U.S.NRC
United States Nuclear Regulatory Commission
Protecting People and the Environment

NUREG/CR-7100
SAND2012-0323P

Direct Current Electrical Shorting in Response to Exposure Fire (DESIREE-Fire): Test Results

Final Report

Office of Nuclear Regulatory Research

AVAILABILITY OF REFERENCE MATERIALS IN NRC PUBLICATIONS

NRC Reference Material

As of November 1999, you may electronically access NUREG-series publications and other NRC records at NRC's Public Electronic Reading Room at http://www.nrc.gov/reading-rm.html. Publicly released records include, to name a few, NUREG-series publications; *Federal Register* notices; applicant, licensee, and vendor documents and correspondence; NRC correspondence and internal memoranda; bulletins and information notices; inspection and investigative reports; licensee event reports; and Commission papers and their attachments.

NRC publications in the NUREG series, NRC regulations, and *Title 10, Energy*, in the Code of *Federal Regulations* may also be purchased from one of these two sources.

1. The Superintendent of Documents
   U.S. Government Printing Office
   Mail Stop SSOP
   Washington, DC 20402–0001
   Internet: bookstore.gpo.gov
   Telephone: 202-512-1800
   Fax: 202-512-2250
2. The National Technical Information Service
   Springfield, VA 22161–0002
   www.ntis.gov
   1–800–553–6847 or, locally, 703–605–6000

A single copy of each NRC draft report for comment is available free, to the extent of supply, upon written request as follows:

Address: U.S. Nuclear Regulatory Commission
Office of Administration
Publications Branch
Washington, DC 20555-0001
E-mail: DISTRIBUTION.RESOURCE@NRC.GOV
Facsimile: 301–415–2289

Some publications in the NUREG series that are posted at NRC's Web site address http://www.nrc.gov/reading-rm/doc-collections/nuregs are updated periodically and may differ from the last printed version. Although references to material found on a Web site bear the date the material was accessed, the material available on the date cited may subsequently be removed from the site.

Non-NRC Reference Material

Documents available from public and special technical libraries include all open literature items, such as books, journal articles, and transactions, *Federal Register* notices, Federal and State legislation, and congressional reports. Such documents as theses, dissertations, foreign reports and translations, and non-NRC conference proceedings may be purchased from their sponsoring organization.

Copies of industry codes and standards used in a substantive manner in the NRC regulatory process are maintained at—

The NRC Technical Library
Two White Flint North
11545 Rockville Pike
Rockville, MD 20852–2738

These standards are available in the library for reference use by the public. Codes and standards are usually copyrighted and may be purchased from the originating organization or, if they are American National Standards, from—

American National Standards Institute
11 West 42nd Street
New York, NY 10036–8002
www.ansi.org
212–642–4900

Legally binding regulatory requirements are stated only in laws; NRC regulations; licenses, including technical specifications; or orders, not in NUREG-series publications. The views expressed in contractor-prepared publications in this series are not necessarily those of the NRC.

The NUREG series comprises (1) technical and administrative reports and books prepared by the staff (NUREG–XXXX) or agency contractors (NUREG/CR–XXXX), (2) proceedings of conferences (NUREG/CP–XXXX), (3) reports resulting from international agreements (NUREG/IA–XXXX), (4) brochures (NUREG/BR–XXXX), and (5) compilations of legal decisions and orders of the Commission and Atomic and Safety Licensing Boards and of Directors' decisions under Section 2.206 of NRC's regulations (NUREG–0750).

U.S.NRC
United States Nuclear Regulatory Commission
Protecting People and the Environment

NUREG/CR-7100
SAND2012-0323P

Direct Current Electrical Shorting in Response to Exposure Fire (DESIREE-Fire): Test Results

Final Report

Manuscript Completed: December 2011
Date Published: April 2012

Prepared by:
Steven P. Nowlen, Jason W. Brown, Tara J. Olivier, and Francis J. Wyant

Sandia National Laboratories
Risk and Reliability Analysis Dept. 6761
P.O. Box 5800
Albuquerque, NM 87185-0748

Gabriel Taylor, NRC Project Manager

NRC Job Code N6579

Office of Nuclear Regulatory Research

ABSTRACT

This report presents the results of a series of fire tests performed to assess cable failure modes and effects behavior for direct current (dc)-powered control circuits. The project, known as the Direct Current Electrical Shorting in Response to Exposure Fire (DESIREE-Fire) test project, was sponsored by the U.S. Nuclear Regulatory Commission Office of Nuclear Regulatory Research. The tests were performed by and at Sandia National Laboratories in Albuquerque, NM. The program was conducted with the collaboration of the Electric Power Research Institute (EPRI) and its member utilities. EPRI representatives participated in all phases of program planning, execution, data analysis, and data reporting by providing both peer review and in-kind material support.

The test program involved a series of both small- and intermediate-scale fire tests. Each test exposed one or more electrical control cables commonly used in the existing fleet of U.S. nuclear power plants (NPPs) to fire exposure conditions. Each test cable was connected to one of several circuit simulator units designed to mimic the behavior of typical NPP components. The simulated dc-powered control circuits included motor-operated valves, solenoid-operated valves of various sizes, and a medium voltage circuit breaker unit. Cable electrical performance is monitored throughout each test to determine both the timing and mode of circuit faulting behavior. This report focused on a factual reporting of the test program and test data. Insights regarding dc-powered control circuit cable failure modes and effects are to be addressed separately via a Phenomena Identification and Ranking Table (PIRT) exercises to qualitatively rank fire-induced electrical circuit phenomena and an expert elicitation to provide quantitative numerical estimates to the likelihood of various fire-induced circuit failure configurations. One PIRT panel focused on electrical behavior and the second on implications for probabilistic risk assessment.

TABLE OF CONTENTS

LIST OF FIGURES

LIST OF TABLES

EXECUTIVE SUMMARY

Overview

Cables can be subject to damage induced by the exposure to fires from external ignition sources. In nuclear power plants (NPPs), hundreds of miles of cables are used to power, control room and monitor plant equipment. Fire-induced cable damage can cause required safety circuits to fail, and potentially in unique and undesired ways. Fire-induced cable failure can cause loss of function equipment failures (i.e., loss of system or component availability). However, fire-induced cable failures are unique because they can potentially cause spurious operation of plant equipment and/or false indications to control operators. This report describes the most recent effort by the U.S. Nuclear Regulatory Commission (NRC) Office of Nuclear Regulatory Research (RES) to investigate cable failure modes and effects for NPP control circuits.

Several testing programs have studied cable failure modes and effects phenomena. This includes testing by the Nuclear Energy Institute (NEI) and Electric Power Research Institute (EPRI) during 2001 (with NRC/RES collaboration – see NUREG/CR-6776, "Cable Insulation Resistance Measurements Made During Cable Fire Test"), the NRC "Cable Response to Live Fire (CAROLFIRE)" (NUREG/CR-6931) testing of 2006, and the Duke Energy testing of 2006. Internationally, efforts were also undertaken by L'Institut de Radioprotection et de Sûreté Nucléaire (IRSN) in France during 1997 and 2008. These previous tests have all focused primarily on control circuits powered by an alternating current (ac) source, a common circuit type used for various NPP functions including safe shutdown.

In addition to ac circuits, NPPs also rely on circuits powered from direct current (dc) sources such as the station batteries. This typically includes various circuits relied upon for post-fire safe shutdown. Of the previous test programs, only the Duke Energy tests included any testing of dc-powered control circuits and those tests were limited in scope and left many questions unanswered. The Duke tests did provide indications that failures in the dc-powered cables might be unique in comparison to ac-powered counterparts. Differences in circuit design practices between ac and dc systems coupled to the Duke results made it a questionable practice at best to extrapolate from ac-based test results to dc-powered circuits. Given the general lack of knowledge and the importance of dc-powered control circuits to post-fire safe shutdown, the NRC initiated this effort to investigate dc-powered cable failure modes and effects.

The tests described in this report were conducted by Sandia National Laboratories (SNL) beginning in the July 2009 and continuing through February 2010. The project conducted 59 small-scale tests and 17 intermediate-scale tests. In total, the tests involved over 225 individual circuit trials. All of the detailed test data is presented in Appendices B-G. The electronic data and photos are available in electronic format in the companion CD-ROM provided with this publication.

This project provided enhanced quality through collaboration with the U.S. NPP industry as represented by EPRI and its member utilities. EPRI participated in all aspects of the program including providing peer review during development of the test plan, support in the design of the test circuits, in-kind material support, consulting through the course of the actual testing, peer review during the data analysis process, and peer review of this report. In-kind material support included samples of Kerite® cables, samples of armored cables, a medium-size (1-inch)

solenoid-operated valve (SOV), a coil assembly for a very large direct-acting SOV, two medium voltage switchgear breaker units, and the battery cells used in the dc power supply. EPRI partners also supported the design of the test circuits to ensure they were both representative of actual plant practices and capable of detecting the failure behaviors. This collaborative research partnership greatly improved the overall testing approach and quality.

dc-Powered Circuit Insights

The dc circuit testing approach paralleled the recently completed CAROLFIRE project. As in the earlier project, two scales of fire testing were conducted. A small-scale radiant heating facility call *Penlight* was used to perform limited scope preliminary tests under closely controlled laboratory conditions. These early tests provided initial data on the dc-powered cable failure behaviors and also provided an opportunity to verify the operability and refine the dc test circuits and operating procedures. More complex tests at a larger, intermediate scale were also performed using an open flame test setup with more realistic exposure conditions involving cables in random fill cable trays and conduits.

A variety of cables were used during testing in order to highlight any failure behaviors attributable to the polymeric formulations used in cable construction. Most of the tested cables were drawn from stocks left over from the CAROLFIRE project, and all are representative of the cables used in U.S. NPPs. As noted above, testing also included two types of cables, Kerite® and armored, provided through EPRI. All of the tested cables were of a multi-conductor configuration and were predominantly of a control cable configuration.

One unique aspect of this project was the use of a rather substantial battery bank as the dc power source. One of the major limitations of the dc tests conducted by Duke Energy was that those tests relied on a relatively small and non-representative set of batteries (a bank of ten 12Vdc automotive batteries). Thanks to in-kind EPRI support and involvement, this project used a set of 60 much larger battery cells to form a nominal 125Vdc power supply. The battery cells, while not as large as a true set of Class 1E station batteries, were judged by EPRI collaborators to be a reasonable representation of such a battery set given the test conditions. To provide a sense of scale, the completed battery bank weighed over 2000 kg (over 4800 lb). The total available short circuit fault current at the output terminals of the battery bank was estimated at over 13,000 amperes (A).

For testing, a total of eight dc-powered control circuits were developed. Seven of these were based on actual NPP-type electrical components; namely, two reversing motor-operated valve (MOV) circuits, two small pilot SOV circuits, one 1-inch SOV, one valve coil for a very large direct acting SOV, and two medium voltage switchgear breaker units. The eighth circuit was a purpose-built system looking for intercable hot shorts (HSs) (cable-to-cable conductor short circuits).

The scope of this report is limited to the objective reporting of the test data. It is not the intent of this report to interpret the test results beyond a factual representation of the progression of events observed in each test. The NRC is conducting follow-on work that will use this test data to develop best estimate probabilities of spurious operations given cable damage via an expert elicitation panel. In addition, another project will evaluate the fire-induced electrical circuit failure phenomena by performing a Phenomena Identification and Ranking Table (PIRT) exercise.

That said, there are several general observations that were made through the course of testing that are worthy of note:

- The arcing observed in conjunction with the cable faulting was more energetic for the dc-powered cables than was the corresponding behavior in ac-power cables. Both ac- and dc-powered cables displayed arcing, but the arcs formed by the faulting dc-powered cables were more substantial, more sustained, and more damaging.
- Faulting of the dc-powered cables often led to destructive damage to the cable conductors (open circuit/conductor breakage). Destructive damage at this level has not been observed for ac-power control cables.
- In some cases the dc-powered cables were left energized even after they had experienced destructive damage as described immediately above. This behavior was more common for tests involving larger (15A, 25A, or 35A) fuses.
- For any given dc-circuit, the two paired fuses (one on the positive leg and one on the negative leg) did not necessarily clear at the same time. Many factors contribute to this behavior. For example, the time/current clearing relationship varies somewhat even within a single batch of like fuses so that one fuse may clear more quickly than another given the same fault current. Also, some fuse blows resulted from circuit-to-circuit interactions through the ground plane (multiple shorts to ground) so that the two fuses involved in the fault might be of different sizes (e.g., the fault currents might be routed through a 10A fuse from one circuit and a 5A fuse from another circuit). In such cases the lower amperage fuse would typically clear leaving the higher amperage fuse intact.
- In general, more long-duration HSs and spurious operations were observed for the dc-powered circuits than had been observed in corresponding ac-powered circuits.

ac-Powered Circuit Insights

The final issue investigated during Direct Current Electrical Shorting in Response to Exposure-Fire (DESIREE-Fire) was the question of how the sizing of control power transformers (CPTs) would impact the likelihood of spurious operation in ac-powered control circuits. This was an issue that was also investigated in the prior CAROLFIRE test program with inconclusive results. During the original NEI/EPRI circuit tests of 2001, it had been noted that multiple current leakage paths that formed during the cable degradation process would lead to saturation of the power-limited CPTs and to degradation of the source voltage. In some cases the voltage degraded to below the minimum pick-up voltage of the motor contactors. This effect was attributed with reducing the Spurious Actuation (SA) probability by a factor of two compared to non-power-limited circuits.

CAROLFIRE investigated a range of CPT sizes (i.e., 100VA to 250VA) but could not reproduce the voltage degradation effect to nearly the degree observed by NEI/EPRI. Differences in the characteristics of the motor contactors used in each program were thought to have been a contributing factor to the difference in test results.

For DESIREE-Fire the control circuit simulator units used in CAROLFIRE were rebuilt using the same model of motor control contactors as the original NEI/EPRI tests. Two of the four contactor sets were provided by EPRI as a part of the collaboration. However, only one case out of a total of 42 total circuit failure trials appears to have experienced voltage degradation that actually prevented a SA; namely, Penlight Test #17. This case involved Surrogate Circuit Diagnostic Unit (SCDU)-1 with a 100VA CPT (note that larger 150VA CPTs were used in the original NEI/EPRI tests). A second test, intermediate-scale test 4, also showed signs of

substantial source voltage degradation but only after SAs had already occurred. This second test involved SCDU-4 with a 75VA CPT.

Overall, like CAROLFIRE, the DESIREE-Fire tests failed to reproduce the voltage degradation effect to nearly the degree observed by NEI/EPRI despite the inclusion of smaller CPTs in the testing protocol. None of the tests involving the two larger CPTs (150VA and 200VA) showed degradation of source voltage sufficient to prevent a SA. Other trials involving the smaller 75VA and 100VA CPTs (i.e., other than Penlight Test #17 and Test IS4) were conducted and did not experience sufficient voltage degradation to prevent SA.

ACKNOWLEDGMENTS

The authors gratefully acknowledge the contributions of the many people who helped ensure the success of this project. Within the NRC we especially acknowledge the support and guidance provided by Harold “Harry” Barrett of NRR. His drive to see these tests through from beginning to end has been greatly appreciated. We also acknowledge the support of our Office of Nuclear Regulatory Research sponsors, Gabriel Taylor and Mark Henry Salley. Mark is a relentless supporter of the need for fire research and that is greatly appreciated. Gabe not only dealt with program oversight but also supported data analysis, which was no ordinary task. It is also important that we acknowledge the critical contributions of the Electric Power Research Institute (EPRI) collaborative team. It is clear that the collaboration was a major success, leading to many improvements in the quality of the test program. Many key aspects of the program were ultimately decided based on input from individuals brought to the project through the EPRI collaboration. Many organizations and individuals participated over the course of the project, but we want to especially acknowledge those who stuck with the project from beginning to end; namely, Ken Canavan, Dan Funk, Jeffro Wagner, Dennis Henneke, Kiang Zee, Ashley Mossa, Ken Caraway, Steve Graham, Dave Miskiewicz, and Ed McCann. Finally, we acknowledge the contributions made to the program via the in-kind material support also arranged via the EPRI collaboration and the relentless efforts of Ken Canavan. Kirtland Air Force Base kindly loaned us a switchgear-breaker unit for use in testing. EPRI arranged and paid for a replacement breaker when the Kirtland breaker was unexpectedly damaged in testing. Target Rock provided two solenoid valve assemblies. Duke Energy, VC Summer, Progress Energy, and Energy Northwest all provided cables for testing.

The authors also acknowledge and thank the following individuals and organizations for providing peer review comments on the preliminary draft of this report:

Dennis Henneke, GE-Hitachi
Chris Pragman, Exelon Energy
Dr. Vyto Babraskus, Fire Science and Technology Inc.
Mano Subudhi, Brookhaven National Laboratory (BNL)
Jeffro Wagner, SCANA Corp., South Carolina Electric & Gas, VC Summer
Ken Caraway, Electric Power Research Institute (EPRI)
Dr. Ogura, Dr. Kasahara and the Fire Protection Working Group, Japan Nuclear Energy Safety Organization (JNES)

The authors also acknowledge and thank student intern, Roushan Ghanbari from Sandia National Laboratories for her help with assisting with this report.

ACRONYMS

A	ampere
ac	alternating current
AOR	air-operated valve
ASTM	American Society of Testing and Materials
AWG	American Wire Gauge
CAROLFIRE	cable response to live fire (an NRC/RES project)
CPG	chlorinated poly ethylene
CPT	control power transformer
CSPE	chloro-sulphorated polyethylene
dc	direct current
DCCCS	direct current control circuit simulators
DESIREE-Fire	direct current electrical shorting in response to exposure-fire
DNF	did not fail
EMRV	electromagnetic relief valve
EPR	ethylene propylene rubber
EPRI	Electric Power Research Institute
FB	fuse blow
FR	A cable insulation product designation of the Kerite company thought to stand for either “fire retardant” or “fire resistant” depending on the source consulted
HS	hot short
HT or HTK	A cable insulation product designation of the Kerite company standing for “high temperature” or “high temperature Kerite”
IN	information notice
IRMS	Insulation Resistance Measurement System
ISRN	L'Institut de Radioprotection et de Sûreté Nucléaire
JNES	Japan Nuclear Safety Organization
LC	large coil
LER	licensee event report
MOU	memorandum of understanding
MOV	motor-operated valve
NEI	Nuclear Energy Institute
NIST	National Institute of Standards and Technology
NOS	new old stock
NPP	nuclear power plants
NRC	Nuclear Regulatory Commission
NRR	NRC Office of Nuclear Reactor Regulation
PE	polyethylene
PIRT	phenomena identification and ranking table
PORV	power-operated relief valve
PRA	probabilistic risk assessment
PVC	polyvinyl chloride
RES	NRC Office of Nuclear Regulatory Research
RIS	regulatory issue summary
SA	spurious actuation
SCDU	surrogate circuit diagnostic unit
SDP	significance determination process
SNL	Sandia National Laboratories
SOV	solenoid-operated valve

SR	silicone rubber
SRV	safety relief valve
SWGR	switchgear
TP	thermoplastic
TS	thermoset
XLPE	cross-linked polyethylene
XLPO	cross-linked polyolefin

1. BACKGROUND AND INTRODUCTION

1.1 Overview

This report describes a series of cable fire tests performed by Sandia National Laboratories (SNL) under the sponsorship of the U.S. Nuclear Regulatory Commission (NRC) Office of Nuclear Regulatory Research (RES). This effort was conducted in collaboration with the Electric Power Research Institute (EPRI) and its member utilities via a NRC-RES/EPRI Memorandum of Understanding (MOU). This effort is known as the Direct Current Electrical Shorting In Response to Exposure-FIRE (DESIREE-Fire) project and was designed to provide data to support the evaluation of potential risks associated with the fire-induced cable failure modes and effects for dc-powered electrical control circuits including, in particular, Hot Short (HS) and Spurious Actuation (SA) phenomena.[1]

While the DESIREE-Fire project involved collaboration between the RES and EPRI, SNL acted as the primary test laboratory and the contents of this report were produced exclusively by SNL. EPRI and its industry members provided peer review of this report in lieu of a full public comment process.

The DESIREE-Fire project complements previous research conducted in the Cable Response to Live Fire (CAROLFIRE) project in 2006 [1]. As a result of these two testing project similarities, this report relies on the readers' understanding of the CAROLFIRE testing approach, as the DESIREE-Fire project applied similar test methods. Although this report does provide a general overview of the testing approach and detailed discussion on where DESIREE-Fire deviated from the CAROLFIRE approach, the reader unfamiliar with the CAROLFIRE testing should consult NUREG/CR-6931, "Cable Response to Live Fire (CAROLFIRE)," for full understanding of the testing approach and reasoning.

1.2 Background

In the late 1990s, a series of licensee event reports (LERs) identified plant-specific problems related to potential fire-induced electrical circuit failures that could affect equipment necessary to achieve and maintain safe shutdown. The NRC staff issued Information Notice (IN) 99-17, "Problems Associated with Post-Fire Safe-Shutdown Circuit Analyses," on June 3, 1999, to document additional problems [2]. In 2001, the nuclear industry, under the coordination of the Nuclear Energy Institute (NEI), performed a series of cable functionality testing to advance the nuclear industry's understanding of fire-induced circuit failures, particularly spurious equipment actuations initiated by circuit failures. The results from these 18 tests were then presented to an expert panel, which developed risk insights into the phenomena of fire-induced failures of electrical cables. The results of the expert panel were documented in an EPRI Technical Report No. TR-1006961, entitled, "Spurious Actuation of Electrical Circuits Due to Cable Fires" [3].

Following this work, the NRC held a public workshop on risk-informing post-fire safe-shutdown circuit analysis inspection on February 19, 2003, at NRC headquarters offices in Rockville, Maryland. Information collected from stakeholders during the workshop was used by the NRC staff to risk-inform the inspection procedures. The results of the workshop were documented in Regulatory Issue Summary (RIS) 2004-03, "Risk-Informed Approach for Post-Fire Safe-

[1] A "hot short" is defined as a short circuit between an energized "source" conductor and a normally non-energized "target" conductor. A "spurious actuation" is defined as inadvertent energization of a device due to a hot short.

Shutdown Circuit Inspections" [4], which separated circuit configurations into three individual categories, or bins, of circuit failure likelihood based on research and test results:

- Bin 1: Circuit configurations most likely to fail.
- Bin 2: Circuit configurations that need more research.
- Bin 3: Circuit configurations unlikely or least likely to fail.

The CAROLFIRE project, completed in 2006, was undertaken by RES to provide additional data for resolving Bin 2 circuit configurations. The results of the 96 tests performed under CAROLFIRE are documented in NUREG/CR-6931 [1].

At the same time CAROLFIRE was ongoing, Duke Energy was conducting their own cable performance testing at Intertek ETL SEMKO testing laboratories (formerly known as Omega Point Laboratories) in San Antonio, Texas. Unlike previous testing, these tests also included limited testing of direct current (dc) circuits. The results from this testing suggested that the fire-induced cable failure modes and effects for dc circuits may differ from that observed for alternating current (ac) circuits. While the results of the Duke Energy tests remain proprietary, NRC did prepare a public report on the test effort [5].

Of the few fire induced-circuit failure tests projects recently conducted to explore failure modes and effects of control cables when damaged by fire, only the Duke Energy tests have included dc-powered control circuits, and in that one case the tests conducted were sharply limited in both scope and number. Circuits powered by a dc power source constitute a significant fraction of the safety-related circuits in commercial nuclear power plants (NPPs) and they are characterized by differences in operating characteristics and design as compared to ac control circuits. Based on industry feedback from the NFPA-805 pilot applications and other ongoing circuit analysis efforts (e.g., inspection and enforcement activities, other NFPA-805 transition projects, and Fire Probabilistic Risk Assessment [PRA] upgrade projects), some of the most challenging potential HS-induced SAs, from a consequence standpoint, are associated with control circuits powered by ungrounded dc sources (e.g., power-operated relief valves (PORVs), letdown valves, reactor head/pressurizer vent valves, safety relief valves (SRVs), and breaker circuits).

What remained unclear was the extent to which the existing, largely ac, test data could be extrapolated to dc-powered control circuits. Parameters of interest include the likelihood of SA and HS duration for dc-powered control circuits of various configurations. The lack of either a sufficient set of dc circuit test data or a technical basis for extrapolation of the ac test data represents a significant uncertainty associated with the analysis of dc circuits.

1.3 Purpose and Objectives

The primary objective of the DESIREE-Fire project is to address analytical uncertainties by providing fire-induced cable failure modes and effects data for dc-powered control circuits, and to provide that data in a manner that allows for a direct comparison to the previously developed ac-powered control circuit failure response data. The tests are designed to investigate a number of key variables that may influence the observed failure behavior including cable type, control circuit configuration, fire exposure conditions, and cable routing configuration. The tests are patterned on the recently completed CAROLFIRE tests.

The DESIREE-Fire project also involved several secondary objectives. First, the ac circuit simulators developed for CAROLFIRE (the Surrogate Circuit Diagnostic Units, SCDUs) were

again used in the DESIREE-Fire testing to expand the data set for ac control circuits and to address Bin 2 Item D which was not fully addressed by the CAROLFIRE testing. Bin 2 Item D, related to control power transformer (CPT) sizing effects on SA likelihood. Second, similar to CAROLFIRE, thermal exposure and cable thermal response data was recorded such that the observed electrical failures can be correlated to the cable thermal response. These secondary objectives focus on expanding the existing data to support further development of cable thermal response predictive models and provide explicit data on cable electrical failure thresholds under dc power conditions. Lastly, the DESIREE-Fire provides test results on Kerite® FR control cable electrical performance during elevated thermal conditions. This data will be used to address questions related to the thermal performance of this specific cables type [6].[2]

1.4 Project Planning and General Approach

The draft project plan for DESIREE-Fire was developed over the course of several months and included several rounds of review and revision. The first draft of the test plan was issued in July 2008 and included a 30-day public comment period (see Federal Register notice 73 FR 53452) starting September 16, 2008, and ending October 24, 2008. A revised plan addressing the public comments was then circulated among the NRC staff and EPRI partners and underwent several revisions as details of the program developed. Input from EPRI led to refinements to various aspects of the test plan including, in particular, the design of the dc test circuits and battery power supply system. These aspects of the test plan continued to develop as EPRI in-kind material support made available a number of NPP components that were incorporated into the test circuits (i.e., solenoid-operated valves [SOVs] and a switchgear breaker unit). Input from EPRI also helped to refine aspects of the test circuits to better represent industry practice (e.g., fuse selection and sizing). The peer review group during the planning process[3] included several industry representatives through EPRI and NRC technical experts specializing in the areas of post-fire safe-shutdown circuit analysis, fire PRA, fire protection, and electrical engineering. The peer review effort was a very detailed and extensive iterative process that resulted in an improved project plan and overall testing approach. The final project plan,[4] while unpublished, can be found on the enclosed CD and on the NRC website (www.NRC.gov).

The tests were performed beginning with the small-scale tests performed during July 2009. The intermediate-scale tests began in October 2010 and continued through February 2010. All tests were performed using SNL fire test facilities in Albuquerque, New Mexico.

The project employed basic quality assurance provisions, but was not subject to a strict quality assurance program. The instruments (voltage and current transducers) used in the SCDUs and the dc Control Circuit Simulator panels (dc-SIM panels) were covered by manufacturer-supplied certificates of calibration, but were not included in the SNL instrument calibration system for verification or recertification at the completion of testing. Hence, the SCDU and DC-SIM panels voltage and current data are to be taken as ”indication only” and should be viewed as providing absolute indications of circuit behavior during testing. All of the other instruments used in

[2] A separate preliminary report on the Kerite cable testing has been published by SNL as cited here. The Kerite cable test results are included in this report, but only in the general context of dc cable failure modes and effects. Issues specific to the Kerite cable are deferred to the separate SNL report.

[3] Peer reviewers were technical experts not directly involved in the original development of the project plan but could conduct a detailed independent review of the plan and provide objective comments to improve the overall research product.

[4] The test plan has not been published but has been posted as a public document on the NRC web site. Citation is as follows: Nowlen, S.P., Wyant, F.J., Brown, J., *Project Plan for Direct Current Electrical Shorting In Response to Exposure FIRE (DESIREE-Fire)*, July 10, 2009.

testing, and in particular the various thermocouples and temperature measurement instrumentation, were subject to the SNL calibration process, which provides calibration services traceable to the National Institute of Standards and Technology (NIST) standards.

All tests followed a proscribed test protocol including pre- and post-test checklists. Field notes were maintained by the lead test engineer documenting all variable aspects of the individual tests and recording field observations during each test. All data processing and plotting was performed using commercial software (Microsoft Excel®, SigmaPlot®). The original data files in their native format have been preserved for archival purposes. All data from the testing program is publically available without restriction on the enclosed CDs at the back of this report and on the NRC website (www.NRC.gov).

1.5 Scope of this Report

This report includes a summary description of all tests performed including experimental setups, test matrices, and a description of instrumentation fielded during each experiment. The processed data can be found on the enclosed CD. The report also presents the data gathered for each test. Interpretation of the test data is limited to a factual description of the circuit faulting behavior. This includes a detailed timeline characterizing the circuit faulting behavior highlighting, in particular, the onset and duration of HSs and SA. This report does not delve into a statistical analysis of data trends nor into the interpretation of test results as they might apply to risk analysis. Those aspects of data analysis and interpretation lie outside the scope of this project and are the subject of planned RES follow-on activities (see Section 0 for additional discussion).

1.6 Report Organization

This balance of this report is organized as follows:

- **Section 2** provides general background discussions describing previous test programs investigating related phenomena. Section 2 also provides an overview of the testing needs addressed by DESIREE-Fire.

- **Section 3** describes the general approach taken by DESIREE-Fire. Included in Section 3 are summary descriptions of the test facilities, test protocols, and cables used in testing.

- **Section 4** provides summary descriptions of the test circuits used to assess cable electrical performance, including both the dc and ac-based systems. A summary description of the dc battery bank is also provided. Note that detailed descriptions of the test circuits are provided in Appendix A.

- **Section 5** presents the two test matrices, one for the small-scale Penlight tests and one for the intermediate-scale tests.

- **Section 6** provides summary descriptions of the test results for each of the various electrical test circuits. That is, the discussions in Section 6 are organized by test circuit rather than by test number or test date. More detailed presentation of the test data is deferred to Appendices B through G.

- **Section 7** presents summary discussions highlighting general insights gained from the testing.

- **Section 8** identifies referenced documents.

- **Appendix A** provides detailed descriptions of the test circuits, the dc battery bank and other test support systems used in testing. There are five sub-appendices (Appendices A.1 through A.5) each covering a specific dc-powered control circuit. Appendix A.6 covers the ac-powered SCDU systems. Appendix A.7 covers the battery bank. Appendix A.8 covers other test support systems including temperature monitoring, computers, software, and the data file formats and structure.

- **Appendices B through G** are provided on the enclosed CDs and present, in detail, the test data for each individual test and test circuit. Together, these six appendices cover every test performed and every circuit tested. The appendices are organized by test circuit and, for each circuit, cover all of the tests that included that circuit. Each of these appendices is divided into two subsections, the first presenting the small-scale Penlight test data and the second covering the intermediate-scale tests. The appendices are associated with test circuits as follows:

    - Appendix B: The dc-powered motor-operated valve (MOV) circuits
    - Appendix C: The dc-powered SOV circuits
    - Appendix D: The dc-powered 1-inch SOV and large coil circuits
    - Appendix E: The dc-powered switchgear breaker circuit
    - Appendix F: The dc-powered intercable circuit
    - Appendix G: The ac-powered SCDU circuits

2. OVERVIEW OF TESTING NEEDS ADDRESSED BY DESIREE-FIRE

2.1 Cable Failure Modes and Effects for dc-powered Control Circuits

As discussed in Section 1.2 above, almost all of the previous testing for fire-induced cable failure modes and effects has focused on ac-powered control circuits. There are several characteristics associated with dc-powered control circuits that are unique as compared to ac control circuits. Hence, the extrapolation of the ac circuit test results to dc circuits might not be valid or appropriate if cable failure modes and effects for dc-powered control circuits differ from the corresponding behaviors in ac circuits. It was this particular area of uncertainty that was the primary focus of the DESIREE-Fire project; that is, to provide data on the failure modes and effects behavior for dc-powered control circuits that could be directly compared to the corresponding data already available for ac-powered control circuits.

Without an understanding of how cable faults in dc circuits differ from ac circuits, the identification of important circuit characteristics for dc systems is, at best, speculative. Based on input obtained during the test plan development and peer review process, three dc circuit characteristics that differ from ac control circuits were identified before testing as those most likely to impact the cable failure modes and effects behaviors. These are the following:

- Fusing: dc-powered control circuits tend to use larger fuse sizes for over-current protection than the comparable ac control circuits. Several factors contribute to this design choice. Ultimately, fuses are sized to protect the cables from current overload and breaker/fuse coordination is maintained consistent with the general treatment of coordination for other plant circuits. The result of this design difference may be that over-current protection devices would not open as readily as the corresponding devices in an ac circuit. This could allow dc circuit faults to persist for a longer period of time before a “fuse-blow” and circuit de-energizing as compared to a corresponding ac circuit. One observation made during testing was that the dc-powered cables displayed far more energetic arcing behaviors during the process of conductor-to-conductor and conductor-to-ground shorting. This behavior may be at least in part a reflection of the larger fuses in the circuits. Overall, fuse design practices may impact HS behaviors including both likelihood and duration, although the net effect of the higher fusing and the anticipated arcing-fault behaviors remains unknown.

- No zero-crossing: By definition, ac circuits have “zero-crossing” points as a result of the sinusoidal waveform signal. In contrast, dc circuits use a constant voltage potential to operate and by definition have no “zero-crossing” behavior. The impact of a constant circuit voltage on the cable faulting behavior as compared to a zero-crossing fault behavior is unclear. The lack of a zero-crossing characteristic, especially when coupled to a higher amperage over-current protection device, may contribute to the observed arcing fault behavior. That is, as noted above, dc-powered conductors were observed to display more energetic and sustained arcing type faults and the lack of a zero-crossing feature might contribute to this behavior. Whether this behavior increases or decreases the duration of HSs is unknown.

- Ungrounded power supply: The information gathered during the development of the test plan (i.e., EPRI input, NRC staff input, and our own research) confirmed that most plants utilize ungrounded dc power sources (i.e., ungrounded battery banks). In contrast, most ac power supply systems are grounded. The nature of the cable shorting

behaviors possible given an ungrounded power source may be more complicated than those associated with a grounded power source. For a grounded circuit, a short between the any single energized conductor and ground would induce a fault current and potentially trigger circuit protection (fuses or breakers) if the conductor-to-ground resistance was low enough. In contrast, for an ungrounded power supply, a single bolted fault between an energized (either positive or negative polarity) conductor and ground (i.e., a single low-resistance conductor-to-ground short) will not induce any fault current and will not trigger circuit over-current protection. Such a fault would only act to ground one side of the battery set. Furthermore, multiple shorts to a grounded raceway (i.e., a cable tray, conduit or grounded conductors if present) could result in the raceway acting as a conductor of power from one circuit to another. That is, if the battery bank becomes grounded on the positive potential, then the ground plane itself can act as a conductor directly to the positive side of the battery bank for any circuit connected to the same battery bank. These complexities could impact both HS duration and SA likelihood.

The intent of the test program was to provide data that will assist staff in assessing the potential risk implication of fire-induced damage to dc-powered cables and control circuits. The tests were designed to explore these and other relevant behaviors for a range of dc-powered control circuits and cables. Summary descriptions of the various dc-powered control circuits tested are provided in Section 0, and more complete descriptions are provided in Appendices A.1 through A.5.

2.2 Cable Failure Modes and Effects for ac Control Circuits

The testing included use of the ac-powered MOV control circuits, referred to as the SCDUs, originally developed for the CAROLFIRE project. The use of this equipment served two purposes. First, these tests represent, in effect, a “target of opportunity” to expand the existing ac control circuit data set. Second, the use of both the ac and dc-powered control circuits in the same tests allows for a direct cross-comparison of observed behaviors. Testing of the ac circuits also provides an opportunity to address one lingering issue not fully resolved by the CAROLFIRE study: namely, the impact of CPT sizing on the likelihood of spurious operations (Bin 2 Item D from RIS 2004-03 [4]). As noted in the CAROLFIRE report, the results for this specific item were ambiguous at best. The dc testing program offers an opportunity to further explore this behavior.

The ac-based SCDUs were deployed in a manner similar to that employed in CAROLFIRE, although some changes were made. In particular, all four sets of motor contactors used in the original design were replaced by Joslyn-Clark contactor sets that are considered representative of those used during industry testing of 2001. Two of the four replacement contactor sets had been used during prior testing by Duke Energy and were provided by EPRI (i.e., as a part of EPRI’s in-kind material support). Two additional contactor sets were purchased directly from the manufacturer. Section 0 provides a summary description of the SCDU and Appendix A.6 provides a more detailed description that includes the system design changes implemented for DESIREE-Fire.

2.3 Fire and Fire Response Characterization

One of two major objectives of the CAROLFIRE project was to explore key behaviors associated with the thermal response of cables exposed to a fire environment. In particular,

CAROLFIRE included a substantial effort to characterize cable heating behavior under a range of fire conditions and to correlate the cable thermal response to electrical performance and failure. These efforts led to improvements in fire modeling techniques and development of the THIEF model as documented in Volume 3 of the CAROLFIRE report [1]. The DESIREE-Fire testing project also included the gathering of fire exposure and cable thermal response data. However, the level and extent of thermal monitoring was not as extensive as in the previous testing program.

With respect to cable thermal response, the DESIREE-Fire testing again included cables instrumented for thermal response in a manner that will allow for correlation to electrical failure. Testing also included thermocouples and other instruments deployed to characterize the local thermal environment to which the cables are exposed. It was not generally anticipated that the failure thresholds for the electrical cables under dc conditions will differ substantially from the cable failure thresholds observed under ac conditions. Accordingly, the DESIREE-Fire tests' thermal exposure conditions were based on cable failure threshold data obtained during testing with ac-powered cables.

2.4 Supplemental Data on Cable Failure Characteristics

Several cable types were tested to evaluate the cables' thermal performance. Although not identified during the development of the DESIREE-Fire test plan, the addition of these tests required little effort and provided needed data for resolution of cable performance issues. The cables tested included samples of vintage (1970s) Kerite® HTK and Kerite® FR. These cables were supplied through the NRC-RES/EPRI MOU as new old stock (NOS). With the use of the electrical monitoring equipment, the failure point as these cables are exposed to a thermal insult can be determined.

3. APPROACH

3.1 Project Planning and General Approach

An extended process of project planning was undertaken to ensure that the testing program and protocols would address the identified data needs. Preliminary planning involved several conference calls between the NRC (including both RES and NRC Office of Nuclear Reactor Regulation [NRR] staff) and SNL. Based on these early discussions a straw-man definition of the overall project goals and technical approach was developed. Several key parameters that would need to be dealt with as a part of test planning were identified, including:

- selection of dc test circuits (i.e., focus on circuits used in safety related systems);
- test circuit design parameters and objectives;
- circuit monitoring objectives and instruments;
- dc power source characteristics (e.g., voltage level, battery characteristics, and number of power supplies);
- power source, circuit, and instrument grounding; and
- cable types to be used in testing.

From these discussions, SNL developed a preliminary test plan that was issued by the NRC for public comment in September 2008. Several comments were, in fact, received as a result of the public comment process and addressed in subsequent revisions. One key element that developed as a result of the public comment process was that industry, as represented by EPRI, cited their interest in establishing a collaborative involvement in the project. Subsequent discussions did lead to a formally established NRC-RES/EPRI MOU collaboration.

The NRC-RES/EPRI MOU collaboration had a major impact on development of the final test plan. A series of conference calls between the NRC, SNL, and the EPRI collaborative team were held over the course of the next several months and during these calls detailed aspects of the test program were discussed. Several rounds of comment and revision of the test plan were undertaken to address concerns and design suggestions, and to incorporate the in-kind material support that developed over the course of these discussions (e.g., to incorporate NPP components made available through the collaboration into the design of the test circuits).

The test plan was nominally finalized in July 2009, and that version is included on the enclosed CD located inside the back cover of this report. However, it should be noted that while the final test plan was “frozen” as a document, additional changes and adjustments were made through the course of the testing to address issues identified as the test plan was implemented. Beginning as early as December 2008 and continuing through July 2010, RES, NRR, SNL, and the EPRI collaborative team participated in weekly teleconferences during which issues were discussed and resolution strategies identified.

To meet the project goals, a fairly large number of tests involving varied arrays of cable types, cable bundling arrangements, heating conditions, circuit types, and cable routing conditions were performed. Based on the success of the CAROLFIRE project approach, it was determined that two scales of testing would be the most beneficial for the DESIREE-Fire project. The two scales of testing are complementary and each provides unique advantages.

Preliminary testing was conducted in a small-scale radiant heat testing apparatus known as Penlight. The small-scale test facility is described more fully in Section 3.2. Penlight allows for well controlled heat exposures that are beneficial for comparison purposes. Penlight tests can

be conducted very efficiently, in a short time, and at relatively low cost. Small-scale testing also provided an opportunity to complete verification of all the test circuits, test procedures, safety procedures, data logging equipment and software. The intermediate-scale tests are far more complex, and therefore more time-consuming and costly. However, they provide more realistic fire exposure and cable loading configurations (e.g., actual open flaming exposure fires and random fill cable trays). Based on the CAROLFIRE results, both testing scales produced similar results relative to the cable failure modes and effects behavior. Hence, the same approach was applied to DESIREE-Fire. In all, of the DESIREE-Fire testing project consisted of 59 Penlight tests and 17 intermediate-scale tests.

The test design was optimized to allow for considerable flexibility as the testing proceeded. As noted above, the test plan was nominally frozen as a document in July 2009. However, the actual implementation of the test matrix allowed for considerable flexibility. Changes were made to cable, circuit, and instrumentation configurations, and to the test procedures to reflect insights gained as the tests proceeded. That is, as experience was gained through the performance of the tests, opportunities for improvement were identified and implemented; hence, the final test plan matrices were modified. Section 5 presents the as tested test matrices.

Each test was based on thermal/fire exposure of a set of sample cables where each cable is connected to one of several electrical performance monitoring systems. Summary descriptions of the various electrical performance monitoring systems are provided in Section 0, and more detailed descriptions are provided in Appendix A. In general, the Penlight tests involved the application of just one or two of the available systems per test. Through the course of the Penlight testing all of the available electrical performance systems were tested. The intermediate-scale tests generally involved simultaneous application of all of the available electrical performance monitoring systems, each connected to one of the sample cables present in the test.

3.2 Penlight Small-Scale Radiant Heating Tests

The small-scale tests for DESIREE-Fire were conducted at the Thermal Test Complex at SNL using a radiant heating apparatus known as Penlight. DESIREE-Fire duplicated the CAROLFIRE test setup in all regards and generally applied the same testing protocols. This section provides a summary description of the Penlight test facility. For a more complete description, refer to the CAROLFIRE report [1].

The Penlight apparatus is placed beneath a ventilation hood as shown in Figure 3-1 and uses computer-controlled, water-cooled quartz lamps to heat a stainless steel shroud. The shroud is painted flat-black and acts as a grey-body radiant heating source, re-radiating heat to a test sample located within the shroud. The exposure temperature is controlled and monitored based on thermocouples mounted on the inner surface of the shroud. Penlight creates a primarily radiant heating environment that is analogous to that seen by an object enveloped in a fire-induced hot gas layer. That is, the hot gas layer thermal exposure environment is dominated by radiant heat exchange between the hot, smoke-filled gases and any immersed objects. The hot, smoke-filled gases act largely as a gray-body radiator. Penlight simulates these conditions with the shroud temperature being analogous to the hot gas layer or smoke temperature. From Volume 2 of CAROLFIRE, Table 3-1 provides a summary of the temperatures and corresponding heat fluxes. Additional insights may be gleaned from that report.

Figure 3-1 The Penlight apparatus

Table 3-1 Relationship between shroud temperature and shroud heat flux assuming an emissivity of 0.815.

Metric Units			Equivalent values in English Units	
Temperature (°C)	**Temperature (°K)**	**Heat Flux (kW/m^2)**	**Temperature (°F)**	**Heat Flux (BTU/ft^2s)**
260	533	3.7	500	0.33
295	568	4.8	563	0.42
300	573	5.0	572	0.44
325	598	5.9	617	0.52
330	603	6.1	626	0.54
350	623	7.0	662	0.62
400	673	9.5	752	0.84
425	698	11.0	797	1.0
460	733	13.4	860	1.2
470	743	14.1	878	1.2
475	748	14.5	887	1.3
500	773	16.5	932	1.5
525	798	18.8	977	1.7
600	873	26.9	1112	2.4
650	923	33.6	1202	3.0
665	938	35.8	1229	3.2
675	948	37.3	1247	3.3
700	973	41.4	1292	3.6
900	1173	87.5	1652	7.7

As in CAROLFIRE, most of the DESIREE-Fire tests were conducted using paired cable lengths supported on a 12-in. (30 cm) wide ladder-back style cable tray[5] suspended through the center

[5] The cable trays procured for DESIREE-Fire were B-Line® Series 2 style steel trays with (per manufacturer specifications) a nominal 3" NEMA VE 1 loading depth, 4" side rail, and 9” rung spacing. The specific part number is 248P09-12-144.

of the Penlight shroud. A limited number of tests were also conducted using the conduit configuration. No tests were conducted using the air drop configuration. The cable trays, conduits and other physical test conditions are effectively identical to those used in CAROLFIRE.

As a general practice, cables were tested in symmetric pairs where one cable would be instrumented with type-K thermocouples inserted just below the outer cable jacket to measure the cable temperature response. A second length of cable would then be routed in a symmetric position on the tray (relative to the shroud) and connected to energized electrical integrity test circuits to monitor electrical performance. This cable pairing approach allows for a direct correlation of temperature response and electrical performance without compromising the electrical integrity of the energized cable. The electrical integrity test circuits used varied between tests and test samples, as further described below.

The exact heating protocol (i.e., the shroud set point temperature) varied from test to test depending on factors such as specific test purpose (e.g., low temperature failure mechanism). In some cases a specific set point value was established and maintained through the entire test. In other cases, the set point was varied through the course of the test. That is, a test would be started at a particular set point value, but that value would be increased as the measured cable temperature approached equilibrium. Step-wise increases were continued at, typically, 10 to 15-minute intervals until cable failure was observed. The actual test profile is unique for each test. The exact heating protocol for each test is specified in the detailed test descriptions provided in Appendices B through G.

3.3 Intermediate-Scale Open Fire Tests

A complementary test set was conducted at a scale more representative of in-plant conditions. These tests involved a more realistic open burn of larger arrays of cable under more varied and representative exposures. These tests were referred to as the Intermediate-scale tests and represent a method of evaluating the fire-induced circuit failure effects at actual scale without expending the time and effort full-scale testing would require. The intermediate-scale test approach is, again, identical to that used during the CAROLFIRE project with only slight modifications. This section provides a summary description of the test facility. For a more complete description, refer to the CAROLFIRE test report [1].

The intermediate-scale testing approach was developed during the CAROLFIRE project where a key goal of the research was to assess different exposure conditions, including cable failures due to a hot gas layer exposure, flame impingement, and fire plume conditions. The design of the Intermediate-test enclosure was based off the American Society of Testing and Materials (ASTM) standard test room specified in ASTM Standard E-603, *Standard Guide for Room Fire Experiments* [7], but is not a true room structure. Rather, it is a far more open configuration that did not restrict air flow to the fire (well-ventilated fire conditions). The test structure is arguably a good analog for a very common in-plant configuration; namely, a beam pocket within a larger room (i.e., a typical in-plant situation where the floor above is supported by massive steel and/or concrete beams creating isolated ceiling-level beam pockets).

The intermediate-scale test assembly is illustrated in Figure 3-2. The test structure consists of a steel framework of which only the upper 40% is enclosed. Overall, the test structure measures approximately 2.4m x 3.7m x 3.0m (8ft x 12ft x 10ft – W x L x H). The upper 1.2m (4ft) of the sides and the structure's top were covered with a 13mm- (½-in) thick "fireproof" wall board

(trade name Durock®).[6] Conduits and trays could be routed in any manner desired. For DESIREE-Fire all raceways were routed as a single straight section passing through the full width of the test structure (i.e., across the 2.4m (8ft) dimension). The raceways used are identical to those used in CAROLFIRE. This test structure acts to focus the fire's heat output initially to this confined volume, creating the desired hot gas layer exposure conditions. As the fire progresses the hot gas layer depth increases, and ultimately smoke and hot gasses spill out naturally from under the sides of the enclosed area. This again would be quite typical of the hot gas layer development behavior for a beam pocket configuration.

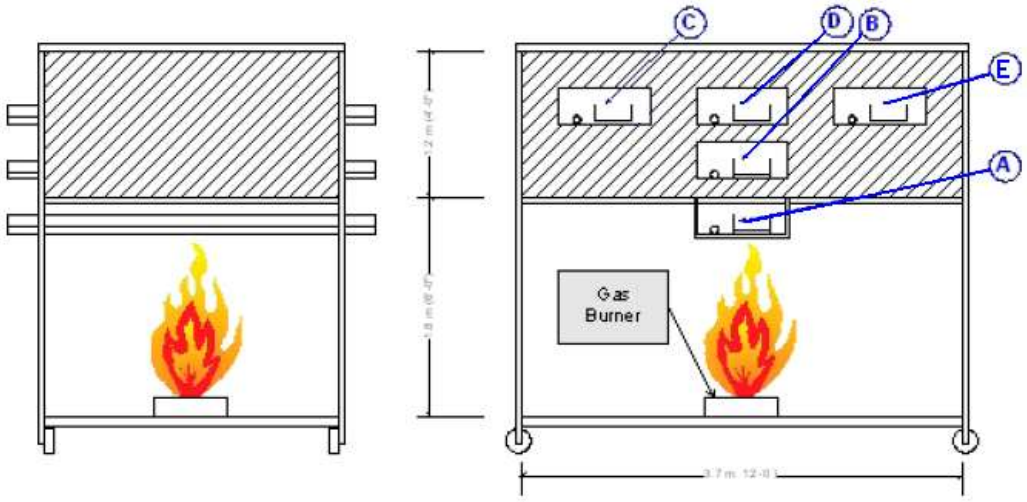

Figure 3-2 Schematic representation of the DESIREE-Fire intermediate-scale test structure.

For DESIREE-Fire five exposure locations[7] were used, namely locations A-E, as illustrated in Figure 3-2 (Note the illustrations of raceway locations A-E in the elevation view figure to the right. These letter designations are used in the test matrices (Section 5) to indicate test object locations.). The detailed test descriptions and test matrices identify cables by location consistent with these labels. Through-wall penetration holes were cut in the side panels to accommodate raceway routing and insulation was placed around the opening between the raceways and enclosure to maintain a hot gas layer within the enclosed portion of the test assembly.

The intermediate-scale test structure was positioned within a larger fire test facility. An existing SNL facility (Building 9830) served as the outer test structure. This isolated the test structure from the ambient environment (e.g., wind effects), allowed for control of bulk air flow conditions through the facility to some extent, and made it possible to gather outlet stack data (temperature, velocity, and oxygen concentration). Figure 3-3 illustrates the placement of the test assembly within the larger facility, and provides overall dimensions for the larger facility.

[6] Durock® is a low-density concrete-based material with fiber-mesh reinforcement. The same material in smaller panels is commonly used as a "'backer board" for tile installation.

[7] Note that two of the cable locations tested in CAROLFIRE were not used during the DESIREE-Fire program. The deleted locations were to the sides of the fire and directly below locations C and E.

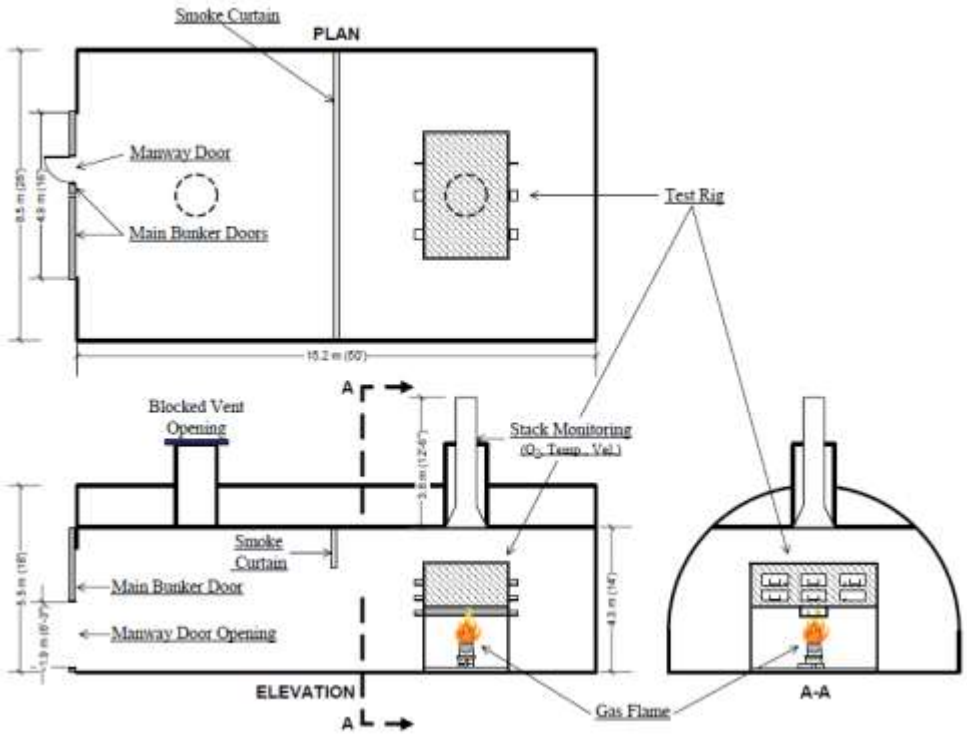

Figure 3-3 Schematic representation of the DESIREE-Fire intermediate test structure located within the outer test facility

The fires in all intermediate-scale tests were initiated using the same gas burner setup as was used in CAROLFIRE. The fuel in all cases was propene (propylene, C_3H_6). The burner used was a square "sand box" diffusion burner. Figure 3-4 provides a photograph of the burner. The top surface of the burner measured 40cm (15.75in) on a side (outside dimensions).

Figure 3-4 Photo of "sand box" diffusion burner

For testing, the burner's top surface was about 0.84m (33in.) above the floor of the enclosure. The burner was always placed in the center of the test structure and directly below cable raceway location A (as shown in Figure 3-2). The flow of gas to the burner was measured and controlled using the same electronic flow control valve as was used in CAROLFIRE [1]. In general, the initial heat release rate allowed for the flame to reach the bottom of the cable tray located in raceway position A. For the majority of the tests, this heat release rate was

maintained for 15 to 20 minutes. The propene flow was subsequently increased every 10 to 30 minutes until the maximum flow rate, if necessary, was reached in order to cause the circuits in the wing positions (i.e., raceway positions C and E) to fail. For details on the heat release rates from each test, please refer to Appendix A.

3.4 Cable Selection

3.4.1 The DESIREE-Fire Cable Set

The CAROLFIRE project undertook an extensive effort to identify and test a variety of representative cable types based on their popularity, thermal robustness, thermo-set (TS) and thermo-plastic (TP) types, tractability, and physical configuration. DESIREE-Fire relied on the CAROLFIRE results in this regard, and most of the cables tested were stocks of unused cables left over from CAROLFIRE. However, not all of the cables tested in CAROLFIRE were re-tested in DESIREE-Fire. Instead, testing focused on a smaller selection of the most popular cable products, and on the 12 American Wire Gauge (AWG) seven conductor cable configurations.

The tested cables are described below with summary information provided in Table 3-2. For this testing project, two cable types were identified as the "core" cable samples, one TS-insulated and the second TP-insulated. These two core cables were the primary focus of the testing. To supplement the two core cable types used, a smaller number of tests used two additional TS-insulated cables and two TP-insulated cables also drawn from the CAROLFIRE materials.

In addition to the CAROLFIRE cables, additional cable types were made available for testing by EPRI through the collaborative agreement. Three general types of cable were made available, namely Kerite® FR, Kerite® HT, and a selection of armored cables.

For convenience, this report identifies the cable materials in the format "insulation/jacket" (e.g., a cable with polyethylene [PE] insulated conductors and a polyvinyl chloride [PVC] jacket would be identified as a PE/PVC cable).

General descriptions of the TS-insulated and -jacketed cables are as follows:

- Cross-linked Polyethylene (XLPE)/Chloro-Sulphonated Polyethylene (CSPE) (Core TS): The most popular insulation material used in the U.S. NPPs is the TS material XLPE. The cable jacket consisted of a CSPE, which is also known by the trade name Hypalon. The cable tested was a Rockbestos-Surprenant Firewall® III product in a seven-conductor (7/c) 12 AWG configuration.
- Ethylene Propylene Rubber (EPR)/Chlorinated-polyethylene (CPE): EPR is the second most popular insulation material and is another TS used during this testing. This EPR-insulated, CPE-jacketed cable was procured from the BICC-Brand® line of products (now marketed by General Cable).
- Silicone Rubber (SR): SR insulation materials are used by a number of U.S. NPPs, particularly in applications inside containment. The SR cable procured consisted of an SR-insulated conductor with a fiberglass braid sheath over the insulated conductor and an overall Amarid braid jacket. This cable was procured as industrial grade from First Capital.
- Cross-linked Polyolefin (XLPO)/XLPE Low Halogen Zero Smoke: An XLPO insulated cable was sought primarily on the basis of existing evidence that XLPO may represent the least robust of the TS materials. However, XLPO is a highly generic material

classification that has been used to label a wide range of actual material formulations. For example, polyethylene is a specific type of polyolefin; hence, all XLPE materials are also legitimately bounded under the more generic classification XLPO. All of the currently available XLPO materials identified during our material search were of a "low halogen zero smoke" type. A Rockbestos XLPO insulated industrial-grade cable was selected and procured. Upon delivery, it was noted that the jacket markings were "XLPE" rather than "XLPO". We contacted Rockbestos and were informed that the material was indeed an XLPE formulation that was being marketed under the more generic XLPO label. The material was tested in a limited number of tests for reference purposes only.

Descriptions of the TP-insulated and -jacketed cables are as follows:

- PE/PVC (Core TP): Of the TP materials, a non-cross-linked PE is one of the two most common general applications, and is considered the most common TP material in use at U.S. NPPs. This cable type is the core TP insulation material used during the DESIREE-Fire testing. This cable was procured as an industrial-grade cable from General Cable.
- Tefzel® 280/Tefzel® 200: Tefzel® is a tradename TP material produced by DuPont Chemical. The material is applied directly as supplied by the manufacturer without modification by the cable manufacturer. The cable tested was procured from Cable USA with a Tefzel® 280 insulation and a Tefzel® 200 jacket. This configuration is considered typical of U.S. NPP usage.
- PVC/PVC: PVC is a TP material very popular for use in the U.S. and abroad as a general commercial- and industrial-grade cable. The PVC/PVC cable used in DESIREE-Fire was procured as an industrial-grade cable from the BICC-Brand® line of products (now marketed by General Cable).

The tested cables included two that were TS-insulated and TP-jacketed as follows:

- XLPE/PVC: XLPE-insulated cables are available in a range of jacket material configurations. An XLPE-insulated and PVC-jacketed cable was procured from General Cable under the BICC-Brand® designation. The cable configuration is considered the most representative of a typical "mixed-type" cable (TS-insulated, TP-jacketed).
- Armored Cable: This cable was provided by Duke Energy and as an XLPE-insulated, PVC-jacketed cable. This cable has a spiral-wound galvanized metal armor below the jacket (the armor is similar in structure and appearance to flexible metal conduit).

The majority of the cables were seven-conductor control cables with a 12 AWG conductor size (7/C-12AWG). The exceptions are the Kerite cables, the armored cable, and the Japanese cable. The Japanese cable is described in Section 3.4.2. The Kerite cables are described in Section 3.4.3. Table 3-2 provides a complete listing of cables tested in DESIREE-Fire.

3.4.2 The Japan Nuclear Safety Organization (JNES) Cable

As part of NRC-Res international collaboration, cable samples provided by JNES were tested as part of the DESIREE-Fire Project. This cable was tested in three Penlight tests and one early limited-scope intermediate-scale test. These particular tests were not included in the original test planning but were conducted at the request of the NRC staff in response to interest expressed by JNES in the work being conducted. At the request of JNES, the cable manufacturer and details of the cable construction are being withheld as proprietary information.

However, JNES did give the NRC and SNL permission to include the test results and a general description of the cable in the DESIREE-Fire report. Hence, the cables are included in the treatment of test data.

The JNES cable was a six-conductor, control-type, metric-specification cable with a 2 mm^2 (0.003 $in^{2)}$ conductor cross section (roughly equivalent to 14AWG). The insulation and jacket were both TS-type materials (i.e., they showed no melting behavior) but the exact material type is unknown. The cable included a spiral-wound copper shield wrap approximately 0.23mm (0.009 in) thick. Both inside and outside this shield wrap was a counter-wrapped thin natural fiber fabric strip (e.g., a cotton canvas type material). Additional filler materials at the center of the cable appeared to be natural fiber (e.g., jute). During testing the copper shield wrap was grounded. The three Penlight tests were run with dc-powered circuits (two with the breaker and one with the MOV circuits) and the one intermediate-scale test used three of the four ac-powered SCDUs.

Table 3-2 DESIREE-Fire cable list.

Cable Function	Insulation and Jacket Materials (I/J)	Material Type (2)	Conductor Size (AWG)	Number of Conductors	Manufacturer	Notes (3)
Control	**XLPE/CSPE**	**TS/TS**	**12**	**7**	Rockbestos-Surprenant	The XLPE cables were from the Firewall III product line, a nuclear-qualified cable brand, but equipment qualification certificates were not requested
Control	XLPO/XLPO	TS/TS	12	7		Industrial-grade cable
Control	SR/Aramid Braid	TS/TS	12	7	First Capital	Industrial-grade cable from a sister company to Rockbestos Surprenant
Control	Tefzel/Tefzel	TP/TP	12	7	Cable USA	Special-order cable with Tefzel-280 insulation and Tefzel-200 jacket
Control	**EPR/CSPE**	**TS/TS**	**12**	**7**	General Cable	Industrial-grade cable
Control	**PE/PVC**	**TP/TP**	**12**	**7**		Industrial-grade cable
Control	PVC/PVC	TP/TP	12	7		Industrial-grade cable
Control	Kerite® FR/ Kerite® FR (with zinc wrap)	Uncert.	12	5	Kerite®	Provided by EPRI 40 mils FR insulation 65 mils FR jacket OD ~1.9 cm (0.74 in) (max)
Control	Kerite® FR/ Kerite® FR (with zinc wrap)	Uncert.	12	10	Kerite®	Provided by EPRI 40 mils FR insulation 80 mils FR jacket OD ~2.69 cm (1.06 in) (max)
Light Power	Kerite® HTK/ Kerite® FR	Uncert.	6	3	Kerite®	Provided by EPRI 55 mils HT insulation 65 mils FR jacket OD ~2.2 cm (0.87 in) (max)
Control	Kerite® FR/ Kerite® FR (with zinc wrap)	Uncert.	12	15	Kerite®	Provided by EPRI 60 mils FR insulation 80 mils FR jacket OD ~3.02 cm (1.19 in) (max)

Table 3-2 DESIREE-Fire cable list (continued).

Cable Function	Insulation and Jacket Materials (I/J)	Material Type (2)	Conductor Size (AWG)	Number of Conductors	Manufacturer	Notes (3)
Control	Kerite® FR/ Kerite® FR	Uncert.	14	9	Kerite®	Provided by EPRI 50 mils FR insulation 65 mils FR jacket OD ~2.16 cm (0.85 in) (max)
Control	Kerite® FR/ Kerite® FR (with zinc wrap)	Uncert.	12	7	Kerite®	Provided by EPRI 40 mils FR insulation 65 mils FR jacket OD ~2.03 cm (0.80 in) (max)
Control	Kerite® FR/ Kerite® FR-III	Uncert.	12	12	Kerite®	Provided by EPRI 60 mils FR insulation 80 mils FR jacket OD ~2.39 cm (0.94 in) (max)
Control	Kerite® FR/ Kerite® FR-II	Uncert.	16	10	Kerite®	Provided by EPRI 50 mils FR insulation 80 mils FR jacket OD ~2.16 cm (0.85 in) (max)
Control	Armored XLPE/PVC	TS/TP	12	8	General Cable	Provided by EPRI
Control	Proprietary	TS/TS	2 mm^2	6	Proprietary (Japan)	Special heat-resistance insulation with radioactive shielding for control, and flame-retardant low hydrochloric acid and special heat-resistance vinyl sheath provided by JNES (Japan) (Note 4)

Additional Notes:

Bold text indicates the "core" program cables; that is, the cables used in the majority of tests.

(1) XLPE = Cross-linked polyethylene; CSPE = Chlorosulfunated polyethylene (also known as Hypalon); XLPO = Cross-linked polyolefin; SR = Silicone rubber; EPR = Ethylene propylene rubber; PVC = Polyvinyl chloride;
PE = Polyethylene (non-cross-linked).

(2) TS = Thermoset; TP = Thermoplastic; shown as: (insulation type)/(jacket type).

(3) All cables are unshielded and unarmored unless specifically stated.

(4) The JNES cable is a metric specification cable. A conductor cross section of 2 mm^2 is roughly equivalent to a 14 AWG conductor.

(5) "Uncert." stands for uncertain.

4. DIAGNOSTIC INSTRUMENTATION SUMMARY

4.1 dc-Powered Test Circuits

The primary focus of this project was on cable failure modes and effects testing for dc-control circuits. Hence, the core of the experimental diagnostic instrumentation was a set of dc-powered control circuit simulators. This section (and its subsections) provides summary descriptions of the dc test circuits and the battery set used to supply power to them during testing. More complete descriptions of the dc-powered test circuits are provided in Appendices A.1 through A.5. Appendix A.7 covers the battery bank.

4.1.1 The dc Battery Bank

The design of the battery bank evolved substantially through the course of the test planning process. The preliminary planning assumed an approach similar to that employed by Duke Energy in its dc tests (2006); namely, use of ten 12V dc deep-cycle automotive batteries connected in series. However, the EPRI collaborative team expressed concern that the automotive batteries would not supply nearly the same short-circuit fault currents that could be generated by an actual set of station batteries. The lower fault current potential was thought to have adversely impacted the Duke Energy tests and it was decided to pursue a more representative battery set if at all possible. In the end, EPRI identified and made available a more representative set of batteries for use in testing.

The battery set made available by EPRI was comprised of 68 Exide model ES-13 calcium flat-plate, lead/acid battery cells that were being taken out of service from the North Anna Nuclear Station technical support center (TSC). The batteries had reached their nominal end of life and were being replaced as a matter of preventative maintenance. The old cells, which were still in serviceable condition, were transported to SNL for use in this test project. All of the cells were tested for serviceability by an independent electrical contractor before receipt at SNL and all the cells used in the program were certified as fully functional in accordance with IEEE Standard 450-2002 *IEEE Recommended Practice for Maintenance, Testing, and Replacement of Vented Lead-Acid Batteries for Stationary Applications* [10].

The battery bank needed to provide a nominal 125Vdc power output, this having been identified by the industry representatives as typical of the dc-control circuit power supplies used in U.S. NPPs. Hence, a total of 60 battery cells were used to construct the battery bank (detailed cell specifications are provided in Appendix A.7). For a sense of scale, each individual cell weighed about 36.7kg (81lb), and together the 60-cell battery bank weighed approximately 2200kg (4860lb). The batteries were housed within a 9.5m- (20ft-) long portable transportainer providing a temperature-controlled environment. The remaining eight cells were retained as replacement spares but were not used in testing because no cell failures occurred over the course of the tests.

The completed battery bank provided an estimated short-circuit output current at the main terminals of over 13,000A. The collaborative partners and the NRC agreed that, while a true station battery set might provide roughly twice that fault current at the battery terminals, the set used was sufficient to meet the needs of testing and that the fault current available to the test circuits could be matched to typical installed end devices through proper sizing of the power supply lead cables. That is, the program used specified lengths of relatively large power cables to supply the individual test circuits (i.e., to connect the battery bank to the dc-SIM panels) so as

to match the available fault current desired by controlling the impedance of the lead cables. Specific guidance regarding lead cable sizing was provided by the EPRI team and was implemented by SNL. Details on the cable dimensions for all of the lead cables used in testing is provided in Appendix A.

The power supply system also included a manually initiated, automatic charging system able to provide both refresh charging and float charging to the battery bank. The charging system was isolated from the battery bank during testing. The batteries were charged regularly throughout the course of the testing program.

Also note that a ground fault detection circuit was provided to detect conductor-to-ground faults that occurred during testing which resulted in grounding of either the positive or negative side of the battery bank. The ground fault circuit is described in Appendix A.7.

4.1.2 The dc Test Circuits

For testing, a total of eight individual dc-powered test circuits were developed. Appendices A.1 through A.5 provide detailed descriptions of these test circuits. The basic circuit diagrams for each circuit as implemented in the testing are also presented. For convenience of reference, six circuit diagrams (Figure 4-1 through Figure 4-6) which reflect the eight different dc-powered circuits are presented collectively at the end of Section 0 (along with the circuit diagram for the ac-powered SCDU, Figure 4-7). The dc test circuits are summarized below.

MOV-1 and MOV-2:
Two separate dc-powered MOV circuits were used in testing. They are referred to as MOV-1 and MOV-2 in the balance of this report.[8] Each MOV circuit was comprised of a matched pair of Joslyn-Clark-brand dc motor control contactors that were electrically and mechanically interlocked. One contactor is designated as the “open” contactor and the second as the “close” contactor (i.e., the contactors that, if energized, would cause the valve to open or close, respectively). The MOV circuit diagram is shown in Figure 4-1. Additional details for this circuit including full circuit and block diagrams are provided in Appendix A.1.

- Note that during post-test evaluation of the test circuits it was discovered that one of the four individual contactors (the MOV-2 close contactor) was incomplete and non-functional. On disassembly, it was discovered that the unit as supplied by the manufacturer was lacking the “moving core” element of the contactor. This is the metal core attached to the moving parts of the contactor that is drawn down when the fixed core coil is energized, causing the contactor to close the main contact sets. Because the moving core was missing, this particular contactor was a passive (or inactive) target. That is, the contactor’s magnetic coil was in place and would represent an inductive load on the circuit just as a fully functional contactor unit would. However, given a hot-short impacting the associated cable conductor, even if energized at full voltage the contactor would not close. This also means that neither the mechanical or electrical interlocks would be engaged, leaving the open contactor as an active target. The full implications of this test anomaly are covered in Appendix A.1. Data analysis has considered the as-operated circuit. The MOV-1 circuit operated as designed.

[8] The reader should note that the dc-powered MOV circuits are consistently referred to as MOV1 and MOV2. As discussed in Section 4.2, testing also involved a set of ac-powered MOV circuits, which are uniformly referred to as the SCDU circuits or as SCDU1 through SCDU4. This convention is maintained throughout the report whenever the various test circuits are discussed.

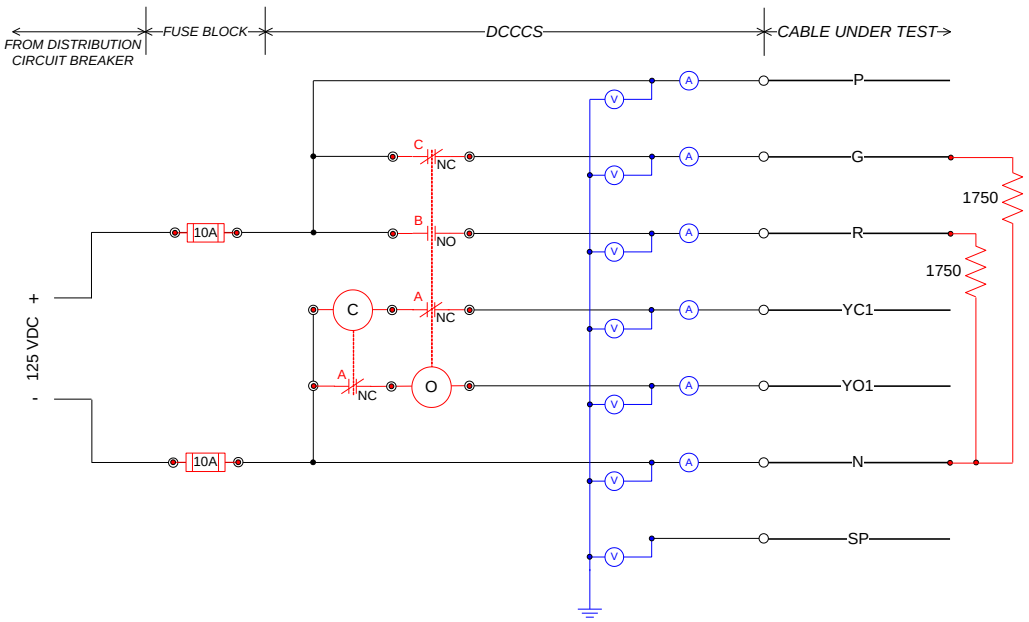

Figure 4-1 The dc test circuit diagram for MOV-1 and MOV-2

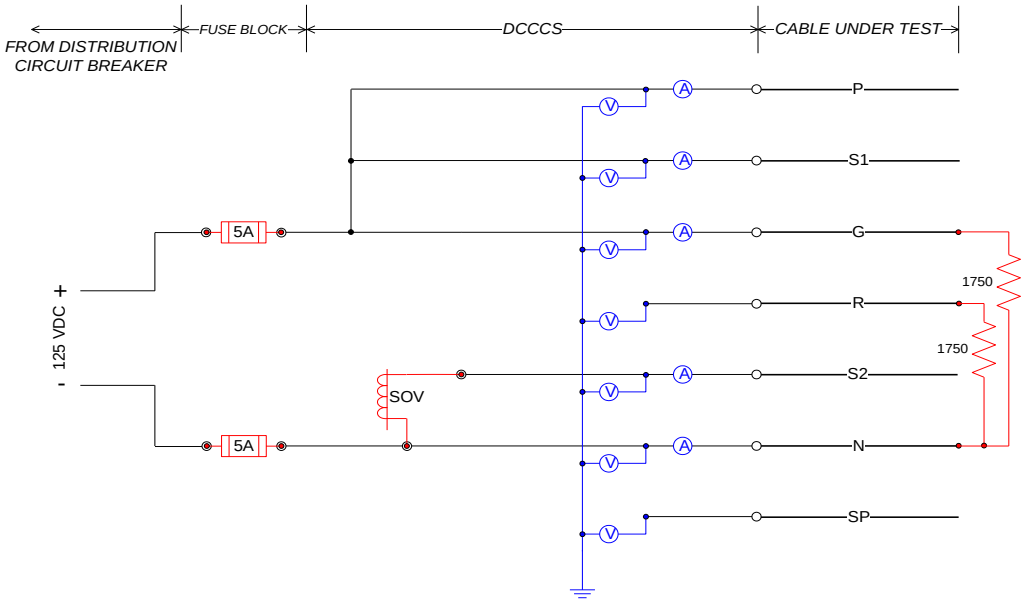

Figure 4-2 The dc test circuit diagram for SOV-1 and SOV-2

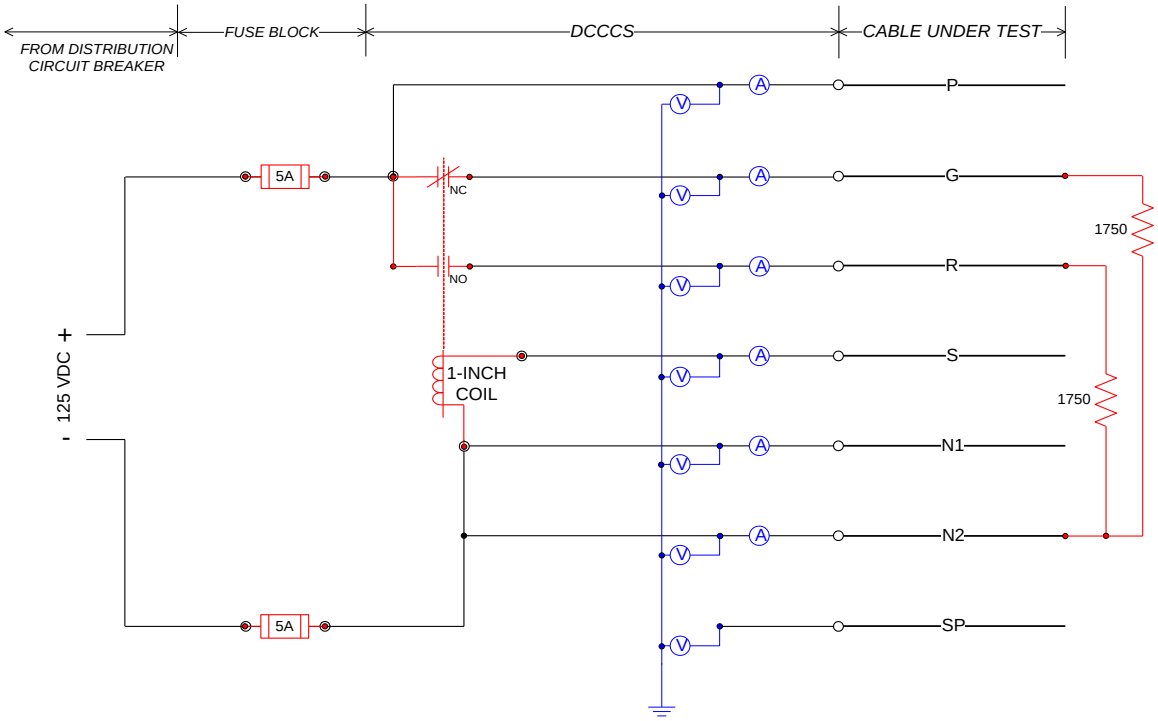

Figure 4-3 The dc test circuit diagram for the 1-in. SOV

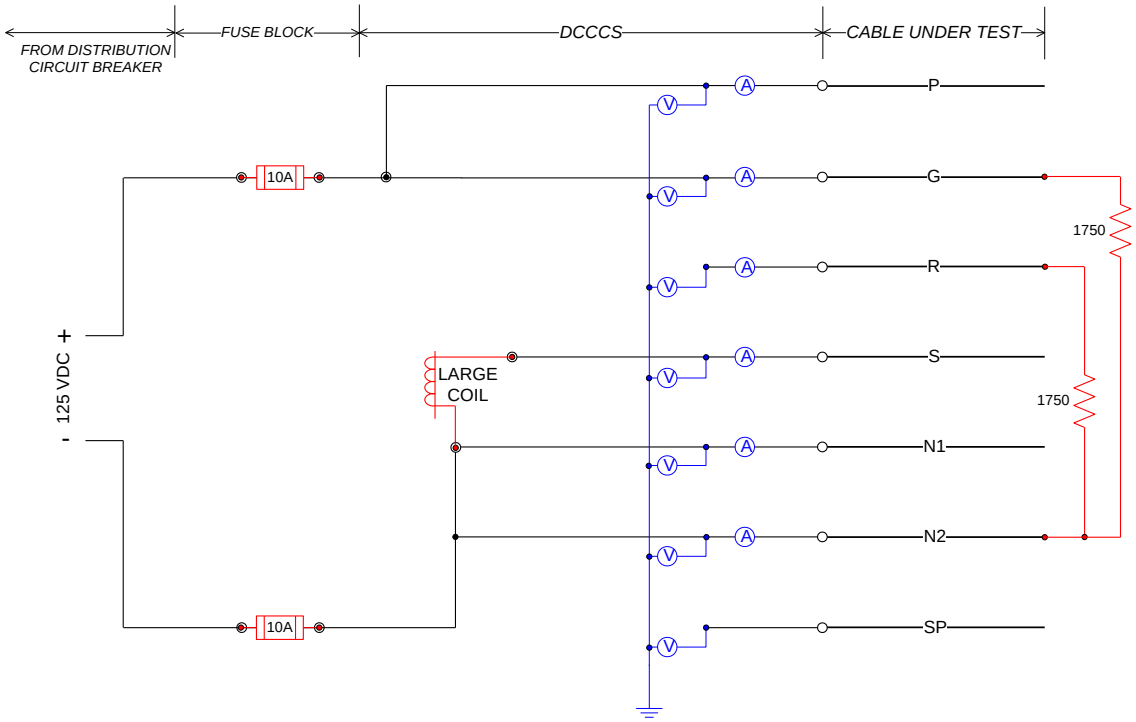

Figure 4-4 The dc test circuit diagram for the large coil

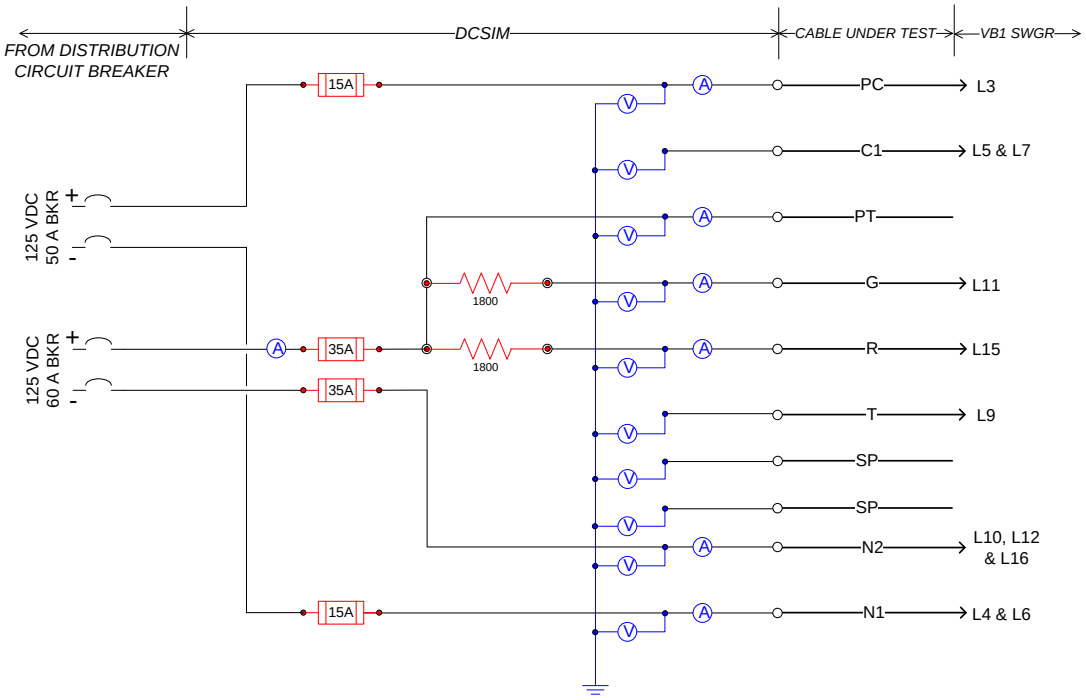

Figure 4-5 The dc test circuit diagram for the switchgear (including both the trip and close circuits)

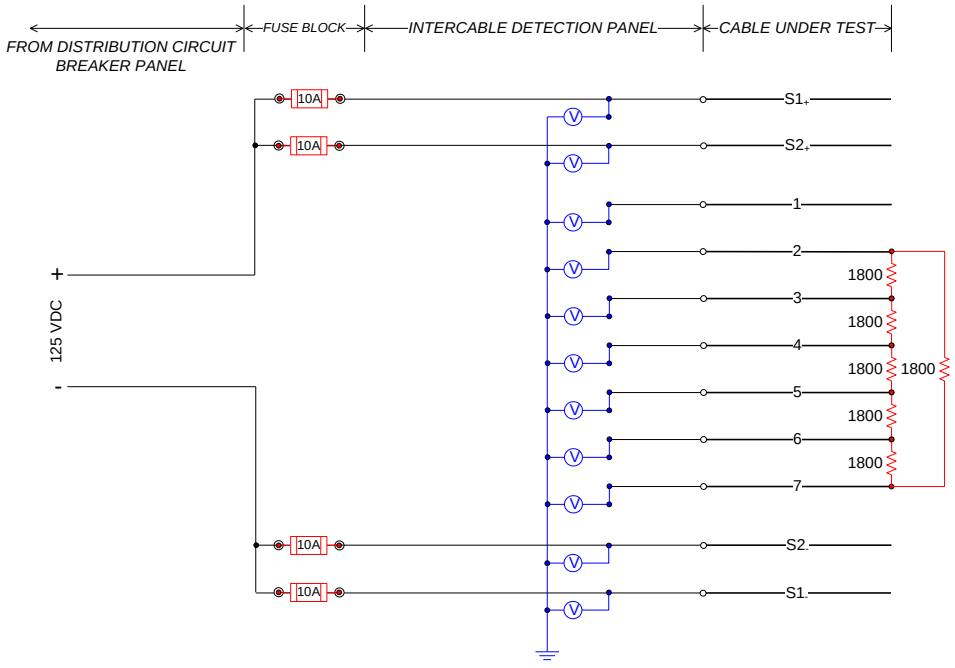

Figure 4-6 Circuit diagram for the intercable shorting circuit

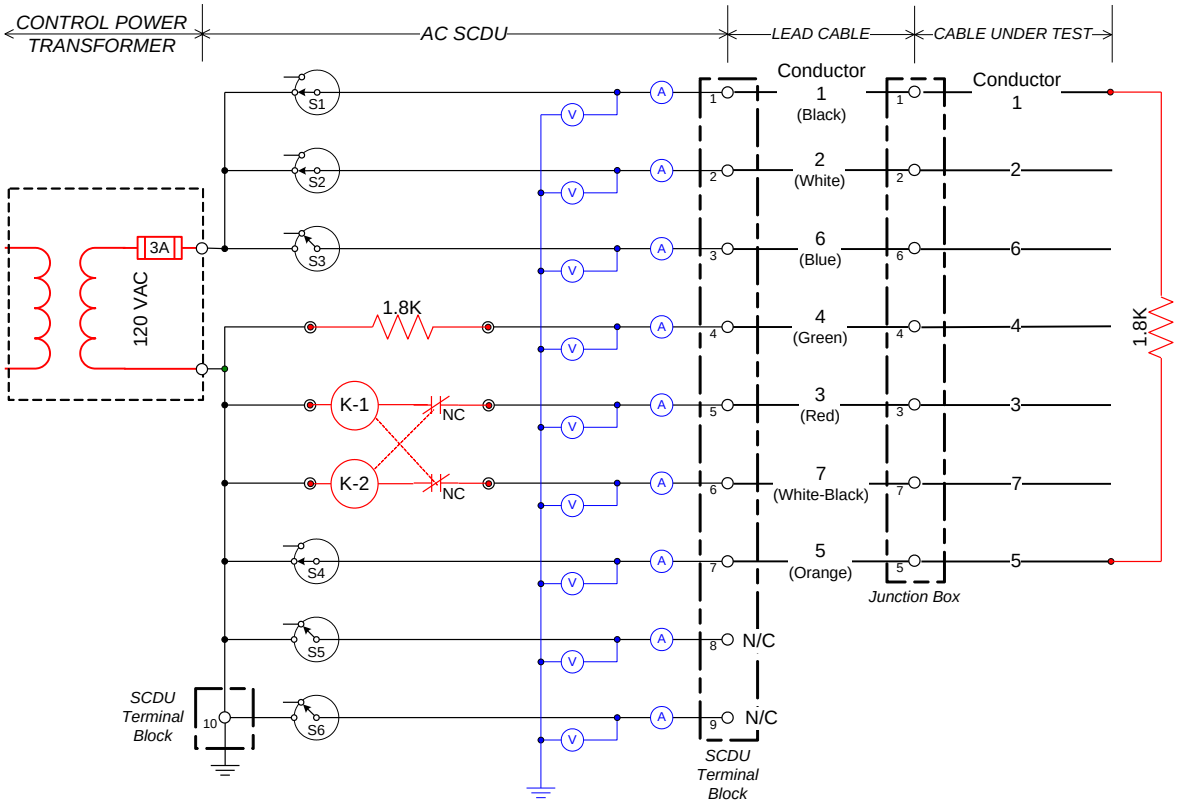

Figure 4-7 Circuit diagram for the SCDU as modified for use in DESIREE-Fire including an active electrical interlock on the contactor pair (K-1 and K-2)

SOV1 and SOV2:

Two separate small SOV circuits were also used in testing (referred to as SOV-1 and SOV-2). The two circuits each include a working solenoid valve of the type commonly used as a pilot control valve, for example, for a larger air-operated valve (AOV). The two valve circuits differed in that one circuit, SOV-2, used a continuous duty "Class H" coil. Based on the manufacturer's literature, the Class H coils will accommodate continuous duty over a wider voltage range; namely, 12% over normal and 28% under normal rated coil voltage. For a nominal 125Vdc coil, this translates to a voltage range of 90 to 180Vdc. The SOV circuit diagram is shown in Figure 4-2. Additional details for this circuit are provided in Appendix A.2.

1-Inch Valve:

One test circuit was built around a relatively large 25mm (1-in.) SOV that was provided by the Target Rock Corporation through the NRC-RES/EPRI collaboration. This was a normally open solenoid valve. The size (1-in.) refers to the nominal inlet and outlet pipe diameter. This was a fully functional valve and was similar to the type of valve that would be used as a head vent valve or in other safety relief applications (but smaller than a typical PORV). The valve assembly included open and close indicator switches that were wired into the valve circuit. The 1-in. valve circuit diagram is shown in Figure 4-3. Additional details for this circuit are provided in Appendix A.3.

- Note that during the course of testing both of the position indicator switches failed closed (first one and later the second). The switches are sealed magnetically activated reed switches and have not been disassembled as a part of postmortem equipment examination. It is suspected that faults propagating through those particular circuit paths may have caused arcing across the switch contact and likely caused the contacts to weld closed. Details on when the failures occurred, the tests impacted by the failures, and the implications for data processing are included in Appendix A.3.

Large Coil:

One circuit was built around the coil assembly for a large, direct-acting SOV. In this case only the coil assembly itself was available (no valve mechanical elements present). Hence, the coil acted as a passive target for HSs. For a sense of scale, the coil assembly itself had a core diameter of approximately 200mm (8-in.) and weighed approximately 114kg (250lb). This coil was also provided by the Target Rock Corporation via the NRC-RES/EPRI collaboration. Originally, one goal of the program was to include a representative PORV valve in the testing program, but a suitable valve was unable to be located. When this valve coil became available, it was decided to include it in the testing program even though it was much larger than a typical PORV would be. Between the 1-in. valve and the large coil, the test circuits are assumed to bound a typical PORV. The large coil circuit diagram is shown in Figure 4-4. Additional details on this circuit are provided in Appendix A.3.

Switchgear:

One test circuit was built around an actual switchgear breaker unit. The units used were fully functional and would open (trip) and close in accordance with the control signals they received. During the course of one particular test, failure of the test cable induced fault currents within the switchgear unit itself that exceeded the ampacity of the 14AWG internal control wiring. This severely damaged the internal unit wiring. The damaged unit was repaired, but was also replaced by a second switchgear unit with more robust internal wiring. The switchgear circuit diagram is shown in Figure 4-5. Appendix A.4 provides a detailed description of both switchgear circuits including a description of the faults that damaged the first unit.

- Note that, as shown at the extreme left of Figure 4-5, the switchgear's trip and close circuits were powered through separate circuit breakers in the dc battery bank power distribution system. This is not typical of in-plant practice, but has no effect on circuit performance. None of the circuit breakers (for any test circuit) ever tripped during testing. Primary circuit protection is provided by the 15A and 35A fuses, also shown in the schematic, and the up-stream circuit breakers were installed as a personnel safety measure (e.g., allowing for individual test circuits to be isolated at the power source). Appendix A.7 provides additional detail on the power distribution system.

Intercable Test Circuit:

The last dc-powered circuit was not designed to mimic any particular control circuit, but rather was designed to monitor for the occurrence of intercable HSs. In particular, there was an interest expressed by the peer team to determine if testing could detect occurrence of the so-called "intercable smart dc hot short"; that is, a short between a target cable and one or more source cables that would result in at least one conductor in the target cable being energized to the positive battery potential and a second conductor in the same target cable being energized

to the negative battery potential. This shorting configuration is the only cable failure mode that can induce spurious operation in certain types of dc circuits.

The intercable test circuit provided for up to two (separately monitored) battery positive source cables/paths, two battery negative source cables/paths, and for a target cable of up to seven conductors. A circuit diagram is shown in Figure 4-6. Conductors 1-7 in this diagram represent the target cable and are generally referred to as T1-T7 in this report. T1 is the conductor at the center of the target cable. In this figure, the source cables/paths are shown as S1+, S2+, S1-, and S2- and the target cable is represented by circuit paths 1 through 7. In the report, these target conductors are typically referred to as T1-T7 and conductor T1 was connected to the center conductor within the target cable.

Each of the six conductors in the outer ring of the target cable (conductors T2-T7) are connected to its two nearest neighbors through 1.8-kΩ resistors (the center conductor is excluded from the resistor network). As a result, conductors T2-T7 will act as a voltage-divider circuit should a smart dc HS form. That is, energizing one conductor (or group of conductors) to the positive battery potential and a second conductor (or group of conductors) to the negative battery potential would result in a voltage cascade from positive to negative across the remaining conductors. This behavior is described in greater detail in Appendix A.5, including illustrative examples. The result of primary interest for this circuit is whether or not such a voltage cascade formed during any given test.

The physical configuration used in testing prevented ground interactions and interactions with the other test circuits. The test cables were placed on an insulating board isolating them from the grounded raceway. The intercable circuit was not co-located with any of the other test circuits, preventing circuit-to-circuit interactions, except to the extent a ground fault in any of the dc-powered circuits will shift the measurement reference potential (i.e., the ground potential relative to battery positive and negative) for all of the dc-powered circuits including the intercable circuit. The test configuration did allow for either hot-short interactions between the source and target cables or fuse blow (FB) failures given interactions between the positive-source cables and the negative-source cables.

The test configuration was not intended to represent any anticipated in-plant conditions. Rather, it was designed to optimize the potential for, and detect, smart dc HSs. The intent is that given that the tests “stacked the deck” in favor of smart dc HS formation, should no such short circuits be observed, this could be taken as evidence that this is a low likelihood failure mode. Overall, caution must be taken in extrapolating from this test circuit to real-life conditions.

4.1.3 Current Transducers

A note needs to be made regarding the current transducers used for monitoring the dc-powered test circuits. The issues identified relative to these transducers are covered in detail in Appendix A.8. The intent here is to summarize the identified issues and the measures taken to address them.

The current transducers used in the dc test circuits were Hall-effect current probes. Hall-effect probes were selected mainly because they are non-intrusive. Duke Energy had used current shunts in its testing. Shunts are low-resistance devices inserted into a circuit path that induce a small voltage drop proportional to current flow. Measuring the voltage drop provides a corresponding current flow. In the Duke Energy tests these shunts proved problematic, in some cases failing due to sustained short-circuit currents. The EPRI collaborative peer team also

expressed concern that the presence of shunts in the various circuit paths could act to limit short-circuit currents, potentially compromising or altering the fuse-blow behavior for the circuits.

Over the course of testing, three issues impacting these transducers were identified as follows:

- **Zero-point drift:** While reviewing data from early tests, it was noted that the zero-point offset (i.e., the transducer output at zero current flow) would drift between the beginning and the end of a given test, and between the end of one test and the beginning of the next test. Discussion with the supplier revealed that dc current flows through the pick-up coils would induce a certain degree of residual magnetism that would be reflected as a non-zero signal output. For ac circuits this effect is self-correcting due to the zero-crossing nature of the power signal, but for dc circuits the lack of a zero-crossing behavior (see Section 2.1 above) means the effect is not self-canceling. The magnetism will fade over time but is an inevitable aspect of the devices when used for dc circuits. This issue was discussed extensively among the peer team and was ultimately addressed through modifications of the testing protocol and during post-test data analysis. The processed data was corrected to reflect the true zero-point offset of each individual current transducer at the beginning of each test, but because the zero-point offset drifts over the course of a given test, the data plots will typically show a slight non-zero current flow at the end of a test when the actual current flows are zero (e.g., fuses have blown and a circuit is deenergized).
- **Transducer sensitivity:** The transducers selected were relatively high range (e.g., +/- 35A or higher) because the peer team wanted to capture the higher short-circuit currents that would be acting to clear circuit fuses. The early tests revealed that this rendered the transducers relatively insensitive to the lower current signals (e.g., those associated with spurious operations, nominally 1A or less) especially given general low-level noise in the data and the zero-point offset issue discussed immediately above. This issue was addressed by amplifying the current signals by making multiple conductor passes through the pick-up coils. This resulted in a corresponding reduction in the maximum range of the transducers (e.g., a +/- 35A transducer becomes a +/- 7A transducer given five loops of the conductor through the pick-up coil). Once the loops were made, the effective range is reduced and current increases above 7A would be reflected as transducer saturation. Reducing the upper limit of the current transducer was an acceptable sacrifice to the peer review committee. The processed data files and all of the plots presented in this report have been corrected for the amplification effect and show the actual (corrected) current values.
- **High-current transducers insensitive to transient behavior:** Each of the main power supply conductors (i.e., between the battery bank and each of the test circuits) were equipped with both lower-range (+/- 35A) and high-range (+/- 500A) current transducers. Despite numerous efforts to address this problem, the high-range current transducers provided little or no data of value. While installation and operability of the transducers was verified (repeatedly) and high-speed data logging was attempted (i.e., at as high as 100 Hz), the 500A transducers were simply not capturing meaningful data signals from the transient short circuits observed. The root cause of this issue has not been traced.

4.2 ac-Powered Test Circuits

DESIREE-Fire included limited testing with the ac-powered SCDU circuits originally designed and built for use in the CAROLFIRE project. The SCDU circuits were nominally designed to

simulate the behavior of a typical ac-powered reversing MOV control circuit. A total of four units were constructed, each representing one complete MOV control circuit.

One issue that had not been fully addressed under CAROLFIRE was that of saturation of the CPTs and degradation of the available voltage to the point where a SA of the contactors was no longer possible. That is, in the EPRI/NEI tests of 2001, multiple leakage current paths led to current draws that exceeded the capacity of the CPTs. CPT voltage output in some EPRI/NEI tests was degraded below the pick-up voltage of the motor control contactors so that even when a HS occurred the contactors did not close. This effect was not observed in any of the CAROLFIRE tests, but one factor that was thought to have influenced the CAROLFIRE results was that the motor control contactors used in CAROLFIRE required far less than the nominal (advertised) power draw for the contactors. A secondary objective for DESIREE-Fire was to re-investigate this aspect of the shorting behavior.

The SCDU motor control contactors were all replaced with contactors identical to those used in the original EPRI/NEI tests.[9] Two of the contactor sets were obtained via the EPRI collaboration and were the units used by Duke Energy in its 2006 testing. Two additional contactor sets were obtained directly from Joslyn-Clark Controls. In addition, the four SCDU units each used a different size CPT; namely, a 75VA for SCDU-4, 100VA for SCDU-1, 150VA for SCDU-2, and 200VA for SCDU-3.

The CAROLFIRE project report [1] and Appendix A.6 provide more detailed descriptions of the SCDU circuits. Appendix A.6 includes a description of the system modifications implemented for DESIREE-Fire. The general circuit schematic for the SCDU is illustrated in Figure 4-7, which, for convenience of reference, is presented along with the dc-powered circuit diagrams at the end of Section 0.

4.3 Other General Instrumentation

The other primary instrumentation utilized in testing was associated with the monitoring of various temperatures. In all cases, temperatures were monitored using Type-K thermocouples. All of the temperature monitoring was performed using calibrated data logging systems and the thermocouples used are batch calibrated. That is, not every thermocouple in a given batch is calibrated because the calibration process itself drives a thermocouple to its performance limits, which can actually alter its calibration. Instead, select samples for any given batch of thermocouples are run through the full calibration process, and, provided no anomalies are identified, the entire batch is considered calibrated. The actual thermocouples used in the calibration process are discarded.

Typical temperature monitoring during the small-scale Penlight tests focused on the Penlight shroud temperature and sub-jacket temperatures for the thermal response sample cables. The intermediate-scale tests included both cable thermal response sample monitoring and the monitoring of the exposure environment (air temperatures) directly above and below the tested cables. The DESIREE-Fire approach temperature monitoring is essentially identical to that described in the CAROLFIRE test report. The major difference is that DESIREE-Fire took a somewhat more minimalistic approach because most of the cables tested in DESIREE-Fire had

[9] Note that at the time of the EPRI/NEI tests the manufacturer of the contactor sets was AO Smith, Clark Controls Division. AO Smith subsequently merged with Joslyn Manufacturing Corp. to become Joslyn-Clark Controls. The same AO Smith model NEMA-1 motor control contactor sets as used by EPRI/NEI and with the exact same model designation (#30U31) remain available through Joslyn-Clark Controls.

already been through extensive testing in CAROLFIRE and there was little need for additional thermal response data for those cables. For those cables that had not been tested before (the Kerite cables, armored cables and the Japanese cable) a somewhat more aggressive approach to cable thermal response measurements was taken (more thermal response cable samples and more thermocouples per sample).

The main objective for DESIREE-Fire relative to cable thermal response was to assess whether the dc-powered circuits experienced faults at substantially different cable temperatures than did the ac-powered circuits from CAROLFIRE. The testing revealed no substantive differences in this regard between the ac and dc circuits.

Beyond the temperature monitoring, the only other data system used was the fuel flow controller for the intermediate-scale gas burner test. Again, the test setup and equipment was the exact same equipment as was used in CAROLFIRE. As in CAROLFIRE, the gas burner flow was set and recorded manually. Flow recording is documented in the test engineer's field notes.

Appendix A.8 provides a more complete description of the various test support systems used in DESIREE-Fire. This includes descriptions of the data logging systems and data analysis processes. Appendix A.8 also describes the content and structure of the processed data files included on the CD provided with this report.

5. TEST MATRICES

Table 5-1 presents the matrix of small-scale Penlight tests performed. Table 5-2 provides the corresponding matrix of intermediate-scale tests. In these two tables the tests are arranged by test number. However, the tests were not performed sequentially in the same order as would be indicated by the test number. Hence, for convenience, Table 5-3 provides an alternate listing of both the Penlight and intermediate-scale tests arranged by the order in which tests were actually performed (i.e., by the date and time of each test). Table 5-3 also provides general comments relating to test anomalies, changes in the test configurations, or changes in the test protocols implemented during the course of testing. Changes in the test circuit configurations or test protocols, in particular, will impact all of the subsequent tests performed.

Note, again, that for both the Penlight and intermediate-scale tests the intent was to mirror as closely as possible the test conditions from the CAROLFIRE project. The intent was to ensure that the results of the DESIREE-Fire tests could be compared directly to those from CAROLFIRE.

In the case of the Penlight tests, the layout of cables, cable types, and exposure temperatures are all quite similar to those used in CAROLFIRE. In the case of the intermediate-scale tests the cable types, cable raceway locations, and gas burner flow rate (heat release rate) settings also mirrored those applied in CAROLFIRE. The primary difference in this regard is that DESIREE-Fire placed no particular emphasis on gathering additional data for use in fire model validation studies, the CAROLFIRE project having provided a wealth of such data. That is, DESIREE-Fire gathered basic cable response and thermal environment temperature data, especially when a cable type not used in CAROLFIRE was being tested (i.e., the Kerite®, JNES, and armored cables), but to a far less extent than did CAROLFIRE. Instead, for DESIREE-Fire resources were focused on providing a wider range, and greater number, of test circuits. This is reflected, for example in the Penlight tests, by DESIREE-Fire's focus on the simple single-cable test configurations as compared to CAROLFIRE, which involved more tests with various cable bundles.

In effect, the same test protocols that were developed as a part of CAROLFIRE were applied in DESIREE-Fire for both test scales. The only significant differences relative to how each test was conducted were those relative to the dc-powered circuits and power supply system. These aspects of the test protocol were mainly associated with ensuring personnel safety during all aspects of testing (e.g., lock-out work procedures) and have no impact on the test conditions seen by the sample cables.

Table 5-1 The DESIREE-Fire small-scale Penlight test matrix.

Burn Test #	Cable Insulation Material										Exposure shroud temperature (C)	Raceway type		Cable Diagnostic System						Date Completed
	Thermosets							Thermoplastics												
	XLPE / CSPE	EPR	SR	Kerite® FR with zinc wrap	Kerite® FR without zinc wrap	Kerite® HTK	Armored	Tefzel	PE / PVC	PVC / PVC		Tray	Conduit	SCDU	SOV1 and SOV2	15-kV Breaker	Large Coil and 1 in. SOV	MOV1 and MOV2	Intercable	
Pre-1 (P)	X										470	X		X						14-Jul-09
Pre-2 (P)	X										470	X		X						14-Jul-09
Pre-3 (P)									X		325	X		X						13-Jul-09
Pre-4 (P)									X		325	X		X						13-Jul-09
1	X										470	X			X					15-Jul-09
2	X										470	X			X					17-Jul-09
3	X										470	X				X				21-Jul-09
4	X										470	X				X				30-Jul-09
5	X										470	X					X			22-Jul-09
6	X										470	X					X			22-Jul-09
7	X										470	X						X		20-Jul-09
8	X										470	X						X		20-Jul-09
9									X		325	X			X					17-Jul-09
10									X		325	X				X				21-Jul-09
11									X		325	X					X			22-Jul-09
12									X		325	X						X		12-Aug-09

Table 5-1 The DESIREE-Fire small-scale Penlight test matrix (continued).

Burn Test #	Cable Insulation Material										Exposure shroud temperature (C)	Raceway type		Cable Diagnostic System						Date Completed
	Thermosets							Thermoplastics												
	XLPE / CSPE	EPR	SR	Kerite® FR with zinc wrap	Kerite® FR without zinc wrap	Kerite® HTK	Armored	Tefzel	PE / PVC	PVC / PVC		Tray	Conduit	SCDU	SOV1 and SOV2	15-kV Breaker	Large Coil and 1-in. SOV	MOV1 and MOV2	Intercable	
13_qual				X							Vary	X		X						26-Jul-09
13				X							350	X		X						27-Jul-09
14				X							450	X		X						28-Jul-09
15				X							300	X		X						28-Jul-09
16				X							470	X		X						28-Jul-09
17_qual						X					Vary	X		X						30-Jul-09
17						X					430	X		X						31-Jul-09
18						X					420	X		X						31-Jul-09
19							X				470	X		X						10-Aug-09
20							X				470	X			X					11-Aug-09
21							X				470	X				X				28-Sep-09
22							X				470	X						X		13-Aug-09
23		X									470	X			X					16-Jul-09
24		X									470	X				X				29-Jul-09
25		X									470	X						X		16-Jul-09
26			X								700	X			X					23-Jul-09
27			X								700	X						X		12-Aug-09
28								X			325	X			X					10-Aug-09

Table 5-1 The DESIREE-Fire small-scale Penlight test matrix (continued).

Burn Test #	Cable Insulation Material										Exposure shroud temperature (C)	Raceway type		Cable Diagnostic System						Date Completed
	Thermosets							Thermoplastics												
	XLPE / CSPE	EPR	SR	Kerite® FR with zinc wrap	Kerite® FR without zinc wrap	Kerite® HTK	Armored	Tefzel	PE / PVC	PVC / PVC		Tray	Conduit	SCDU	SOV1 and SOV2	15-kV Breaker	Large Coil and 1-in. SOV	MOV1 and MOV2	Intercable	
29								X			vary	X				X				29-Jul-09
30								X			325	X						X		13-Aug-09
31										X	325	X			X					17-Jul-09
32										X	325	X				X				24-Sep-09
33										X	325	X						X		12-Aug-09
34	X										525		X		X					11-Aug-09
35	X										525		X			X				25-Sep-09
36	X										525		X				X			12-Aug-09
37	X										525		X					X		23-Sep-09
38									X		450		X		X					11-Aug-09
39									X		450		X			X				24-Sep-09
40									X		450		X				X			12-Aug-09
41									X		525		X					X		14-Sep-09
42	X										430	X				X				25-Sep-09
43									X		275	X						X		24-Sep-09
44					X						325	X						X		5-Oct-09
45	X										460	X							X	9-Oct-09
46		X									325	X							X	8-Oct-09

Table 5-1 The DESIREE-Fire small-scale Penlight test matrix (continued).

Burn Test #	Cable Insulation Material										Exposure shroud temperature (C)	Raceway type		Cable Diagnostic System						Date Completed
	Thermosets							Thermoplastics												
	XLPE / CSPE	EPR	SR	Kerite® FR with zinc wrap	Kerite® FR without zinc wrap	Kerite® HTK	Armored	Tefzel	PE / PVC	PVC / PVC		Tray	Conduit	SCDU	SOV1 and SOV2	15-kV Breaker	Large Coil and 1-in. SOV	MOV1 and MOV2	Intercable	
47									X		350	X							X	8-Oct-09
48										X	400	X							X	8-Oct-09
49					X						400	X						X		9-Oct-09
50					X						450	X						X		12-Oct-09
JPN-1											325	X				X				15-Sep-09
JPN-2											350	X				X				16-Sep-09
JPN-3											350	X						X		23-Sep-09

Table 5-2 The DESIREE-Fire intermediate-scale test matrix.

Burn Test #	Cable Monitoring Devices	LOCATION	CABLE TYPE									RACE-WAY TYPE		RACEWAY LOADING			Completion Date
			XLPE	EPR	PE	XLPO	TEFZEL	ARMOR	KERITE® FR with zinc wrap	KERITE® FR without zinc wrap	JPN	TRAY	CONDUIT	Circuits Only (No Fill)	Bundled Circuits	Circuits Plus Fill	
JPN 1	SCDU 1	E									X	X		X			16-Sep-09
	SCDU 2	B									X	X		X			
	SCDU 3	A									X	X				X	
Pre-1 (IS)	Fill cable only	A										X					6-Nov-09
	SCDU 3, 4	B	X									X		X			
	Lg Coil, 1" Coil	E	X									X		X			
	Intercable Bundle	D	X									X		X			
	SWGR-C, SWGR-T	B	X									X		X			
Pre-2 (IS)	Fill cable only	B										X					4-Nov-09
	MOV-1, SOV-1	A			X							X		X			
	SCDU 1, 2	D			X							X		X			
	MOV-2, SOV-2	E			X							X		X			
1	Fill cable only	A										X					23-Feb-10
	MOV-1, SOV-1, Lg Coil, 1" Coil	B	X									X	X[1]		X	X	
	Intercable Bundle	C	X									X			X		
	MOV-2, SOV-2, SWGR-C[7], SWGR-T[7]	D	X									X			X		

Table 5-2 The DESIREE-Fire intermediate-scale test matrix (continued).

Burn Test #	Cable Monitoring Devices	LOCATION	CABLE TYPE									RACE-WAY TYPE		RACEWAY LOADING			Completion Date
			XLPE	EPR	PE	XLPO	TEFZEL	ARMOR	KERITE® FR with zinc wrap	KERITE® FR without zinc wrap	JPN	TRAY	CONDUIT	Circuits Only (No Fill)	Bundled Circuits	Circuits Plus Fill	
2	Fill cable only	B										X					2-Dec-09
	MOV-1, SOV-1, Lg Coil, 1" Coil	C	X									X			X		
	Intercable Bundle	D	X									X			X		
	MOV-2, SOV-2	A	X									X				X	
3	No circuits in these positions	C&E															17-Feb-10
	MOV-1, SOV-1, Lg Coil, 1" Coil	D	X									X			X		
	Intercable Bundle	A	X									X				X	
	MOV-2, SOV-2, SWGR-C[7], SWGR-T[7]	B	X									X	X[2]			X	
4	SCDU 1, 2, 3, 4	D	X									X			X		12-Nov-09
	MOV-1, SOV-1, Lg Coil, 1" Coil	A	X									X				X	
	Intercable Bundle	B	X									X				X	
	MOV-2, SOV-2, SWGR-C, SWGR-T	C&E	X									X[3]			X		
5	Fill cable only	A										X					1-Mar-10
	MOV-1, SOV-1, Lg Coil, 1" Coil	B			X							X	X[1]			X	
	Intercable Bundle	C			X							X			X		
	MOV-2, SOV-2, SWGR-C[7], SWGR-T[7]	D			X							X			X		

Table 5-2 The DESIREE-Fire intermediate-scale test matrix (continued).

Burn Test #	Cable Monitoring Devices	LOCATION	CABLE TYPE								RACE-WAY TYPE		RACEWAY LOADING			Completion Date
			XLPE	EPR	PE	XLPO	TEFZEL	ARMOR	KERITE® FR with zinc wrap	KERITE® FR without zinc wrap	JPN	TRAY	CONDUIT	Circuits Only (No Fill)	Bundled Circuits	Circuits Plus Fill	
6	SWGR-C[7], SWGR-T[7]	B			X							X	X[4]			X	3-Mar-10
	MOV-1, SOV-1, Lg Coil, 1" Coil	C			X							X			X		
	Intercable Bundle	D			X							X			X		
	MOV-2, SOV-2	A			X							X				X	
7	No circuits in these positions	C&E															4-Mar-10
	MOV-1, SOV-1, SWGR-C[7], SWGR-T[7]	D			X							X			X		
	Intercable Bundle	A			X							X				X	
	MOV-2, SOV-2, Lg Coil, 1" Coil	B			X							X	X[5]			X	
8	SCDU 1, 2, 3, 4	D			X							X			X		17-Nov-09
	MOV-1, SOV-1, Lg Coil, 1" Coil	A			X							X				X	
	Intercable Bundle	B			X							X				X	
	MOV-2, SOV-2, SWGR-C, SWGR-T	C			X							X			X		
9	Fill cable only	A										X					17-Mar-10
	MOV-1, SOV-1, Lg Coil, 1" Coil	B						X	X	X		X				X	
	Intercable Bundle	C		X								X			X		
	MOV-2, SOV-2, SWGR-C[7], SWGR-T[7]	D						X				X		X			

Table 5-2 The DESIREE-Fire intermediate-scale test matrix (continued).

Burn Test #	Cable Monitoring Devices	LOCATION	CABLE TYPE								RACE-WAY TYPE		RACEWAY LOADING			Completion Date
			XLPE	EPR	PE	XLPO	TEFZEL	ARMOR	KERITE® FR with zinc wrap	KERITE® FR without zinc wrap	JPN	TRAY	CONDUIT	Circuits Only (No Fill)	Bundled Circuits	Circuits Plus Fill	
10	MOV-1, SOV-1	C								X		X			X		25-Mar-10
	Lg Coil, 1" Coil	D							X			X			X		
	Intercable Bundle	A		X								X				X	
	MOV-2, SOV-2, SWGR-C[7], SWGR-T[7]	B							X	X		X				X	
11	SCDU 1, 2, 3	A		X								X				X	25-Nov-09
	MOV-1, SOV-1, Lg Coil, 1" Coil	B		X								X				X	
	Intercable Bundle	C		X								X			X[6]		
	MOV-2, SOV-2	D		X								X			X		
12	SCDU 1, 2, 3	C		X								X			X[6]		20-Nov-09
	MOV-1, SOV-1, Lg Coil, 1" Coil	D		X								X			X		
	Intercable Bundle	A		X								X				X	
	MOV-2, SOV-2	B		X								X				X	
Conting #1	Fill cable only	A										X					26-Mar-10
	SWGR-C[7], SWGR-T[7]	B				X						X		X			
	No circuits in other positions																

Table 5-2 The DESIREE-Fire intermediate-scale test matrix (continued).

Burn Test #	Cable Monitoring Devices	LOCATION	CABLE TYPE									RACE-WAY TYPE		RACEWAY LOADING			Completion Date
			XLPE	EPR	PE	XLPO	TEFZEL	ARMOR	KERITE® FR with zinc wrap	KERITE® FR without zinc wrap	JPN	TRAY	CONDUIT	Circuits Only (No Fill)	Bundled Circuits	Circuits Plus Fill	
Conting #2	Fill cable only	A										X					29-Mar-10
	SWGR-C[7], SWGR-T[7]	B					X					X		X			
	No circuits in other positions																

Notes for Table 5-2:

[1] Location B: MOV and SOV circuits located in conduit without fill cables. Large Coil and 1" Valve located within fill tray.
[2] Location B: MOV-2 and SOV-2 circuits in tray with fill cables. SWGR circuits in conduit without fill cables.
[3] Location C: MOV-2 and SOV-2 circuits bundled in tray. Location E: Both SWGR circuits bundled in tray.
[4] Location B: Fill cables in tray. SWGR-C and SWGR-T in conduit.
[5] Location B: MOV-1 and SOV-1 circuits were tested in the tray. Large Coil and 1" Valve were tested in the conduit.
[6] Location C: Cable Sample connected to the 35-A fuses tested on the side of the tray.
[7] Replacement 4.16 kV GE Breaker

Table 5-3 Chronology of DESIREE-Fire tests (both testing scales).

Date	Test #	Comments including changes to test protocols
Begin Penlight testing 7/13/2009		
7/13/2009	Pre-3 (P)	
7/13/2009	Pre-4 (P)	
7/14/2009	Pre-1 (P)	
7/14/2009	Pre-2 (P)	
7/15/2009	1	
7/16/2009	25	
7/16/2009	23	SOV-2 was intentionally fused at 10A rather than 5A for this test only.
7/17/2009	31	
7/17/2009	9	
7/17/2009	2	
7/20/2009	7	
7/20/2009	8	
7/21/2009	3	
7/21/2009	10	
7/22/2009	5	
7/22/2009	11	
7/22/2009	6	Anomalies detected on R conductor for the 1-in. solenoid; test was still conducted. R conductor acted as a positive source conductor.
7/23/2009	26	
7/26/2009	13_qual	
7/27/2009	13	
7/28/2009	14	
7/28/2009	15	
7/28/2009	16	
7/29/2009	24	Conductors passing through the switchgear CT35 transducers were wrapped around the hall effect device five times. The positive battery lead on the 35A switchgear fuse was wrapped twice around the CT500 hall effect device.
7/29/2009	29	
7/30/2009	4	
7/30/2009	17_qual	
7/31/2009	17	
7/31/2009	18	
8/10/2009	19	
8/10/2009	28	All circuits were rewired to include five turns around the CT35 and two turns around the CT500 transducers.
8/11/2009	20	

Table 5-3 Chronology of DESIREE-Fire tests (both testing scales) (continued).

Date	Test #	Comments including changes to test protocols
8/11/2009	34	
8/11/2009	38	
8/12/2009	36	
8/12/2009	40	
8/12/2009	27	
8/12/2009	33	
8/12/2009	12	Penlight apparatus was not functioning properly and had to be shut down before being turned back on. Upon being turned back on, the circuits were experiencing degradation.
8/13/2009	30	
8/13/2009	22	
9/14/2009	41	
9/15/2009	JPN-1	
9/16/2009	JPN-2 & JPN-(IS)1	On this day, both JPN-2 Penlight and JPN-(IS)1 intermediate-scale were run. This was an early intermediate-scale test. Intermediate-scale testing did not resume until November 4, 2009.
9/23/2009	JPN-3	The electrical interlock on MOV-1 would not fully close, it was adjusted to perform as anticipated. The current transducer monitoring the green indication lamp on MOV-1 was replaced. Loose wiring was tightened.
9/23/2009	37	
9/24/2009	43	
9/24/2009	32	
9/24/2009	39	
9/25/2009	35	
9/25/2009	42	
9/28/2009	21	
10/5/2009	44	
10/8/2009	47	
10/8/2009	48	
10/8/2009	46	
10/9/2009	45	
10/9/2009	49	
10/12/2009	50	
Begin primary matrix of intermediate-scale tests 11/4/2009		
11/4/2009	Pre-2 (IS)	
11/6/2009	Pre-1 (IS)	
11/12/2009	4	

Table 5-3 Chronology of DESIREE-Fire tests (both testing scales) (continued).

Date	Test #	Comments including changes to test protocols
11/17/2009	8	The 15-kV Switchgear was damaged during Test IS8.
11/20/2009	12	Anomalies detected on R conductor for the 1-in. solenoid; test was still conducted.
11/25/2009	11	Removed connection to the R position switch on the 1" SOV before test.
12/2/2009	2	CT-500 transducers connected to SCDU data acquisition system (no SCDU circuits). Large coil tested using the 15A fuses for the duration of testing. The voltage transducer monitoring the R conductor on the large coil circuit was replaced. Intercable configuration tested using 5A fuses for the duration of testing. The current transducer monitoring R on the MOV-2 was replaced.
2/17/2010	3	The 5-kV switchgear was installed before Test IS3. The motor starters for both MOV-1 and MOV-2 were transferred to the chassis housing the 1" solenoid and large coil.
2/23/2010	1	
3/1/2010	5	CT-35 transducer monitoring S conductor on the Large Coil started to perform off-normal. This was not detected until data analysis.
3/3/2010	6	
3/4/2010	7	
3/17/2010	9	
3/25/2010	10	
3/26/2010	Conting.-1	Contingency tests - Only cables for 5-kV switchgear were tested in Contingency tests 1 and 2.
3/29/2010	Conting.-2	

6. SUMMARY OF TEST RESULTS

6.1 dc Motor Starter (MOV) Results

6.1.1 Penlight Small-Scale Tests

Fifteen small-scale tests were conducted using the dc MOV starters. Each test included two dc MOV starter circuits. Each MOV circuit consisted of a "Close" contactor unit and an "Open" contactor unit. The contactors are operated via a coil that when energized pulls in a movable core assembly, which forces the main power contacts to close. The main power connections were not used during these tests. The MOV control circuits were designated as MOV-1 (open), MOV-1 (close), MOV-2 (open), and MOV-2 (close).

Table 6-1 provides a summary of the small-scale test matrix. As shown in the table, the scope of these tests covered all of the cable types available for the DESIREE-Fire project. Five TS-insulated cable types and three TP-cables were included in the test series. The MOV circuit cables were exposed to the Penlight thermal environment in a cable tray configuration with the exception of Tests 37 and 41 where the cables were routed through a rigid metal conduit (both circuits and the thermal cable were co-located in the same conduit).

Table 6-1 Small-scale test matrix – dc MOVs.

Burn Test #	Cable Insulation Material								Exposure Shroud Temp (°C)	Raceway Type	
	Thermoset					Thermoplastic					
	XLPE / CSPE	EPR	SR	Kerite®	Armored	Tefzel	PE / PVC	PVC / PVC		Tray	Conduit
7	X								470	X	
8	X								470	X	
12							X		325	X	
22					X				470	X	
25		X							470	X	
27			X						700	X	
30						X			325	X	
33								X	325	X	
37	X								525		X
41							X		525		X
43							X		275	X	
44				FR					325	X	
49				FR					400	X	
50				FR					450	X	
JPN-3	JNES-supplied cable								350	X	

Table 6-2 provides a summary of the small-scale test results for the MOV circuits. Of the 30 circuit tests run, 20 resulted in SAs and 5 in clearing of one or both 10-A fuses as the initial fault mode. The summary table includes the first failure as well as the failure mechanism (e.g., SA or FB). Circuits with an asterisk (*) may have experienced multiple SAs; however, the appropriate appendices should be reviewed for more detailed information on the number of operations and duration of each operation. The longest duration SA was approximately 60 minutes and occurred in Test 43. This particular event preceded other SAs (i.e., locking in for a period of time and subsequently clearing for a period of time) of 23, 10, and 24 minutes, and 31 second durations. With the exception of the 31-second duration, the open coil on MOV-2 experienced

each of the SAs. Figure 6-1 through Figure 6-4 show the temperature profile during the test, the current and voltage response of both MOV circuits during the test (two different time frames), and the behavior of the battery ground-fault monitoring system. Additional information for each test may be found in Appendix B.

Table 6-2 Results summary – dc MOV.

Test #	MOV	Mode	Time to Damage (seconds)	Duration (seconds)	Coil
7	1	SA	538	32	Open
	2	FB	564	- - -	- - -
8	1	SA	538	8	Open
	2	FB	514	- - -	- - -
12	1	SA	859	203	Open
	2	DNF	DNF	- - -	- - -
22	1*	SA	585	2	Open
	2*	SA	596	37	Open
25	1	SA	613	10	Close
	2*	SA	570	2	Close
27	1	DNF	DNF	- - -	- - -
	2	DNF	DNF	- - -	- - -
30	1	SA	1436	90	Open
	2	SA	1076	1439 (~24 minutes)	Open
33	1	FB	627	- - -	- - -
	2	FB	575	- - -	- - -
37	1	SA	1681	30	Close
	2	SA	1723	16	Close
41	1*	SA	2699	60	Open
	2*	SA	1307	98	Close
43	1*	SA	11266	94	Open
	2*	SA	2776	3583 (~60 minutes)	Open
44	1	SA	9073	1203	Close
	2	SA	10043	306	Open
49	1	SA	4394	7	Close
	2	SA	4823	1	Open
50	1	FB	1334	- - -	- - -
	2	SA	1242	22	Close
JPN-3	1	SA	2626	240	Open
	2	SA	2308	194	Open

SA = Spurious Actuation
FB = Fuse Blow
DNF = Did Not Fail

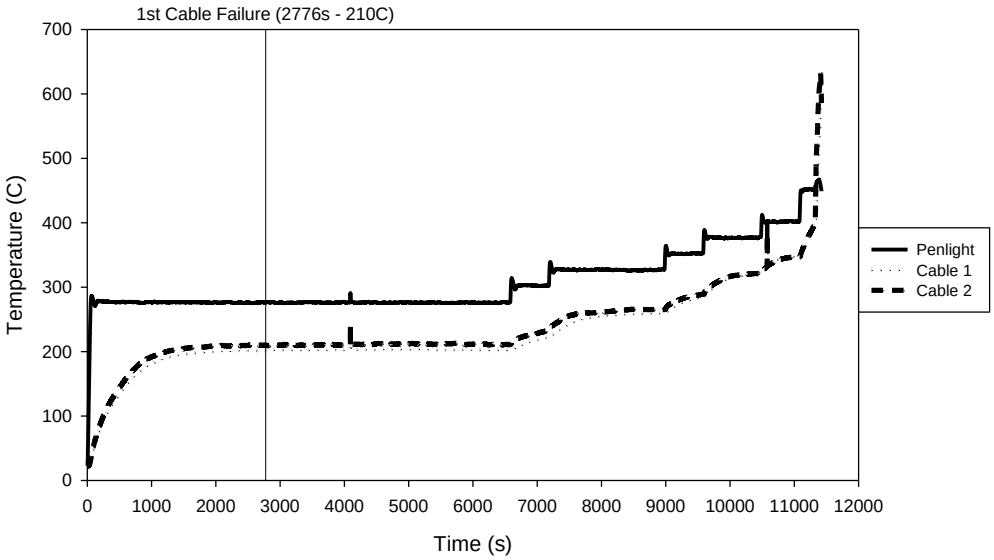

Figure 6-1 Test #43 temperature profile

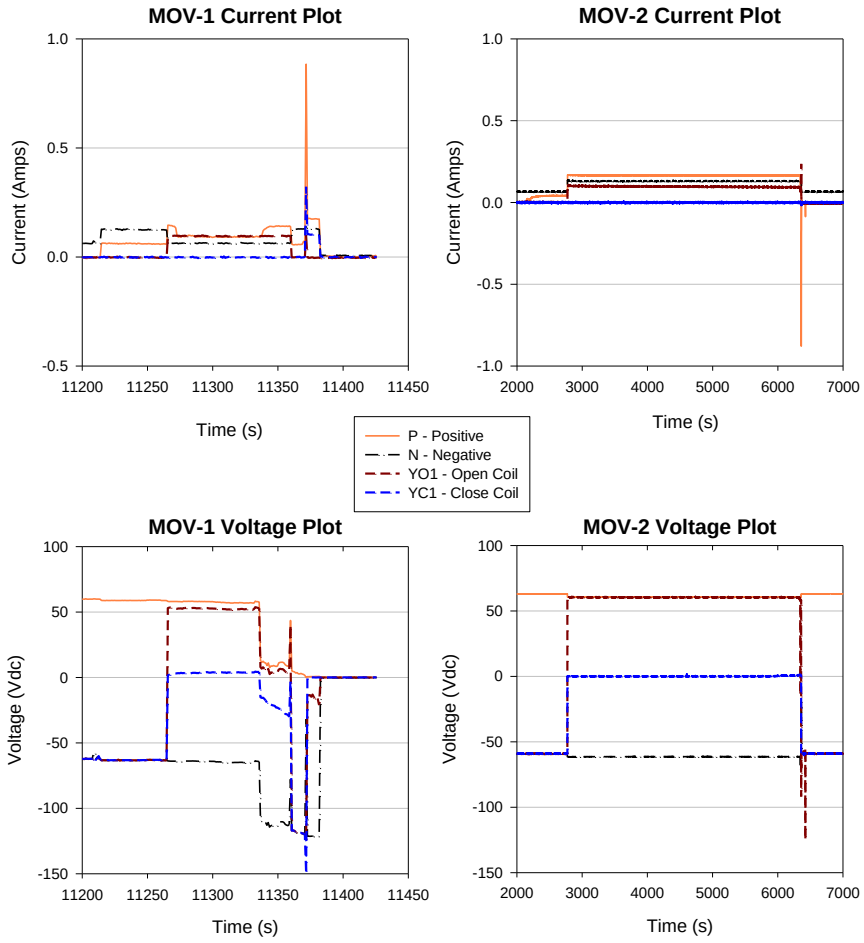

Figure 6-2 Test #43 MOV-1 and MOV-2 voltage/current plots

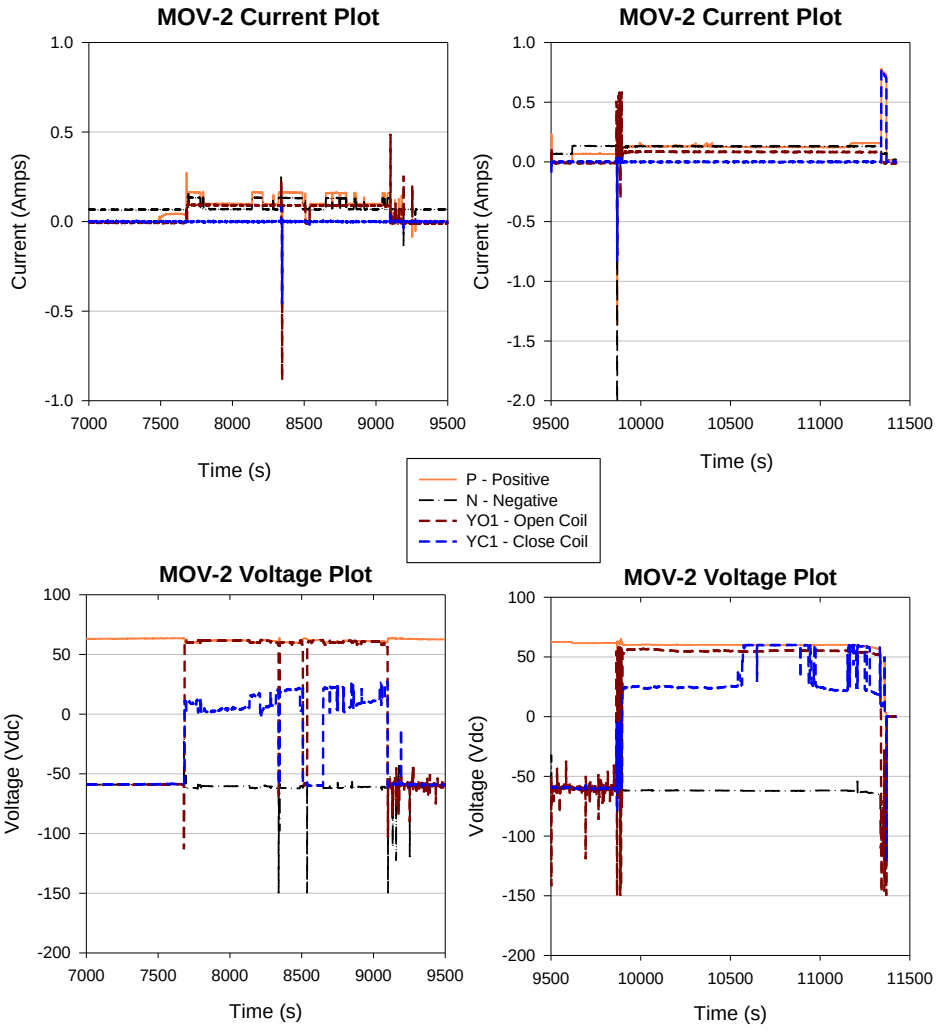

Figure 6-3 Test #43 additional MOV-2 voltage/current plots

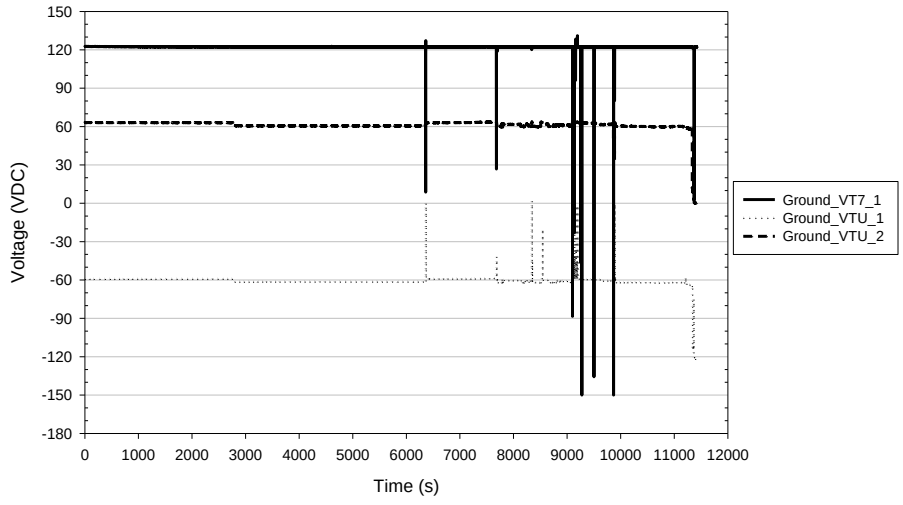

Figure 6-4 Test #43 ground voltage monitoring circuit indication

One test worth noting here is Test 27, during which neither cable failed. This test used the SR-insulated cable. The CAROLFIRE tests had already indicated that this cable was unlikely to fail during Penlight testing, but CAROLFIRE used exclusively ac-powered test circuits. Test 27 was included in DESIREE-Fire to see if the same behavior would apply to a dc-powered circuit. The results indicate that the SR cable behaves similarly for dc circuits as it did with ac circuits; that is, despite a prolonged high-temperature exposure (700 ºC) the cable did not experience electrical shorting. The Penlight tests do not involve cable wetting, which CAROLFIRE showed would cause cable failure following such a thermal exposure.

A second somewhat anomalous test worth noting is Test 43. At the request of the peer review committee, this test involved a TP cable (PE/PVC) and a relatively low Penlight shroud temperature (275 ºC). Given this exposure, the failure time for one of the two test cables was quite extended (i.e., over three hours). This is simply indicative of an exposure placed the cable in thermal equilibrium at a temperature very near its failure threshold. The lower-exposure temperatures were used in testing to provide some assessment as to whether SA durations might be a function of the exposure conditions. Although this methodology differed from the 10- to 20-minute failure threshold used during CAROLFIRE, the peer review committee suggested that DESIREE-Fire provided the opportunity to investigate failure mechanisms for prolonged low-temperature exposures. The actual analysis and assessment of the data in this context lies beyond the scope of this report.

6.1.2 Intermediate-Scale Tests

Thirteen intermediate-scale tests were conducted using the dc MOV starters. Each test included two dc MOV starter circuits. However, unlike the Penlight tests, the two individual MOV circuit test cables were not routed through the intermediate-scale test cell together. For most cases, the MOV-1 cable was routed along with the SOV-1 test cable, and MOV-2 with SOV-2.

Only four TS-insulated cable types and one TP type were included in the intermediate-scale tests. SR, Tefzel, and PVC insulation cables were not connected to the MOV circuits during any of the intermediate-scale tests. Two of the intermediate-scale tests had the MOV-1 cable routed in rigid conduit. The rest of the tests were run with the MOV cables routed in cable trays, usually with other fill cables surrounding the test cables.

Table 6-3 provides the test matrix used for the intermediate-scale tests of the MOV cables. Table 6-4 provides a summary of the intermediate scale test results for the MOV circuits. Of the 26 circuit tests run, 13 resulted in SAs as the initial failure mode and 7 in clearing of one or both 10A fuses. The longest duration of a SA was over 6.5 minutes. Circuits with an asterisk (*) may have experienced multiple SAs; however, the appropriate appendices should be reviewed for more detailed information on the number of operations and duration of each operation. Additional details about each of the MOV intermediate-scale tests are provided in Appendix B.

6.2 Small dc SOV Results

The dc solenoids are operated via an electromagnetic coil that when energized pulls in a movable core, which forces the valve stem to change position. The SOVs are spring-loaded so that when electric power is removed from the solenoid the valve returns to its unpowered condition. The two dc SOV control circuits were designated as SOV-1 and SOV-2.

Table 6-3 Intermediate-scale test matrix for the dc MOV starters.

Burn Test #	Device	Cable Insulation Material								Exposure Location	Raceway Type	
		Thermoset					Thermoplastic					
		XLPE / CSPE	EPR	SR	Kerite®	Armored	Tefzel	PE / PVC	PVC / PVC		Tray	Conduit
Pre-2 (IS)	MOV-1							X		A	X	
	MOV-2							X		E	X	
1	MOV-1	X								B		X
	MOV-2	X								D	X	
2	MOV-1	X								A	X	
	MOV-2	X								C	X	
3	MOV-1	X								D	X	
	MOV-2	X								B	X	
4	MOV-1	X								A	X	
	MOV-2	X								C	X	
5	MOV-1							X		B		X
	MOV-2							X		D	X	
6	MOV-1							X		C	X	
	MOV-2							X		A	X	
7	MOV-1							X		B	X	
	MOV-2							X		D	X	
8	MOV-1							X		A	X	
	MOV-2							X		C	X	
9	MOV-1				FR					B	X	
	MOV-2					X				D	X	
10	MOV-1				FR					C	X	
	MOV-2				FR with zinc					B	X	
11	MOV-1		X							B	X	
	MOV-2		X							D	X	
12	MOV-1		X							A	X	
	MOV-2		X							B	X	

6.2.1 Penlight Small-Scale dc SOV Tests

Ten tests were conducted in Penlight using two small SOV circuits per test for a total of 20 data points. Table 6-5 provides the matrix for the small-scale SOV circuit tests indicating the cable types, raceway configuration, and shroud exposure temperature (ºC). As indicated in the table, only Kerite® and the JNES cables were not tested as one of the small SOV circuit cables.

Table 6-6 provides a summary of the results of the dc SOV cable tests. Of the 20 circuit cables tested, 11 initially failed by SA of the valve, 6 first failed by clearing one or both of the 5A circuit fuses, and 3 cables did not fail. The longest of the SA durations was more than 21 minutes, occurring during Penlight Test #38. The test was concluded before the SA was cleared and denoted with a “greater than” (>) symbol in the summary table. Circuits with an asterisk (*) may have experienced multiple SAs; however, the appropriate appendices should be reviewed for more detailed information on the number of operations and duration of each operation. Additional insights may be gained from Appendix C.

Table 6-4 Intermediate-scale results summary – dc MOVs.

Test #	MOV	Mode	Time to Damage (seconds)	Duration (seconds)	Coil
Pre-2 (IS)	1	FB	343	- - -	- - -
	2	SA	820	401	Open
1	1	SA	1475	83	Open
	2	HS	2617	44	Close
2	1	SA	4247	115	Open
	2*	HS	1116	26	Close
3	1	SA	2784	3	Open
	2*	SA	1078	12	Open
4	1	SA	1859	36	Open
	2	HS	4967	7	- - -
5	1	SA	1717	17	Open
	2*	HS	1500	73	Close
6	1	SA	1480	27	Close
	2	FB	336	- - -	- - -
7	1	FB	324	- - -	- - -
	2	FB	535	- - -	- - -
8	1	SA	1052	97	Close
	2	FB	1743	- - -	- - -
9	1	SA	2611	16	Close
	2	SA	1253	24	Open
10	1*	SA	3584	7	Open
	2	HS	2798	37	Close
11	1	SA	1179	18	Open
	2	FB	2749	- - -	- - -
12	1	FB	3031	- - -	- - -
	2	HS	2233	107	Close
HS = Hot Short; SA = Spurious Actuation; FB = Fuse Blow; DNF = Did Not Fail					

Table 6-5 Small-scale test matrix – small dc SOVs.

Test #	Cable Insulation Material								Exposure Shroud Temp (ºC)	Raceway Type	
	Thermoset					Thermoplastic					
	XLPE / CSPE	EPR	SR	Kerite®	Armored	Tefzel	PE / PVC	PVC / PVC		Tray	Conduit
1	X								470	X	
2	X								470	X	
9							X		325	X	
20					X				470	X	
23		X							470	X	
26			X						700	X	
28						X			325	X	
31								X	325	X	
34	X								525		X
38							X		450		X

Table 6-6 Small-scale test results summary – small dc SOVs.

Test #	SOV	Mode	Time to Damage (seconds)	Duration (seconds)
1	1	FB	597	- - -
	2*	SA	542	21
2	1	FB	648	- - -
	2*	SA	560	23
9	1	SA	864	22
	2*	SA	827	35
20	1	SA	502	24
	2*	SA	508	20
23	1	SA	487	5
	2	FB	498	- - -
26	1	DNF	- - -	- - -
	2	DNF	- - -	- - -
28	1	FB	3384	- - -
	2	SA	3393	297
31	1	SA	517	3
	2	FB	432	- - -
34	1*	SA	1728	3
	2	FB	1644	- - -
38	1	DNF	- - -	- - -
	2	SA	1163	>1312

While no statistical analyses have been performed, there does not appear to be any obvious differences in behavior between the two valve circuits. That is, the presence of the Class H coil in SOV-2 does not appear to have grossly impacted circuit behavior. Both SOV circuits again show similar ratios of FB and spurious operation failures, and there is no obvious distinction relative to SA duration (i.e., neither valve showed an obvious trend towards longer or short duration spurious operation events).

6.2.2 Intermediate-Scale SOV Tests

Thirteen tests were conducted using the small dc SOVs during the intermediate-scale test series. Each test included two dc SOV circuits. Table 6-7 provides the intermediate-scale test matrix for the small SOV circuits indicating the cable types, raceway configuration, and location in the intermediate-scale test cell. As shown in the table, at least one test was run on a small SOV cable that included each of the available TS materials. On the other hand, the SOV circuits tested using TP materials only employed PE/PVC cables, not Tefzel or PVC. The SOV cables were generally run in cable trays, and bundled with other cables. Only two tests were conducted that routed a SOV-1 cable through the rigid metal conduit at location B in the intermediate-scale test cell.

A summary of the SOV circuit responses to the cable damage caused by the intermediate-scale fire environments is provided in Table 6-7. Of the 26 SOV circuit cables tested, 14 resulted in an initial SA failure while the rest (12) were characterized by initially clearing of one or both 5A circuit fuses. The longest duration of a spurious SOV actuation occurred during Test IS9 on SOV-1 where the event lasted for just less than two minutes. Circuits with an asterisk (*) may have experienced multiple SAs; however, the appropriate appendices should be reviewed for more detailed information on the number of operations and duration of each operation. As was

observed for the Penlight test, while no statistical analyses have been performed, there do not appear to be any obvious differences behavior between the two valve circuits.

Table 6-7 Intermediate-scale test matrix for the small SOVs.

Burn Test #	Device	Cable Insulation Material								Exposure Location	Raceway Type	
		Thermoset					Thermoplastic					
		XLPE / CSPE	EPR	SR	Kerite®	Armored	Tefzel	PE / PVC	PVC / PVC		Tray	Conduit
Pre-2 (IS)	SOV-1							X		A	X	
	SOV-2							X		E	X	
1	SOV-1	X								B		X
	SOV-2	X								D	X	
2	SOV-1	X								C	X	
	SOV-2	X								A	X	
3	SOV-1	X								D	X	
	SOV-2	X								B	X	
4	SOV-1	X								A	X	
	SOV-2	X								C	X	
5	SOV-1							X		B		X
	SOV-2							X		D	X	
6	SOV-1							X		C	X	
	SOV-2							X		A	X	
7	SOV-1							X		B	X	
	SOV-2							X		D	X	
8	SOV-1							X		A	X	
	SOV-2							X		C	X	
9	SOV-1				FR					B	X	
	SOV-2					X				D	X	
10	SOV-1				FR					C	X	
	SOV-2				FR with zinc					B	X	
11	SOV-1		X							B	X	
	SOV-2		X							D	X	
12	SOV-1		X							D	X	
	SOV-2		X							B	X	

6.3 Large dc Coil and 1-Inch Solenoid Operated Valve (1”) Results

The dc solenoids are operated via an electromagnetic coil that when energized pulls in a movable core, which forces the valve stem to change position. The 1-in. SOV is spring-loaded so that when electric power is removed from the solenoid the valve returns to its unpowered condition. The large coil consisted solely of a large (approximately 0.4m high by 0.3m diameter) electromagnetic coil enclosed in a stainless steel container. No movable core was part of the large coil unit. The two control circuits for these devices were designated as Large Coil (LC) and 1-Inch SOV (1-in.).

6.3.1 Penlight Small-Scale dc Large Coil and 1” SOV Tests

Five tests were conducted in Penlight using the large coil and the 1-in. SOV circuits. Table 6-8 provides the test matrix for the small-scale tests of these SOV circuits indicating the cable types,

raceway configuration, and shroud exposure temperature (ºC). As indicated in the table, only XLPE/CSPE and PE/PVC cables were tested with these circuits.

The large coil is a low pick-up coil and the manufacturer[10] (Target Rock) has designed the magnetics of the coil to pick between 60V to 70V. This large coil has a 36-ohm (+/- 6%) resistance.

Table 6-9 provides a summary of the results of the large coil and 1" SOV cable tests. Of the ten circuit cables tested, seven initially failed by SA of the valve coil and three first failed by clearing one or both of the circuit fuses. The longest of the SA durations was just over one minute, occurring during Penlight Test #40. Circuits with an asterisk (*) may have experienced multiple SAs; however, the appropriate appendices should be reviewed for more detailed information on the number of operations and duration of each operation. Additional details may be found in Appendix D.

Table 6-8 Small-scale test matrix – large coil and 1" SOV.

Test #	Cable Insulation Material								Exposure Shroud Temp (ºC)	Raceway Type	
	Thermoset					Thermoplastic					
	XLPE / CSPE	EPR	SR	Kerite®	Armored	Tefzel	PE / PVC	PVC / PVC		Tray	Conduit
5	X								470	X	
6	X								470	X	
11							X		325	X	
36	X								525		X
40							X		450		X

Table 6-9 Small-scale test results summary – large coil and 1" SOV.

Test #	SOV	Mode	Time to Damage (seconds)	Duration (seconds)
5	LC	SA	616	2
	1"*	SA	643	5
6	LC	FB	677	- - -
	1"	SA	597	<1
11	LC*	SA	1000	52
	1"*	SA	798	11
36	LC	FB	1743	- - -
	1"	SA	1611	13
40	LC*	SA	4100	64
	1"	FB	4167	- - -

During Penlight small-scale Test #11, both the large coil and the 1-inch SOV experienced multiple SAs during the course of the test run. For the large coil the first SA lasted 52 seconds and the second, which occurred about five minutes later, lasted over 1000 seconds, until the circuit fuse cleared. Similarly, the first 1-inch SOV SA lasted 11 seconds and the second lasted 798 seconds, also starting about five minutes after the end of the first one. The end of the second SA of the 1-in. SOV was caused by the clearing of its circuit fuse.

[10] Point of contact is Steve Pauly.

Figure 6-5 through Figure 6-7 provide the temperature profile during Penlight Test #11, the current and voltage response of both circuits during the test, and the behavior of the nominal 125Vdc battery ground monitoring system.

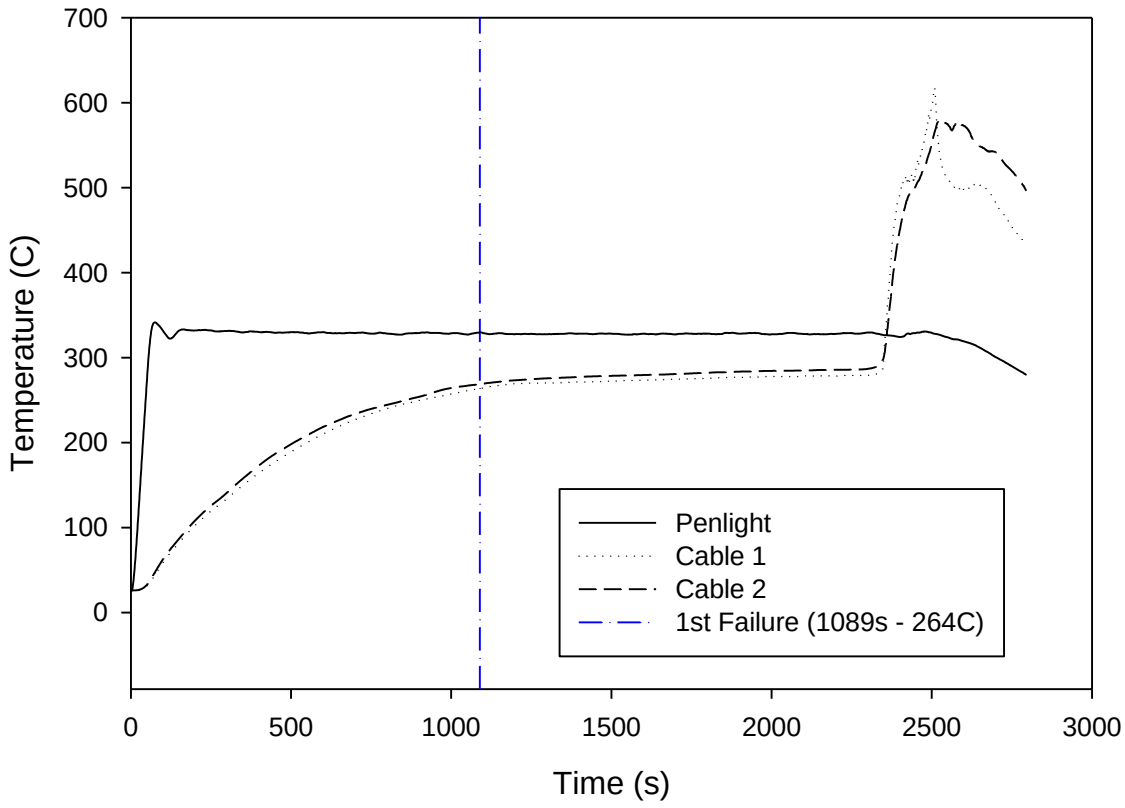

Figure 6-5 Penlight Test #11 temperature profile

6.3.2 Intermediate-Scale dc Large Coil and 1" SOV Tests

Thirteen tests were conducted using the large coil and 1-in. SOV circuit cables. Table 6-10 provides the intermediate-scale test matrix for these large coil and 1-in. SOV circuits indicating the types of cables tested, the raceway configuration, and the location in the intermediate-scale test cell. As shown in the table, at least one test was run with the large coil and 1-in. circuit cables that included each of the available TS materials except for SR. On the other hand, these SOV circuits tested using TP materials only employed PE/PVC cables, not Tefzel or PVC. The large coil and 1-in. cables were generally run in cable trays bundled with other cables except for Test IS7, where the cables were routed through rigid metal conduit in test cell location B.

A summary of the large coil and 1-in. SOV circuits' response to the cable damage caused by the intermediate-scale fire environments is provided in Table 6-12. Of the 13 1-in. SOV circuit cables tested, 7 resulted in an initial SA failure while 5 were characterized by initially clearing of one or both circuit fuses; no failures occurred during Preliminary Test 1 (Pre-1 (IS)). The longest duration of a spurious 1-in. SOV actuation occurred during Test IS6, where the event lasted for just less than 1.5 minutes.

Table 6-10 Intermediate-scale test results summary – 1-in. SOV.

Test #	SOV	Mode	Time to Damage (seconds)	Duration (seconds)
Pre-2	1	FB	312	- - -
	2	SA	953	67
1	1	FB	1375	- - -
	2	SA	2512	11
2	1	SA	3909	68
	2	SA	1030	79
3	1	FB	3066	- - -
	2*	SA	1361	2
4	1	FB	1671	- - -
	2	SA	5216	33
5	1	FB	1556	- - -
	2*	SA	1646	12
6	1	SA	1400	101
	2	FB	191	- - -
7	1	SA	302	61
	2	FB	466	- - -
8	1	SA	960	92
	2	FB	2354	- - -
9	1	SA	2584	112
	2	SA	1552	28
10	1	FB	3646	- - -
	2	FB	2502	- - -
11	1	FB	1569	- - -
	2	SA	2858	59
12	1	SA	3131	5
	2	FB	2314	- - -

Of the 13 large coil circuit cables tested, five resulted in an initial SA failure while seven were characterized by initially clearing of one or both circuit fuses; no failures occurred during Pre-1 (IS). The longest duration of a spurious large coil actuation occurred during Test IS8, where the event lasted for just less than two minutes. Circuits with an asterisk (*) may have experienced multiple SAs; however, the appropriate appendices should be reviewed for more detailed information on the number of operations and duration of each operation. Additional insights may be gained from Appendix D.

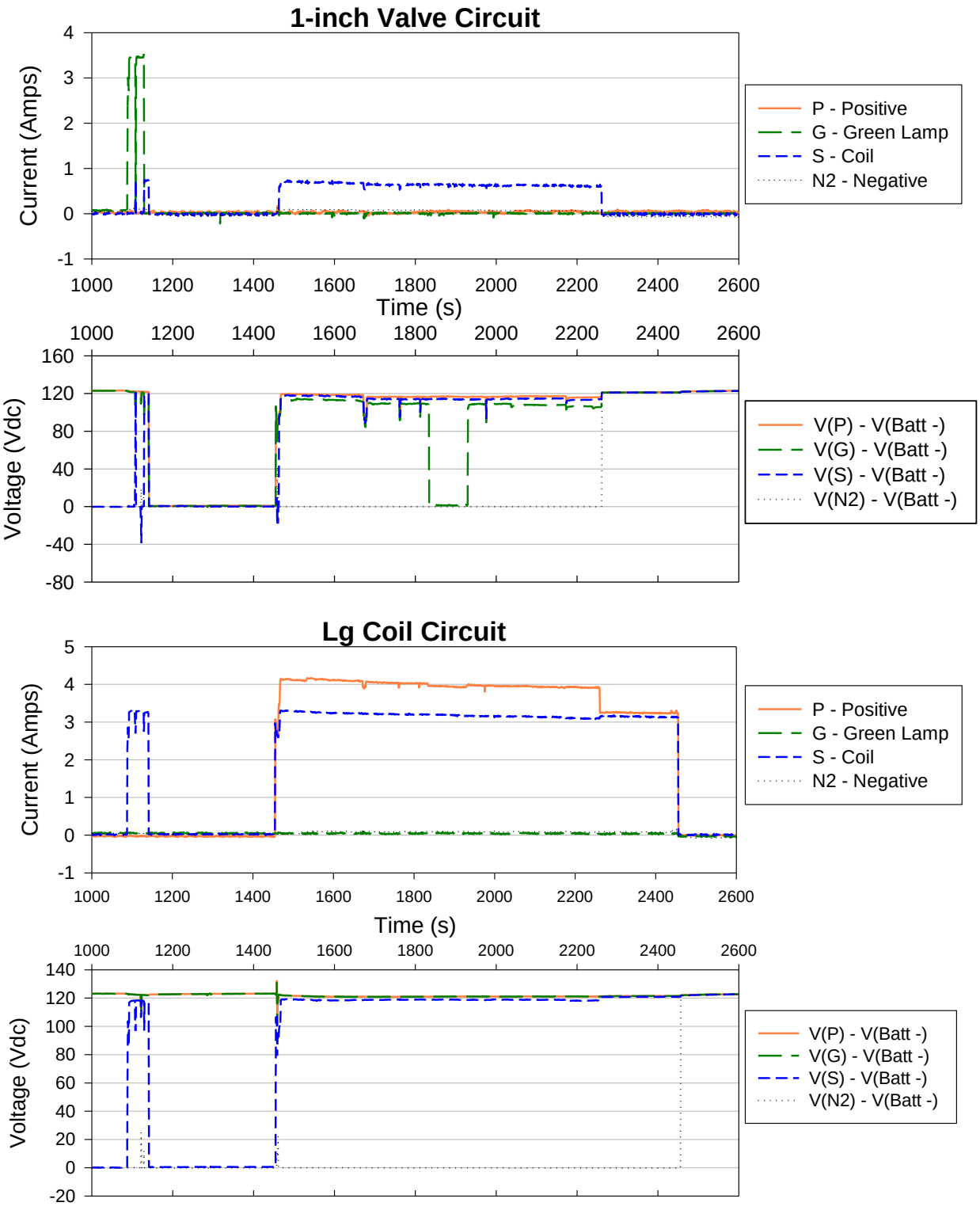

Figure 6-6 Penlight Test #11 1-inch SOV and large coil voltage/current plots

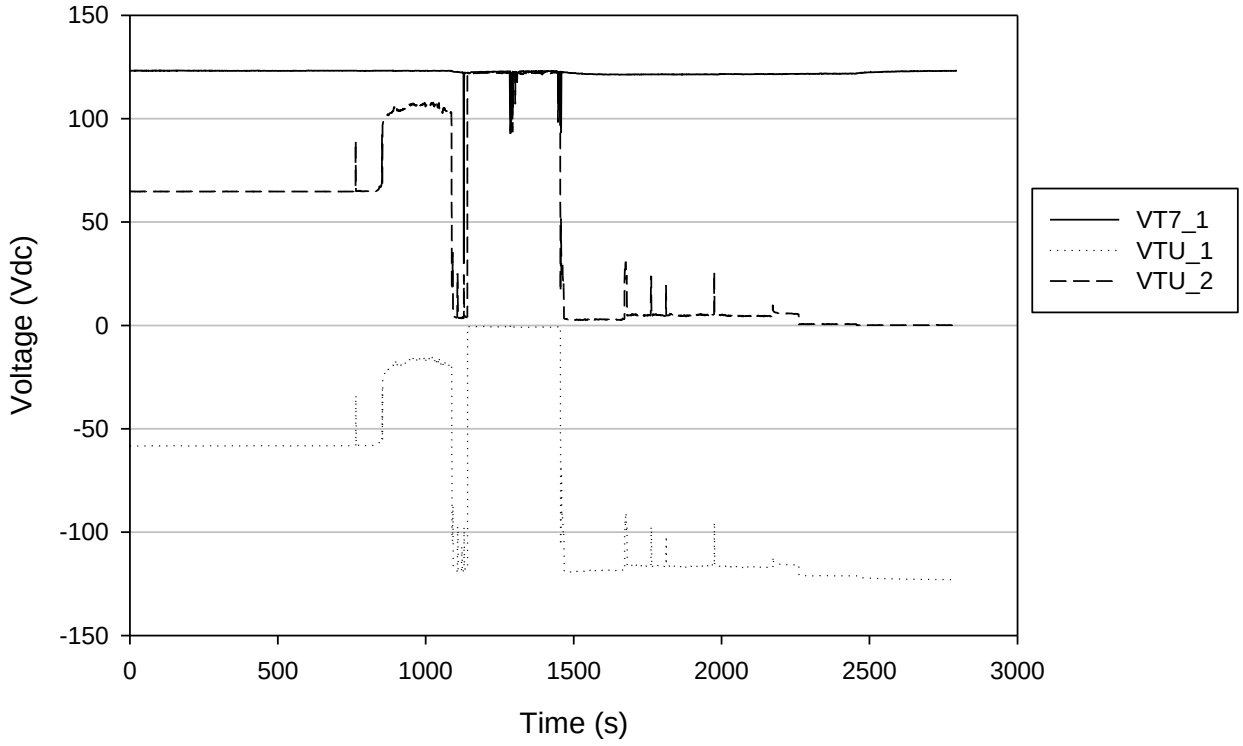

Figure 6-7 Test #11 ground voltage monitoring circuit indication

Table 6-11 Intermediate-scale test matrix for the large coil and 1" SOV.

Burn Test #	Cable Insulation Material								Exposure Location	Raceway Type	
	Thermoset					Thermoplastic					
	XLPE / CSPE	EPR	SR	Kerite®	Armored	Tefzel	PE / PVC	PVC / PVC		Tray	Conduit
Pre-1 (IS)	X								E	X	
1	X								B	X	
2	X								C	X	
3	X								D	X	
4	X								A	X	
5							X		B	X	
6							X		C	X	
7							X		B		X
8							X		A	X	
9					X				B	X	
10				FR with zinc (LC), FR (1" SOV)					D	X	
11		X							B	X	
12		X							D	X	

Table 6-12 Intermediate-scale test results summary – large coil and 1" SOV.

Test #	SOV	Mode	Time to Damage (seconds)	Duration (seconds)
Pre-1 (IS)	1"	Circuits did not fail		
	LC			
1	1"*	SA	1361	16
	LC*	SA	1449	1
2	1"	FB	3975	- - -
	LC	FB	4492	- - -
3	1"*	SA	2188	33
	LC	FB	2288	- - -
4	1"	FB	1671	- - -
	LC	FB	1675	- - -
5	1"	FB	655	- - -
	LC	SA	819	89
6	1"	SA	1548	89
	LC	FB	1317	- - -
7	1"	SA	1713	49
	LC	FB	1426	- - -
8	1"	FB	1137	- - -
	LC	SA	943	117
9	1"	SA	628	10
	LC	FB	765	- - -
10	1"	SA	2635	9
	LC	FB	2890	- - -
11	1"*	SA	1310	2
	LC	SA	1432	1
12	1"	FB	3032	- - -
	LC*	SA	2746	51

6.4 Switchgear Results

Medium voltage breakers, or "switchgear," are designed to provide three-phase electrical power to big loads such as large pump motors. The large circuit breaker (switchgear) is operated by the action of one of two electromagnetic coils contained within the unit. The "close" coil controls the closing of the primary circuit breaker contacts. The other, the "trip coil," controls the opening of the primary contacts. These circuits are typically associated with separate and independent cables connected to the control panel on the circuit breaker. These two control circuits are also fused separately as well with the trip circuit fused much higher than the closing circuit (e.g., 35A versus 15A).

For DESIREE-Fire, the two circuit cables were kept separate with the exception of one intermediate-scale test. The two circuits were identified as "Close" and "Trip."

6.4.1 Penlight Small-Scale Switchgear Tests

Ten Penlight small-scale tests were conducted using the two circuit breaker circuit cables. The initial condition of the circuit breaker at the start of every Penlight test was Open with the actuating spring charged. Table 6-13 provides the test matrix for the small-scale tests of these circuits indicating the types of cables tested, the raceway configuration, and the shroud exposure temperature (ºC).

Table 6-13 Small-scale test matrix – switchgear.

Test #	Cable Insulation Material								Exposure Shroud Temp (ºC)	Raceway Type	
	Thermosets					Thermoplastics					
	XLPE / CSPE	EPR	SR	Kerite®	Armored	Tefzel	PE / PVC	PVC / PVC		Tray	Conduit
3	X								470	X	
4	X								470	X	
10							X		325	X	
21					X				470	X	
24		X							470	X	
29						X			325	X	
32								X	325	X	
35	X								525		X
39							X		470		X
42	X								430	X	
JPN-1	JNES cable only								varies	X	
JPN-2	JNES cable only								350	X	

Table 6-14 provides a summary of the results of the switchgear cable tests. Of the 20 circuit cables tested, 9 initially failed by SA of the actuating coil and 10 first failed by clearing one or both of the circuit fuses. The longest of the SA duration was over 23 minutes, occurring during Penlight Test #29 on the close coil circuit. Circuits with an asterisk (*) may have experienced multiple SAs; however, the appropriate appendices should be reviewed for more detailed information on the number of operations and duration of each operation. Additional insights may be gained from Appendix E.

During Penlight small-scale Test #21, both the close coil and the trip coil circuits experienced a very large fault wherein both the 15A and 35A negative side fuses cleared simultaneously. Both positive side fuses were found to be intact during the post-test examinations.

Throughout the course testing, it was not uncommon to see the cable connected to the trip coil experience prolonged arcing behavior and conductor severance, but only a limited number of tests were investigated in greater detail. Photos from Penlight Tests 3, 10, 29, and JPN2 may be found in Appendix E under their respective test sections. It should be emphasized, however, that these tests were not the only ones to experience this type of arcing behavior or conductor severance. The photos from these experiments were to illustrate some of the behavior observed during the course of testing this particular circuit.

Table 6-14 Small-scale test results summary – switchgear.

Test #	Coil	Mode	Time to Damage (seconds)	Duration (seconds)
3	Close	SA	721	13
	Trip	FB	698	- - -
4	Close*	SA	625	1
	Trip*	SA	626	6
10	Close	FB	911	- - -
	Trip	DNF	- - -	- - -
21	Close	FB	963	- - -
	Trip	FB	963	- - -
24	Close	FB	2193	- - -
	Trip	FB	2288	- - -
29	Close	SA	3530	1396
	Trip	FB	3488	- - -
32	Close	SA	607	13
	Trip	SA	620	11
35	Close	SA	1692	87
	Trip	FB	1738	- - -
39	Close	FB	3616	- - -
	Trip	FB	4175	- - -
42	Close	SA	6120	16
	Trip	SA	6137	26

6.4.2 Intermediate-Scale Switchgear Tests

As shown in Table 6-15, 12 of the intermediate-scale fire tests included cables that provided control to the close and trip circuits for a large circuit breaker. Two different classes of circuit breaker were tested: 15kVac and 5kVac. For the most part, the circuit breakers were open with their trip springs charged at the beginning of the test. A few of the later tests were conducted with the circuit breaker starting in the closed position with the spring charged. Additionally, three tests were conducted with the breaker in the closed position and with conductor C1 electrically connected to PC through a jumper. This arrangement was introduced in order to test the behavior of the anti-pump relay in the close circuit inside the breaker.

Like the Penlight tests, the initial intermediate-scale tests involved the 15-kV circuit breaker. However, during one intermediate-scale test, IS Test 8, a severe short in the switchgear close test cable caused internal wiring inside the circuit breaker to overheat and generated a lot of smoke in the immediate vicinity of the circuit breaker. The test director immediately isolated both switchgear circuits by opening the 50- and 60-A breakers, providing battery power to the trip and close circuits. Appendix A.4 provides details of this incident and the results of the post-test investigation. After failure of the first breaker, a second, 5-kV class switchgear breaker was obtained by EPRI for use in the remainder of the intermediate-scale tests.

A summary of the switchgear circuits' response to the cable damage caused by the intermediate-scale fire environments is provided in Table 6-16. Of the 12 switchgear circuit tests conducted, seven resulted in an initial SA failure while four were characterized by initially clearing of one or both circuit fuses. During Test IS8, a severe HS damaged the switchgear's internal panel wiring and both the close and trip circuits had to be isolated from the battery.

Most of the SAs were of nominally short durations. Additional insights may be gained from Appendix E.

Table 6-15 Intermediate-scale test matrix for the switchgear.

Burn Test #	Cable Insulation Material									Exposure Location	Raceway Type	
		Thermosets					Thermoplastics					
	XLPE / CSPE	EPR	SR	Kerite®	XLPO	Armored	Tefzel	PE / PVC	PVC / PVC		Tray	Conduit
Pre-1 (IS)	X									B	X	
1	X									D	X	
3	X									B		X
4	X									E	X	
5								X		D	X	
6								X		B		X
7								X		D	X	
8								X		C	X	
9						X				D	X	
10				FR with zinc						B	X	
Cont-1					X					B	X	
Cont-2							X			B	X	

During the conduct of the intermediate-scale testing, it was decided to test the functionality of the anti-pump feature in the 5-kV switchgear unit. This was accomplished by installing a jumper between the terminal block points for PC and C1 in the dc-SIM panel before closing the dc disconnect switch. This energized the anti-pump relay once dc power was applied to the circuit. The breaker was then closed using the manual push button on the front of the switchgear cabinet. This initial condition was implemented for IS Tests #10, Contingency-1, and Contingency-2.

The expectation was that once the breaker tripped open, then the continuous power being supplied to the anti-pump relay (52Y) through the closed 52Y/a contact would prevent a spurious reclosure of the circuit breaker main contacts. The anti-pump feature appeared to allow a reclosure of the breaker following a trip during the Contingency-1 test. Around the time of the three SAs, the battery negative was in a transition to becoming shorted to ground. If the potential difference between C1 and N1 momentarily dropped below the holding voltage and current needed to keep the anti-pump relay engaged, then it is possible that the relay dropped out, allowing voltage from C1 to re-energize the close coil.

Table 6-16 Intermediate-scale test results summary – switchgear.

Test #	SWGR Size	Bkr Cond At Start	Mode	Time to Damage (seconds)	Duration (seconds)	Coil
Pre-1 (IS)	15 kV	OPEN	SA	502	1	Close
1	5 kV	OPEN	FB	1255	-.-.-	Close
3	5 kV	OPEN	SA	1460	8	Close
4	15 kV	OPEN	FB	4766	-.-.-	Close
5	5 kV	OPEN	SA	1424	5	Close
6	5 kV	CLOSED	SA	850	<1	Trip
7	5 kV	CLOSED	SA	1095	<1	Trip
8	15 kV	OPEN	HS	1102	35	Trip
9	5 kV	CLOSED	FB	1920	-.-.-	Close
10	5 kV	CLOSED w/ Jumper	SA	3108	37	Trip
Cont-1	5 kV	CLOSED w/ Jumper	SA	406	1	Trip
Cont-2	5 kV	CLOSED w/ Jumper	FB	337	-.-.-	Trip

*Note: The SWGR circuit was not tested in intermediate scale tests 2, 11, and 12.

6.5 Intercable Test Circuit Results

The DESIREE-Fire tests included an “intercable” test circuit. The test circuit itself is described in brief in Section 4.1.2 and in detail in Appendix A.6. The test results for this circuit are described in detail in Appendix F. As noted in these descriptions, the circuit and test configurations optimized the potential for intercable interactions involving, in particular, the so-called “smart dc hot short”; that is, an intercable short such that one conductor (or group of conductors) in a target cable becomes energized at the positive battery potential and a second conductor (or group of conductors) in that same target cable becomes energized at the negative battery potential. Should such a short form that impacts the target cable, a voltage cascade from positive to negative across the outer ring of conductors would form. Hence, the test result of primary interest for this circuit is whether or not such a voltage cascade formed.

6.5.1 Penlight Small-Scale Intercable Tests

Four Penlight small-scale tests were conducted using the intercable circuit bundles. Table 6-17 provides the test matrix for the small-scale tests of these circuits indicating the cable types, raceway configuration, and nominal shroud exposure temperature (ºC). For the penlight tests, the bundle of five cables was placed on a non-conductive piece of insulation to provide isolation from the grounded cable tray. The only way to clear the positive and negative fuses would be through intercable shorting; however, shorting through the target cable was the primary interest.

Zip ties were used on the ends of the cable (i.e., far removed from the interior of Penlight) and therefore did not contribute to cable performance. Table 6-18 provides a summary of the results of the intercable cable tests.

Table 6-17 Small-scale test matrix – intercable circuits.

Burn Test #	Cable Insulation Material								Exposure Shroud Temp (C)	Raceway Type	
	Thermosets					Thermoplastics					
	XLPE / CSPE	EPR	SR	Kerite	Armored	Tefzel	PE / PVC	PVC / PVC		Tray	Conduit
45	X								460	X	
46		X							470	X	
47							X		350	X	
48								X	400	X	

Table 6-18 Small-scale test results summary – intercable circuits.

Test #	Mode	Time to Damage (seconds)
45	HS	1550
46	HS	1000
47	HS	2240
48	HS	550

Of the four intercable bundles tested, all indicated cable-to-cable interactions between the target cable and one or more of the energized source cables. This was not unexpected given the test configuration, which, as noted above, was designed to optimize the potential for such interactions. In Tests 45, 46, and 48 the intercable interactions occurred only after the target cable had failed internally. This is apparent in that as the target conductors become energized (in either the positive or negative direction relative to ground) all of the conductors in the outer ring (conductors 2-7) will become energized to the same voltage level. Often in such cases, the central conductor, which was not a part of the target cable resistor network, would show an independent intermediate voltage, indicating that gross cable damage had not propagated fully to the center conductor. Previous testing has consistently shown that the conductors in the outer ring will generally fail first with the inner conductor (or conductors) failing some time later. Hence, the intercable test results are consistent with prior testing in this regard.

Penlight Test 47, involving the PE/PVC TP cable, is the only test that shows signs of the anticipated voltage cascade across the target conductors beginning to form. Figure 6-8 illustrates the results for this test. Approximately 2240 seconds into the test, initial intercable interactions were observed. It was not until 4350 seconds into the experiment, however, that positive and negative interactions occurred. The Target 5 conductor shorted to a positive source, which is indicated by the 10Vdc increase. Concurrently, Target 2 shorted to a negative source and decreased by approximately 10Vdc. This cascade effect illustrates the fact that the target cable had not completely failed internally before the interaction with two of the source cables. Had internal shorting occurred before intercable behavior, the conductors of the target cable would become energized to the same voltage level.

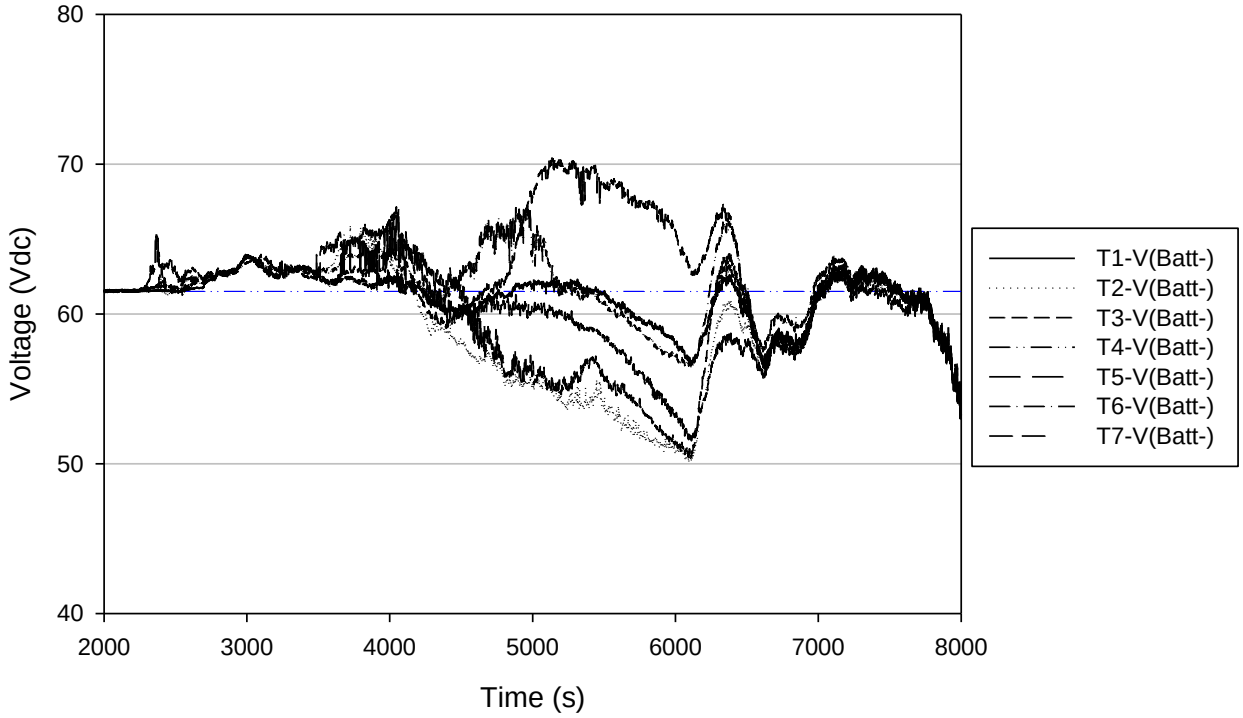

Figure 6-8 Penlight Test #47 cascade effect indicating intercable interaction

6.5.2 Intermediate-Scale Intercable Circuit Tests

Thirteen intermediate scale tests were conducted using the five cable intercable bundles designed to reveal cable-to-cable interactions. Table 6-19 provides the test matrix for the intercable circuits indicating the cable types, raceway configuration and location in the intermediate-scale test cell.

A summary of the intercable circuits' response to the cable damage caused by the intermediate scale fire environments is provided in Table 6-20. Of the 13 circuit tests conducted, seven resulted in an indication of intercable (source-to-target) interactions. However, in all 7 cases, the target cable had failed internally before the intercable interactions. The source circuit fuses cleared, indicating intercable shorting between the source cables, before any interactions with the target cable in five of the tests. No cable failures occurred during the intermediate-scale Preliminary Test 1 (Pre-1 (IS)).

Table 6-19 Intermediate-scale test matrix for the intercable circuits.

Burn Test #	Cable Insulation Material								Exposure Location	Raceway Type	
	Thermoset					Thermoplastic					
	XLPE / CSPE	EPR	SR	Kerite®	Armored	Tefzel	PE / PVC	PVC / PVC		Tray	Conduit
Pre-1 (IS)	X								D	X	
1	X								C	X	
2	X								D	X	
3	X								A	X	
4	X								B	X	
5							X		C	X	
6							X		D	X	
7							X		A	X	
8							X		B	X	
9		X							C	X	
10		X							A	X	
11		X							C	X	
12		X							A	X	

A typical case is illustrated by Test IS10. During this test it appears that the center conductor in the target cable had not shorted to the outer ring of conductors during the early part of the intercable interaction. Figure 6-9 provides a plot of the target conductor voltages measured during Test IS10, where T1 is the center conductor. Note that most of the voltage signals (T2 through T7) overlap completely, indicating that all six conductors in the outer ring were shorted together. This case simply indicates that the outer ring of conductors in the target cable had all shorted together, and that the negative source cable was interacting with those conductors through a high-resistance intercable short. The center conductor of the target cable retained some degree of insulation resistance relative to the other conductor in the target cable; hence, it shows an intermediate voltage between the outer ring conductors and ground. At approximately 750 seconds, the central conductor shorts more completely to the outer ring conductors and the positive source conductors become the predominant source for the intercable shorting. Again, the energizing voltages were insufficient to induce a SA for this case.

Table 6-20 Intermediate-scale test results summary – intercable circuits.

Test #	Mode	Time to Damage (seconds)
Pre-1 (IS)	n/a	No failure
1	HS	2520
2	FB	1110
3	HS	461
4	FB	1675
5	FB	1760 & 2026
6	FB	336
7	FB	448
8	HS	1481
9	HS	1602
10	HS	514
11	HS	3184
12	HS	1222

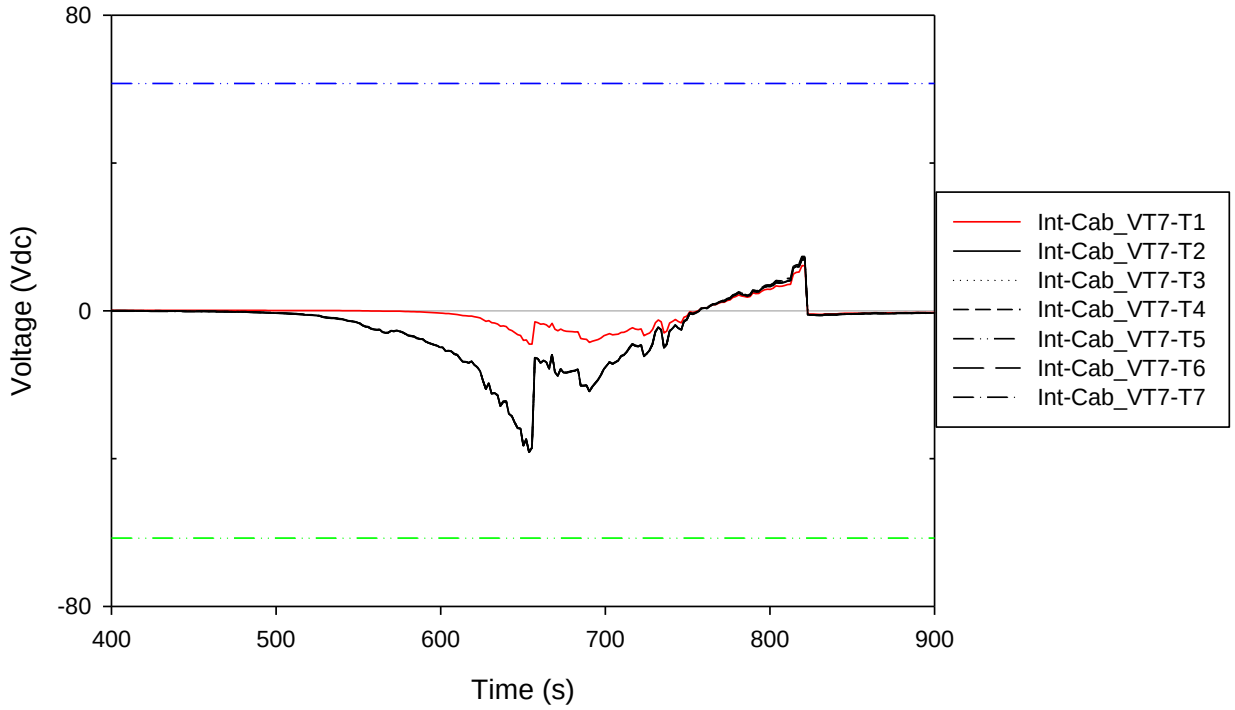

Figure 6-9 Intercable target conductor voltages measured during intermediate-scale test IS10

6.5.3 Summary of the Intercable Circuit Tests

The tests did show a number of intercable HSs occurring, but that is not unexpected given that the test configuration was designed to optimize the potential for intercable HSs. HSs were observed in 4-of-4 Penlight tests and 7-of-12 intermediate-scale tests (where failure occurred; in one intermediate-scale test the circuit did not fail). In no case was an intercable smart dc HS observed. Penlight Test 47 involved the only substantive case where sign of a potentially forming smart dc HS appeared, and in that case the signs were rather weak. The energizing voltage difference observed on the target cable reached a maximum of only about 15Vdc, indicating that the cable-to-cable resistance values, while degrading, remained quite high. The voltages imposed on the target conductors in this case were not sufficient to induce a spurious operation.

6.6 SCDU Test Results

Four ac-powered SCDUs were used to simulate ac MOV control circuits. The four separate units were designated as SCDU-1, SCDU-2, SCDU-3, and SCDU-4. The units were originally built for, and used in, the CAROLFIRE project. Each SCDU includes a pair of ac-powered NEMA Class 1 motor starter contactor units and a CPT that provides 120Vac (nominal) power to the control circuit. A detailed discussion of the SCDU systems is provided in Appendix A.6.

For the purposes of DESIREE-Fire the original CAROLFIRE motor control contactor units were replaced with Joslyn-Clark units identical to those used in the original NEI-EPRI tests. Of the

four contactor sets, all had intact electrical interlocks, but only three of the four had intact mechanical and electrical interlocks in place. SDCU-1 utilized one of two contactor sets provided by EPRI and that particular set did not have mechanical interlocks in place. SNL tested the unit as received from EPRI.

The primary objective for DESIREE-Fire relative to the SCDUs was to investigate the impact of CPTs effect on the likelihood of SAs. In the original NEI/EPRI tests of 2000 there was an apparent effect on SA likelihood due to saturation of the limited-power CPTs, which led to degradation of the source voltage to below the contactor minimum pick-up voltage before SAs could occur in some tests. Overall, the CPT effect was attributed with reducing SA likelihood by a factor of two based on expert judgment [3]. This same effect was *not* observed in any of the CAROLFIRE tests, but those tests had used different contactor sets that had lower power demand and lower pick-up voltages. DESIREE-Fire includes follow-up investigations on this specific issue.

Each SCDU supplies circuit power through a CPT of specified rating: SCDU-1 used a 100VA CPT, SCDU-2 used a 150VA CPT, SCDU-3 used a 200VA CPT, and SCDU-4 used a 75VA CPT. The intent was to attempt to determine what, if any, impact on a nominal 100VA circuit that a CPT of a given rating might have on limiting the available voltage-current to induce a SA of one of the two target motor starters. The secondary side of all CPTs was grounded on the return side and fused at 3A on the line side. For each of the circuits, the two MOV contactor coils were identified as Target 5 and Target 6.

Note that after completion of Test IS12, the SCDU data logging capability was re-tasked to allow for high-speed monitoring of certain of the dc current transducer signals. Hence, the intermediate-scale tests performed after Test IS12 did not utilize the SCDUs.

6.6.1 Penlight Small-Scale Tests

Thirteen small-scale Penlight tests were conducted using the SCDUs. With the exception of Tests #13-Qual and #17-Qual, each Penlight test included two of the four available SCDU circuits. Table 6-21 provides a summary of the small-scale test matrix for these 13 tests. As shown in the table, the scope of these tests covered Kerite® cable types available for the DESIREE-Fire project; however, the four preliminary tests used XLPE/CSPE and PE/PVC cables. One armored cable test was included in the test series.

Table 6-22 provides a summary of the small-scale test results for the SCDU circuits. Of the 24 circuit tests run, nine resulted in SAs and 13 in clearing of the circuit fuse. The longest duration of a SA was 57 minutes.

Figure 6-10 shows the current and voltage response of all the conductors of the cable connected to SCDU-1 during Penlight Test 17. Recall that SCDU-1 had a 100-VA CPT. In this one case it appears that the degradation in the source voltage, beginning around 1750 seconds, was sufficient to prevent the actuation of either target coil despite HSs to both target conductors. This voltage degradation effect is likely due to the limited capacity of the 100VA CPT to supply all of the leakage currents being developed at that time. This effect was not noted in any of the other Penlight test results.

Table 6-21 Small-scale test matrix – ac MOVs.

Burn Test #	Cable Insulation Material								Exposure Shroud Temp (ºC)	Raceway Type	
	Thermoset					Thermoplastic					
	XLPE / CSPE	EPR	SR	Kerite®	Armored	Tefzel	PE / PVC	PVC / PVC		Tray	Conduit
Pre-1 (P)	X								470	X	
Pre-2 (P)	X								470	X	
Pre-3 (P)							X		325	X	
Pre-4 (P)							X		325	X	
13_qual				FR-z					Varied	X	
13				FR-z					350	X	
14				FR-z					450	X	
15				FR-z					300	X	
16				FR-z					470	X	
17_qual				HTK					Varied	X	
17				HTK					430	X	
18				HTK					420	X	
19					X				470	X	

Notes: FR-z refers to Kerite® FR with a zinc wrap.
HTK refers to Kerite® HTK (high temperature cable).

Table 6-22 Results summary – ac MOV Penlight tests.

Test #	SCDU	Mode	Time to Failure (seconds)	HS/SA Duration (seconds)	Coil
Pre-1 (P)	1	SA/HS	550	41	T6/T5
	2	SA	563	41	T6
Pre-2 (P)	1	SA	1186	64	T6
	2	SA	1226	54	T6
Pre-3 (P)	1	FB	886	- - -	- - -
	2	FB	912	- - -	- - -
Pre-4 (P)	1	SA/HS	878	292	T6/T5
	2	SA	845	27	T5
13-Qual	1	SA	3360	~1440	T6
13	1	SA	4575	~1	T6
	2	FB	4590	- - -	- - -
14	1	FB	964	- - -	- - -
	2	FB	964	- - -	- - -
15	1	DNF	- - -	- - -	- - -
	2	DNF	- - -	- - -	- - -
16	1	FB	834	- - -	- - -
	2	FB	750	- - -	- - -
17-Qual	1	FB	2769	- - -	- - -
17	1	FB	1848	- - -	- - -
	2	FB	1900	- - -	- - -
18	1	FB	5807	- - -	- - -
	2	SA	5665	35	T6
19	1	FB	586	- - -	- - -
	2	FB	585	- - -	- - -

6.6.2 Intermediate-Scale SCDU Tests

Six intermediate-scale tests were conducted involving the SCDUs. Table 6-23 provides the test matrix for the intermediate scale tests that included the SCDUs. This matrix shows the cable types, raceway configuration, and location in the test cell.

Table 6-24 summarizes the results of the intermediate scale SCDU tests. Of the 18 SCDU circuits tested, seven initially experienced a SA of one of the motor starter units, nine cleared the circuit fuse as the initial failure, and two circuits did not fail in one of the tests. The longest duration for a spurious operation was 102 seconds on SCDU-1 during Test IS8.

Insofar as the effect that the CPTs had on limiting SAs in the SCDU circuits, it does not appear that the CPTs limited the ability of the circuit voltage-current to any degree that would prevent the occurrence of a SA during any of the intermediate-scale tests. Figure 6-11 illustrates one of the more pronounced cases where degradation of the source voltage was observed, but only after SAs had already occurred. Shown below in Figure 6-10 and Figure 6-11 are the voltage and current plots for SCDU-4 (75VA CPT) during Test IS4.

Test IS4 does show substantial degradation of the source voltage, but only relatively late in the test and well after SA had occurred on contactor T5. As shown in Figure 6-11, the T5 motor starter experiences a HS and causes a SA at 4606 seconds. At 4619 to 4627 seconds, the T6 motor starter conductor also experiences a HS but does not actuate because the energized T5

device has locked the T6 contactor out mechanically and electrically. At 4657 seconds, the circuit voltage dropped below the drop-out threshold for SCDU-4 contactor T5 and shortly thereafter both T5 and T6 begin chattering in response to continued HSs, but neither contactor locked in. This occurred during the time that multiple leakage current flow paths have evidently developed, yet there is still enough source voltage and current available to elicit responses from the motor starters. The SCDU-4 circuit fuse clears at 4672 seconds.

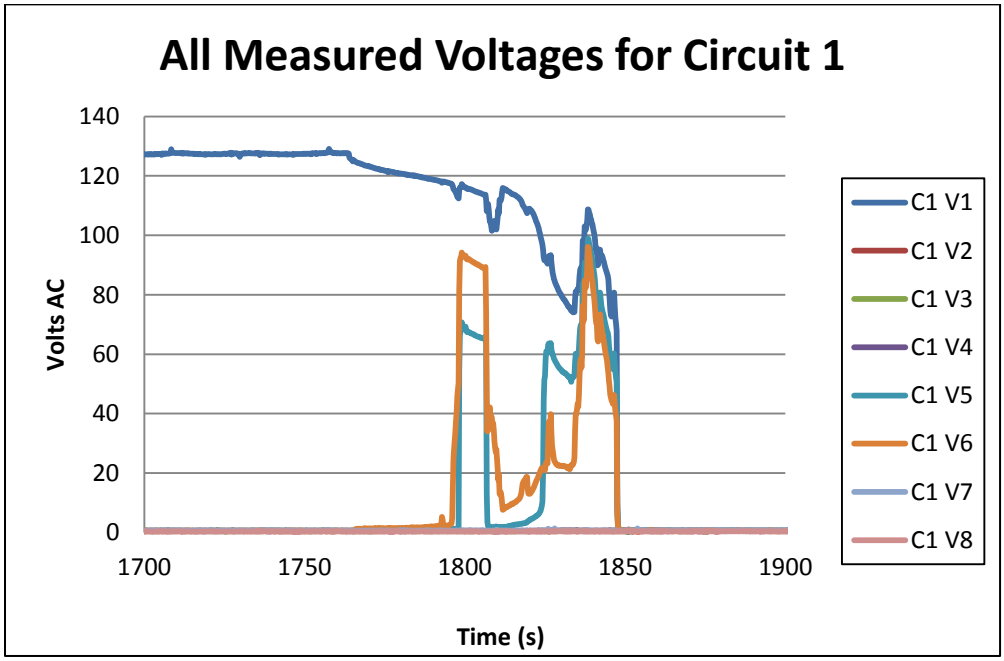

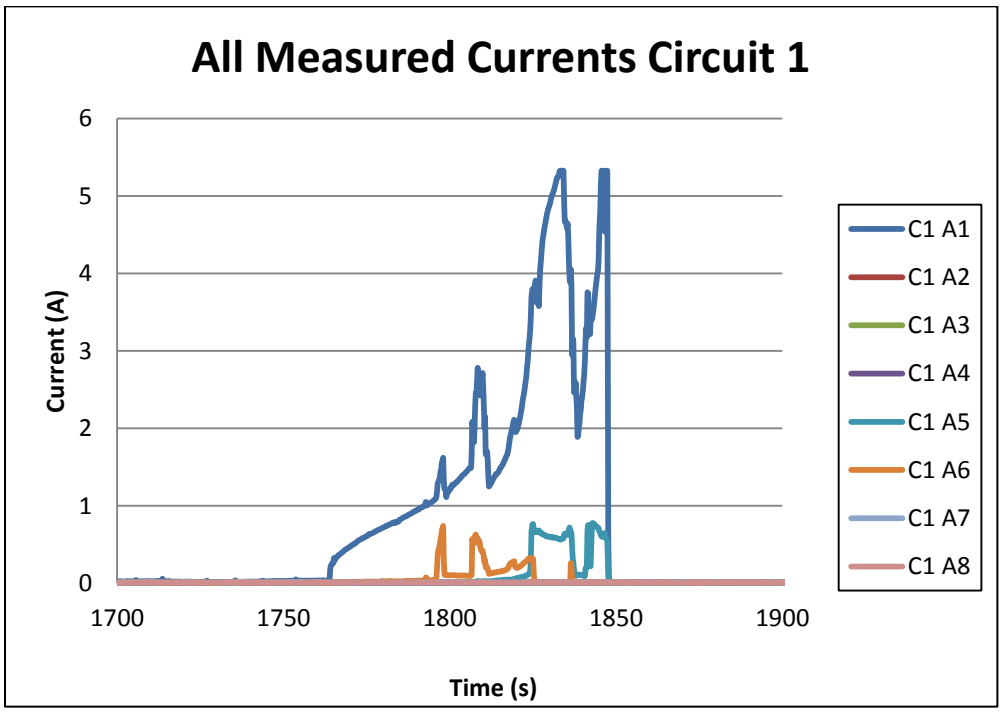

Figure 6-10 Penlight Test #17 SCDU-1 voltage and current plots

Table 6-23 Intermediate-scale test matrix for the SCDU circuits.

Burn Test #	SCDU ID	Cable Insulation Material								Exposure Location	Raceway Type	
		Thermoset					Thermoplastic					
		XLPE / CSPE	EPR	SR	Kerite®	Armored	Tefzel	PE / PVC	PVC / PVC		Tray	Conduit
Pre-1 (IS)	3	X								C	X	
	4	X								C	X	
Pre-2 (IS)	1							X		D	X	
	2							X		D	X	
4	1	X								D	X	
	2	X								D	X	
	3	X								D	X	
	4	X								D	X	
8	1							X		D	X	
	2							X		D	X	
	3							X		D	X	
	4							X		D	X	
11	1		X							A	X	
	2		X							A	X	
	3		X							A	X	
12	1		X							C	X	
	2		X							C	X	
	3		X							C	X	

Table 6-24 Intermediate-scale test results summary – SCDUs.

Test #	SCDU	Mode	Time to Damage (seconds)	Duration (seconds)
Pre-1 (IS)	3	DNF*	- - -	- - -
	4	DNF	- - -	- - -
Pre-2 (IS)	1	FB	628	- - -
	2	FB	633	- - -
4	1	SA	4381	44
	2	SA	4015	48
	3	SA	4602	4
	4	SA	4606	41
8	1	SA	1174	102
	2	FB	2035	- - -
	3	FB	515	- - -
	4	FB	1732	- - -
11	1	SA	895	5
	2	FB	921	- - -
	3	FB	811	- - -
12	1	SA	3795	62
	2	FB	3541	- - -
	3	FB	2923	- - -

* DNF indicates SCDU did not fail.

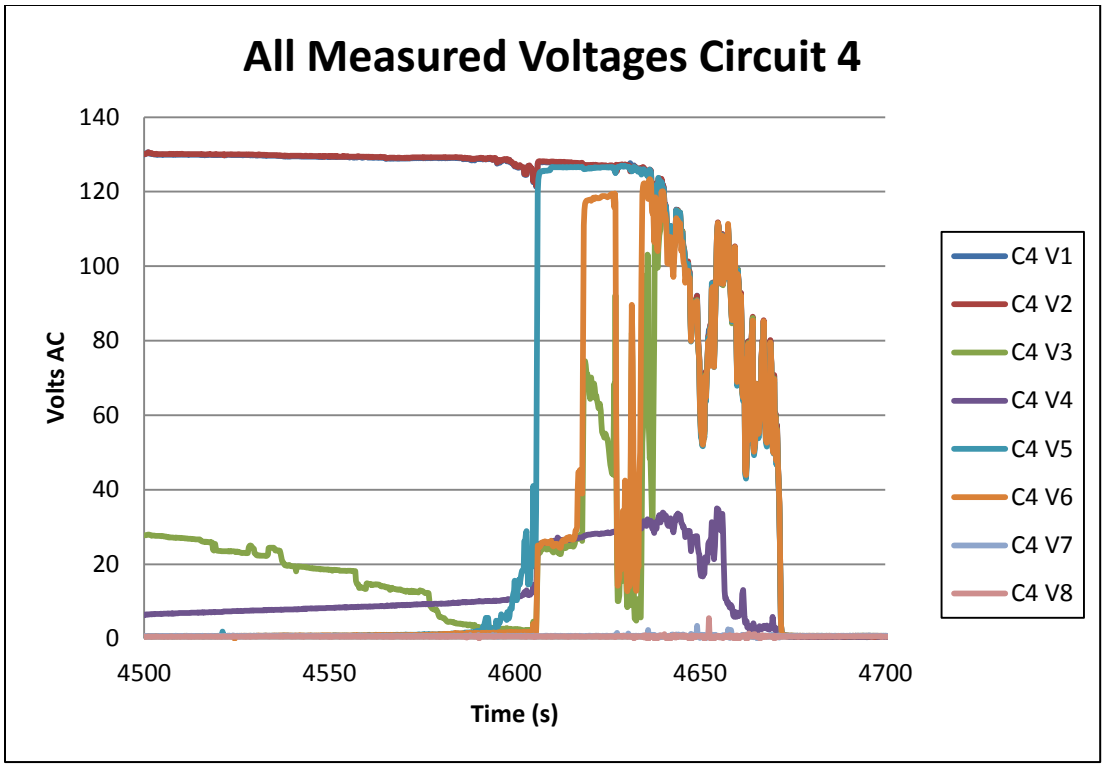

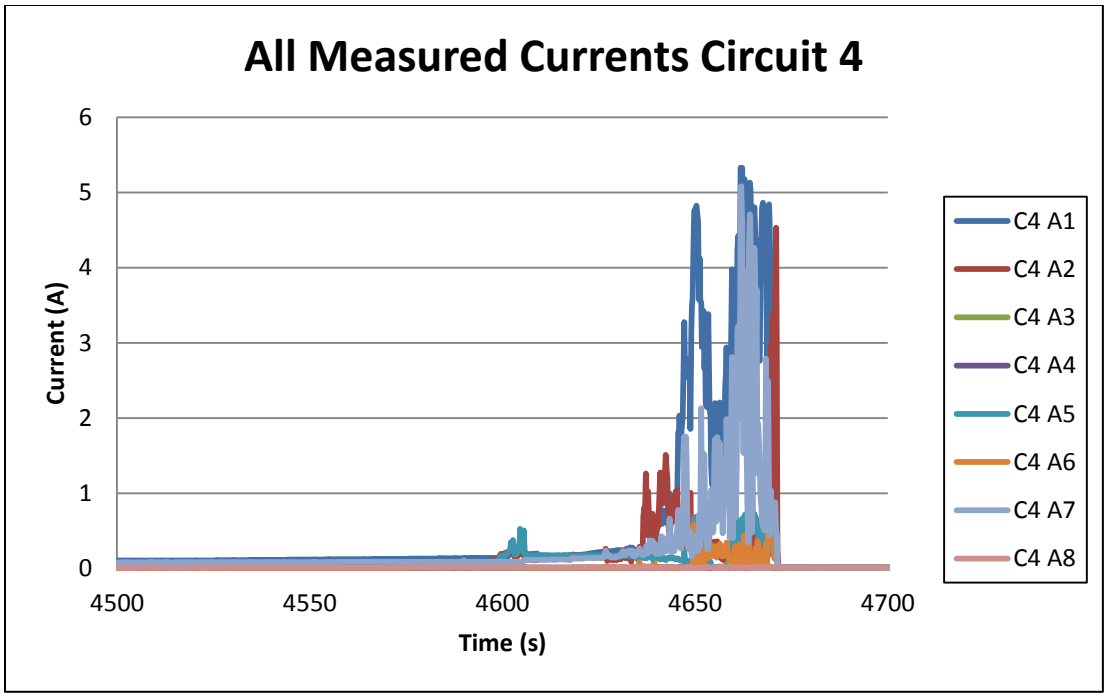

Figure 6-11 Test IS4 intracable target conductor current and voltage plots for SCDU 4

7. CONCLUSIONS AND GENERAL INSIGHTS

As a part of the DESIREE-Fire project, a total of 59 small-scale tests and 17 intermediate-scale tests were conducted. In all, the combined small- and intermediate-scale tests represent a total of over 225 individual circuit failure trials considering the number of individual circuits used in each of the tests. The testing focused mainly on dc-powered control circuits, but also involved limited testing of ac-powered circuits as a follow-up to one unresolved issue from the previous CAROLFIRE test program. Additionally, the inclusion of Kerite®, armored, and Japanese cables provided an opportunity to gain further insights on their failure modes and effects.

7.1 dc-Powered Circuits

The scope of this report is limited to objective reporting of the test data. It is not the intent of this report to interpret the test results beyond a factual representation of the progression of events observed in each test. The NRC already has plans in place to assemble two expert panels whose charter will be to interpret the test results and assess their implications for various applications. One panel will focus on the electrical aspects of the data and the second will deal with the statistical and risk aspects. Both panels will be conducted using the Phenomena Expert Elicitation process. In addition, as part of the following work under the electrical expert panel, the NRC plans to issue a NUREG report with some ac and dc circuit testing results analysis.

That said, there are four general observations on the behavior of the dc-powered cables as compared to previously tested ac-powered cables that were made through the course of DESIREE-Fire testing that are worthy of note:

- The faulting behavior of the dc-powered cables was more energetic than comparable ac-power cables observed in prior testing efforts. Both ac- and dc-powered cables displayed arcing behavior when short circuits form. However, with the dc-powered cables, the arcs were more substantial, more sustained and more damaging.
- Related to the first observation, short-circuit faulting in the dc-powered cables often led to destructive damage to the cable conductors. That is, it was often observed that the arc formed during faulting was sufficient to sever a conductor or even an entire multiconductor cable. The effect observed was analogous to welding operations where the welding rods are consumed in the process. This sort of destructive damage was not seen as the result of ac-power cable short circuits. Open circuits are a unique failure mode that was not observed in the ac testing but was common in the dc testing.
- In some cases the dc-powered cables were left energized even after they had experienced destructive damage as described immediately above. This behavior was tied to the fuse sizes used. Typically, the smaller 5A and 10A fuses would clear, de-energizing the conductors once failures occurred. However, as the fuse size increased, it became more common for the conductors to be left severely damaged but still energized. This behavior was not observed for the ac-powered cables, but none of the ac-powered cable tests have used fuses as large as those used in some of the tested dc-powered circuits.
- Corresponding to the prior observation, the positive and negative fuses for any given dc circuit did not necessarily clear at the same time. It was not uncommon to have one blown fuse while the other remained functional. An actively fused conductor could become grounded (through the tray, for example) and a transition of the relative ground

potential (i.e., from positive to negative or vice versa) could generate a sufficient amount of current to cause the intact fuse to clear.

- In general, more long-duration HSs and spurious operations were observed for the dc-powered circuits than had been observed in corresponding ac-powered circuits.

7.2 ac-Powered Circuits

The final issue investigated during DESIREE-Fire was the question of how the sizing of CPTs would impact the likelihood of spurious operation in ac-powered control circuits. This was an issue that was also investigated in the prior CAROLFIRE test program with inconclusive results. During the original NEI/EPRI circuit tests of 2000, it had been noted that multiple current leakage paths that formed during the cable degradation process would lead to saturation of the power-limited CPTs and to degradation of the source voltage. In some cases the voltage degraded to below the minimum pick-up voltage of the motor contactors. This effect was attributed with reducing the SA probability by a factor of two compared to non-power-limited circuits by an expert panel examining the NEI/EPRI data [3].

CAROLFIRE investigated a range of CPT sizes (i.e., 100VA to 250VA) but could not reproduce the voltage degradation effect to nearly the degree observed by NEI/EPRI. Differences in the characteristics of the motor contactors used in each program were thought to have been a contributing factor to the different test result.

For DESIREE-Fire, the ac-powered MOV simulator circuits, the SCDUs, were rebuilt using the exact same model of motor control contactor as had been used by NEI/EPRI and additional tests were run. The motor contactor sets all included electrical interlocks, and three of the four included mechanical interlocks as well.

For DESIREE-Fire only one case out of a total of 42 total circuit trials appears to have experienced a similar level of voltage degradation sufficient to have actually prevented a SA despite formation of HSs to the target (contactor coil) conductors; namely, Penlight Test #17. This case involved SCDU-1 with a 100VA CPT. A second test, intermediate-scale Test IS4, also showed signs of substantial source voltage degradation, but only after SAs had already occurred in the target circuit. This second test involved SCDU-4 with a 75VA CPT.

Overall, like CAROLFIRE, the DESIREE-Fire tests failed to reproduce the voltage degradation effect to nearly the degree that had been observed by NEI/EPRI despite the use of CPTs with just half the capacity of those used in the NEI/EPRI tests. None of the tests involving the two larger CPTs (150VA and 200VA) showed substantive degradation of source voltage sufficient to prevent a SA from locking in. Other trials of the smaller CPTs (75VA and 100VA) also did not experience sufficient voltage degradation to prevent SA lock-in.

8. REFERENCES

1. **NUREG/CR-6931**, "Cable Response to Live Fire (CAROLFIRE)," U.S. Nuclear Regulatory Commission, Washington, DC, April 2008, a report in three volumes:
   Volume 1: Nowlen, S.P., Wyant, F.J., *Test Descriptions and Analysis of Circuit* Response, SAND2007-600/V1, U.S. NRC, Washington, DC, April 2008.
   Volume 2: Nowlen, S.P., Wyant, F.J., *Cable Fire Response Data for Fire Model Improvement,* SAND2007-600/V2.
   Volume 3: McGrattan, K., *Thermally-Induced Electrical Failure (THIEF) Model,* NISTIR 7472.

2. **Information Notice 99-17**, "Problems Associated with Post-Fire Safe-Shutdown Circuit Analyses," U.S. Nuclear Regulatory Commission, Washington, DC, June 3, 1999.

3. **Report TR-1006961**, "Spurious Actuation of Electrical Circuits Due to Cable Fires, Results of an Expert Elicitation," Electric Power Research Institute, Palo Alto, CA, 2002.

4. **Regulatory Issue Summary (RIS) 2004-03**, **Rev. 1,** "Risk-informed Approach for Post-Fire Safe-Shutdown Circuit Inspections," U.S. Nuclear Regulatory Commission, Washington, DC, December 29, 2004.

5. **U.S. Nuclear Regulatory Commission**, "Results and Observations from Duke Armored Control Cable Fire-Induced Spurious Operation Testing," U.S. NRC, available through the NRC Agency-Wide Document Access and Management System (ADAMS) using accession numbers ML071200168 and ML071200168.

6. **SAND2010-4936**, Nowlen, S.P., and Brown, J., "A Preliminary Look at the Fire-Induced Electrical Failure Behavior of Kerite® FR Insulated Electrical Cables - A Letter Report to the U.S. NRC/RES," Sandia National Laboratories, Albuquerque, NM, July 2010.

7. **Standard E 603-06**, *Standard Guide for Room Fire Experiments,* American Society of Testing and Materials, 100 Barr Harbor Drive, P.O. Box C700, West Conshohocken, PA 19428-2959, 2006.

8. **NUREG/CR-6850, EPRI TR 1011989**, Nowlen, S.P., Najafi, B, et al., "EPRI/NRC-RES Fire PRA Methodology for Nuclear Power Facilities," a report in two volumes, a joint publication of the U.S. Nuclear Regulatory Commission and Electric Power Research Institute, September 2005.

9. **Inspection Manual Chapter 06.09, Attachment F**, "Fire Protection Significance Determination Process," U.S. Nuclear Regulatory Commission, February 28, 2005 (http://www.nrc.gov/readingrm/doc-collections/insp-manual/manual-chapter/index.html).

10. **Standard 450-2002**, "IEEE Recommended Practice for Maintenance, Testing, and Replacement of Vented Lead-Acid Batteries for Stationary Applications," Published by The Institute of Electrical and Electronics Engineers, Inc., 3 Park Avenue, New York, NY 10016-5997, April 2003.

Appendix A. Test Support Systems

A.1 Direct Current (dc)-Powered Motor-Operated Valve (MOV) Circuits

A typical dc MOV control circuit is illustrated in Figure A-1. This drawing was derived from a Reactor Core Isolation Cooling (RCIC) MOV found at a currently operating U.S. nuclear power plant. This circuit has also been used as an analysis example during the annual Office of Nuclear Regulatory Research (RES)/Electric Power Research Institute (EPRI) fire probabilistic risk assessment (PRA) training course. The corresponding block diagram displayed in Figure A-2 illustrates the basic MOV location with respect to the various control and power distribution cabinets. Note that the specific conductors present in each connecting cable are indicated on the block diagram (e.g., conductors P, N, YC1, G, R, etc.) and these designations correspond to the conductor designations in the circuit diagram. The target cable of concern to be studied in this test series is cable A, which is highlighted in the block diagram.

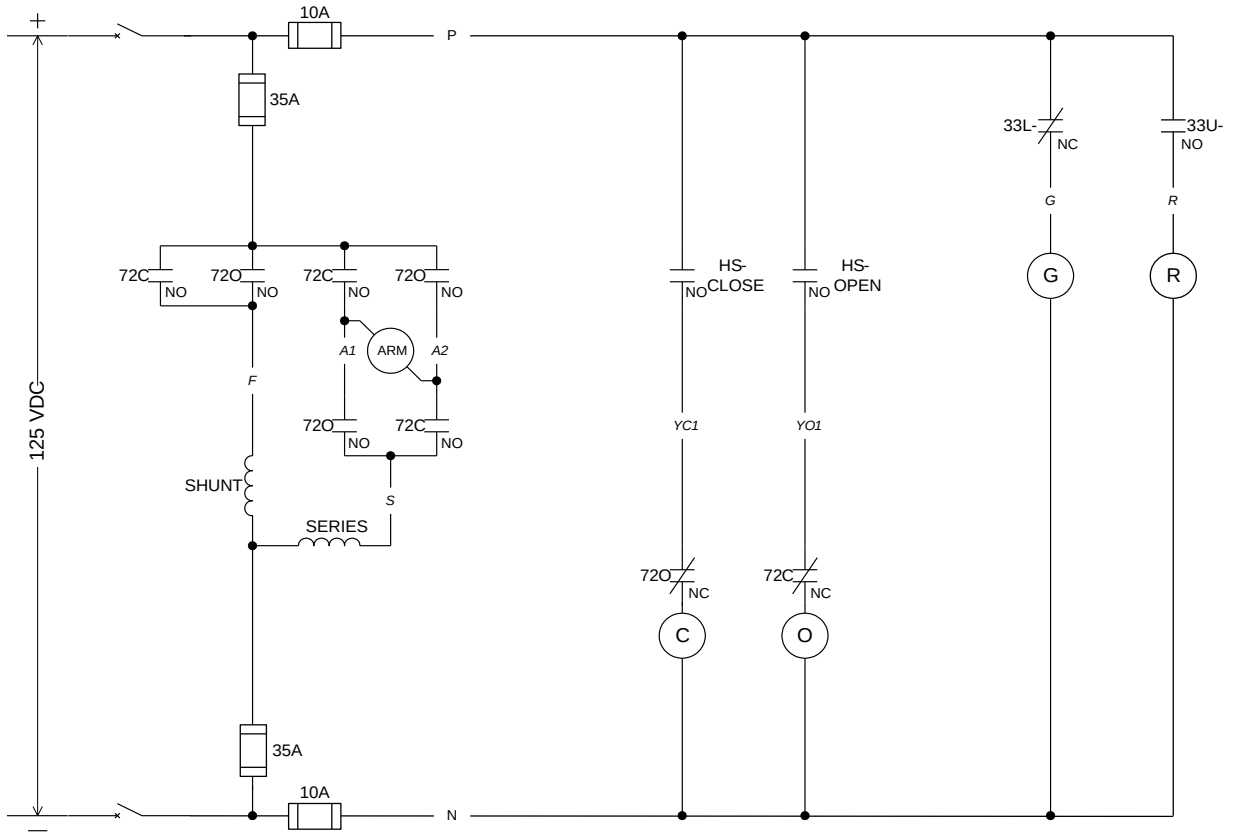

Figure A-1 Electrical schematic diagram of a typical dc MOV

Figure A-1 depicts the dc MOV control circuit with the valve position contacts in the condition they would be in when the valve is fully closed and not operating. The principal circuit failure mode of concern is a hot short leading to the spurious opening of the MOV.

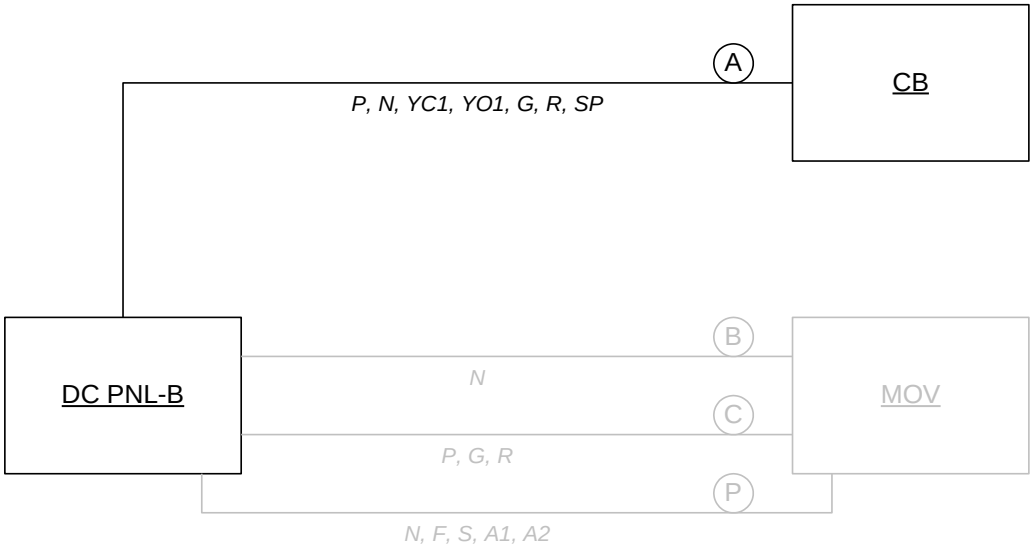

Figure A-2 Block diagram of a dc MOV

The right-hand portion of the circuit schematic diagram (Figure A-1) is of primary interest to this effort as this represents the control portion of the circuit. This is that portion of the circuit fed through the two 10-ampere (A) fuses. That portion to the left of center represents the motor of the MOV itself (that part fed through the 35-A fuses). The intent is not to simulate this portion of the circuit.

With respect to spurious actuation potential, Cable A as shown in the block diagram is the target of interest. This cable does contain all of the conductors necessary to cause a spurious actuation of the valve circuit, and the dc-simulator (dc-SIM) panel for this circuit is based on connections to this cable. The corresponding dc-SIM panel unit implementation is illustrated in Figure A-3. Table A-1 identifies the conductor-to-conductor interactions required to occur within Cable A to cause a specific circuit malfunction, including spurious opening of the valve.

Table A-1 Identification of specific intracable induced circuit failure modes for the dc MOV.

Circuit Failure Effect	Will occur if any of these conductors…	Come into contact with any of these conductors…	Notes
Valve spuriously opens	P, G	YO1	
Loss of valve control	N	YO1, R	Circuit fuse(s) will blow if an attempt is made to open the valve while this internal short condition exists.
Loss of circuit power (blown fuse(s))	P, G	N	
Erroneous/spurious valve position indication	P, G	R	
Loss of valve position indication	—	—	Open circuit failure of conductor G or N.

It is also worthwhile noting that no immediate discernible effect occurs if conductors P, YO1, YC1, or R experience an open circuit failure (conductor break) as the initial failure mode.

The line drawing for the dc MOV control circuit layout may be found in Figure A-3 and the corresponding component arrangements may be seen in

Figure A-4 and Figure A-5. The latter two drawings provide a visual depiction and orientation of components that were used to monitor the specific circuit performance.

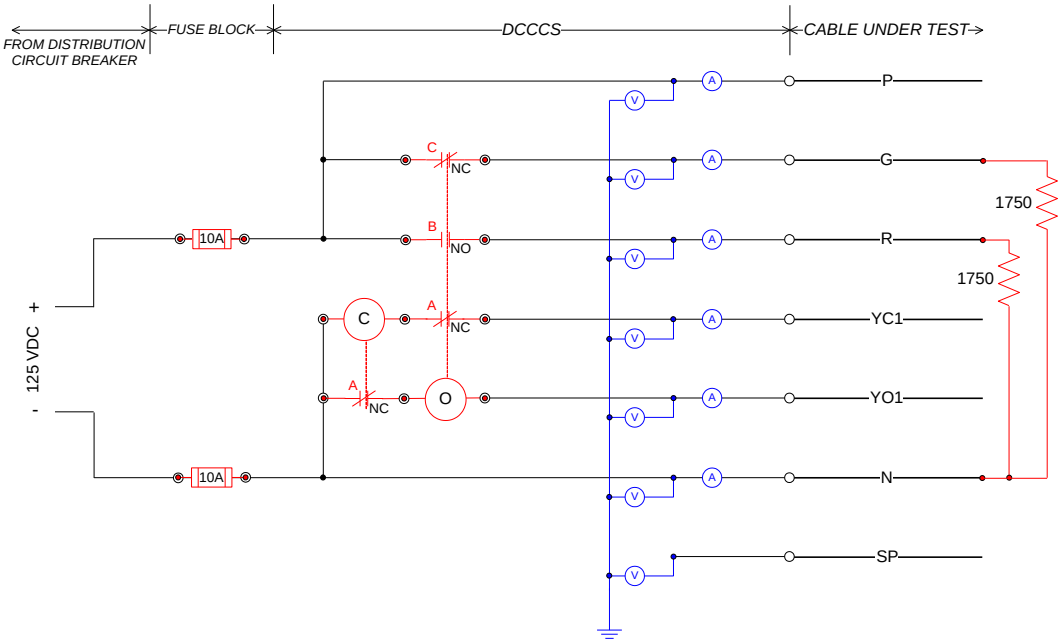

Figure A-3 dc-SIM panel layout for the control circuit on a dc MOV

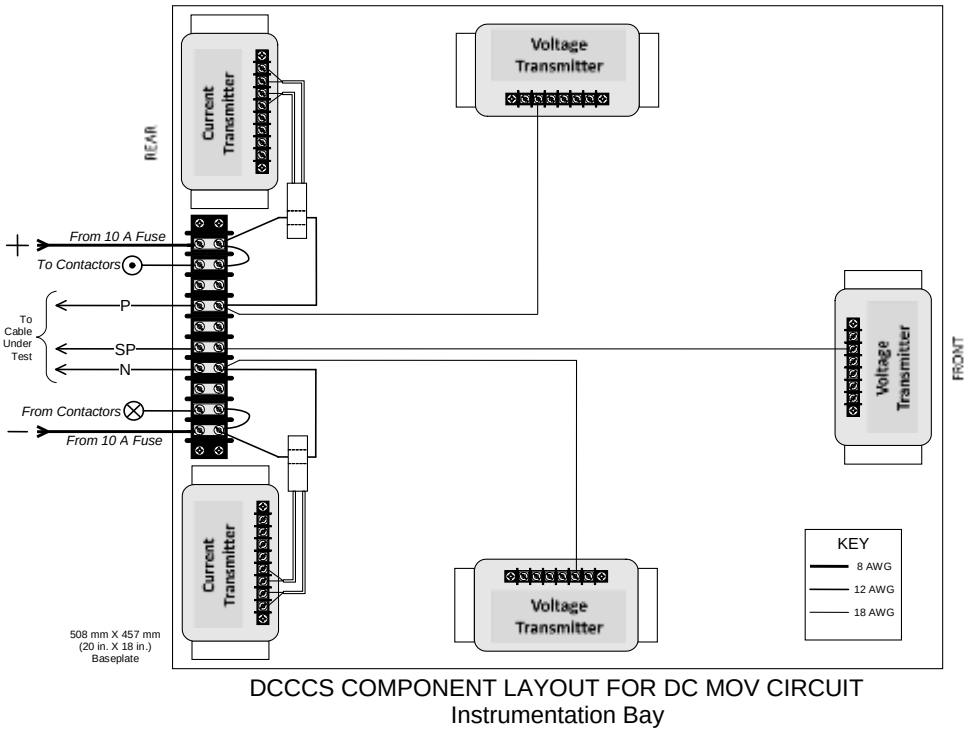

DCCCS COMPONENT LAYOUT FOR DC MOV CIRCUIT
Instrumentation Bay

Figure A-4 dc-SIM panel component arrangement for the dc MOV circuit instrumentation bay

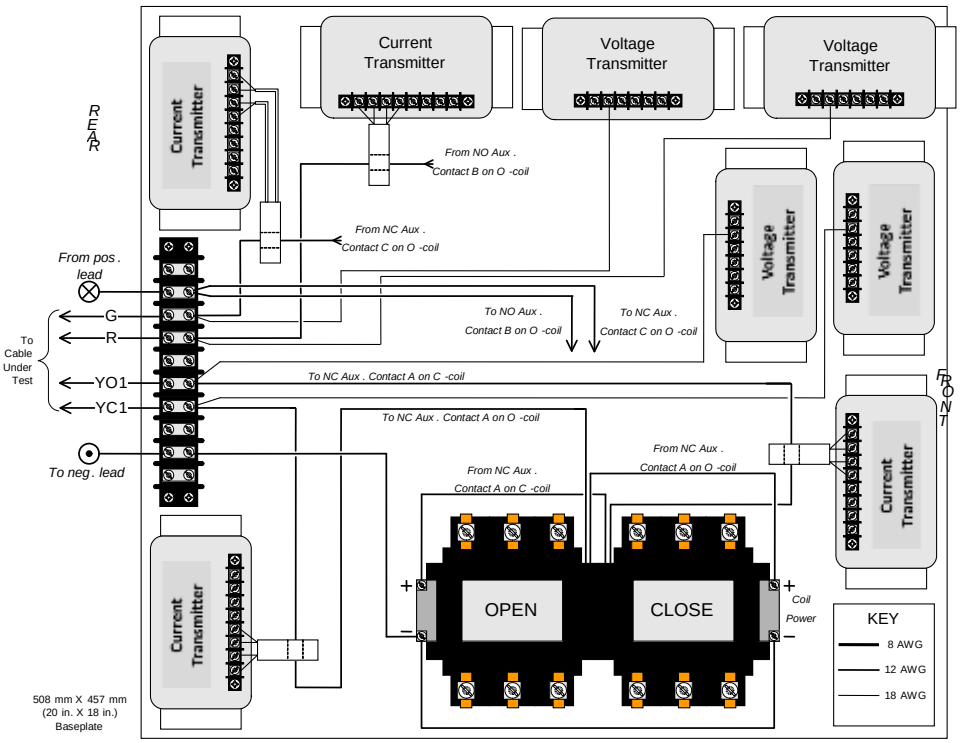

DCCCS COMPONENT LAYOUT FOR DC MOV CIRCUIT
Contactors Bay

Figure A-5 dc-SIM panel component arrangement for the dc MOV circuit contactors bay

The motor starters for MOV circuits were procured through Joslyn Clark[1] and the details, including model numbers and description, may be found in Table A-2.

Table A-2 Description of the motor controller from Joslyn Clark.

250 Volts DC Max		
NEMA Size	Description	Reference No.
1	Open Type dc Coil 2 Pole N.O.	7401-1020-12
Modification & Accessories		
NEMA Size	Description	Reference No.
1	N.O. & N.C. Aux	5M65
1	Mechanical Interlock	5999-4737
1	Reversing Base Plate	23082.79-1

To confirm proper circuit wiring, a procedure was followed to verify current and voltage readings for both circuits. The results of the testing were as anticipated; however, they did not reveal a defect with one of the connected motor controllers. This defect was not observed until a subsequent equipment analysis.

[1] Additional information may be ascertained from the Joslyn Clark catalogue which is available at http://www.joslynclark.com/downloads.htm.

As a part of post-test data analysis, pick-up and drop-out voltage tests were conducted for each of the four individual relay contactor units and the results are summarized in Table A-3. This was not performed before testing because the relay contactor units were delivered by Joslyn-Clark nearly three months late. By the time the units arrived, construction of the entire set of dc surrogate circuits had been completed (with the exception of these relays), and all preparations for testing had been completed. A decision was made to measure the coil resistance for each unit, but to defer the pick-up and drop-out testing and proceed with fire testing.

Table A-3 dc MOV coil characterizations.

Device	Cold Coil Resistance (Ω)	Average Pickup Voltage (Vdc)	Average Pickup Current (A)	Average Dropout Voltage (Vdc)	Average Dropout Current (A)
MOV-1 (open)	154.9	29.0	0.1785	26.6	0.1625
MOV-1 (close)	154.6	89.3	0.4873	4.8	0.0263
MOV-2 (open)	155.3	50.7	0.2867	7.3	0.0420
MOV-2 (close)	155.3	N/A	N/A	N/A	N/A

The close contactor unit for MOV-2 was found to not have a metal slug as part of its movable core assembly. Thus it was incapable of operating when the coil was energized. Current and voltage can still be monitored but implications are discussed below.

During the post-test examination, three of the four in-service relay contactor units tested out as expected, but the fourth unit, the “close” unit in circuit MOV-2, failed to pick up (close) despite application of up to 170 Vdc. An external physical inspection revealed no obvious flaw and the contactor could be closed manually. Also, the voltage and current observed during the pick-up test indicated that the relay coil was in place and operating as expected. A coil resistance measurement also yielded a value that was consistent with pre-test readings.

At this point a decision was made to disassemble the non-functional unit. A second working unit was also disassembled for comparison. This inspection revealed that the moving core was missing from the non-functional unit. Figure A-6 shows the functional unit with the moving core in place and Figure A-7 shows the non-functional unit with the moving core absent. Figure A-8 shows the two units side by side. The relay was received from the manufacturer without the moving core. An inspection was also performed for a fifth (spare) relay contactor unit, and it was found that the spare contactor was also missing the moving core. Hence, two of five relay contactor units obtained directly from Joslyn-Clark were non-functional.

The implications for the data analysis are summarized as follows:

- Circuit MOV-1 is not effected in any way.
- For circuit MOV-2, the “open” contactor was fully functional but the “close” contactor was a non-functional passive coil target only. The “close” contactor was present as an inductive load on the circuit, but the relay would never have closed during testing.
- The data can still be analyzed and interpreted, including for spurious actuations, but the following cases need to be considered:
    - Given an initial hot short to the close coil, the electrical and mechanical interlocks will <u>not</u> engage. A subsequent hot short to the open coil would cause the open coil to close and would trip the close coil out of the circuit via the electrical interlock.

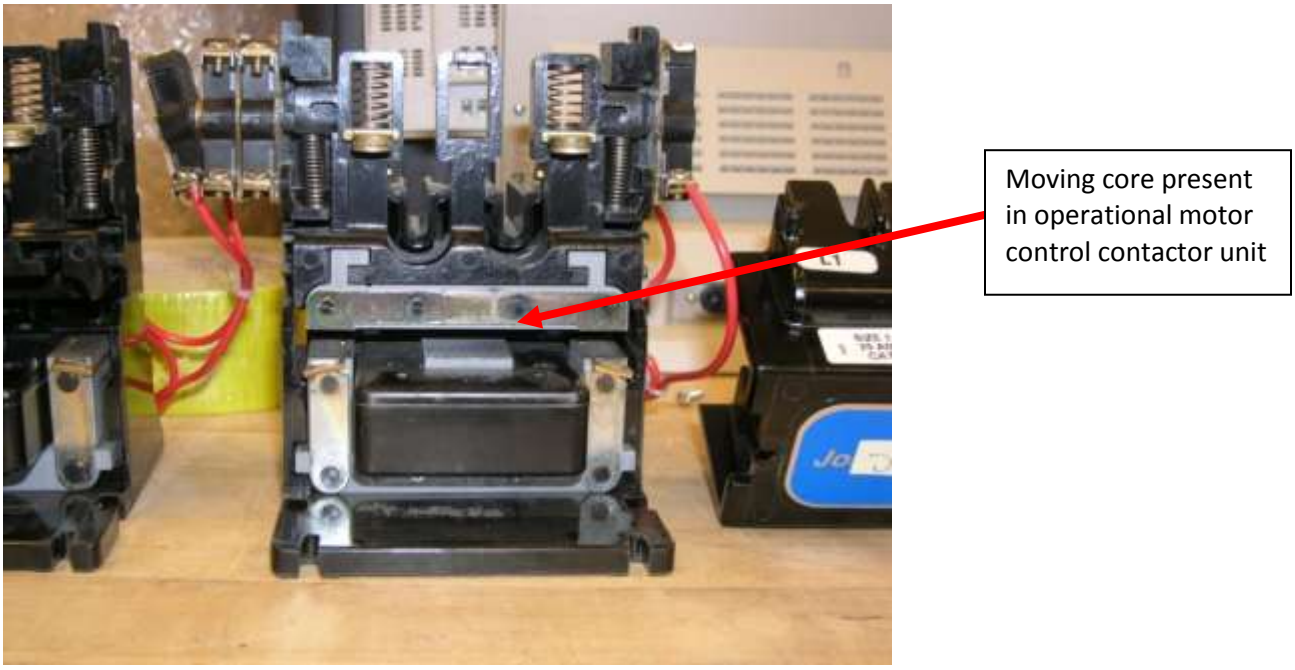

Figure A-6 Open motor controller with functional moving core for the MOV-2 circuit

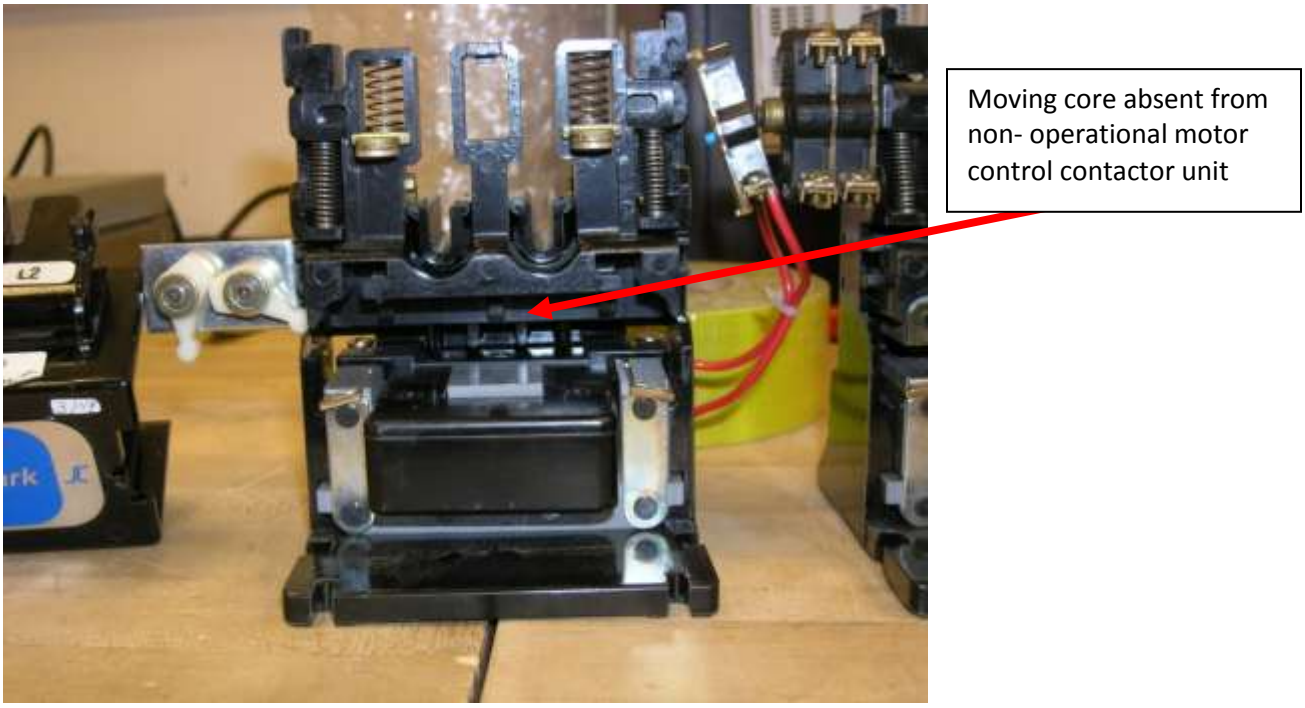

Figure A-7 Close motor controller missing the metal driver for the moving core for the MOV-2 circuit

Figure A-8 Side-by-side comparison of the open and closed motor contactors for the MOV-2 circuit

- Given an initial hot short to the open coil, the open contactor would close, triggering both the mechanical and electrical interlocks. A subsequent hot short to the close coil would behave exactly as if the close contactor was fully functional (i.e., there would be an indication of voltage applied to that circuit path but no current flow).
- Overall, it was not possible to electrically engage (i.e., induce current flow) in both the open and close coils simultaneously despite the non-functional close contactor unit.

A.2 dc-Powered Solenoid-Operated Valve (SOV) Circuits

A.2.1 Circuit Used During Testing

A schematic of a typical small SOV control circuit is shown in Figure A-9. This schematic was derived from an actual plant circuit, and has been used as an example analysis case in the RES/EPRI fire PRA training program. The corresponding block diagram is shown in Figure A-10. The corresponding dc-SIM panel implementation for this circuit, assuming fire-induced failure of Cable B as shown in the block diagram, is the potential concern, is illustrated in Figure A-11. The potential component layout for the SOV circuits may be seen in Figure A-12.

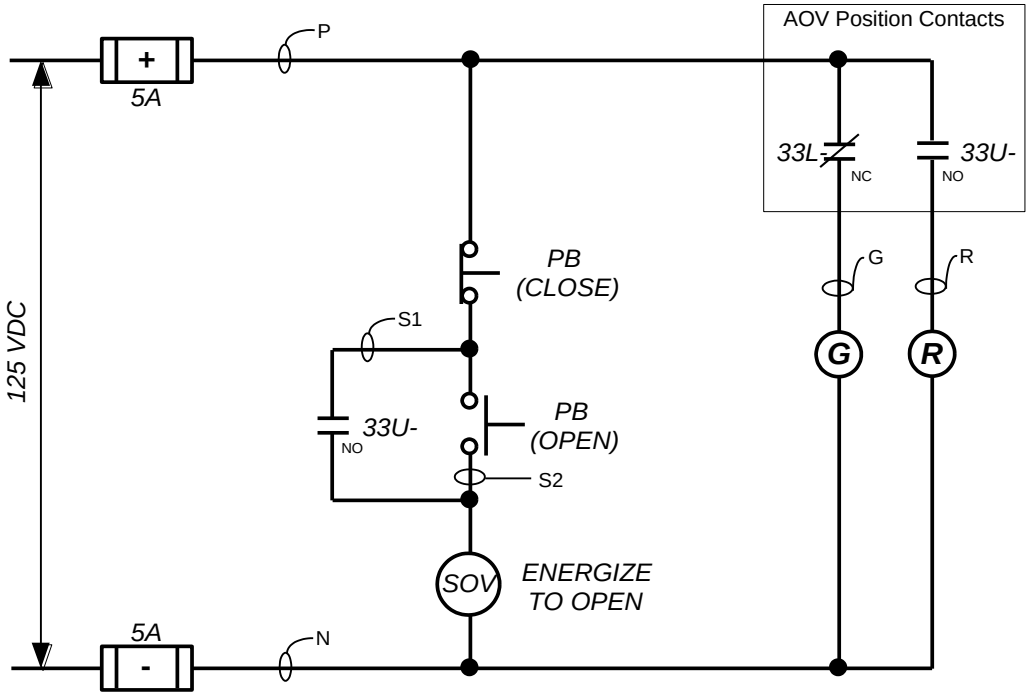

Figure A-9 Electrical schematic diagram for a small SOV

The small solenoid valve is shown in its normally closed position. Table A-4 identifies the conductor-to-conductor interactions required to occur within Cable B to cause a specific circuit failure mode, including spurious opening of the valve.

It is also worthwhile noting that no immediate discernible effect occurs if conductors P, N, S1, S2, or R experience an open circuit failure (conductor break) as the initial failure mode.

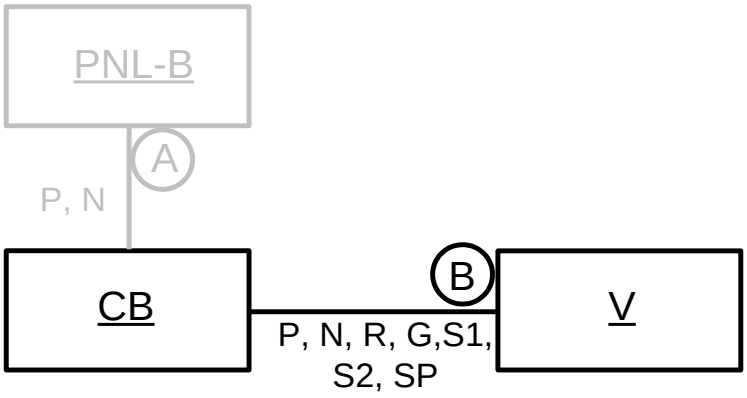

Figure A-10 Block diagram of a small SOV

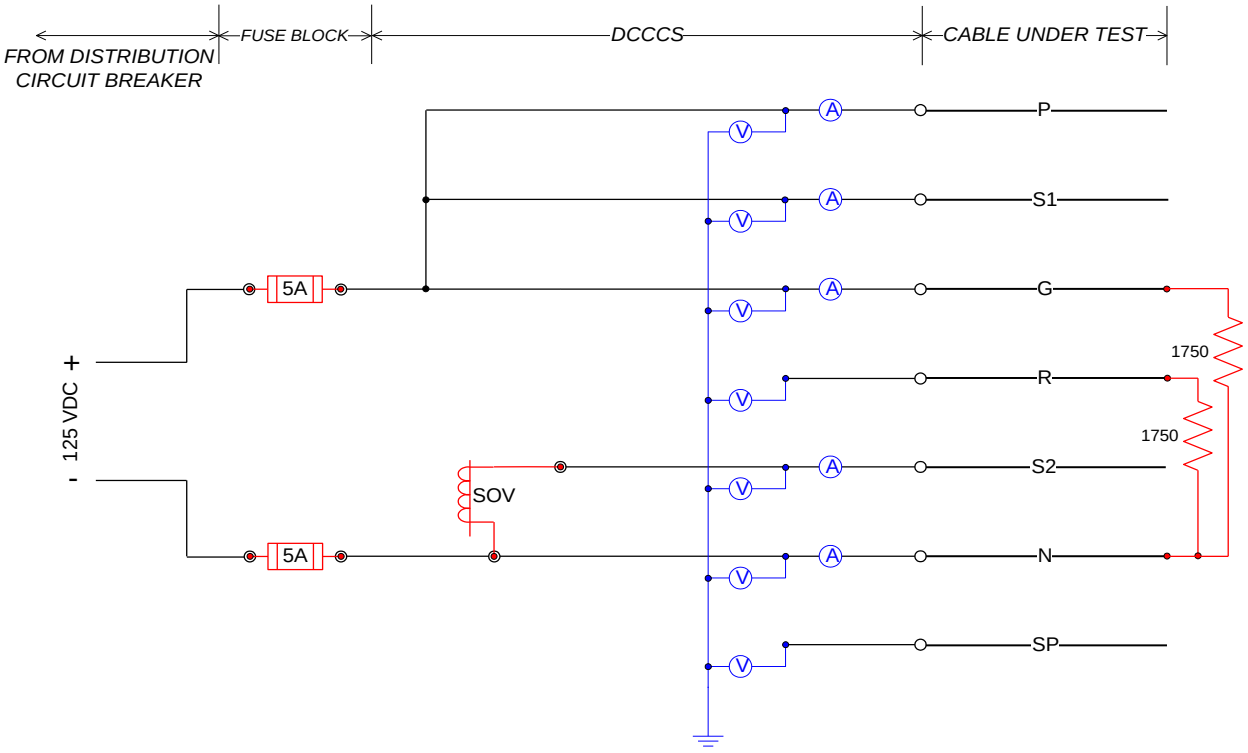

Figure A-11 dc-SIM panel layout for a small SOV dc circuit

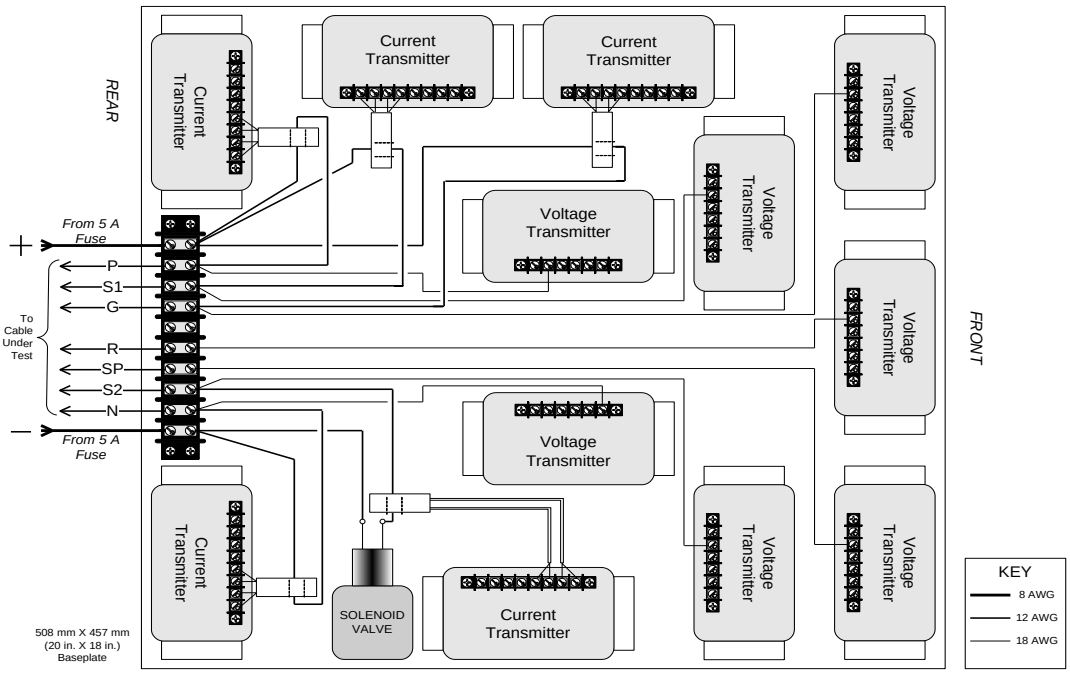

Figure A-12 dc-SIM panel component arrangement for a small SOV dc circuit

Table A-4 Identification of specific intracable induced circuit failure modes for the small SOV.

Circuit Failure Effect	Will occur if any of these conductors…	Come into contact with any of these conductors…	Notes
Valve spuriously opens	P, S1, G	S2	
Loss of valve control	N	S2, R	Circuit fuse(s) will blow if an attempt is made to open the valve while this internal short condition exists.
Loss of circuit power (blown fuse(s))	P, S1, G	N	
Erroneous/spurious valve position indication	P, S1, G	R	
Loss of valve position indication	—	—	Open circuit failure of conductor G.

A.2.2 Alternate SOV Circuit Designs That Were Not Tested but May Exist in Plants

One variation of the basic small solenoid valve circuit is one where the connections to the valve position limit switches and status-indicating lamps are reversed (see Figure A-13). This change then results in a slight change to the conductors connecting the control board (CB) to the valve (V) as shown in Figure A-14. Note that Cable B now does not require conductor P at the valve. P has been replaced with a second spare conductor. Figure A-15 shows the resulting layout of the dc-SIM panel for this modified control circuit for a small SOV. Note that the dc-SIM panel layout for this SOV control circuit scheme requires the use of a separate and

independent cable conductor that is protected and isolated from the fire. It is needed to provide power to one side of the resistors that simulate the status-indicating lamps and tie into the R and G conductors of the cable under test at the other end.

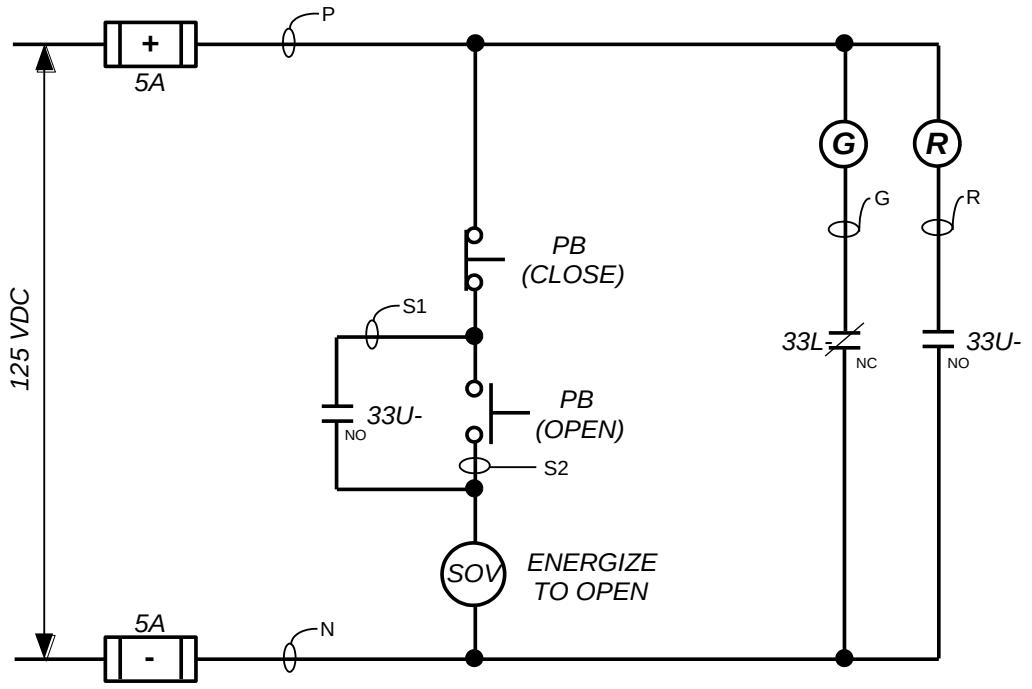

Figure A-13 Electrical schematic diagram for a small SOV with position contacts and status-indicating lamps reversed (not tested)

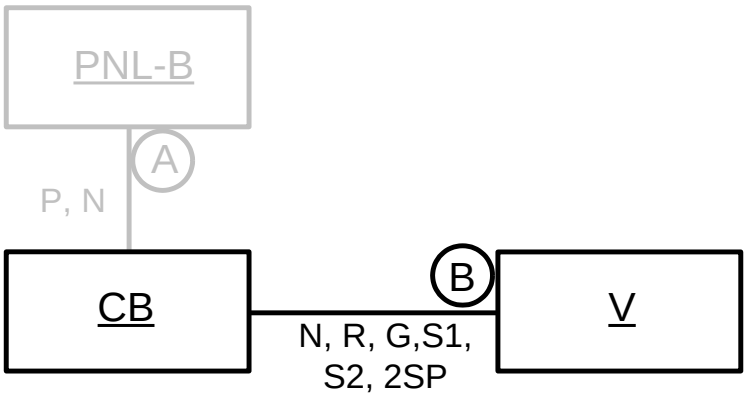

Figure A-14 Block diagram of a small SOV with position contacts and status-indicating amps reversed (not tested)

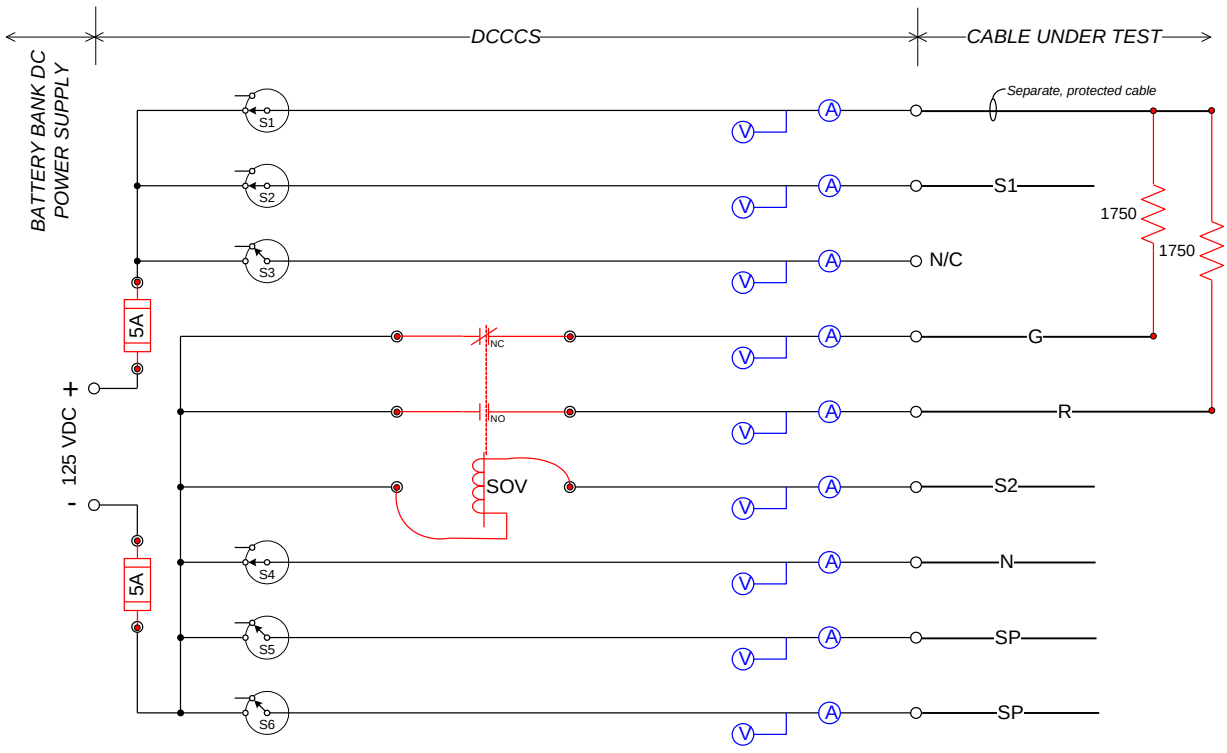

Figure A-15 dc-SIM panel layout for a small SOV dc circuit with position contacts and status-indicating lamps reversed (note the use of a separate independent and protected cable to make needed circuit connections) (not tested)

The small solenoid valve with the valve position limit switches and status-indicating lamps reversed is shown in its normally closed position. Table A-5 identifies the conductor-to-conductor interactions required to occur within Cable B to cause a specific circuit failure mode, including spurious opening of the valve. Note that no immediate discernible effect occurs if conductors N, S1, S2, or R experience an open circuit failure (conductor break) as the initial failure mode.

Table A-5 Identification of specific intracable induced circuit failure modes for the small SOV with position contacts and lamps reversed. (not tested)

Circuit Failure Effect	Will occur if any of these conductors…	Come into contact with any of these conductors…	Notes
Valve spuriously opens	S1 / P	S2	
Loss of valve control	N, G	S2	Circuit fuse(s) will blow if an attempt is made to open the valve while this internal short condition exists.
Loss of circuit power (blown fuse(s))	S1	N, G	
Erroneous/spurious valve position indication	N	R	
Loss of valve position indication	—	—	Open circuit failure of conductor G.

Although reversing the indicating lights is an option, because of the specific valve chosen for creation of the SOV circuit, the circuits may only be tested in the normal configuration. After experimental results and experiences are gleaned, this possibility may be revisited.

The SOV circuits utilized two ASCO RedHat[2] general service solenoid valves throughout the testing program. Information for these two solenoids may be found in Table A-6.

Table A-6 SOV information.

Circuit	Item	Series	Part Order Number
SOV-1	Solenoid Operated Valve	ASCO RedHat Series 8320	8320G172
SOV-2	Solenoid Operated Valve with Class H Coil	ASCO RedHat Series 8320	EFHT8320G172

Based on recommendations from the peer review committee, SOV-2 used a continuous-duty Class H coil. Continuous-duty Class H coils are required for battery-charging circuits where wider voltage ranges are typically encountered. Based on the manufacturer's literature, the Class H coils will accommodate continuous duty over a wider voltage range; namely, 12% over normal and 28% under normal rated coil voltage. For a nominal 125-Vdc coil, this translates to a voltage range of 90 to 180-Vdc.

Also note that the wiring of the dc SOVs was not polarity-specific. That is, the two lead wires to the solenoid coil could be connected without consideration of the power source polarity. A member of the peer team clarified that dc solenoids are often configured with an integral (internal) rectifier, so that they will operate correctly regardless of whether the source applied is alternating current (ac) or dc, and regardless of the dc polarity applied. The SOVs used in DESIREE-Fire appear to be of this type (internally rectified). Hence, a "reverse polarity" dc hot short on an SOV such as those tested here would still cause a spurious operation. A reverse polarity short on a dc solenoid without the internal rectifier would not cause a spurious operation.

Note that the test data has been reviewed for this effect, and no cases were observed that appeared to involve a reverse polarity short to the SOVs. Given the test configurations, a reverse polarity short would require, at a minimum, the following events to occur:

- A positive source conductor must short to the (nominally) negative side of the valve coil. That is, a positive source must short to either conductor N or G as shown in the circuit schematic, thereby "back-feeding" a positive potential to the nominally negative side of the coil. Further, this short circuit must result in clearing of the negative fuse for this circuit (i.e., instead of the positive fuse). Note that the positive source could come from intracable shorting (i.e., with conductor S1) or from intercable shorting to a second cable.
- Because the negative fuse must clear, an independent negative energizing source would need to come into contact with the (nominally) positive side of the valve coil (conductor S2). Given the test configuration, this would require either an intercable hot sort or multiple shorts to ground on the negative battery potential that included conductor S2.

[2] Additional information may be ascertained from the ASCO catalogue, which is available at http://www.ascovalvenet.com/AscoValvenet/Applications/LiteratureRequest/PublicSite/LRPublicWeb.aspx?action=add.

The SOV solenoids were electrically characterized following the intermediate scale tests in order to determine their actual pick-up and drop-out voltage and current thresholds. Table A-7 provides a summary of each SOV's electrical characteristics. Note that the two valves have essentially identical electrical characteristics; that is, the Class H coil appears to have no impact on pick-up voltage, pick-up current, or drop-out voltage.

Table A-7 Small dc SOV solenoid characterizations.

Device	Cold Coil Resistance	Average Pick-up Voltage (Vdc)	Average Pick-up Current (A)	Average Dropout Voltage (Vdc)	Average Dropout Current (A)
SOV-1	1280	56.9	0.042	43.8	0.033
SOV-2	1270	55.2	0.042	43.8	0.033

A.3 dc-Powered 1-Inch Solenoid Valve and Large Coil

A.3.1 Alternate PORV and 1-inch SOV Circuit Designs Not Tested

The power-operated relief valve (PORV) simulated circuit, Figure A-16, was of similar construction to that shown for the SOV in Figure A-9. This design was also based on circuits used in the fire PRA training course. For the PORV circuit, the valve coil is much larger coil and the fusing is correspondingly larger. The block diagram, Figure A-17, is also similar. The dc-SIM panel implementation of this circuit is shown in Figure A-18. Again, the dc-SIM panel implementation assumes that fire-induced failure of Cable B in the block diagram is the potential spurious actuation concern.

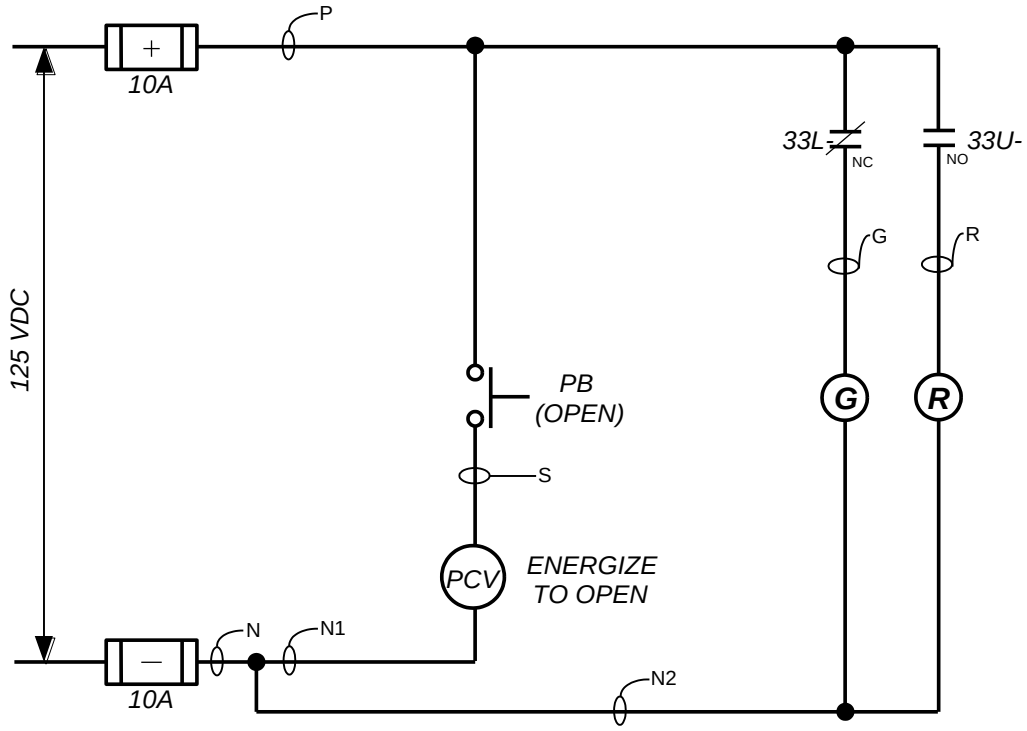

Figure A-16 Electrical schematic diagram of a typical PORV

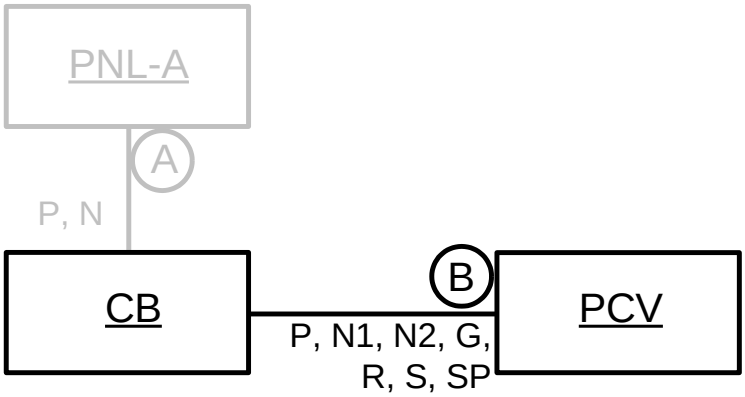

Figure A-17 Block diagram of a dc PORV

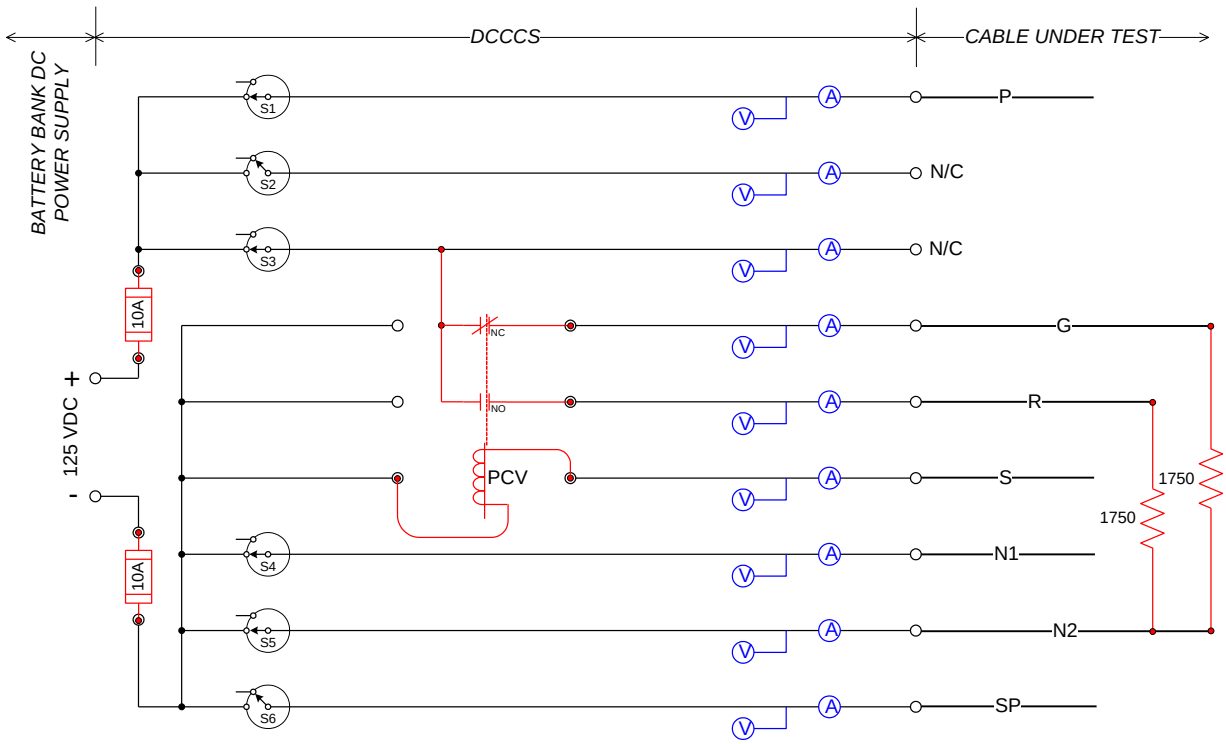

Figure A-18 dc-SIM panel layout of a typical dc PORV control circuit

Figure A-18 shows the PORV in its normally closed position. Table A-8 identifies the conductor-to-conductor interactions required to occur within Cable B to cause a specific circuit failure mode, including spurious opening of the valve.

It is also worthwhile noting that no immediate discernible effect occurs if conductors P, N1, S, or R experience an open circuit failure (conductor break) as the initial failure mode.

Table A-8 Identification of specific intracable induced circuit failure modes for the PORV.

Circuit Failure Effect	Will occur if any of these conductors…	Come into contact with any of these conductors…	Notes
Valve spuriously opens	P, G	S	
Loss of valve control	N1, N2	S, R	Circuit fuse(s) will blow if an attempt is made to open the valve while this internal short condition exists.
Loss of circuit power (blown fuse(s))	P, G	N1, N2	
Erroneous/spurious valve position indication	P, G	R	
Loss of valve position indication	—	—	Open circuit failure of conductor N2 or G.

One variation of the basic PORV circuit is one where the connections to the valve position limit switches and status-indicating lamps are reversed (see Figure A-19). This change then results in a slight change to the conductors connecting the control board (CB) to the valve (V) as shown in Figure A-20. Note that Cable B now does not require conductor P at the valve. P has been replaced with a second spare conductor. Figure A-21 shows the resulting layout of the dc-SIM panel for this modified control circuit for a PORV. Note that the dc-SIM panel layout for this valve control circuit scheme requires the use of a separate and independent cable conductor that is protected and isolated from the fire. It is needed to provide power to one side of the resistors that simulate the status-indicating lamps and tie into the R and G conductors of the cable under test at the other end. A second conductor in that separate cable is used to tie the downstream ends of the position switch contacts to N2 in the test cable.

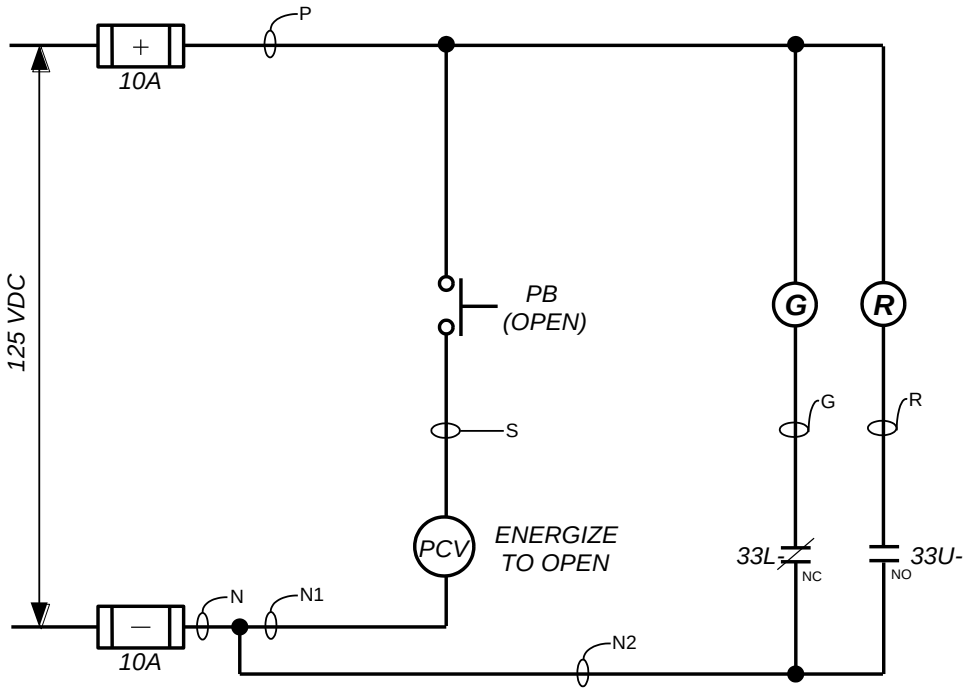

Figure A-19 Electrical schematic diagram for a PORV with position contacts and status-indicating lamps reversed (not tested)

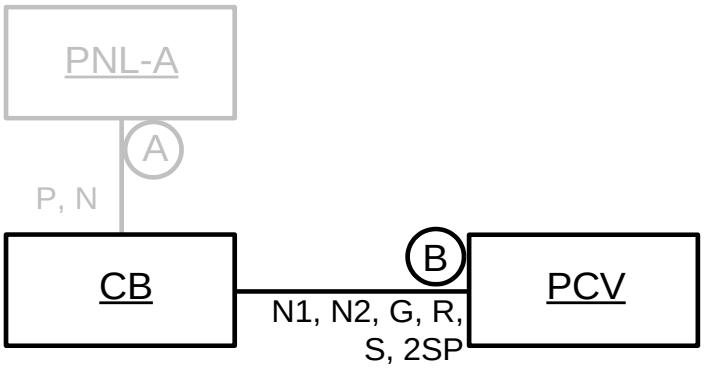

Figure A-20 Block diagram of a PORV with position contacts and status-indicating lamps reversed (not tested)

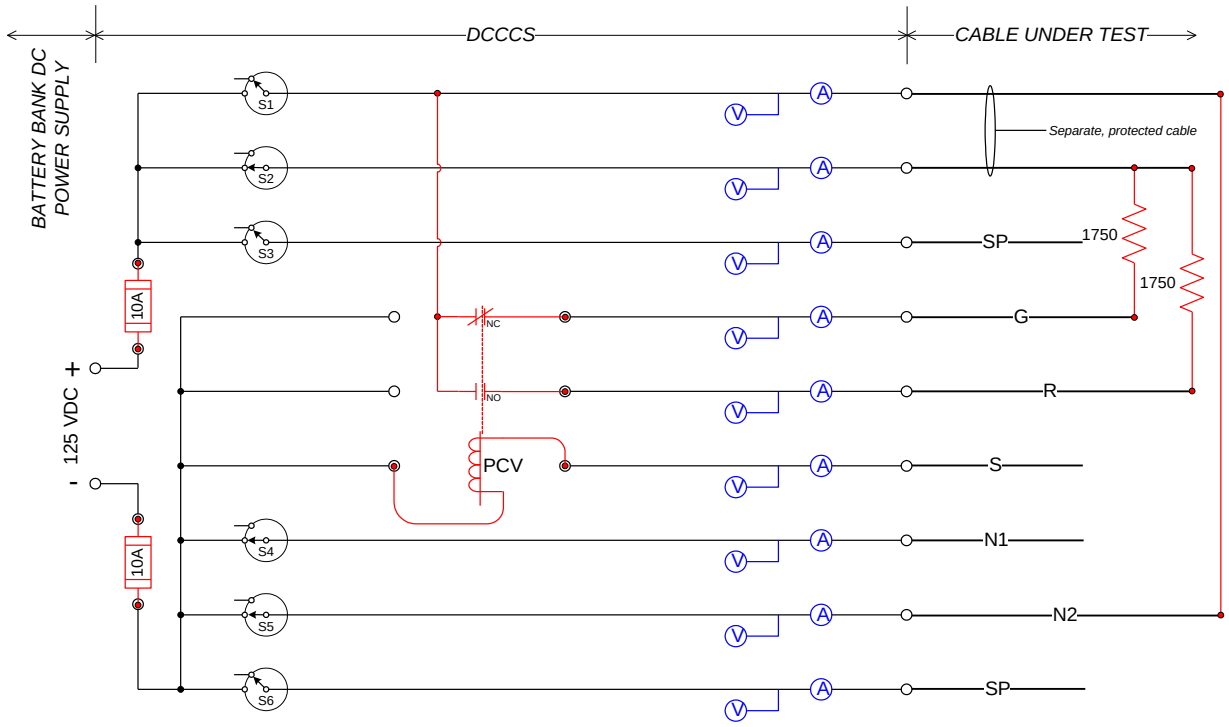

Figure A-21 dc-SIM panel layout for a PORV dc circuit with position contacts and status-indicating lamps reversed (not tested)

The PORV with the valve position limit switches and status-indicating lamps reversed is shown in Figure A-21 in its normally closed position. Table A-9 identifies the conductor-to-conductor interactions required to occur within cable B to cause a specific circuit failure mode, including spurious opening of the valve. Note that no immediate discernable effect occurs if conductors N1, S, or R experience an open circuit failure (conductor break) as the initial failure mode.

Table A-9 Identification of specific intracable induced circuit failure modes for the PORV with position contacts and lamps reversed. (not tested)

Circuit Failure Effect	Will occur if any of these conductors…	Come into contact with any of these conductors…	Notes
Valve spuriously opens	—	—	No energized conductors in Cable B.
Loss of valve control	N1, N2	S	Circuit fuse(s) will blow if an attempt is made to open the valve while this internal short condition exists.
Loss of circuit power (blown fuse(s))	—	—	No energized conductors in Cable B.
Erroneous/spurious valve position indication	N1, N2	R	
Loss of valve position indication	—	—	Open circuit failure of conductor N2 or G.

Another variant of the basic PORV circuit to be explored is one where the valve actuating coil is isolated by double switch contacts (see Figure A-22). This change is implemented to assess

how much less vulnerable this design is to a spurious operation over the standard, non-isolated design. Cable B, connecting the control board (CB) to the valve (V) as shown in Figure A-23, is still the target cable of concern. Figure A-24 shows the resulting layout of the dc-SIM panel for this version of the PORV control circuit.

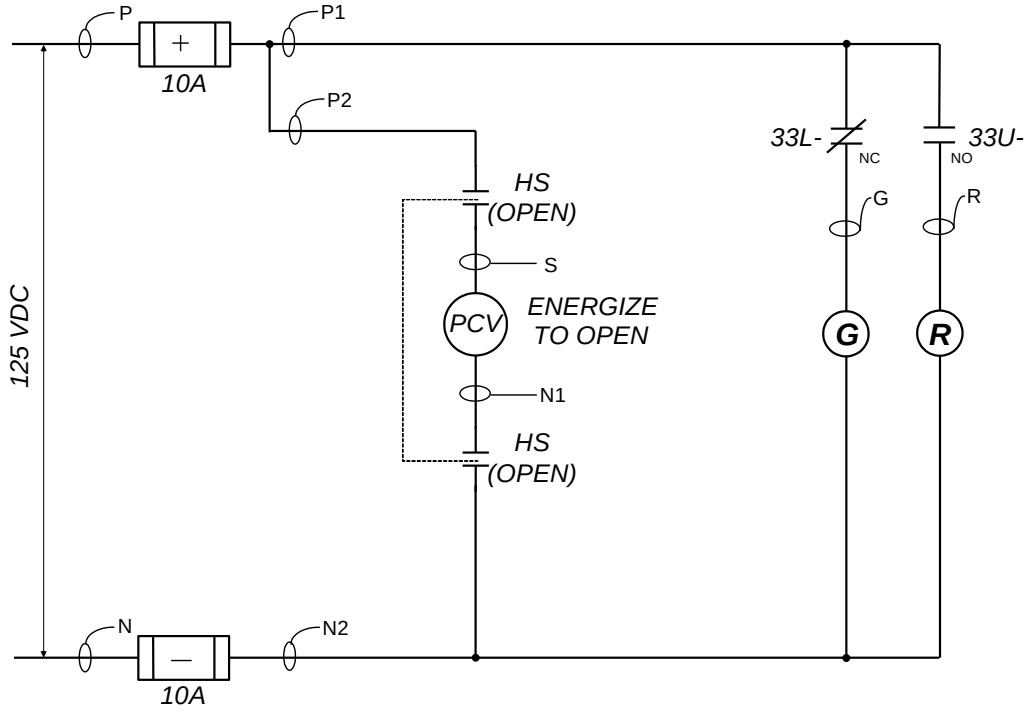

Figure A-22 Electrical schematic diagram of a PORV with double contacts (not tested)

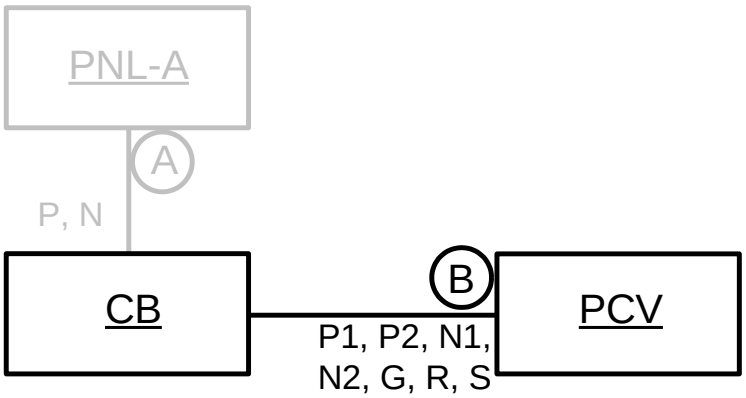

Figure A-23 Block diagram of a PORV with double contacts (not tested)

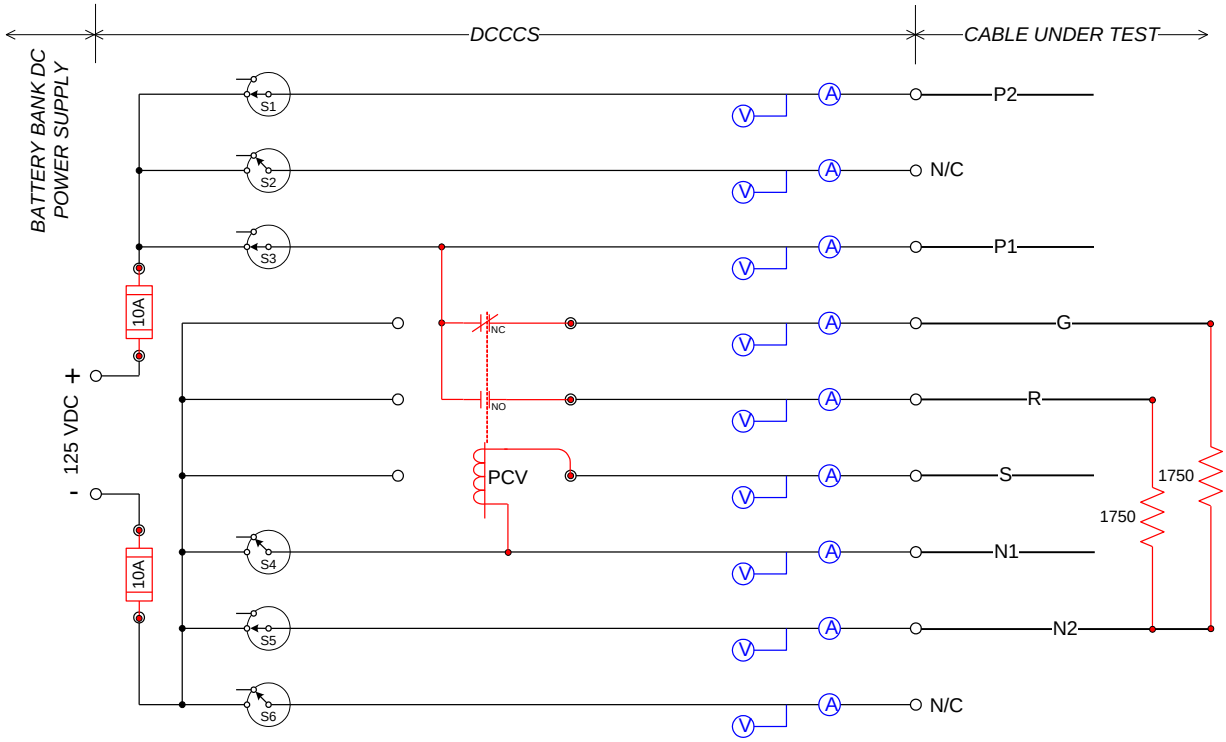

Figure A-24 dc-SIM panel layout for the PORV with double contacts (not tested)

The PORV with the dual isolation switches is shown in Figure A-24 in its normally closed position. Table A-10 identifies the conductor-to-conductor interactions required to occur within Cable B to cause a specific circuit failure mode, including spurious opening of the valve.

Table A-10 Identification of specific intracable induced circuit failure modes for the PORV with double contacts. (not tested)

Circuit Failure Effect	Will occur if any of these conductors…	Come into contact with any of these conductors…	Notes
Valve spuriously opens	P1, P2, G → S **AND** N2 → N1		
Loss of valve control	N2	S, R	Circuit fuse(s) will blow if an attempt is made to open the valve while this internal short condition exists.
Loss of circuit power (blown fuse(s))	P1, P2, G	N2	
Erroneous/spurious valve position indication	P1, P2, G	R	
Loss of valve position indication	—	—	Open circuit failure of conductor N2 or G.

Note that no immediate discernible effect occurs if conductors P1, P2, N1, S, or R experience an open circuit failure (conductor break) as the initial failure mode.

A.3.2 Tested Circuits for 1-inch SOV ASSEMBLY and Large Coil

Two valves were obtained for the purposes of Direct Current Electrical Shorting in Response to Exposure-Fire (DESIREE–Fire), namely a “1-Inch Valve” and a “Large Coil.” The line illustrations providing the overall description of the circuits may be found in Figure A-25 and Figure A-27. Potential component layouts for each of the two valves may be found in Figure A-26 and Figure A-28. Because of time constraints and the limited amount of experiments, it was decided to focus on the normal configuration rather than the reversed indicating light option. After initial results and experimental experiences, this option may be revisited.

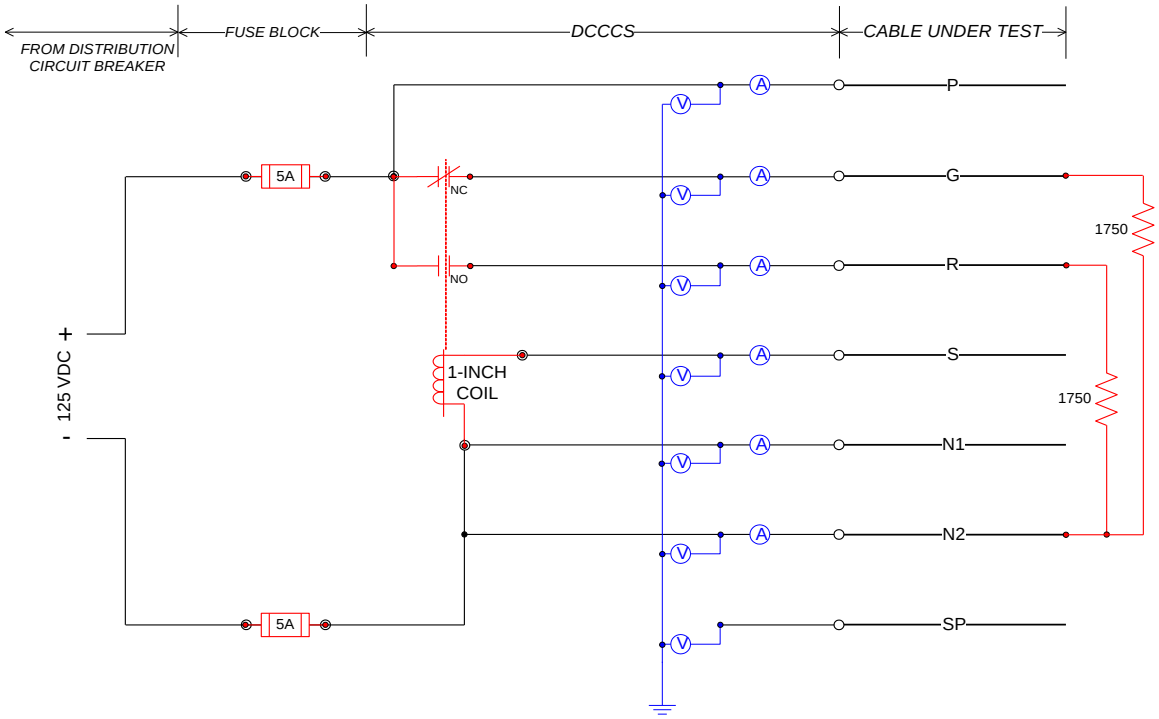

Figure A-25 Line drawing of the dc-SIM panel layout for a 1-inch coil circuit

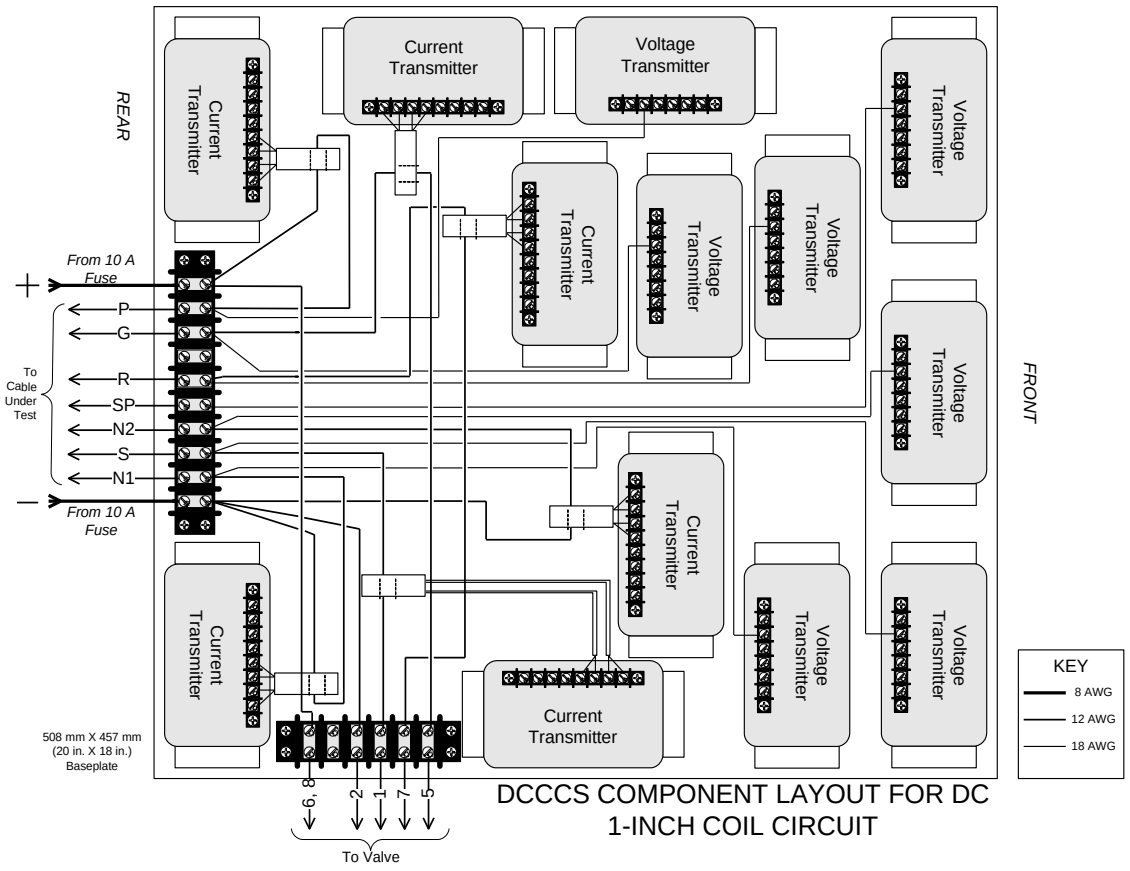

Figure A-26 Component layout for the dc 1-inch coil circuit

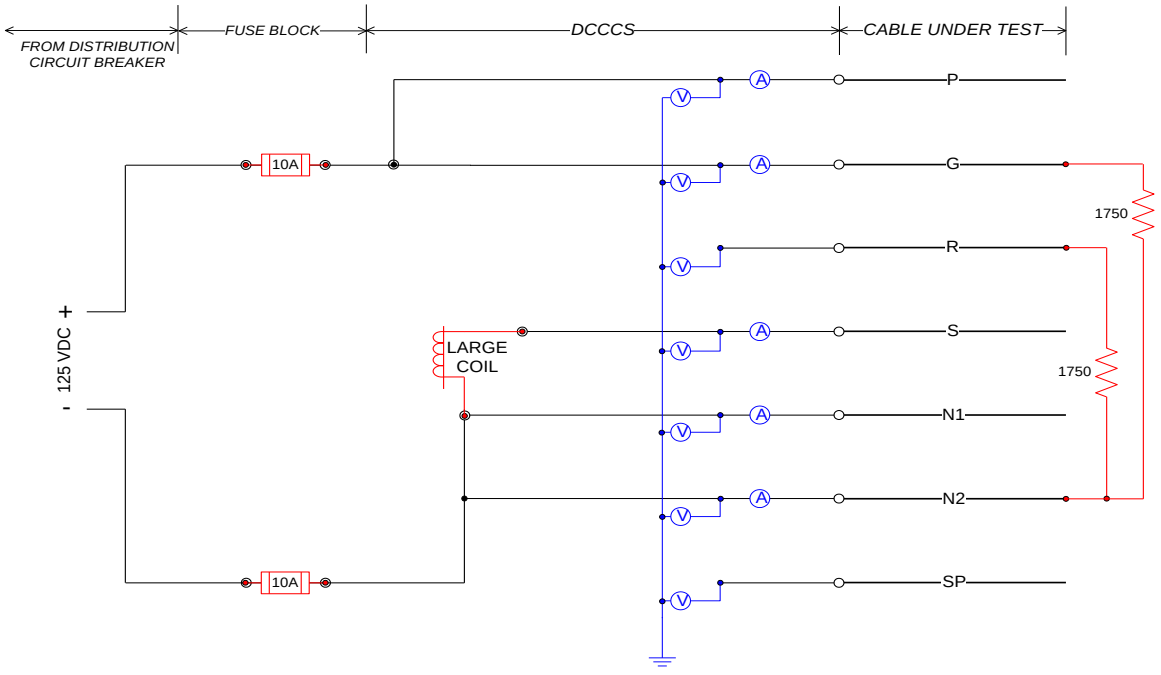

Figure A-27 Line drawing for the dc large coil circuit

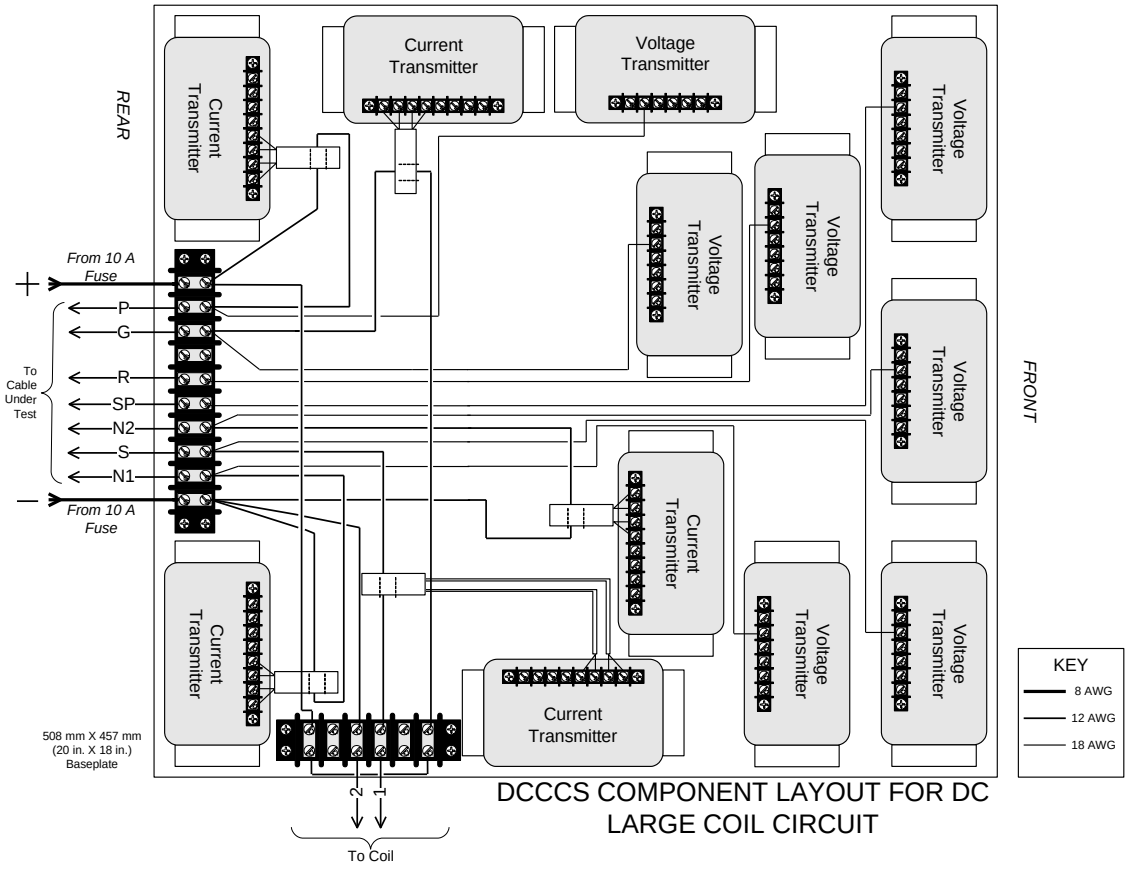

Figure A-28 Component layout for the dc large coil circuit

The 1-Inch SOV solenoid was electrically characterized following the intermediate-scale tests in order to determine its actual pick-up and drop-out voltage and current thresholds. Table A-8 provides a summary of the SOV's electrical characteristics. Since it has no moving parts to determine when pick-up or drop-out occurs, the large coil was not characterized electrically.

Table A-11 1-inch SOV solenoid characterizations.

Device	Cold Coil Resistance	Average Pick-up Voltage (Vdc)	Average Pick-up Current (A)	Average Dropout Voltage (Vdc)	Average Dropout Current (A)
1-inch coil	158.8	47.9	0.30	17.2	0.11
Large Coil	36	N/A	N/A	N/A	N/A

A.4 dc-Powered Switchgear Breaker Circuit

A.4.1 General Design Information

There were two different SWGR breaker circuits used during DESIREE testing. The first SWGR circuit is displayed in Figure A-29. The internal manufacturer's wiring of this SWGR was reversed based on the assumed manufacturer's wiring displayed in Figure A-31. The second SWGR circuit is displayed in Figure A-30. During intermediate scale test #8, the first SWGR had an incident which acknowledged this wiring defect. This is described in detail in Section A.4.2. The reverse wiring did not affect the functionality of the SWGR. The block diagram provided in Figure A-32 depicts the location of the switchgear in the NPP and Cable A represents the test cable. The corresponding dc-SIM panel implementation is illustrated in Figure A-33. Note that the dc-SIM panel breaker design includes both 15-A and 35-A fuses, each set feeding different portions of the control circuit. In this case, the larger fuse set powers the breaker trip circuit and the smaller set powers the breaker close portion of the circuit.

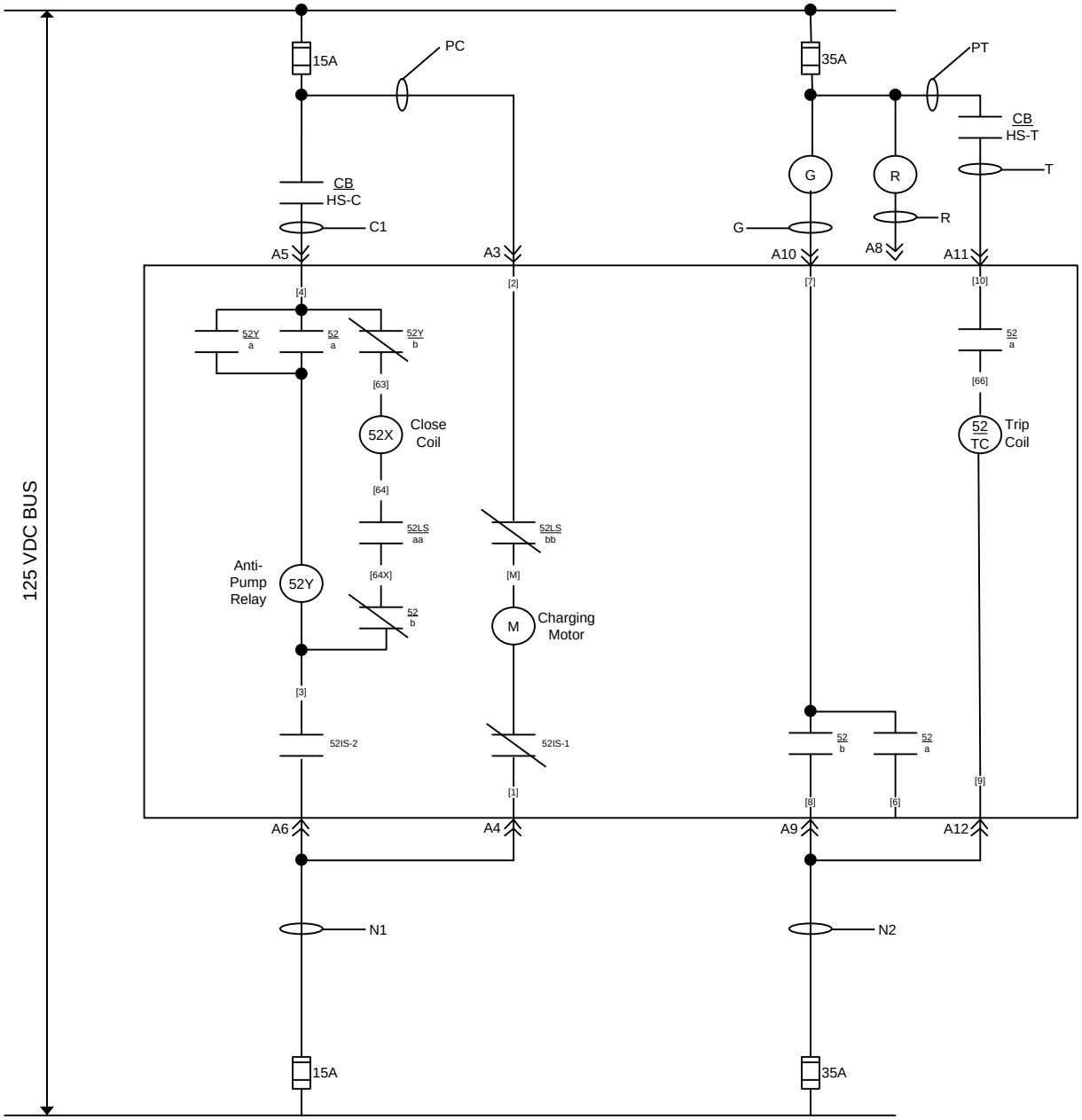

Figure A-29 Line Drawing for dc SWGR 1 Circuit

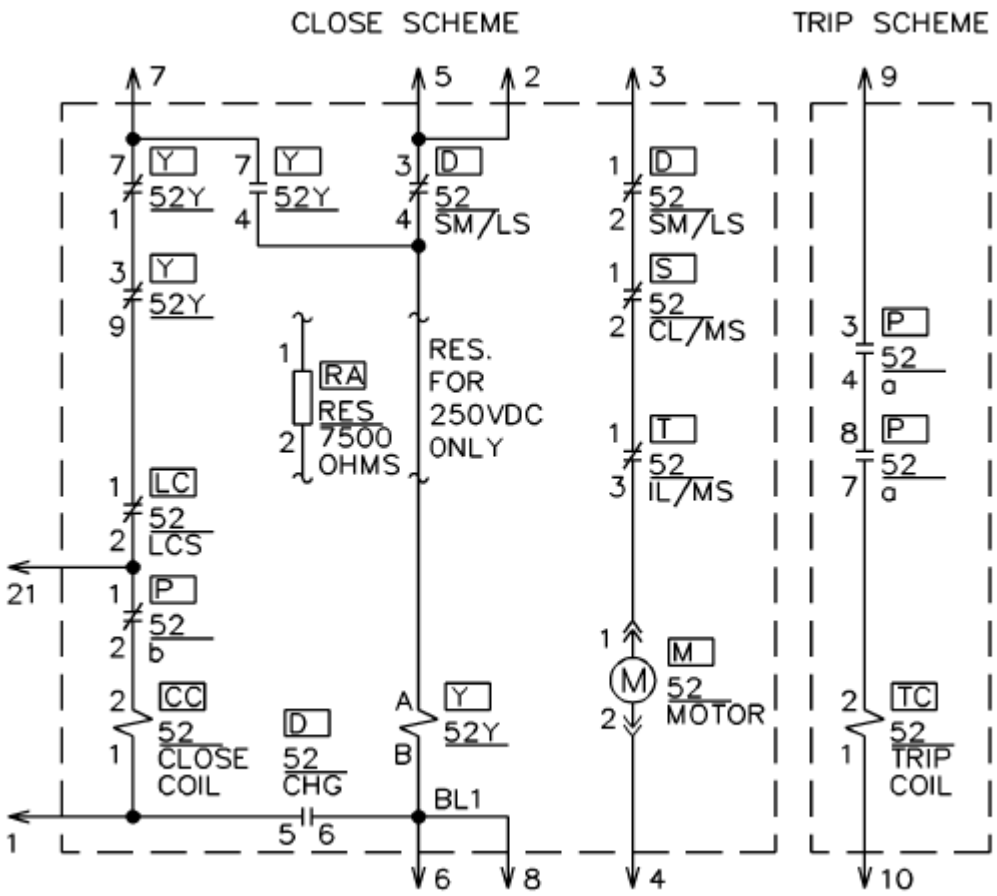

Figure A-30 Line Drawing for dc SWGR 2 Circuit

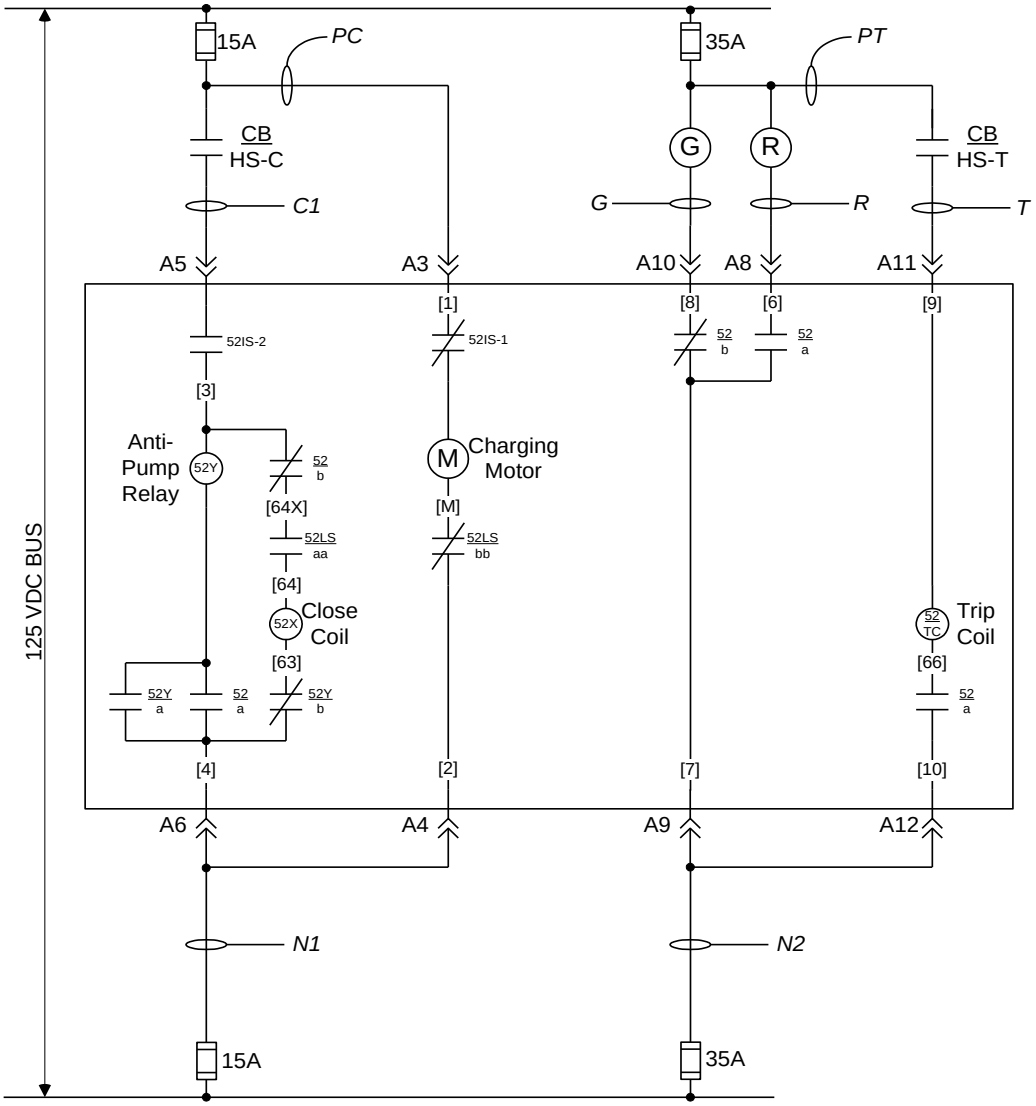

Figure A-31 Electrical schematic diagram for typical 4160-VAC switchgear, manufacturer's wiring

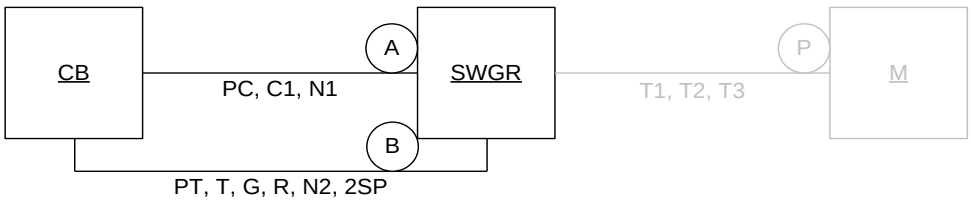

Figure A-32 Block diagram for typical 4160-VAC switchgear

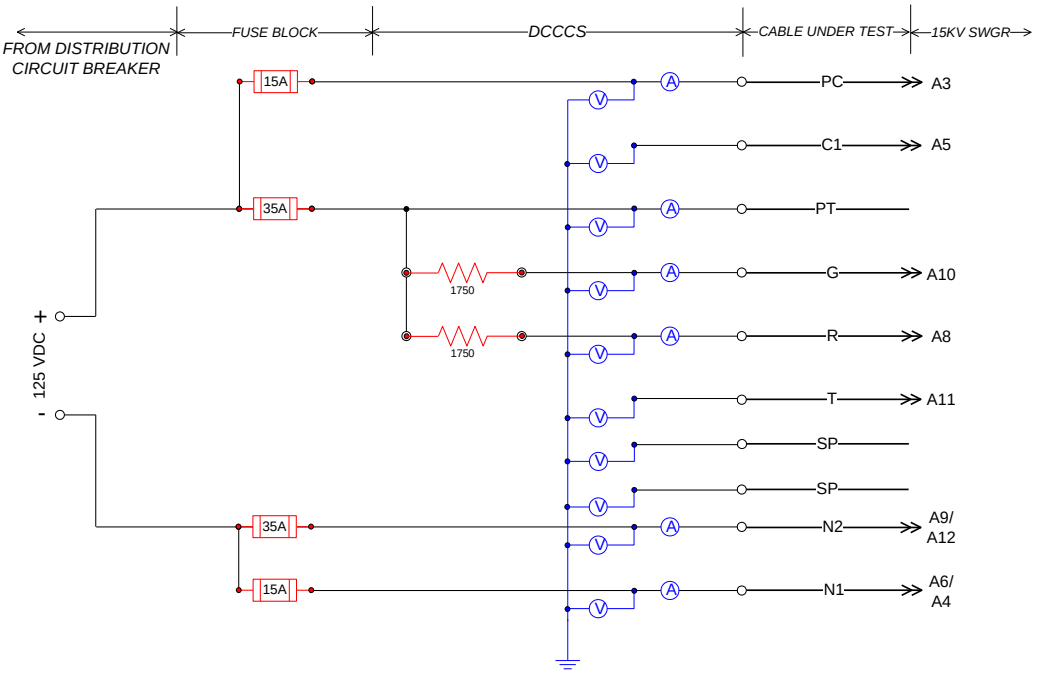

Figure A-33 dc-SIM panel layout for the control circuit on a typical 4160-VAC switchgear

Figure A-34 shows a representative schematic of a dc control circuit for a 4.16-kV vacuum-operated circuit breakers. The anti-pumping circuitry shown in red is of interest in this test program to determine the effects that it has on limiting the occurrence of multiple repetitive spurious actuations, or actuation after the breaker had been tripped by operator actions.

This aspect of the circuit, the anti-pumping feature, was not simulated; rather, it was an inherent feature of the breaker units used in testing. Breaker spurious actuation status and the "Y" anti-pumping coil status were monitored during the testing and recorded on the data acquisition system.

Note that in practice, the trip and close circuits were powered through separate breakers in the dc battery bank power distribution system. This is not typical of in-plant practice, but has no effect on circuit performance. Primary circuit protection is provided by the 15-A and 35-A fuses, and the breakers were installed as a personnel safety measure. Appendix A.7 provides additional detail on the power distribution system.

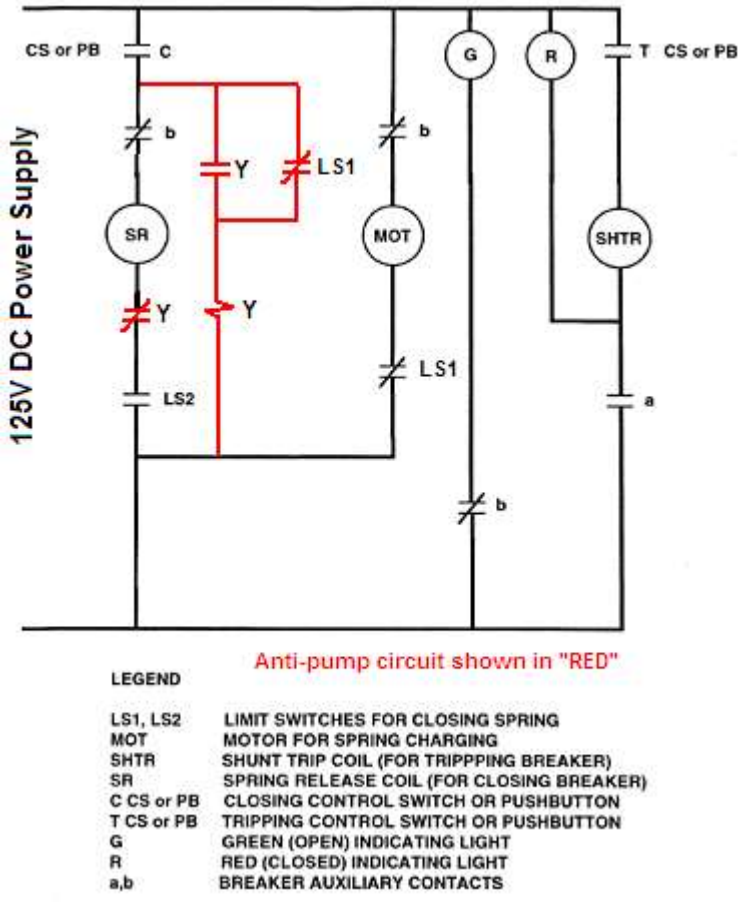

Figure A-34 4.16-kV circuit breaker schematic

Figure A-35 and Figure A-36 represent the layout of components for the switchgear circuit within the simulator racks.

A.4.2 15-kV Circuit Breaker Damage Post-Event Investigation

A.4.2.1 Introduction and Purpose

This section describes the events leading up to and the post-event investigation of the DESIREE-Fire intermediate-scale test that led to damage occurring to the 15-kV circuit breaker being used as part of the test series.

On November 17, 2009, Test IS8 was conducted. This test consisted of 13 separate test circuits being served by 17 different test cables. All of the test cables were seven-conductor, No. 12 AWG wires with polyethylene (PE) insulation and enclosed within a polyvinyl chloride (PVC) outer jacket. All of the test cables were laid in standard ladder-type trays with other, so-called “fill” cables. The fill cables were used to provide additional fuel during the fire and were typically of the same type (i.e., TS or TP) to the cable under test. These additional cables were not grounded. The two cables supporting the switchgear (SWGR) close and trip circuits were located in the C position of the intermediate-scale test cell (Figure 3-2 in the main body of this report). They were bundled together with two other test cables—one supporting the MOV-2 circuit and the other supporting the SOV-2 circuit—along with additional fill cables. The principal thermal exposure mode at the C position in the test cell is by hot gas layer rather than by direct plume impingement. The heat source for the test cell is a gas burner located at the

intersection of the long and short centerlines of the cell, and located directly below the center of the cable tray at Position A. The heat release rate is controlled by a gas flow control valve.

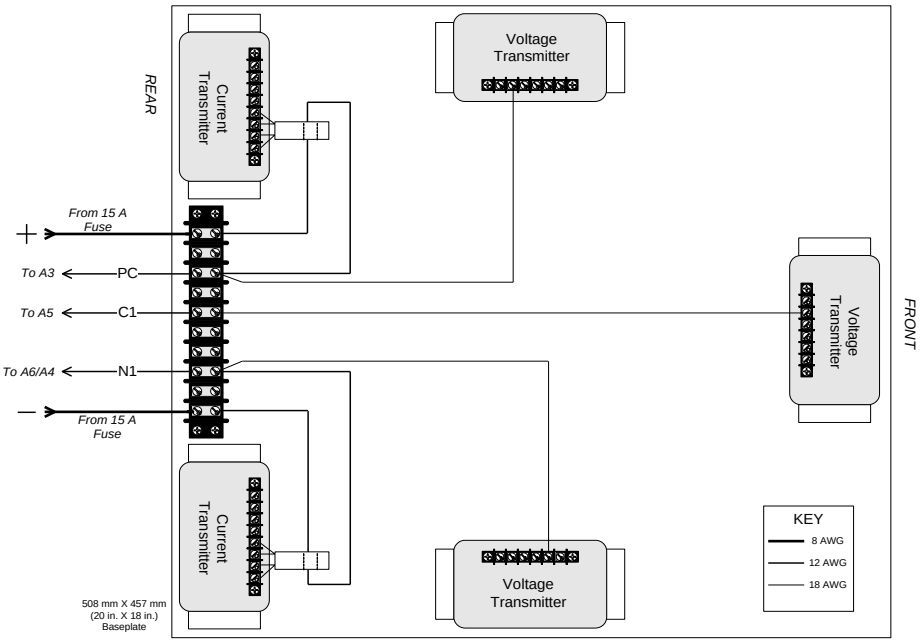

Figure A-35 dc-SIM panel component arrangement for the switchgear control circuit—close circuit (15-A) bay

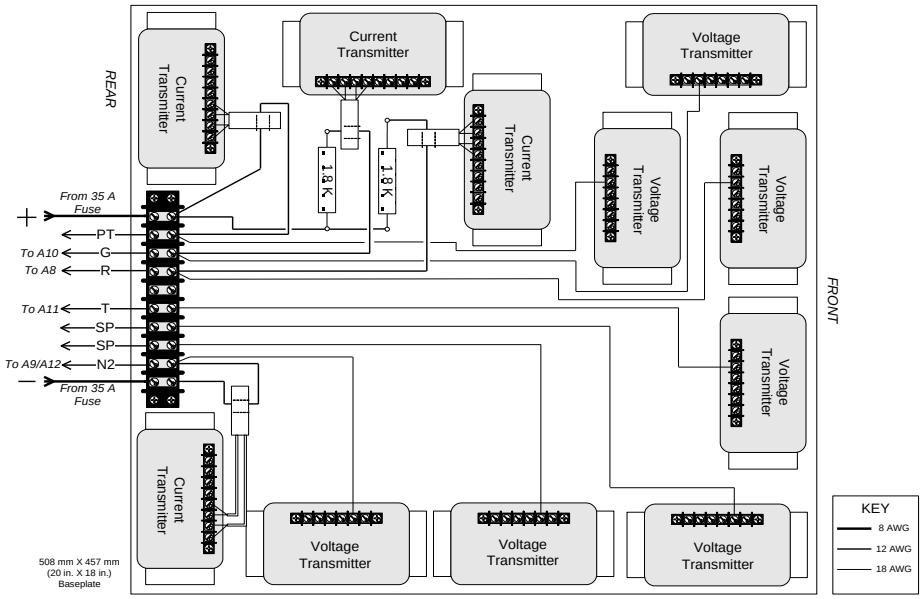

Figure A-36 dc-SIM panel component arrangement for the switchgear control circuit—trip circuit (35-A) bay

Briefly, the test was started at 11:34:25 a.m. At 11:55:34 (approximately 21 minutes into the test) smoke was discovered coming from the interior of the circuit breaker. Flame was not observed. Power to both the close and trip circuits was isolated by opening the 50-A and 60-A circuit breakers. The test run continued for another 21 minutes before being shut down.

A.4.2.2 Test Setup

The 15-kV circuit breaker was connected to the two test cables by a single return cable from the back side of the intermediate-scale Test Cell. Appendix A.7 provided additional detail on the characteristics (wire gauge and lengths) for the various lead cables and a general description of the overall battery power system. To summarize, the two switchgear circuit cables (close and trip) were connected to the circuit lead cables, run from the dc-SIM panels in the instrument trailer to the igloo test bunker, by use of a junction box located on the floor of the test bunker. Battery power to the switchgear circuits came into the dc-SIM panels via load cables from the two breaker panels located on the side of the battery trailer. The switchgear's close circuit was routed through a 50-A circuit breaker in the breaker panel and the trip circuit through a 60-A circuit breaker. The cables feeding the individual circuit breakers were run through conduit from the main battery disconnect switch, also located on the outside of the battery trailer. It should be noted that these breakers were provided mainly for personnel protection and were not intended to provide primary protection to the test circuit. Primary protection is provided by the individual trip and close circuit fuses.

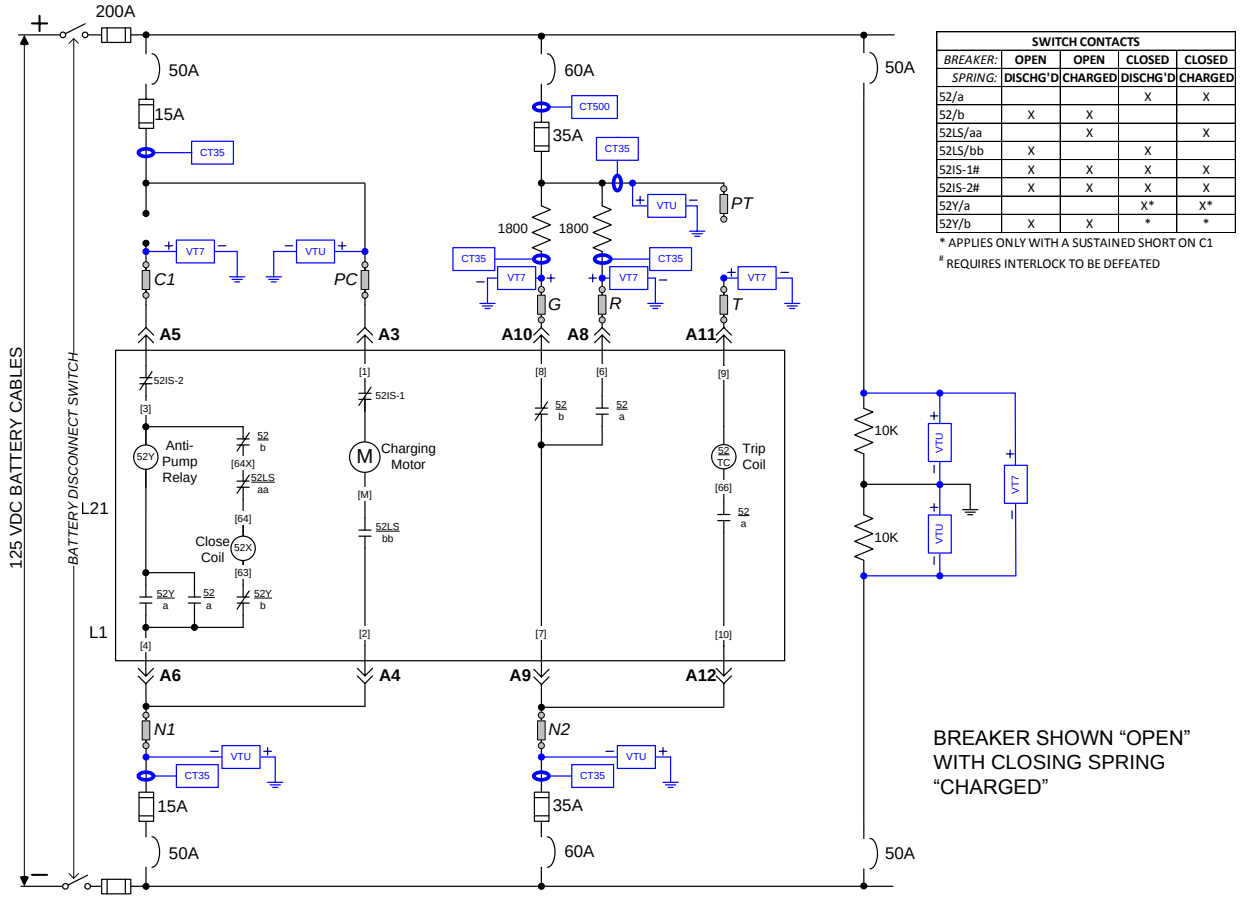

Elementary Diagram for DSE 15KV Switchgear 125VDC Control Circuit
(from Fig. 1-6 in SU-6150-2A, MARCH 1978)

Figure A-37 Elementary diagram for the 15-kV switchgear showing normal connections to the test cables

Figure A-37 shows the normal configuration of the switchgear circuit connections to the dc-SIM panel and the interfacing test cables. In the figure, the diagnostic information is represented by boxes designated as "CT35" for current transmitters, "VT7" for bidirectional voltage transmitters, and "VTU" for unidirectional voltage transmitters. Also indicated in the figure are

the various isolation devices for the circuits, including fuses, circuit breakers, and the main battery disconnect switch. The ground monitoring circuit is also shown. The positions of the contacts internal to the switchgear shown in the figure represent the configurations for the breaker in its normal pre-test setup (i.e., OPEN with the spring charged).

Figure A-38 shows the normal connections made from the switchgear return cable at the A connector panel on the front of the switchgear unit. None of the other connector pins on the B, C, or D connector panels were used during any of the DESIREE-Fire tests.

CLOSE CIRCUIT CABLE

PC connects to **A3**
C1 connects to **A5**
N1 connects to **A4** & **A6**
SP1 not connected
SP2 not connected
SP3 not connected
SP4 not connected

TRIP CIRCUIT CABLE

PT not connected
G connects to **A10**
R connects to **A8**
T connects to **A11**
SP1 not connected
SP2 not connected
N2 connects to **A9** & **A12**

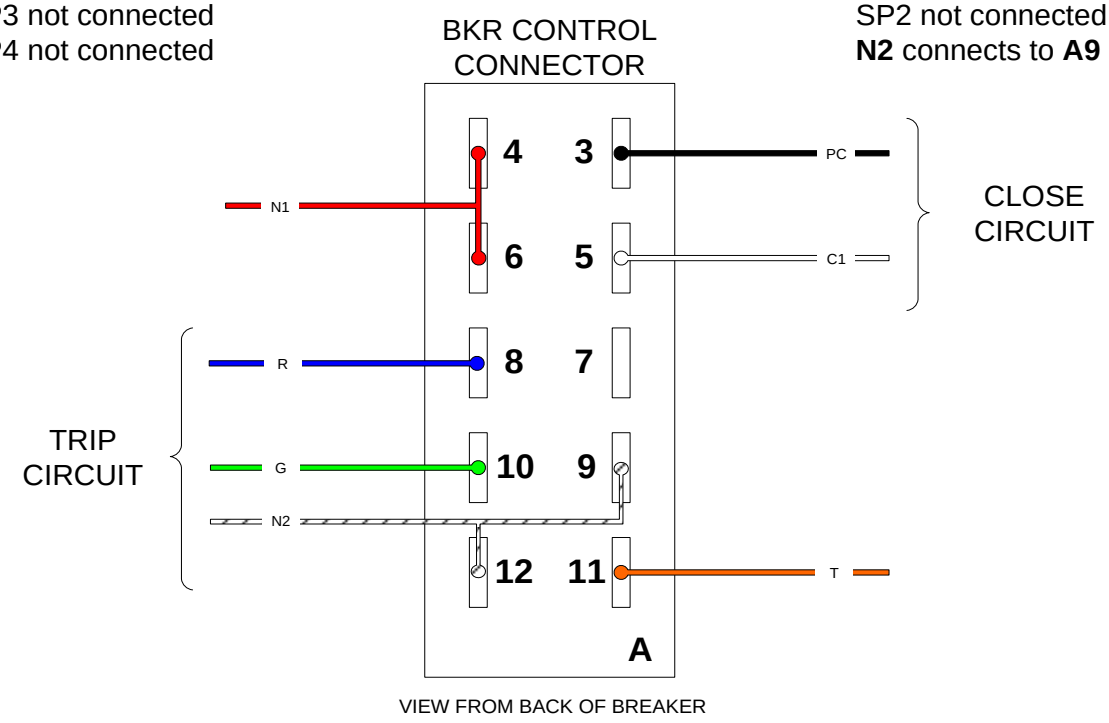

Figure A-38 Normal connection arrangement of the switchgear return cable to the switchgear connection panel

A.4.2.3 Description of Event

Figure A-39 provides the current and voltage plots for PT, N2, and G at the time of the event. Notice that the current rise for PT and N2 cuts off at 7 A. This is because the current transducer is rated at 35 A and was set up with five turns of the conductor through its pick-up coil; thus there is a multiplication effect associated with the transducers. A 7-A conductor current is amplified by a factor of five and appears to the transducer to be a 35-A current, which saturates the transducer. The drop-off occurred because one of the switchgear internal panel wires that was also exposed to that current acted as a slow-blow fuse and opened because so much heat was generated that the copper conductor in the 16-gauge panel wire melted. That phenomenon is what stopped further damage from occurring.

Figure A-40 provides the plot of the data generated by the CT-500 current transducer over the period of the event. Note that no indication of high current input from the battery was recorded during the time of the event.

A.4.2.4 Event Investigation

On November 18, 2009, an investigation of the event took place. The scope of the investigation included the wiring of the switchgear from the test and return cables, the interior wiring of the switchgear, and the connection of the test cables to the dc-SIM panels. Attachment 2 provides the handwritten notes taken by one of the investigators during this activity.

One of the first things discovered by the investigators was that the connections made at the terminal block from the switchgear return cable were reversed (left to right) from what they should have been. This is explained above.

Figure A-41 shows a photo of the front of the switchgear. No physical damage is evident in this view. Figure A-42 and Figure A-43 show different views of the damaged panel wires immediately behind the connector block. Figure A-44 shows damage to some of the wires inside the bundle behind the connector block. Figure A-45 and Figure A-46 show damage to the wires located in the wireway between the connector block and the auxiliary contacts. Figure A-47 shows wire damage near the auxiliary contact and Figure A-48 shows wire damage at the auxiliary contacts.

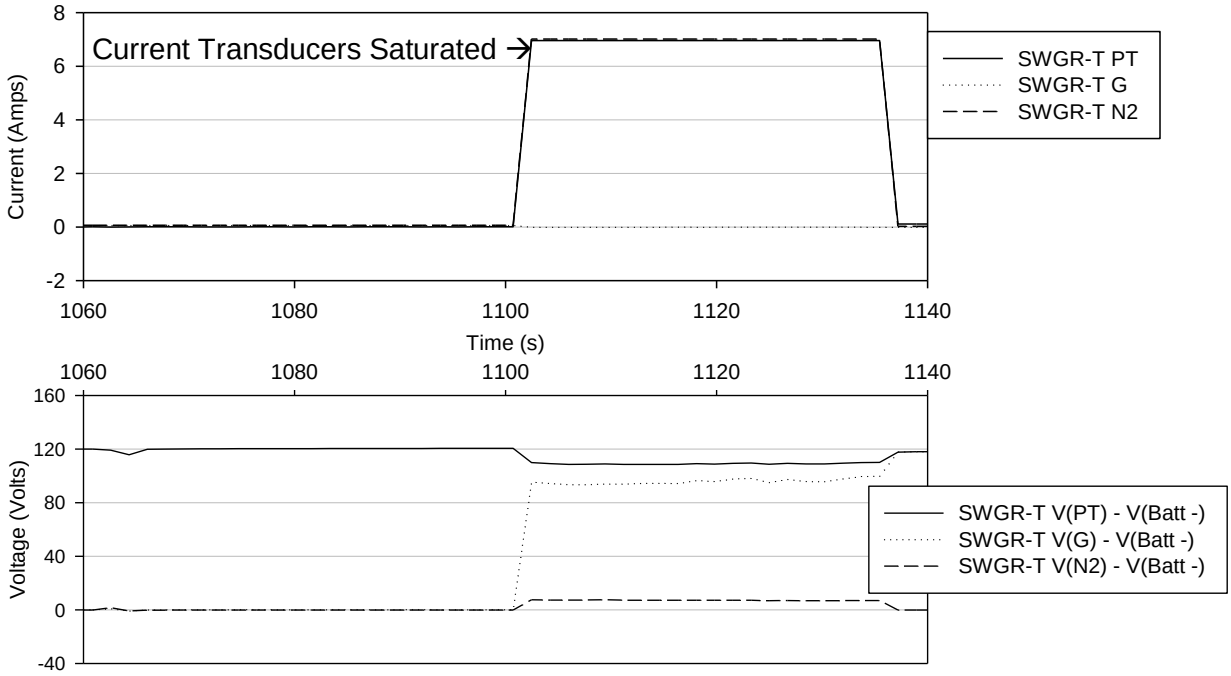

Figure A-39 Test IS8 current/voltage plots for SWGR PT, N2, and G at 1100 seconds

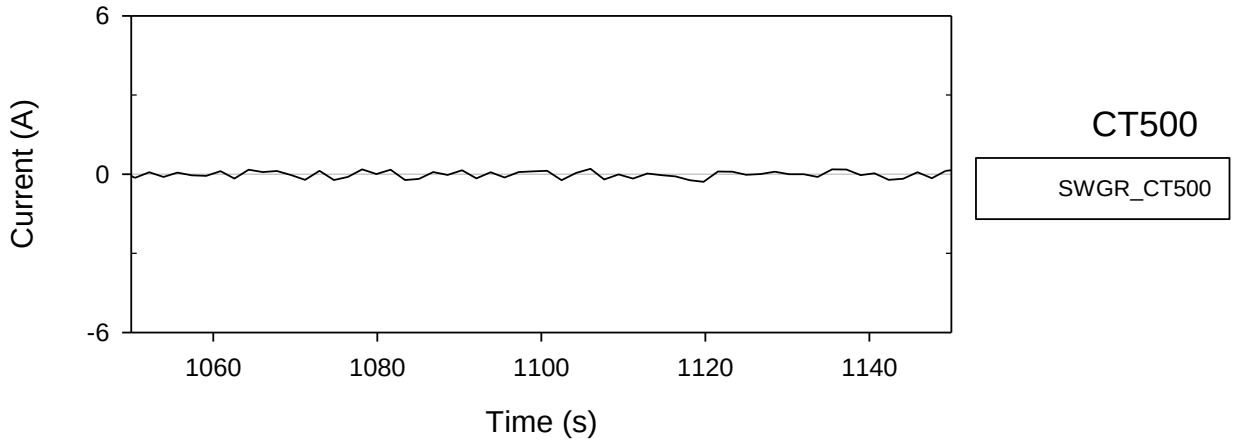

Figure A-40 Data recorded from the CT-500 current transducer during the event

Figure A-41 Front of the switchgear unit. The return cable connections are being made at the left side.

Figure A-42 Damaged panel wires immediately behind the connector block

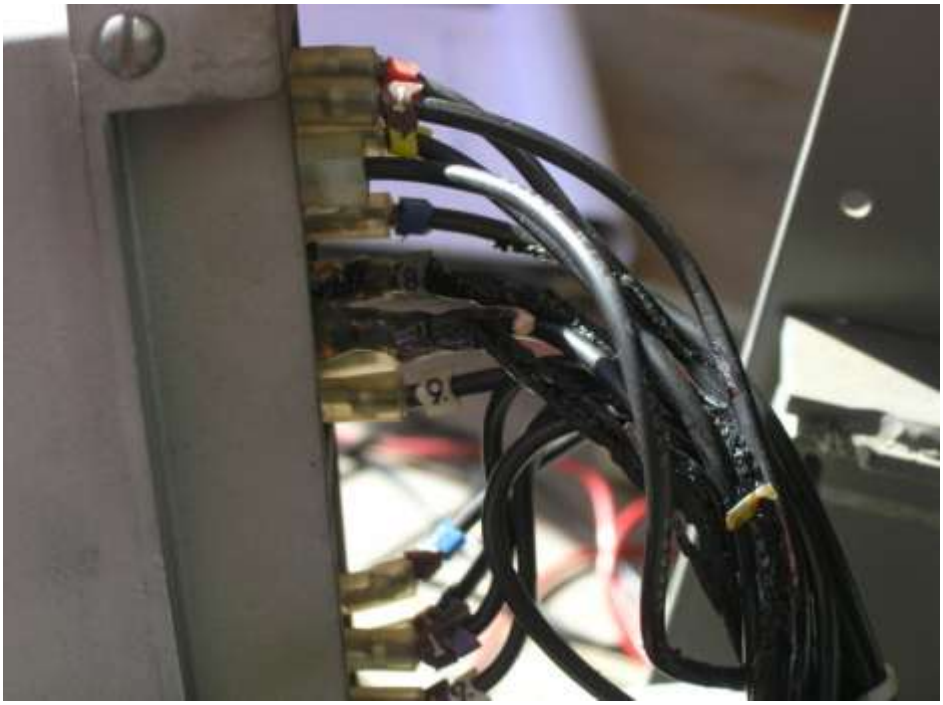

Figure A-43 Another view of damaged panel wires immediately behind the connector block

Figure A-44 Damage to some of the wires inside the bundle behind the connector block

Figure A-45 Damage to the wires located in the wireway between the connector block and the auxiliary contacts

Figure A-46 Another view of damage to the wires located in the wireway between the connector block and the auxiliary contacts

Figure A-47 Panel wire damage near the auxiliary contacts

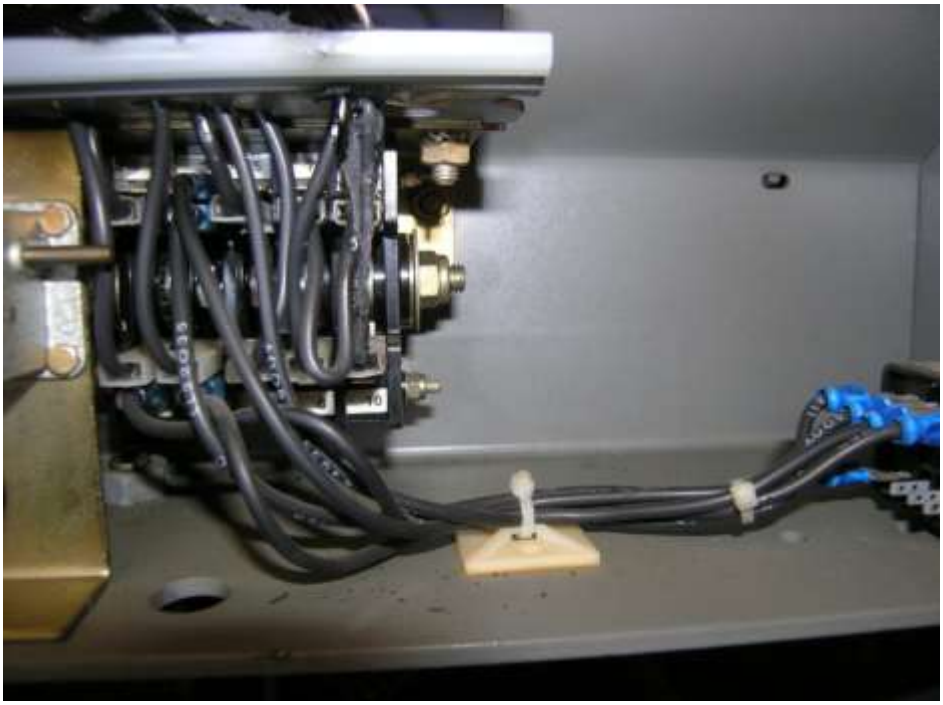

Figure A-48 Panel wire damage at the auxiliary contacts

Severe damage was experienced by the internal conductors leading from G at connection panel point A10 to the 52/b auxiliary contact and then to N2 at connection point A9. These wires are identified as 8 and 7, respectively, in Figure A.4-8. Other internal panel wires located and routed in close proximity to 7 and 8 also incurred some damage, but to a much lesser extent.

Figure A-49 and Figure A-50 are analogs of Figure A-37 and Figure A-38 showing the actual circuit configuration versus the expected circuit configuration. These figures show the effect of reverse connecting the return cable conductors to the switchgear connection panel. Figure A-49 shows the internal wiring of the switchgear close and trip circuits turned over because of the reverse wiring. Figure A-50 shows the reverse connections made at the switchgear connection panel.

Because the same internal panel wires 7 and 8 were connected between conductors G and N2 the interposing auxiliary contact 52/b is closed. This condition did not depend on the correct wiring of the return cable. Thus it was determined that the internal switchgear damage would likely have occurred given the same shorting circumstances even if the return cable had been correctly connected to the circuit breaker control connector.

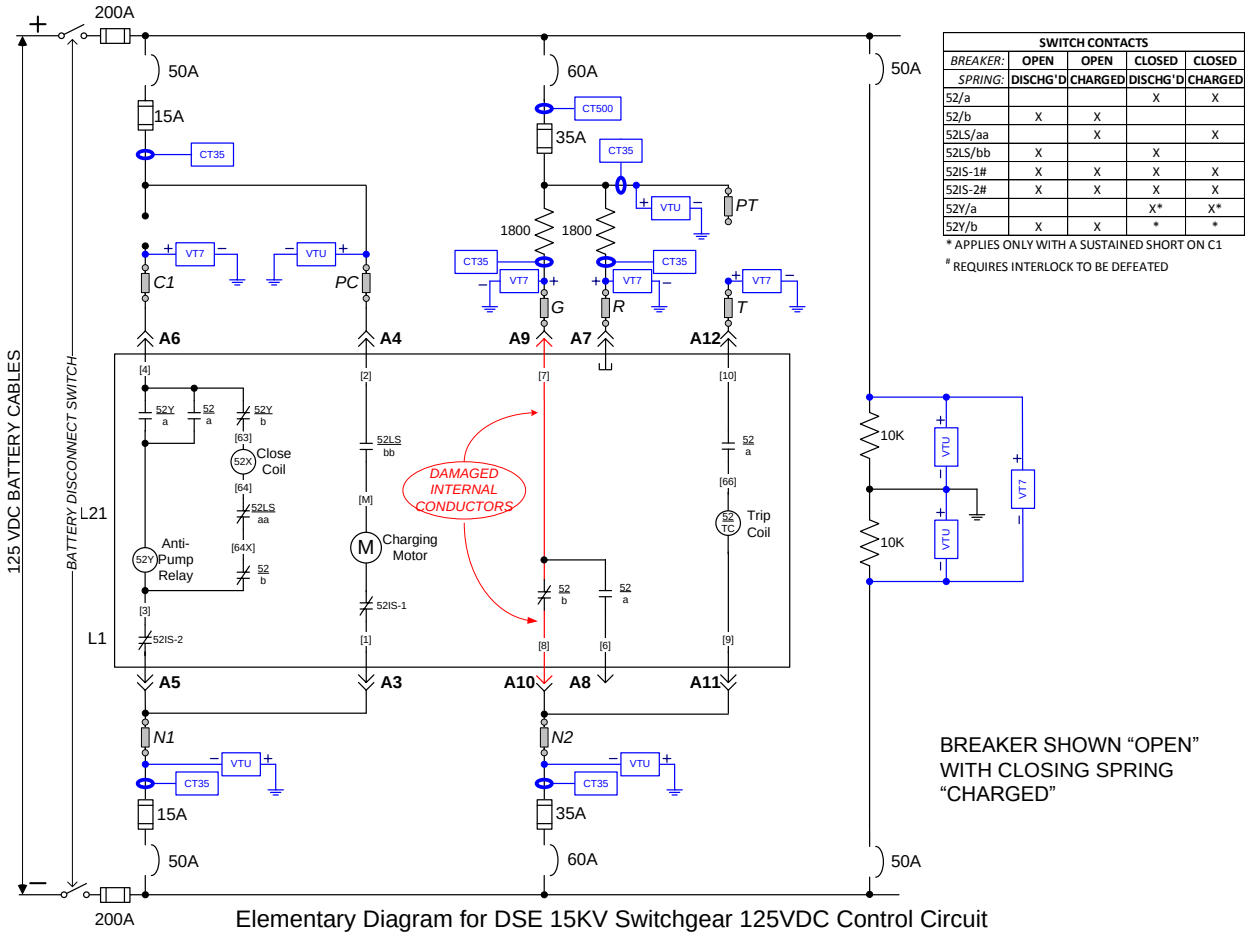

Elementary Diagram for DSE 15KV Switchgear 125VDC Control Circuit Showing Reversed Connections

Figure A-49 Internal switchgear wiring connections resulting from reverse connections at the terminal panel

A.4.2.5 Summary and Conclusions

The results of the investigation determined a number of issues regarding the use and operation of the 15-kV circuit breaker unit as part of the DESIREE-Fire tests:

- No double-check of the connection to the circuit breaker was made after the final hookup.
- It was determined that the sizes of the fuses on the close and trip circuits were too large to protect the 16-gauge internal panel wiring.
- The instrumentation being used on the switchgear circuits was not able to provide the data needed to clearly identify the cause of the large current that resulted in damage.
- It is likely that the damage would have occurred even if the connection to the breaker's control panel had been installed correctly.

CLOSE CIRCUIT CABLE

PC connected to **A4**
C1 connected to **A6**
N1 connected to **A3** & **A5**
SP1 not connected
SP2 not connected
SP3 not connected
SP4 not connected

TRIP CIRCUIT CABLE

PT not connected
G connected to **A9**
R connected to **A7**
T connected to **A12**
SP1 not connected
SP2 not connected
N2 connected to **A10** & **A11**

REVERSED CONNECTION DIAGRAM

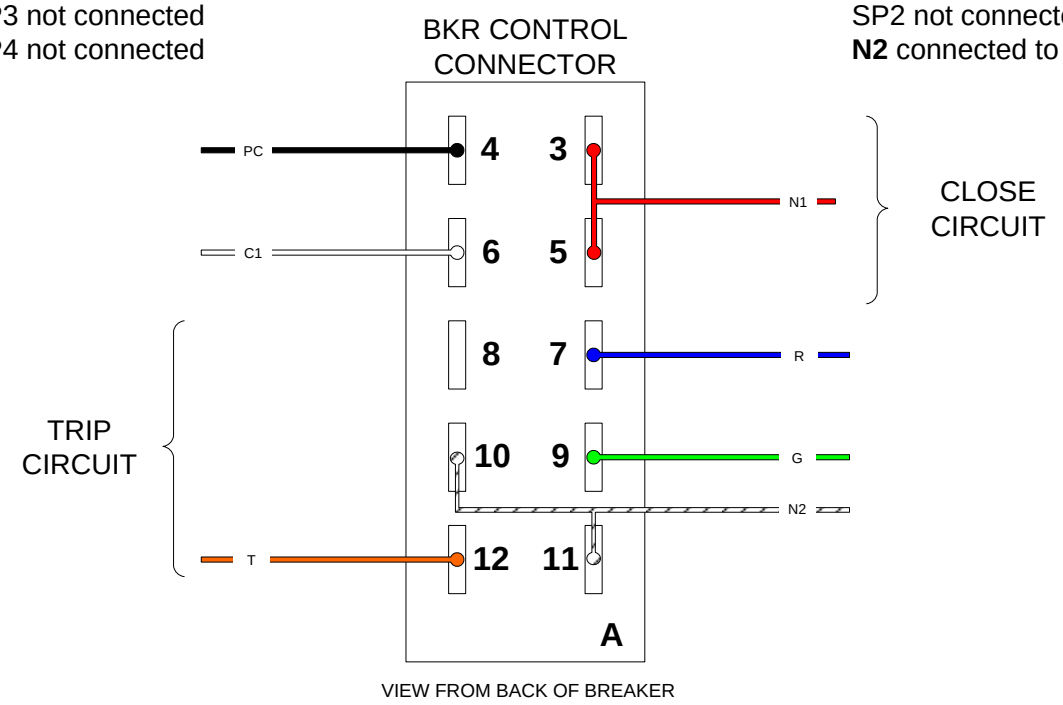

Figure A-50 Reversed connections made at the terminal panel

A.4.3 The Replacement 4.16-kV GE PowerVac® Breaker

After damaging the 15-kV breaker, a refurbished medium voltage circuit breaker configured with a 125-VDC control circuit that uses 20-A and 35-A fuses for the close and trip circuits was donated through the EPRI collaboration. The breaker was a -5kV class GE PowerVac®, Model VB1-4.16-250, 1200 A, 4.16 kV.

From the manufacturer's summary description, the vacuum circuit breaker uses sealed vacuum power interrupters to establish and interrupt a primary circuit. Primary connections to the associated metalclad switchgear are made by horizontal bars and disconnect fingers, electrically and mechanically connected to the vacuum interrupters. The operating mechanism provides direct motion at each phase location in order to move the movable contact of the vacuum interrupters from an open position to a spring-loaded closed position and then back to the open position on command.

The ML-18 and ML-18H mechanisms are of the stored-energy type and use a gear motor to charge a closing spring. During a closing operation, the energy stored in the closing spring is used to close the vacuum interrupter contacts, compress the wipe springs that load the contacts, charge the opening spring, and overcome bearing and other friction forces. The energy then stored in the wipe springs and opening spring will open the contacts during an opening operation.

Closing and opening operations are controlled electrically by the metalclad switchgear or remote relaying. Mechanical control is provided by manual close and trip buttons on the circuit breaker. The closing spring may be manually charged.

Figure A-51, Figure A-52, and Figure A-53 provide representative drawings for the new switchgear.

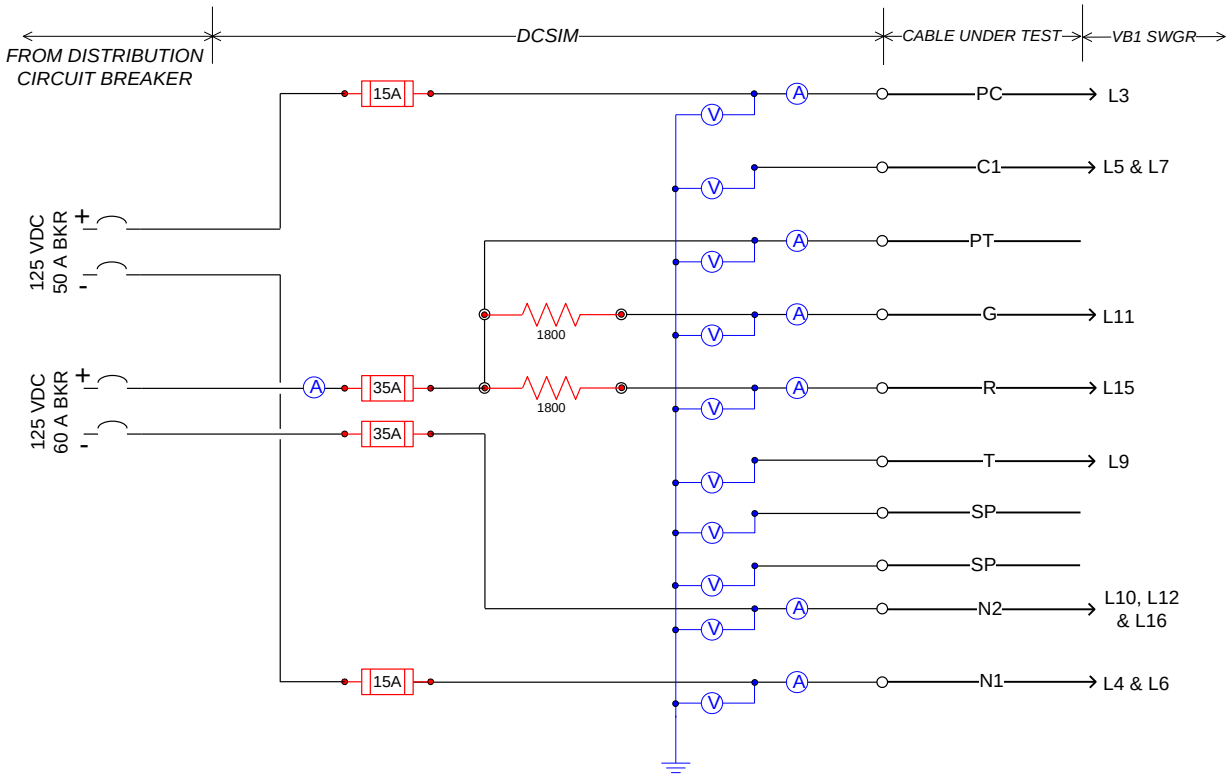

Figure A-51 dc-SIM panel layout for the control circuit on the GE VB1 SKV switchgear dc control circuit

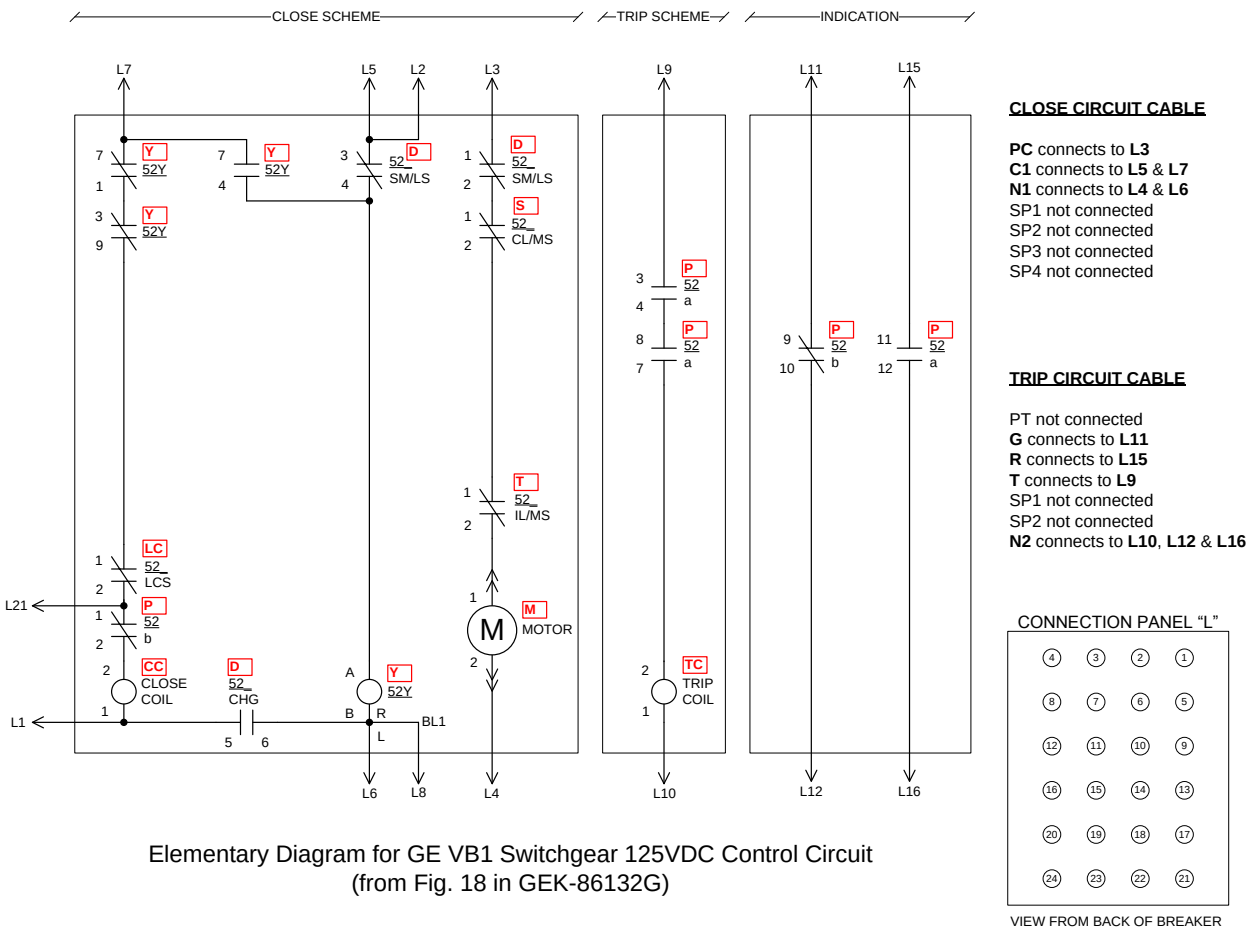

Elementary Diagram for GE VB1 Switchgear 125VDC Control Circuit
(from Fig. 18 in GEK-86132G)

Figure A-52 GE VB1 5-kV circuit breaker elementary diagram

CLOSE CIRCUIT CABLE

PC connects to **L3**
C1 connects to **L5** & **L7**
N1 connects to **L4** & **L6**
SP1 not connected
SP2 not connected
SP3 not connected
SP4 not connected

TRIP CIRCUIT CABLE

PT not connected
G connects to **L11**
R connects to **L15**
T connects to **L9**
SP1 not connected
SP2 not connected
N2 connects to **L10**, **L12** & **L16**

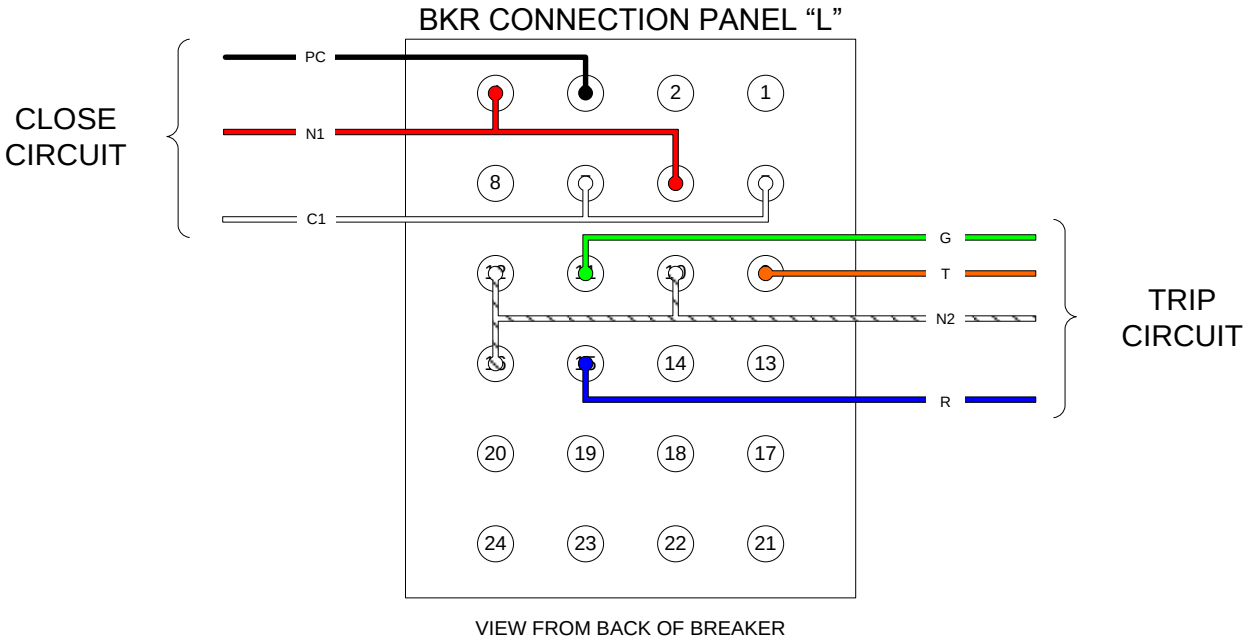

Figure A-53 GE VB1 5-kV circuit breaker connection diagram

A.5 dc-Powered Intercable Short Detection Circuit

One specific goal of the CAROLFIRE tests was to explore the potential for risk-relevant electrical shorting interactions between two separate cables (i.e., intercable shorts that might cause a spurious operation). DESIREE-Fire provided an opportunity to explore similar behaviors for dc-powered cables. Limited exploration of intercable interaction potential using the dc battery bank was performed.

Figure A-54 depicts a simple configuration, contrived to provide a solid chance of inducing proper polarity shorting within the target cable from the positive and negative source cables. Note that all of the conductors in a particular source cable were energized to the same polarity and their voltage being monitored as a group (i.e., one voltage monitor per source cable). The seven individual conductors in the target cable were monitored for voltage. Additionally, the outer six conductors of the target cable (2 through 7) were connected together in a resistance network so that "float" voltages were distributed among the separate conductors. Figure A-55, Figure A-56, and Figure A-57 provide the electrical schematic and resistor connection arrangement, respectively. Also note that conductor number 1 was not part of the resistance network, but was monitored for changes in voltage.

During the Penlight testing, the marinate board provided electrical isolation from the ground plane so that multiple shorts to ground do not result in a fuse actuation and to limit the possibility of forming a ground bias of the battery by the first short to ground, by either of the source cables. Throughout the intermediate-scale experiments, however, the intercable bundle was placed in various locations in the cable tray (i.e., in direct contact with the tray, positioned between fill cables, and on top of the fill cables). The specifics for each test can be found in Appendix F.

In these intercable tests, the target cables were not connected to anything other than voltage monitoring instruments. In this configuration, shorting between the source and target cables will be indicated by a change in voltage potential. Figure A-58, Figure A-59, and Figure A-60 show examples of how the voltage readings on individual target conductors are expected to vary depending upon which of the target conductors are directly energized by the positive and negative sources. These are ideal conditions and do not assume any intracable interactions have occurred within the target. Both thermoset (TS) and thermoplastic (TP) cables were used throughout the Penlight and intermediate-scale experiments.

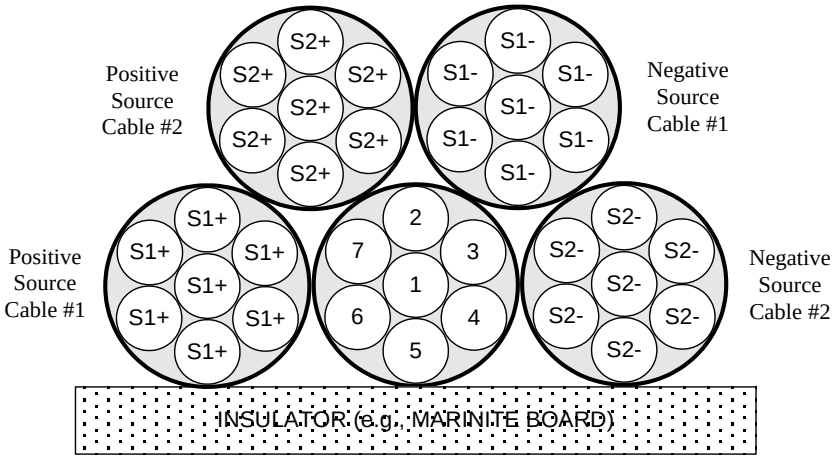

Figure A-54 Cable grouping with multiple source cables surrounding the target

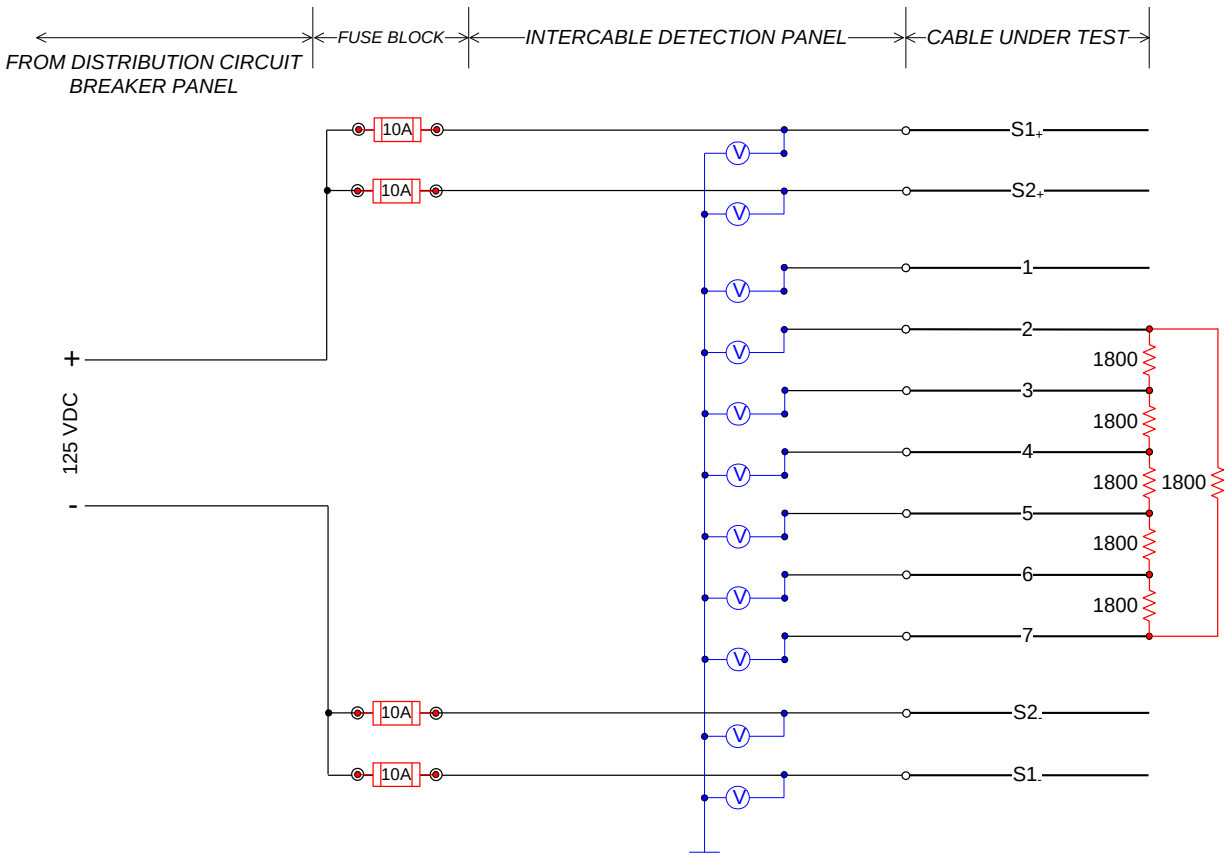

Figure A-55 Intercable monitoring and power circuit where four source cables are separately powered and fused from the battery; the seven conductors of the target cable are individually monitored for voltage and interconnected with a resistance network

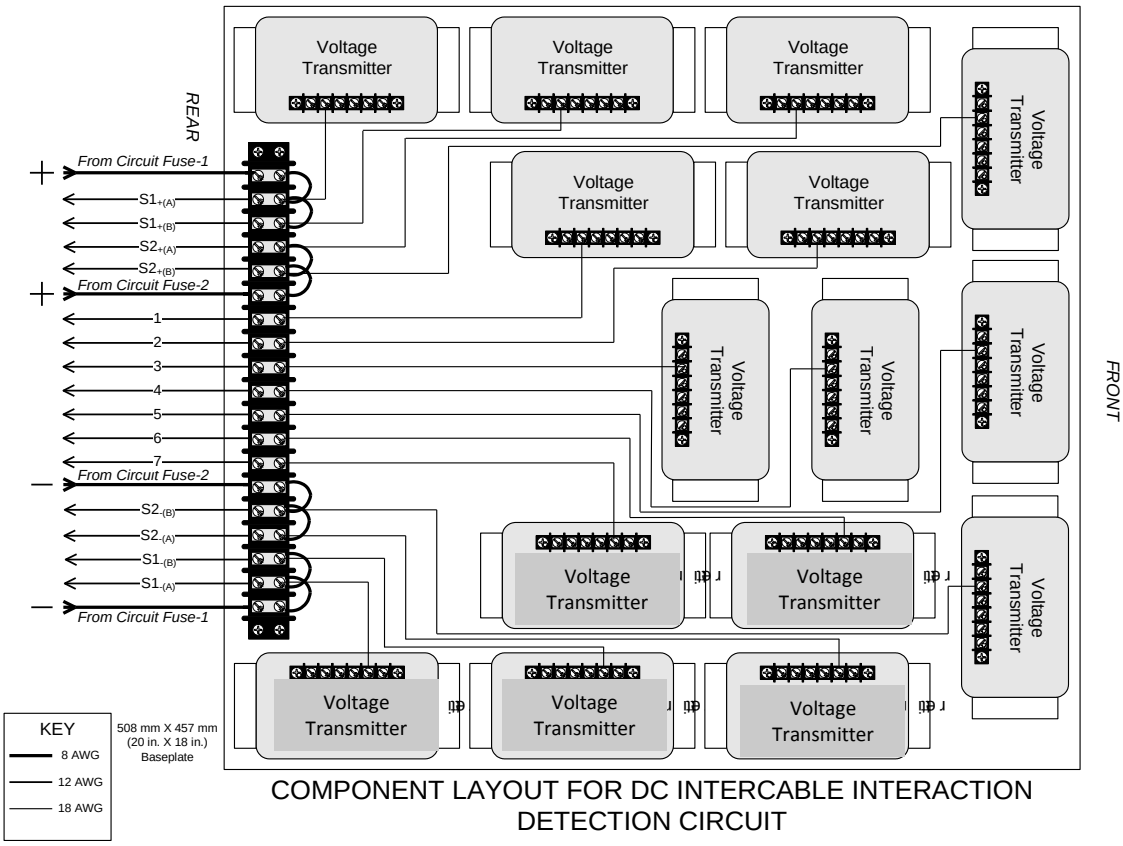

COMPONENT LAYOUT FOR DC INTERCABLE INTERACTION DETECTION CIRCUIT

Figure A-56 Component layout for intercable monitoring and power circuit where four source cables are separately powered and fused from the battery; the seven conductors of the target cable are individually monitored for voltage and interconnected with a resistance network

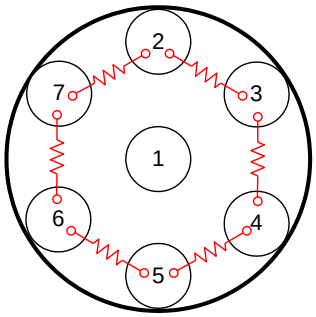

Figure A-57 Intercable configuration showing the network of resistors connected to the individual conductors of the target cable

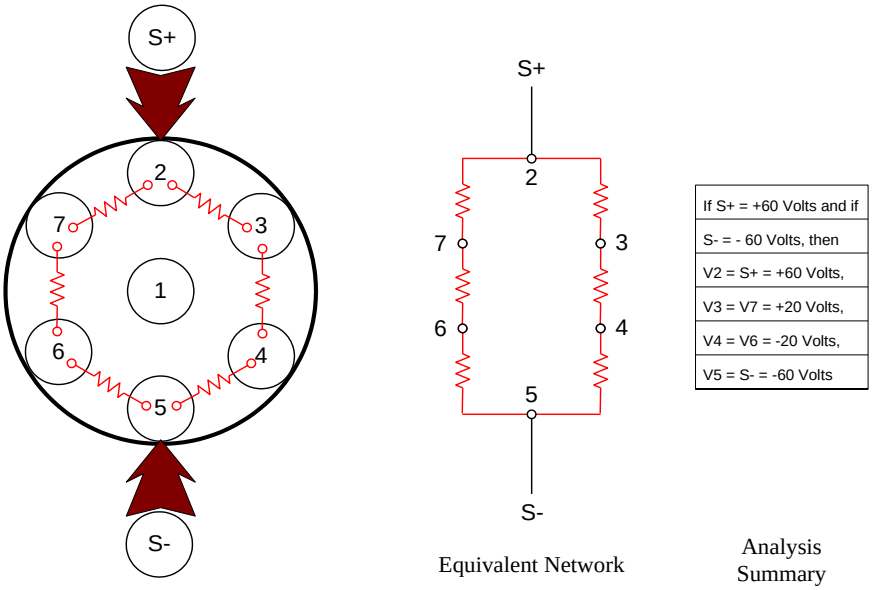

Figure A-58 Cable network analysis for the case of a positive interaction on conductor 2 and a negative interaction on conductor 5 (180-degree separation)

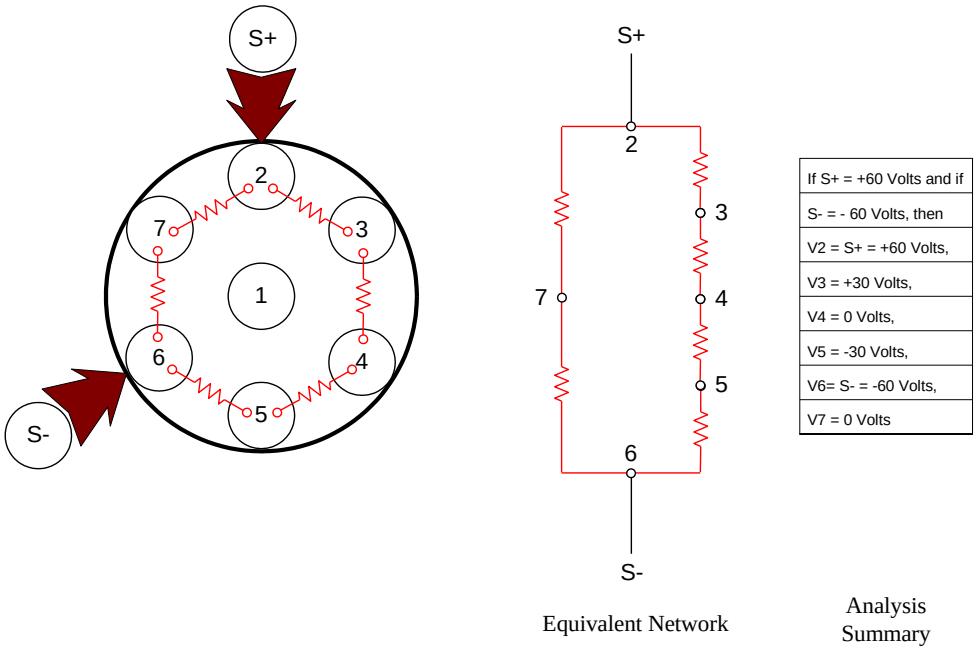

Figure A-59 Cable network analysis for the case of a positive interaction on conductor 2 and a negative interaction on conductor 6 (120-degree separation)

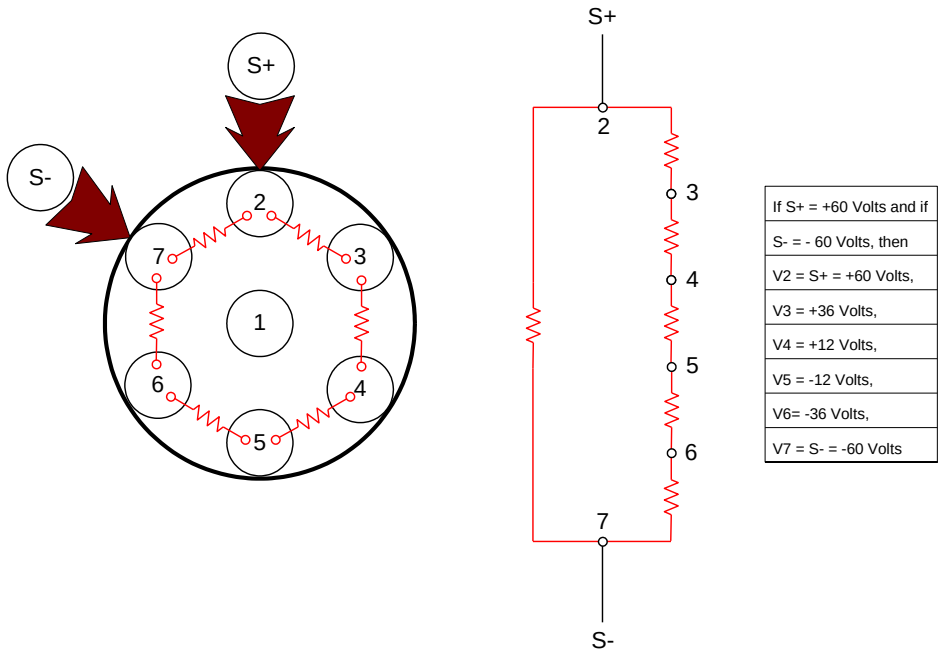

Figure A-60 Cable network analysis for the case of a positive interaction on conductor 2 and a negative interaction on conductor 7 (60-degree separation)

A.6 ac-Powered Surrogate Circuit Diagnostic Unit

Figure A-61 depicts the electrical schematic drawing of a simplified ac MOV control circuit. The block diagram is shown in Figure A-62 with the target Cable B highlighted. The contacts shown in Figure A-61 indicate that the valve is in the closed position; therefore the failure modes of concern are those cases wherein the valve could be made to spuriously open.

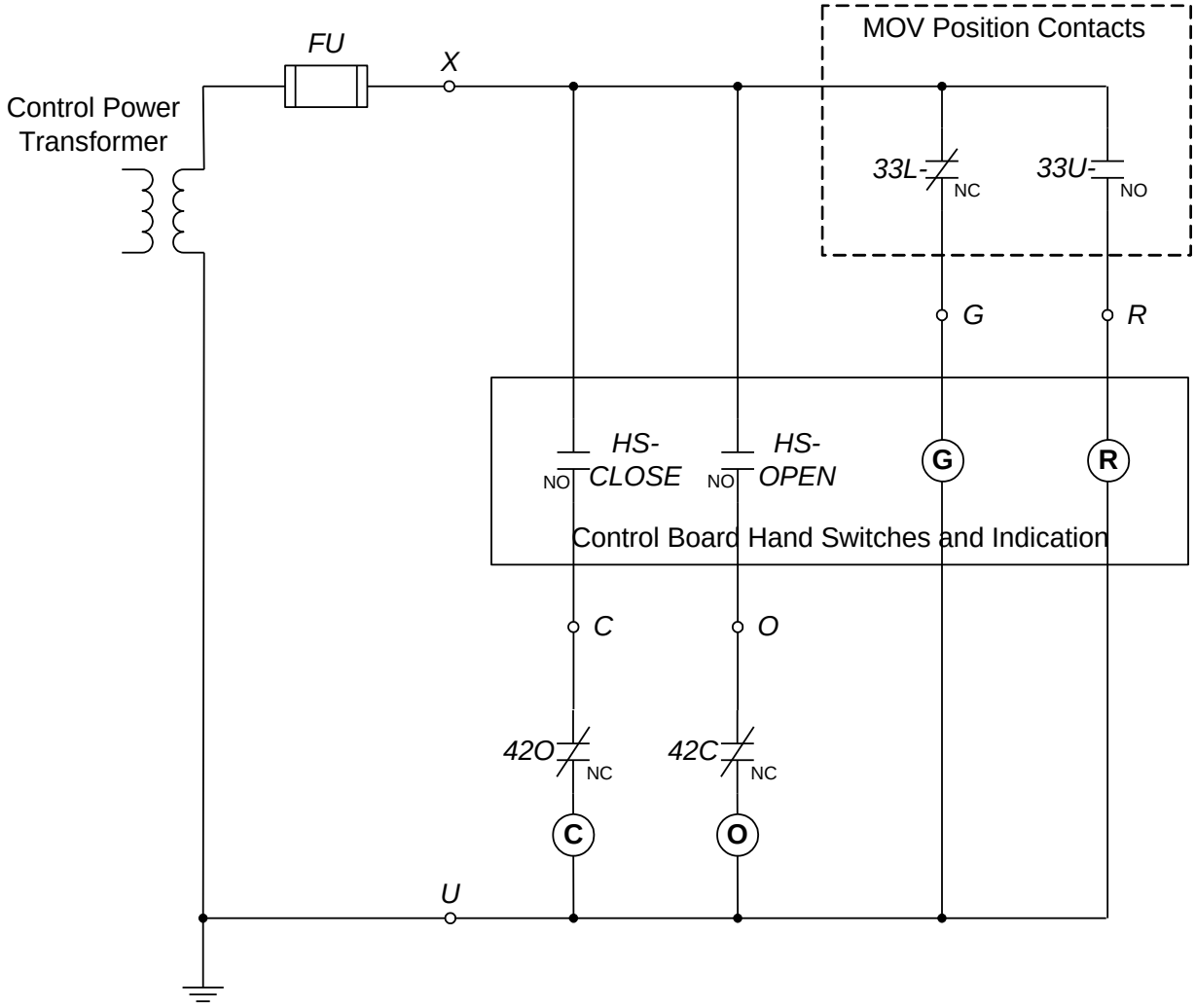

Figure A-61 Simplified ac-powered MOV control circuit, with control panel transformer (CPT)

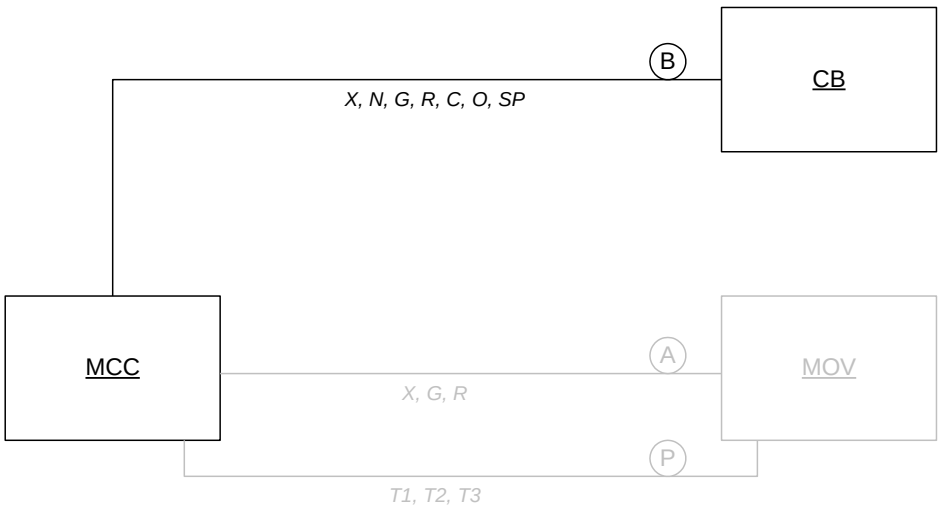

Figure A-62 Block diagram for simple ac-powered MOV control circuit

Figure A-63 shows an analog of the simulated ac MOV control circuit that was employed during the early EPRI/Nuclear Energy Institute (NEI) tests and during CAROLFIRE. An 120V ac power source, a 1750-ohm resistor representing an indicator lamp, and two relay coil targets are connected to the simulated circuit. A seven-conductor cable connected to the Surrogate Circuit Diagnostic Unit (SCDU) is the device under test. Although it is possible to encounter a circuit in a NPP that is supplied with power directly for a power source, typically a CPT is used. Testing of the circuit in Figure A-63 would provide little to no information on the effects of a CPT in limiting the probabilities of spurious actuation and therefore was not tested in this testing program.

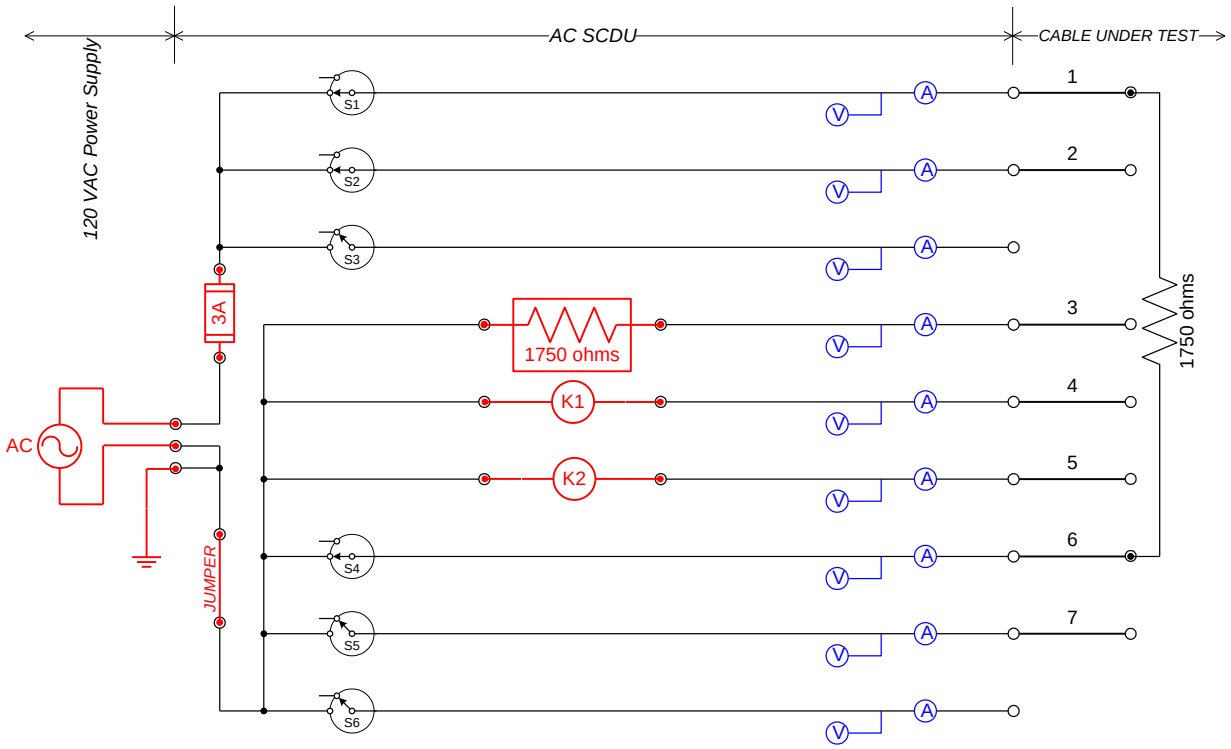

Figure A-63 Simulated ac MOV control circuit, without CPT (not tested)

Figure A-64 shows the same control circuit being powered through a CPT. It should be noted that by changing the switch arrangements, these cable configurations can be easily changed, for example, to connect the ungrounded spare conductor (#7) to ground, or, if desired, to change conductor #2 from an energized state to an ungrounded spare.

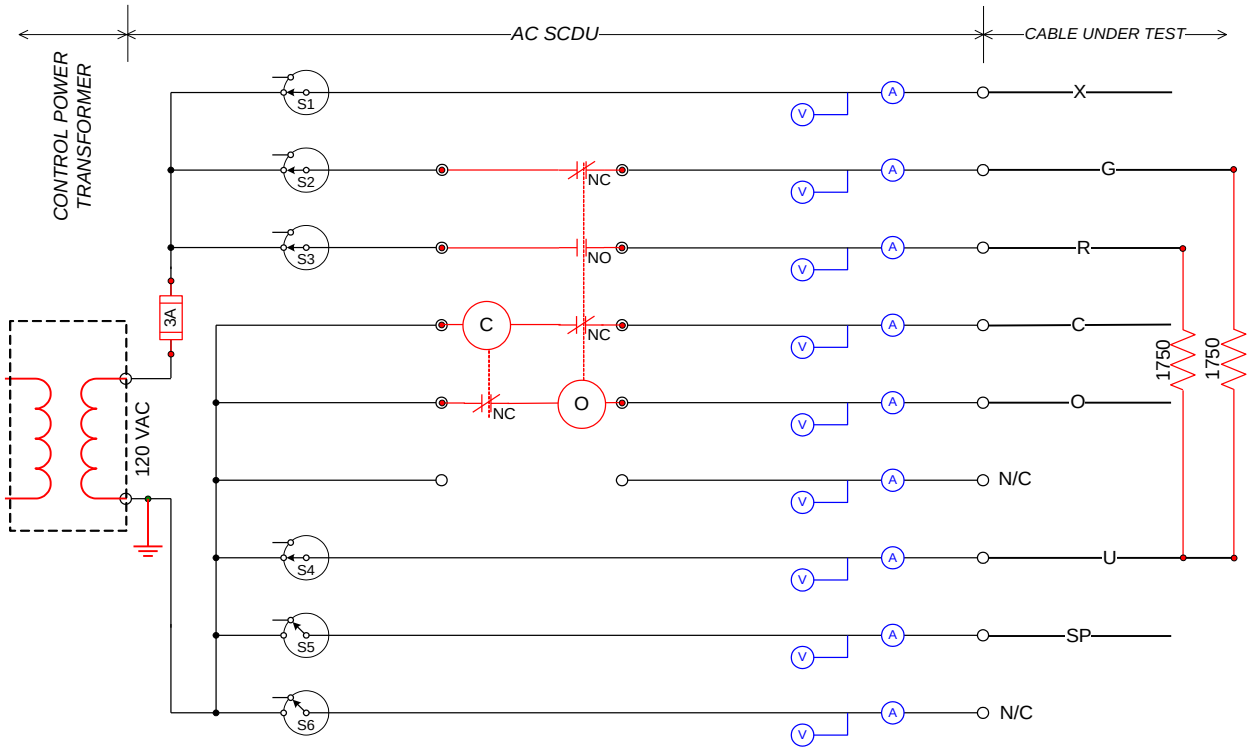

Figure A-64 Simulated ac MOV control circuit, with CPT

The motor starters used during CAROLFIRE were, in hindsight, found to require far less motive power to lock in and hold a spurious actuation signal than anticipated. The intent in CAROLFIRE had been to obtain motor starters that required a nominal 100 VAC of power to lock in a relay actuation. In practice, while the relays obtained were cited as 100 VAC relays, it actually took a much smaller power level to lock in an actuation (on the order of 60 VAC). As a result, CAROLFIRE was unable to resolve one of the original Regulatory Information Summary (RIS) 2004-03, "Risk-Informed Approach for Post-Fire Safe-Shutdown Circuit Inspections," unresolved issues; namely, that item related to how CPT size relative to the nominal circuit required power would impact spurious actuation likelihood. The CPT units used in CAROLFIRE were sized against the anticipated 100-VAC power requirement for the relays. Given the actual power requirement of the relays, the CPTs were, in effect, over-sized. As a result, the CAROLFIRE tests did not experience the same type of CPT power drawdown observed in the original NEI/EPRI testing program.

To rectify this problem the existing motor starter relays were replaced with Joslyn-Clark[3] (current part number is T30U031) for the DESIREE-Fire test series. SCDU-1 and SCDU-2 were replaced with the original motor starter sets used during the NEI tests while SCDU-3 and SCDU-4 were replaced with newly purchased motor starter sets, identical sets of these

[3] Note that the EPRI test report (TR-1003326, page 4-13) cites "AO Smith (Clark Controls Division) Catalog #30U031" as the make and model of the motor starters used in that test program. AO Smith has since merged with Joslyn controls. The combined company is known as Joslyn-Clark Controls. The same model motor starter relays are sold under the Joslyn-Clark brand using essentially the same catalog number (T30U031).

controllers. All of the sets of motor starters included the mechanical interlock devices except SCDU-2, which was used as shipped by EPRI.

These interlocks more realistically represented the actual plant circuit implementation and provided a new aspect to the test data not previously explored. Although the original intention was to test the ac systems for each intermediate-scale experiment, a decision was made to shift the large ranged dc-rated current transducers (i.e., CT500) for each dc circuit onto the SCDU's high-speed data acquisition system. As such, only the first seven tests (i.e., JPN-IS1, Prelim1, Prelim2, ISTest4, ISTest8, ISTest11, and ISTest12) included the SCDU circuits.

Table A-12 identifies the conductor-to-conductor interactions required to occur within Cable B to cause a specific circuit malfunction, including spurious opening of the valve. It is also worthwhile noting that no immediate discernible effect occurs if conductors X, O, C, or R experience an open circuit failure (conductor break) as the initial failure mode.

Table A-12 Identification of specific intracable induced circuit failure modes for the ac MOV.

Circuit Failure Effect	Will occur if any of these conductors…	Come into contact with any of these conductors…	Notes
Valve spuriously opens	X, G	O	
Loss of valve control	U	O, R	Circuit fuse(s) will blow if an attempt is made to open the valve while this internal short condition exists.
Loss of circuit power (blown fuse(s))	X, G	U	
Erroneous/spurious valve position indication	X, G	R	
Loss of valve position indication	—	—	Open circuit failure of conductor G or U.

The MOV contactors were electrically characterized following the intermediate-scale tests in order to determine their actual pick-up and drop-out voltage and current thresholds. Table A-13 provides a summary of each MOV contactor's electrical characteristics.

Table A-13 ac MOV contactor coil pick-up and drop-out characteristics.

Device	Average Pick-up Voltage (Vdc)	Average Pick-up Current (A)	Average Drop-out Voltage (Vdc)	Average Drop-out Current (A)
SCDU-1 (T5)	93.9	0.07	71.7	N/A
SCDU-1 (T6)	80.5	0.08	67.1	N/A
SCDU-2 (T5)	81.1	0.08	60.1	N/A
SCDU-2 (T6)	79.7	0.08	69.5	N/A
SCDU-3 (T5)	82.3	0.09	64.6	N/A
SCDU-3 (T6)	83.2	0.08	57.5	N/A
SCDU-4 (T5)	85.1	0.08	59.7	N/A
SCDU-4 (T6)	85.0	0.08	57.2	N/A

A.7 The dc Battery Bank and Power Distribution System

A.7.1 Overview

The battery bank was built to supply a nominal 125-Vdc power source. The batteries were obtained through the NRC-RES/EPRI memorandum of understanding (MOU) and were being taken out of service from the North Anna Nuclear Station Technical Support Center as a part of preventative maintenance. The battery cells had reached their nominal end-of-life conditions, but were still in serviceable condition and were transported to Sandia National Laboratories (SNL) for use in this test project.

A.7.2 Basic Design Parameters

The dc power supply battery bank was constructed using a set of Exide model ES-13 calcium flat plate, lead/acid, nominal 2.1-Vdc uninterruptible power supply (UPS) battery cells. Each cell contains approximately 9.1 liters (2 gallons) of sulfuric acid as the electrolyte. A total of 60 cells were used in the main battery bank. Eight spare cells were also available, but were not used in the program as no cell failures occurred during testing.

Before installation, all of the individual battery cells were tested by an independent testing laboratory using IEEE Standard 450-1995, *IEEE Recommended Practices for Maintenance, Testing and Replacement of Vented Lead-Acid Batteries for Stationary Applications* [1]. All of the cells used in testing, including the spare cells, were certified as being in good working condition.

Cell handling was performed in accordance with IEEE Standard 484-2002, *IEEE Recommended Practice for Installation Design and Implementation of Vented Lead-Acid Batteries for Stationary Applications* [2]. Load/capacity calculations were performed in accordance with IEEE Standard 485-1997, *IEEE Recommended Practice for Sizing Lead-Acid Batteries for Stationary Applications* [3].

The basic design parameters of the battery bank are summarized as follows:

- Cell type: Exide ES-13, lead alloy acid-filled cells
- Nominal open circuit voltage: 2.06 V
- Nominal cell float voltage: 2.17–2.26 V
- Total cell count in main battery bank: 60
- Nominal bank float voltage: 125 V
- Available short circuit current at the battery terminals: approximately 13,680 A
- Cell-to-cell connections: Exide lead-plated copper bars and bolts

Table A-14 and Table A-15 provide additional physical information for the individual battery cells as provided by Exide.

Table A-14 Exide battery cell dimensions from the manufacturer's literature.

Exide Calcium Flat Plate Battery Cell						
	Overall Dimensions					
Model Type	Container Length		Container Width		Height	
ES-13	(in.)	(mm)	(in.)	(mm)	(in.)	(mm)
	4.87	124	10.8	274	18.7	475

Table A-15 Exide battery cell weight from the manufacturer's literature.

Exide Calcium Flat Plate Battery Cell								
	Weights -- Volumes							
Model Type	Unpacked		Domestic Packed		Electrolyte Only			
ES-13	(lbs)	(kg)	(lbs)	(kg)	(lbs)	(kg)	(gal)	(liters)
	81	36.7	83	37.6	20	9.1	2.0	7.6

A.7.3 Battery Banking Housing and Connections

The battery cells were installed in a portable transportainer providing personnel protection, spill containment (in the event of a cell leak or rupture), environmental protection to the cells, and the ability to transport the cells between testing sites. The transportainer was provided with both heating and cooling to ensure that the cells did not deviate from the manufacturer-specified operating or storage conditions. Figure A-65 provides a nominal schematic of the battery cell layout within the transportainer.

Intercell connections were removed during transport. Once in place on site, the intercell connection plates were installed in accordance with manufacturer specifications. The connections were also tested for continuity using a micro-ohm meter and in accordance with manufacturer specifications. Any out of compliance connections were reworked to ensure an acceptable level of terminal-to-terminal resistance and consistency between connections. Figure A-66 provides a photograph of the battery cells during work to install the cell-to-cell connector plates.

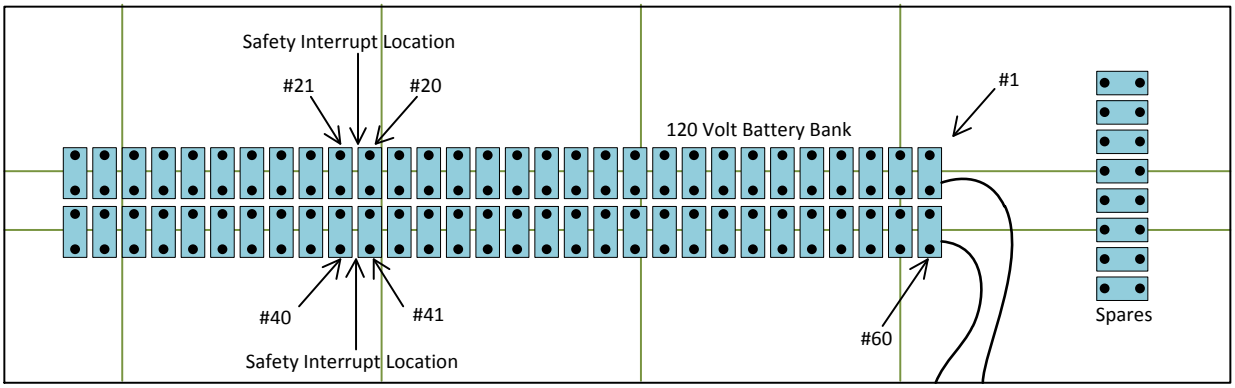

Figure A-65 Battery enclosure layout

Figure A-66 Photo of the battery assembly

An automatic charging system capable of recharging the cells over night was also installed. The charger was capable of providing both a freshening charge and float charging. All cells received a freshening charge when they arrived at SNL. Once installed, the battery bank also received a freshening charge. The bank was then recharged periodically throughout the course of testing. In general, the bank would be recharged at least weekly during the small-scale tests where the loads on the cells were relatively modest. During the larger--scale tests, the cells would be charged as a minimum after completion of two tests. The charger was secured and disconnected from the battery bank during testing.

The battery bank was ungrounded, although ground faults during testing were expected and a ground-fault monitoring circuit was included in the test design and monitored during testing.

A.7.4 Power Distribution

The battery bank was connected to the dc-SIM panels via a series of fuses and breakers. The power distribution system is illustrated schematically in Figure A-67. In order, progressing from the battery cells to the dc-SIM panels, were the following electrical features:

- The main terminal of the battery bank was connected to the power distribution system via two single-conductor 4/0 power cables (the battery bank was ungrounded).
- A primary disconnect switch.
    - 250 - 125 VDC bus - 200-A contacts.
- 200-A fuse on each of the main output cables (integral to the disconnect switch).
    - Two each Littelfuse fuse, part number JTD-200ID.
- A dc breaker distribution panel fed by 4/0 cables from the output of the 200A fuses and with separate breakers for each test branch circuit.
    - Two-pole dc circuit breakers rated at 250 Vdc.
    - Circuit breaker capacities range from 30 A to 60 A depending on the specific circuit.

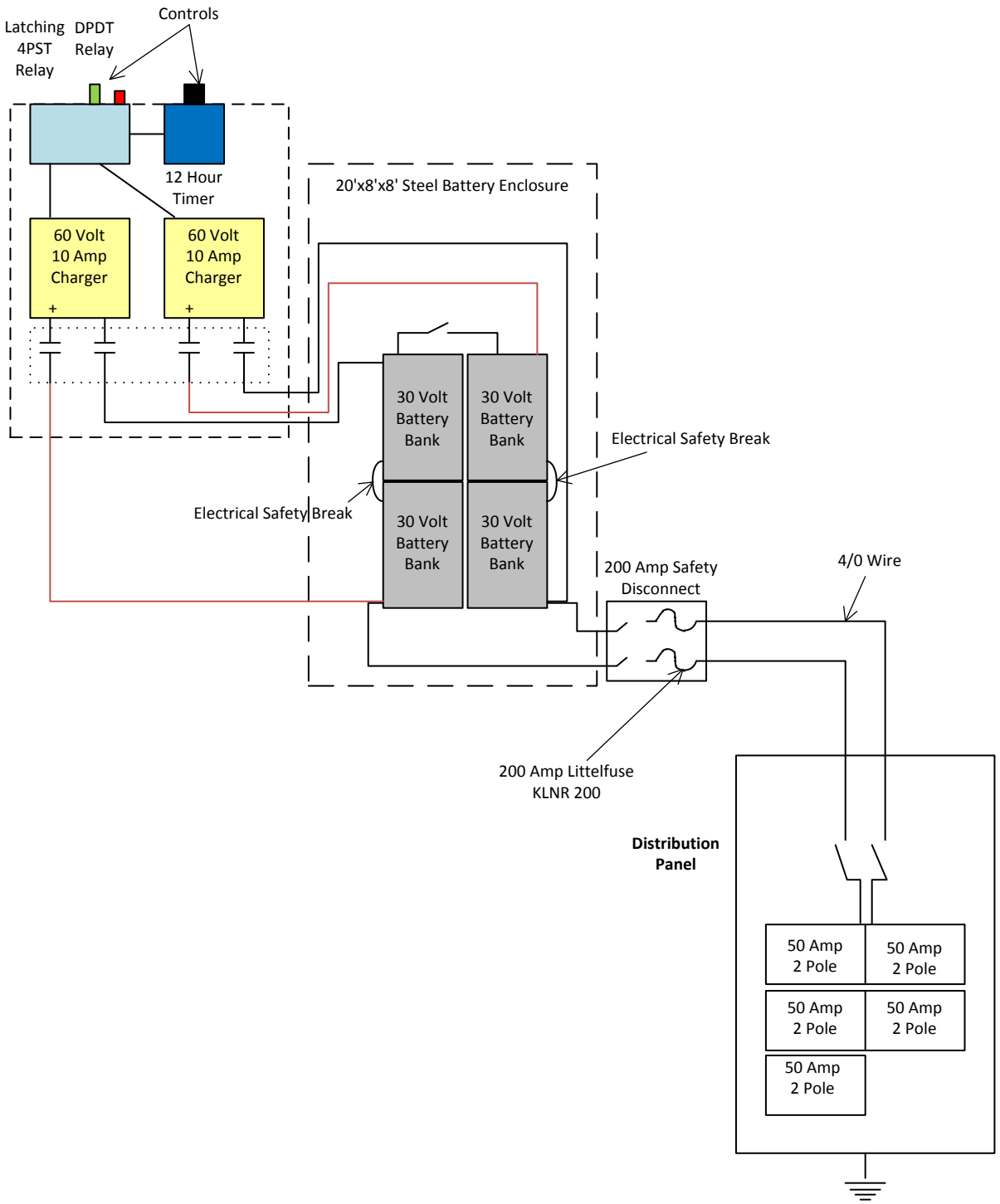

Figure A-67 dc power skid schematic

- 3/C, 8 American Wire Gauge (AWG) power cables connecting the dc breaker panel to the dc-SIM panels (each test circuit was serviced by an individual cable).
- A fuse on each incoming power feed cable to the dc-SIM panel.
    - Fuse sizes are specific to each test circuit. Refer to the corresponding circuit descriptions for details.
- 12 AWG cables connecting the dc-SIM panels to the test cables.

Figure A-68 provides a second schematic of the connections and cable lengths for each connection from the battery to the dc-SIM panels and to the test cables, including the lead cable to the switchgear unit itself. This figure includes specification of each cable's wire gauge and length (e.g., for use in calculating voltage drops).

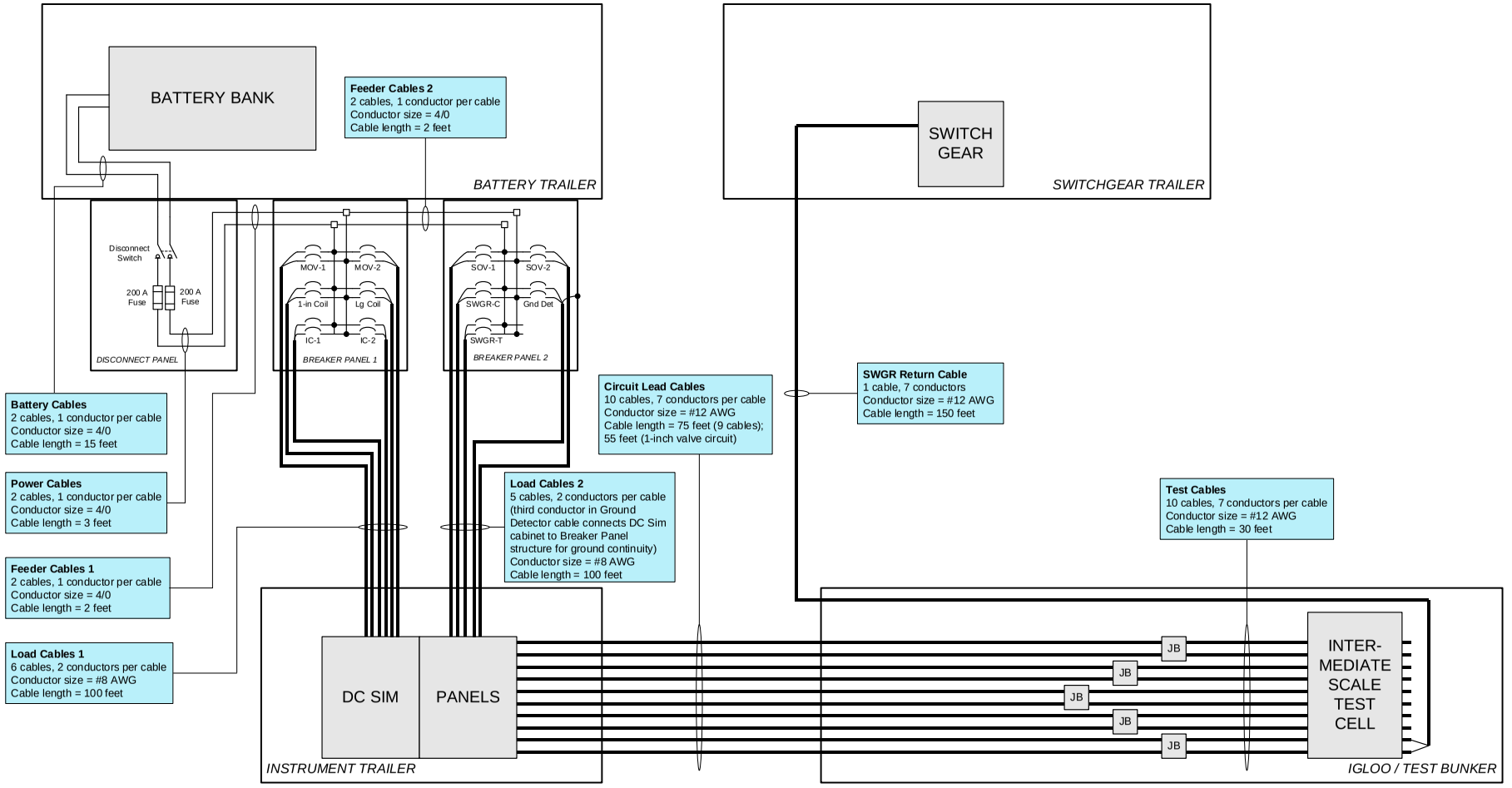

11/23/2009

Figure A-68 dc power connection layout for the intermediate-scale tests

It should be noted that for each of the test circuits, the primary circuit protection is provided by the individual circuit fuses. These fuses are intended to represent typical plant practices. The other circuit protection features (i.e., the breakers, 200-A main output fuses, and primary disconnect switch) are all provided for personnel protection and safety. These additional protective devices were selected to provide appropriate breaker-fuse coordination, but are not intended to represent in-plant practice.

A.7.5 Battery Bank Ground Fault Detection Circuit

The dc battery bank was nominally an ungrounded power supply system. A ground fault detection circuit provided the opportunity to monitor for shorts between the battery bank and ground (ground faults). Figure A-69 and Figure A-70 illustrate the line drawing as well as the component layout for this circuit.

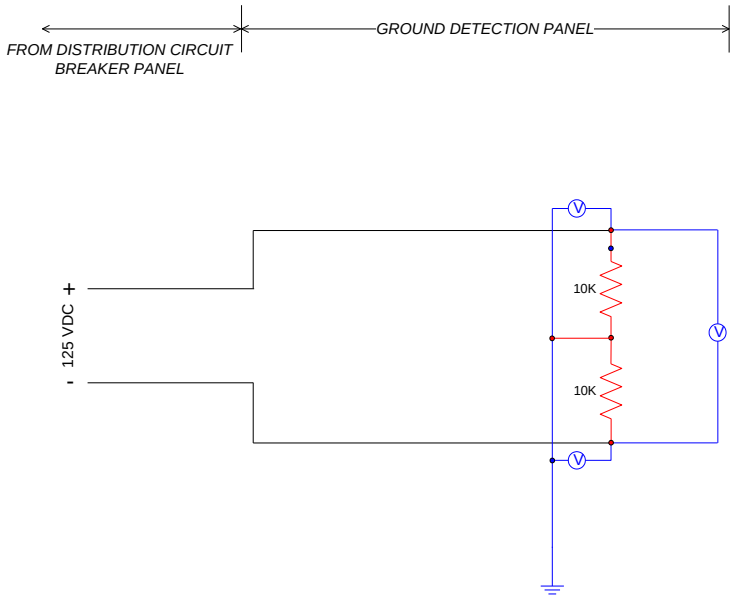

Figure A-69 Line drawing for the dc ground detection circuit

In practice, the ground detection circuit provides a monitored high-resistance (10,000-Ω) path between each side of the battery bank and the local ground plane. Under normal conditions (i.e., no ground faults present) the voltage monitor on the far right will read a nominal 125-VDC battery voltage, and each of the other two voltage transducers, those measuring across the two ballast resistors, reads exactly one-half that value. Should a ground fault occur on either side of the battery bank, the overall bank voltage would not change, but the voltages across the ballast resistors would both change. If, for example, there is a ground fault on the positive leg of the battery bank, the voltage across the positive-side ballast resistor would drop to zero, and that across the resistor on the negative side would rise to the full battery bank potential of 125-VDC.

To ensure proper operation, all experimental systems and equipment were connected to a common ground plane (e.g., facility ground). The voltage transducers for the various dc circuit simulator panels measured circuit path voltages relative to this same common ground plane. This is important to the data analysis because, while the dc battery bank is nominally ungrounded, the ground fault monitoring circuit does establish a nominal reference ground for

the battery bank. That is, when measured relative to ground, the positive side of the battery bank is nominally +62.5Vdc and the negative side is nominally -62.5Vdc. Any battery ground faults that form over the course of testing (i.e., due to shorting between a conductor connected to battery positive or battery negative and ground) will result in changes to measured voltages on various individual circuit/conductor traces. These changes may not indicate a fault in that particular circuit/cable, but rather, may be strictly an artifact of the battery ground fault. This effect is illustrated in detail in the discussion of individual test results.

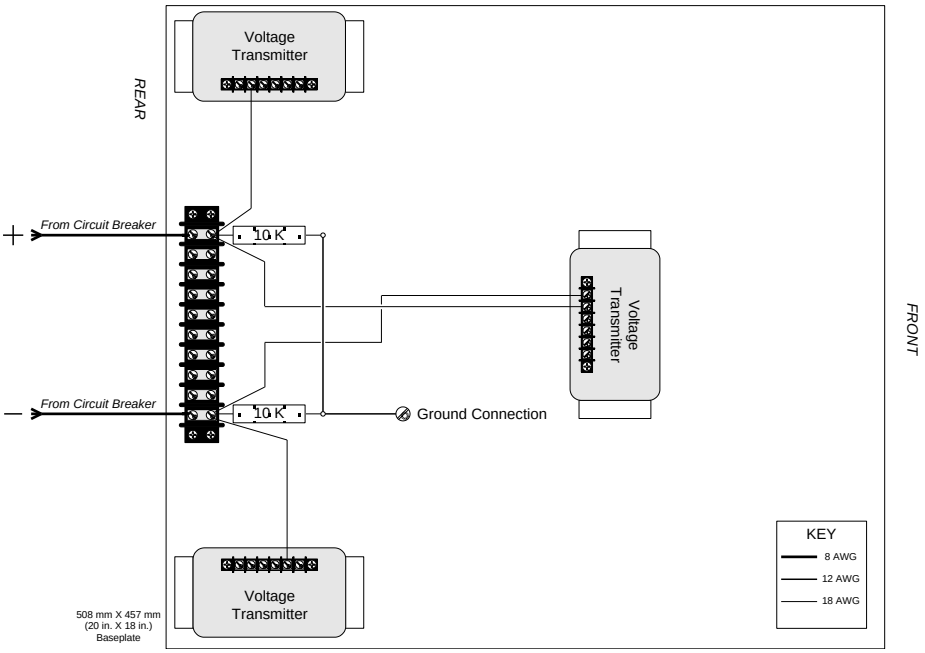

Figure A-70 Component layout for the dc ground detection circuit

A.8 Other Systems and Additional Information

This section of the appendix is dedicated to the other support systems that were necessary for the successful implementation and completion of the experimental series.

A.8.1 Transducers

A.8.1.1 Current Transducers

A note should be made regarding the current transducers[4] used for monitoring the dc-powered test circuits. The transducers were based on Hall-effect current probes. Hall-effect probes were selected mainly because they are non-intrusive. Duke Energy had used current shunts in its testing. Shunts are low-resistance devices inserted into a circuit path that induce a small voltage drop proportional to current flow. Measuring the voltage drop provides a method to calculate current flow. In the Duke Energy tests these shunts proved problematic, in some cases failing due to sustained short-circuit currents. The EPRI peer team also expressed concern that the presence of shunts in the various circuit paths could act to limit short-circuit currents, potentially compromising or altering the fuse-blow behavior for the circuits.

The current transducers were selected in two sizes. Most had a range of +/– 35 Adc (Ohio Semitronics Model CTL-51/35, signal conditioner Model CTA201RX5), but the main input power leads to each circuit were also equipped with larger +/– 500 A transducers (Ohio Semitronics Model CTL-601/500, signal conditioner Model CTA201X5). The intent was for the smaller transducers to pick up the smaller currents associated with normal circuit operation and early faulting behavior, and the larger transducers would pick up the higher-current behavior anticipated as gross cable failures occurred. Through the course of testing, three separate issues arose that impact the analysis and interpretation of the test data.

The first issue encountered was an apparent drift in the zero-point offset of the transducers between the beginning and the end of a given test, and between the end of one test and the beginning of the next test. This problem was observed early during the Penlight test series. The supplier's technical support was contacted and the source of the problem was identified. The Hall-effect sensors are basically magnetic coils that react to the fields created by the flow of electrical current producing a proportional voltage signal. When these devices are subjected to dc current flows, they will retain a certain degree of residual magnetism that is reflected as a non-zero voltage output. The magnetism will fade over time, and can be reversed by sending a reverse current signal through the pick-up core, but is an inevitable, but unadvertised, aspect of the devices when used for dc circuits. A separate drift existed during the first few minutes that instrument power (i.e., 120 VAC to turn on the equipment) was applied. These two unique occurrences prevented the uniform application of a zero-point offset.

These issues were discussed among the full peer team and potential options were explored. One option was to replace the Hall-effect transducers with shunts, but this was rejected for the same reasons that Hall-effect transducers were selected in the first place (as described above). Instead, a decision was made to continue the test program using the Hall-effect transducers and to deal with the offset issue in data analysis. To support the required data analysis adjustments, the testing protocol was modified in two ways. First, the transducers were energized up to 30

[4] All transducers were procured through Ohio Semitronics. Additional information may be ascertained from their catalog found on their website: https://www.ohiosemitronics.com/.

minutes before the beginning of a test to ensure that they were fully “warmed up” before testing. Second, data logging was initiated before energizing the test circuits and a set of baseline test data without any current flow was collected. Third, once the test circuits were energized (i.e., the connections to the battery bank were closed) an additional period of baseline data logging was allowed. Finally, after the completion of a given test, a period of post-test data was gathered with the battery engaged and continuing until after the battery bank was disconnected from the circuits.

The analysis of test data has “corrected” the current transducer data by subtracting out the pre-test, pre-battery initiation, zero current offset value for each transducer. That is, the pre-test zero condition data are used to calculate an average zero-point offset for each current transducer, and that value is subtracted from all test readings. Note that this approach provides a nominal correction but is imperfect. This is because, as noted, the zero-point offset drifts through the course of a test depending on the current flow experienced by the transducer. No attempts were made to correct the data beyond reflecting the pre-test offset. The result is that the current measurements at the end of the test may indicate a small current flow even after the circuits are fully de-energized.

The second issue identified was related to transducer sensitivity. The 35-A transducers were chosen at the outset because the peer team was interested in the characteristics of the short circuit currents, which were expected to be much larger than the normal circuit operating currents. However, this meant that the transducers were not especially sensitive to the normal circuit operating currents (typically 1 A or less). The early tests also showed that the transient short circuit current pulses were simply too fast for the data logging system to fully catch (i.e., the transducers would “see” the fault, but there was no assurance that the true peak current was being captured). After discussion with the peer team, a decision was taken to increase the sensitivity of the current transducers by looping the conductors repeatedly through the Hall-effect sensor coils. That is, by looping a conductor through the transducer five times, the signal strength sensed by the transducer is multiplied by five. In this manner, all of the 35-A transducers were amplified by a factor of five (five loops) and the 500-A transducers by a factor of two (two loops). This amplification effect was reversed during data processing so that the processed data files and all of the plots presented in this report show the corrected data and the actual (corrected) current values.

The final issue that was identified for the current transducers impacted the larger 500-A transducers only. The data from early tests showed that these transducers did not appear to be picking up the current signals at all. Diagnosis of the installed transducers showed that they were properly wired and that they could detect a steady current flow as expected. However, even after amplification of the signal by a factor of two, the transducers still appeared insensitive to the current transients. That is, even when a 35-A transducer (effectively reduced to +/-7 A transducers by the amplification) saturated, the 500-A transducers will not show a corresponding current flow. Several measures were taken in an attempt to address this issue. The final measure taken was to shift all of the 500-A transducers to a data logging system capable of much higher logging speeds (100 Hz). The system used for monitoring the high-ranged current transducers was, in fact, the system normally used to record data from the SCDU circuits. Even this change did not yield the desired result. Again, operability of the revised data logging system was verified, but still the 500-A transducers were not providing meaningful data signals when the transient short circuits were observed. The root cause of this issue has not been traced. It is thought that the larger Hall-effect coils may simply not be fast enough to respond to the transient faulting behaviors that seem to be manifested in tenths of a second. Overall, the 500-A transducers provided little or no data of value.

A.8.1.2 Voltage Transducers

Two types of voltage transducers were used for each circuit. When directly fed from a pole off the battery, a unidirectional transducer (Ohio Semitronics Model VTU-005X5) was used for monitoring the voltage. Typically, as an example, positive and negative source conductors were monitored using these types of transducers.

When a conductor was not tied to a specific battery terminal, such as a spare, a bi-direction transducer (Ohio Semitronics Model VT7-005X5-11) was used to monitor the voltage. This provided an opportunity to learn how the conductor was being affected by the other failing conductors.

A.8.2 Fuses, Fuse Holders, and Terminal Blocks

The fuses for the dc circuits were ordered through Ferraz-Shawmut.[5] The MOV circuits were fused with 10-A, fast-acting, midget fuses (Model Number ATM10) and connected with a two-pole fuse block (Model Number 30352). The SOV circuits were typically fused with 5-A, fast-acting, midget fuses (Model Number ATM5). The 1-inch valve and the switchgear close circuits were fused at 15 A using the ATM15, fast-acting, midget fuses. The large coil was fused with 25-A, fast-acting, midget fuses. The switchgear trip circuit was fused at 35 A, Model Number FRZ A2Y35-1.

Except for the 35-A fuses on the switchgear circuit, the fuses were housed within two-pole fuse blocks (Model Number 30352). The 35-A fuses were connected by two-pole fuse blocks, Model Number 20606.

The terminal blocks (Buchanan Model 223) used in each circuit were rated for up to 600 VDC.

A.8.3 Thermocouples

This test series provided additional cable thermal response data for the fire model improvement effort started in the CAROLFIRE test program.[6] In this particular program, providing cable thermal response data was a secondary objective. However, measurements of the cable thermal response are important to characterize the environmental conditions leading to the failure, and additional data in this regards is considered quite valuable. As a “target of opportunity,” cable thermal response data was gathered during the tests in a manner similar to that employed in CAROLFIRE, albeit with somewhat less instrument density.

As noted for CAROLFIRE, it is not appropriate to instrument any single cable for both thermal and electrical response. This is because installation of a thermocouple on, or within, a cable could impact the electrical failure behavior. Instead, the approach applied involves mirroring a cable being monitored for electrical performance with a second cable (in an adjacent or symmetric location) that monitored thermal response. Figure A-71 provides a graphical depiction of this dual-cable setup. In the majority of the small-scale tests, however, the orientation more often resembled Figure A-72.

[5] Additional information on the Ferraz-Shawmut fuses may be ascertained from their website at http://us.ferrazshawmut.com/.
[6] CAROLFIRE Final Report, 2007.

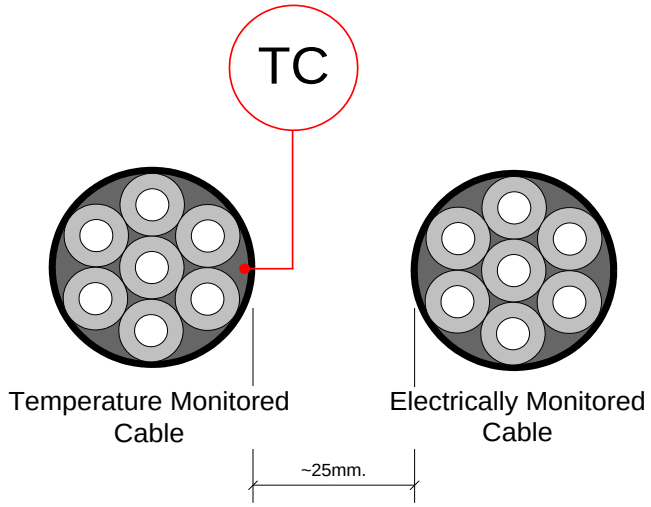

Figure A-71 Example thermocouple arrangement for temperature monitoring of seven-conductor cable located near the electrically monitored cable in tray. Cables were in contact during conduit tests

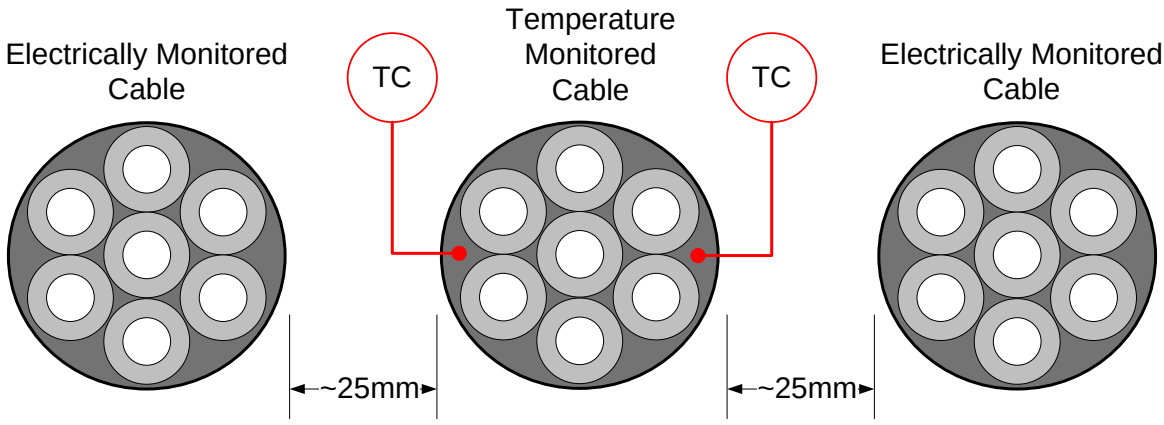

Figure A-72 Alternative orientation for the two electrically monitored cables and the thermally monitored cable

Thermocouples measured the thermal response of cables upon heating. In Penlight, Type K thermocouples placed just below the outer cable jacket were used for cable thermal response monitoring, a technique proven during the CAROLFIRE tests. In this process, a small slit is cut in the jacket, allowing insertion of the thermocouple bead. The bead itself can typically be inserted to a distance of approximately 2.5 to 10 cm (1 to 4 in.) along the length of the cable, placing it well away from the cut in the outer jacket. Placement distance does vary depending on the cable type. The slit was then closed and secured with a single layer of fiberglass tape.

For the armored cables, a pilot hole was drilled through the armor to allow for the insertion of a thermocouple next to the conductors. After the hole was drilled, a probe was used to further widen the gap for the thermocouple. In similar fashion, the bead was inserted approximately 2.5 cm to 10 cm(1 to 4 in.) and the pilot hole was sealed with fiberglass tape.

Where it was necessary to do so, such as in the Kerite® tests, the configurations of the thermocouple-instrumented cables/bundles exactly mimicked the configurations employed by the electrically monitored cables/bundles. The principal exceptions to this approach were those cases where three-cable bundles were run through a conduit. Here only a single thermocouple-instrumented cable was included with the bundle due to space constraints within the conduit.

Thermocouples were also widely used throughout the intermediate-scale experiments; however, because of the extensive effort expelled on circuit preparation, thermally monitored cables were not as prevalent. Instead, air temperatures were gathered at each test position. In Position A and Position B, the middle of the tray was assumed to be the hottest exposure area for the involved circuits and, as such, only the air temperatures at the center of the tray were monitored. In the three remaining positions, air temperatures were captured at 0.91 m (3 feet), the middle, and 2.13 m (7 feet) of the 3.05 m (10-foot) tray. The only tests that contained thermocouple instrumented cables were ISTest9 and ISTest10, the Kerite® and armored cable tests, respectively.

During the course of testing, there were instances when the recorded thermocouple data yielded erratic results, such as pronounced increases and/or decreases in temperature. An example of this may be observed in the air temperature for B-Position in ISTest10 at approximately 2800 seconds. Possible causes of this behavior may include failure at the junction point between the thermocouple connector and the thermocouple lead (e.g., debris interference, thermal impact) or interaction with electrical arcing; however, subsequent investigation of the off-normal readings did not occur upon the conclusion of this test or others with similar results. The data from the effected thermocouple should be discarded after the gross failure.

A.8.4 Data Acquisition System[7]

The dc circuits were connected to a National Instruments screw terminal block (Model Number SCXI-1300), 32-channel amplifier (Model Number SCXI-1102), and 12-slot chassis (Model Number SCXI-1001). The temperature data was collected by a similar system; however, it used a 4-slot chassis (Model Number SCXI-1000) rather than the 12-slot. The SCDU circuits, and later the CT500 current transducers, were monitored on a National Instruments SCB-100.

These system interfaces were controlled by LabVIEW Developer Suite, a software program developed by National Instruments.

A.8.5 Computers/Software

Individual computers were connected to the data acquisition systems for the dc circuits, ac circuits, and temperature data. This was to prevent data loss in the event of a system or power failure.

[7] Additional information about the National Instruments data acquisition systems may be ascertained from their product website at http://www.ni.com/.

The dc system was connected to a Hewlett-Packard desktop, Workstation XW4100 with a Pentium 4 Processor.

The ac system was connected to a Dell desktop, Precision 350 with a Pentium 4 Processor.

The temperature data acquisition system was connected to a Hewlett Packard laptop, Compaq nc6230 with an Intel Centrino Processor.

All three systems were operated on Windows XP.

A.8.6 Data Files

A list of the data files for each test may be found in Table A-16 and Table A-17.

Table A-16 Matrix of the Penlight data files.

DESIREE-Fire Penlight Data Matrix			
Burn Test #	**Data Files**		**Date Completed**
	Circuit	**Temperature**	
Pre-1 (P)	SCDU-1-2_July-14-2009_Prelim-1	Temperature data was not gathered during the preliminary Penlight tests	July 14, 2009
Pre-2 (P)	SCDU-1-2_July-14-2009_Prelim-2		July 14, 2009
Pre-3 (P)	SCDU-1-2_July-13-2009_Prelim-3		July 13, 2009
Pre-4 (P)	SCDU-1-2_July-13-2009_Prelim-4		July 13, 2009
1	PLTest1_SOV_Circuit.xlsx	PLTest1_SOV_Temperature.xlsx	July 15, 2009
2	PLTest2_SOV_Circuit.xlsx	PLTest2_SOV_Temperature.xlsx	July 17, 2009
3	PLTest3_SWGR_Circuit.xlsx	PLTest3_SWGR_Temperature.xlsx	July 21, 2009
4	PLTest4_SWGR_Circuit.xlsx	PLTest4_SWGR_Temperature.xlsx	July 30, 2009
5	PLTest5_1-inch_Large_Coil_Circuit.xlsx	PLTest5_1-inch_Large_Coil_Temperature.xlsx	July 22, 2009
6	PLTest6_1-inch-Long_Coil_Circuit.xlsx	PLTest6_1-inch-Long_Coil_Temperature.xlsx	July 22, 2009
7	PLTest7_MOV_Circuit.xlsx	PLTest7_MOV_Temperature.xlsx	July 20, 2009
8	PLTest8_MOV_Circuit.xlsx	PLTest8_MOV_Temperature.xlsx	July 20, 2009
9	PLTest9_SOV_Circuit.xlsx	PLTest9_SOV_Temperature.xlsx	July 17, 2009
10	PLTest10_SWGR_Circuit.xlsx	PLTest10_SWGR_Temperature.xlsx	July 21, 2009
11	PLTest11_1-inch_Large_Coil_Circuit.xlsx	PLTest11_1-inch_Large_Coil_Temperature.xlsx	July 22, 2009
12	PLTest12_MOV_Circuit.xlsx	PLTest12_MOV_Temperature.xlsx	August 12, 2009
13_qual	PLTest13-Qual_SCDU_Circuit.xlsx	PLTest13-Qual_SCDU_Temperature.xlsx	July 27, 2009
13	PLTest13_SCDU_Circuit.xlsx	PLTest13_SCDU_Temperature.xlsx	July 27, 2009
14	PLTes14_SCDU_Circuit.xlsx	PLTest14_SCDU_Temperature.xlsx	July 28, 2009

Table A-16 Matrix of the Penlight data files (continued).

DESIREE-Fire Penlight Data Matrix

Burn Test #	Data Files		Date Completed
	Circuit	Temperature	
15	PLTest15_SCDU_Circuit.xlsx	PLTest15_SCDU_Temperature.xlsx	July 28, 2009
16	PLTest16_SCDU_Circuit.xlsx	PLTest16_SCDU_Temperature.xlsx	July 28, 2009
17_qual	PLTest17-Qual_SCDU_Circuit.xlsx	PLTest17-Qual_SCDU_Temperature.xlsx	July 30, 2009
17	PLTest17_SCDU_Circuit.xlsx	PLTest17_SCDU_Temperature.xlsx	July 31, 2009
18	PLTest18_SCDU_Circuit.xlsx	PLTest18_SCDU_Temperature.xlsx	July 31, 2009
19	PLTest19_SCDU_Circuit.xlsx	PLTest19_SCDU_Temperature.xlsx	August 10, 2009
20	PLTest20_SOV_Circuit.xlsx	PLTest20_SOV_Temperature.xlsx	August 11, 2009
21	PLTest21_SWGR_Circuit.xlsx	PLTest21_SWGR_Temperature.xlsx	September 28, 2009
22	PLTest22_MOV_Circuit.xlsx	PLTest22_MOV_Temperature.xlsx	August 13, 2009
23	PLTest23_SOV_Circuit.xlsx	PLTest23_SOV_Temperature.xlsx	July 16, 2009
24	PLTest24_SWGR_Circuit.xlsx	PLTest24_SWGR_Temperature.xlsx	July 29, 2009
25	PLTest25_MOV_Circuit.xlsx	PLTest25_MOV_Temperature.xlsx	July 16, 2009
26	PLTest26_SOV_Circuit.xlsx	PLTest26_SOV_Temperature.xlsx	July 23, 2009
27	PLTest27_MOV_Circuit.xlsx	PLTest27_MOV_Temperature.xlsx	August 12, 2009
28	PLTest28_SOV_Circuit.xlsx	PLTest28_SOV_Temperature.xlsx	August 11, 2009
29	PLTest29_SWGR_Circuit.xlsx	PLTest29_SWGR_Temperature.xlsx	July 29, 2009
30	PLTest30_MOV_Circuit.xlsx	PLTest30_MOV_Temperature.xlsx	August 13, 2009
31	PLTest31_SOV_Circuit.xlsx	PLTest31_SOV_Temperature.xlsx	July 17, 2009
32	PLTest32_SWGR_Circuit.xlsx	PLTest32_SWGR_Temperature.xlsx	September 24, 2009
33	PLTest33_MOV_Circuit.xlsx	PLTest33_MOV_Temperature.xlsx	August 12, 2009
34	PLTest34_SOV_Circuit.xlsx	PLTest34_SOV_Temperature.xlsx	August 11, 2009
35	PLTest35_SWGR_Circuit.xlsx	PLTest35_SWGR_Temperature.xlsx	September 25, 2009
36	PLTest36_1-inch_Large_Coil_Circuit.xlsx	PLTest36_1-inch_Large_Coil_Temperature.xlsx	August 12, 2009
37	PLTest37_MOV_Circuit.xlsx	PLTest37_MOV_Temperature.xlsx	September 23, 2009
38	PLTest38_SOV_Circuit.xlsx	PLTest38_SOV_Temperature.xlsx	August 11, 2009
39	PLTest39_SWGR_Circuit.xlsx	PLTest39_SWGR_Temperature.xlsx	September 24, 2009
40	PLTest40_1-inch_Large_Coil_Circuit.xlsx	PLTest40_1-inch_Large_Coil_Temperature.xlsx	August 12, 2009
41	PLTest41_MOV_Circuit.xlsx	PLTest41_MOV_Temperature.xlsx	September 14, 2009

Table A-16 Matrix of the Penlight data files (continued).

DESIREE-Fire Penlight Data Matrix			
Burn Test #	Data Files		Date Completed
	Circuit	Temperature	
42	PLTest42_SWGR_Circuit.xlsx	PLTest42_SWGR_Temperature.xlsx	September 25, 2009
43	PLTest43_MOV_Circuit.xlsx	PLTest43_MOV_Temperature.xlsx	September 24, 2009
44	PLTest44_MOV_Circuit.xlsx	PLTest44_MOV_Temperature.xlsx	October 5, 2009
45	PLTest45_Intercable_Circuit.xlsx	PLTest45_Intercable_Temperature.xlsx	October 9, 2009
46	PLTest46_Intercable_Circuit.xlsx	PLTest46_Intercable_Temperature.xlsx	October 8, 2009
47	PLTest47_Intercable_Circuit.xlsx	PLTest47_Intercable_Temperature.xlsx	October 8, 2009
48	PLTest48_Intercable_Circuit.xlsx	PLTest48_Intercable_Temperature.xlsx	October 8, 2009
49	PLTest49_MOV_Circuit.xlsx	PLTest49_MOV_Temperature.xlsx	October 9, 2009
50	PLTest50_MOV_Circuit.xlsx	PLTest50_MOV_Temperature.xlsx	October 12, 2009
JPN 1	PLJPN-1_SWGR_Circuit.xlsx	PLJPN-1_SWGR_Temperature.xlsx	September 15, 2009
JPN 2	PLJPN-2_SWGR_Circuit.xlsx	PLJPN-2_SWGR_Temperature.xlsx	September 16, 2009
JPN 3	PLJPN-3_MOV_Circuit.xlsx	PLJPN-3_MOV_Temperature.xlsx	September 23, 2009

Table A-17 Matrix of the intermediate-scale experimental data files.

DESIREE-Fire Intermediate Scale Data Matrix				
Burn Test #	Data Files			Date Completed
	DC Data File	AC Data File	Temperature	
JPN 1	Not Used	9-16-09_Test-JPN-Igl_SCDU-1-2-3 9-16-09_Test-JPN-Igl-2_SCDU-1-2-3 9-16-09_Test-JPN-Igl-3_SCDU-1-2-3	9-16-09_JPN-Igl.csv 9-16-09_J-igl2.csv 9-16-09_J-Ig3.csv	09/16/09
Pre-1 (IS)	11-06-09_Prelim-1_Burnsite.csv	11-06-09_Prelim1_Burnsite	11-06-09_1335.csv	11/06/09
Pre-2 (IS)	11-04-09_Prelim-1_Burnsite.csv	11-04-09_Prelim1_Burnsite	11-4-09_1630.csv	11/04/09
1	02-24-2010_Test-1_Burnsite.csv	02-23-2010_Test-1_Burnsite	2-24-10_1301.csv	02/23/10
2	12-03-09_Test-2_Burnsite.csv	12-03-09_Test-2_Burnsite	12-3-09_1230.csv	12/03/09
3	02-17-2010_Test-3_Burnsite.csv	02-17-2010_Test-3_Burnsite	2-17-10_1327.csv	02/17/10
4	11-12-09_Test-4_Burnsite.csv	11-12-09_Test-4_Burnsite	11-12-2009_1030.csv	11/12/09
5	03-01-2010_Test-5_Burnsite.csv	03-01-2010_Test-5_Burnsite	3-1-10_1340.csv	03/01/10
6	03-03-2010_Test-6_Burnsite.csv	03-03-2010_Test-6_Burnsite	3-3-10_1405.csv	03/03/10
7	03-09-2010_Test-7_Burnsite.csv	03-09-2010_Test-7_Burnsite	3-9-10_1315.csv	03/09/10

Table A-18 Matrix of the intermediate-scale experimental data files (continued).

DESIREE-Fire Intermediate Scale Data Matrix				
Burn Test #	Data Files			Date Completed
	DC Data File	**AC Data File**	**Temperature**	
8	**11-17-09_Test-8_Burnsite.csv**	**11-17-09_Test-8_Burnsite**	**11-17-2009.csv**	**11/17/09**
9	**03-17-2010_Test-9_Burnsite.csv**	**03-17-2010_Test-9_Burnsite**	**3-17-10_.csv**	**03/17/10**
10	**03-25-2010_Test-10_Burnsite.csv**	**03-25-2010_Test-10_Burnsite**	**3-25-10_1040.csv**	**03/25/10**
11	**11-25-09_Test-11_Burnsite.csv**	**11-25-09_Test-11_Burnsite**	**11-25-09_1330.csv**	**11/25/09**
12	**11-23-09_Test-12_Burnsite.csv**	**11-23-09_Test-12_Burnsite**	**11-23-09_1505.csv**	**11/23/09**
Contin 1	**03-26-2010_ContingencyTest-1_Burnsite.csv**	**03-26-2010_ContingencyTest-1_Burnsite**	**3-26-10_1137.csv**	**03/26/10**
Contin 2	**03-29-2010_ContingencyTest-2_Burnsite.csv**	**03-29-2010_ContingencyTest-2_Burnsite**	**3-29-10_1134.csv**	**03/29/10**

A.8.7 Data Processing and Analysis

Both the Penlight and intermediate-scale experiments have associated circuit files that contain the date and test number. The temperature data files (located on the cd) contain the date and nominal test start time of each test. The AC files are analyzed in similar fashion to the CAROLFIRE SCDU files. Essentially, a Microsoft Excel® template was created and may be populated with the relevant data captured from the SCDU system through the "Import Raw Data." As with SCDU files from CAROLFIRE, specific test information had to be included on the Test Conditions sheet in order to correctly synchronize the circuit and fire data start times. Graphs located on separate sheets populate automatically.

The data processing was significantly more complicated on the dc circuit systems. For each pair of circuits (i.e., MOV-1 and MOV-2, SOV-1 and SOV-2, etc.), there was a separate Excel® template and graphing template developed to aid in data analysis. Similar to the SCDU template, a Test Conditions page with specific information, such as circuit data acquisition and fire start times, must be filled out for each experiment. Once this information is entered, the circuit offset, fire offset, and the test duration are calculated and displayed. Time, circuit, and ground data from the raw circuit file may then be copied and pasted into the Raw Data sheet. As described in previous sections, the current offset must be adjusted for each test. Typically, the last 100 seconds before the battery was turned on was averaged and used as the offset. The Processed Data worksheet was used for data manipulation, such as incorporating the current offset information, adjusting the negative voltages monitored on the unidirectional transducers, and the filtering of the ground fault activity. In order to clearly interpret the data, it is important to filter out the ground fault behavior. Figure A-73, Figure A-74, and Figure A-75 display the progression of data analysis beginning with the raw positive, negative, and coil voltage and extending through the filtering of the ground detection circuit. The spurious actuation may be clearly observed in the final graph.

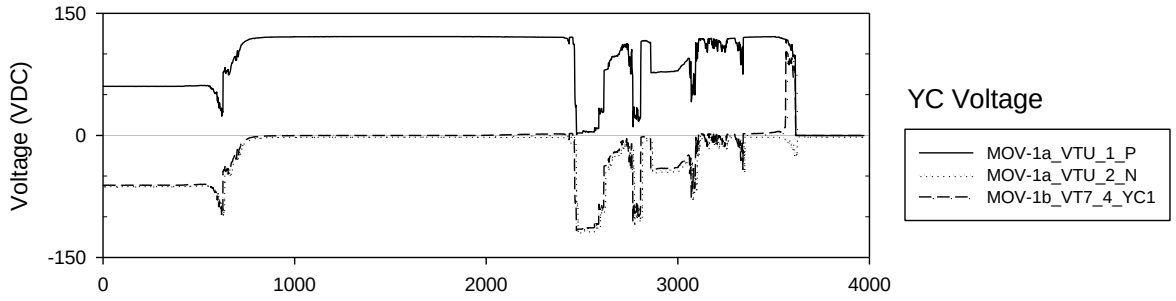

Figure A-73 Unedited voltage data including the positive and negative sources

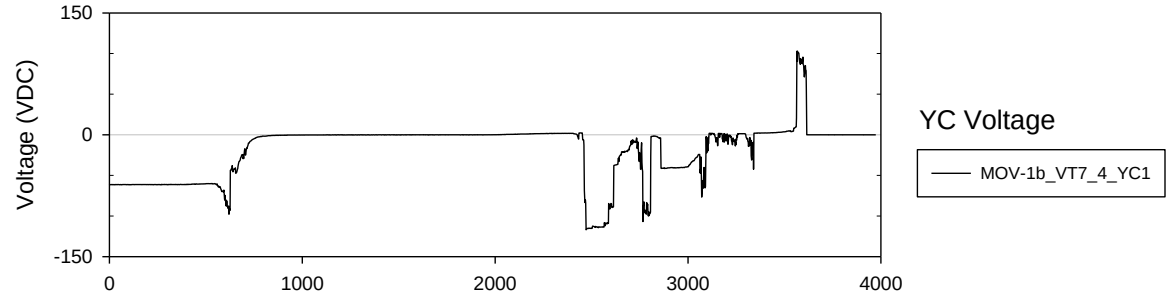

Figure A-74 Raw voltage plot for the MOV-1 close coil

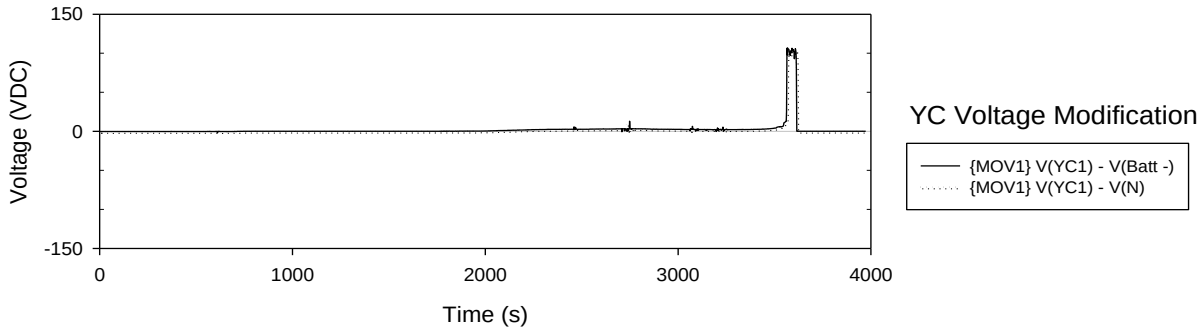

Figure A-75 Voltage with the ground filtered out

The specific ground, current, and voltage information may be copied and pasted into the Final Data worksheet. This worksheet is then used to populate the graphing templates.

SigmaPlot® 11 was used to create the graphs for each circuit, excluding the SCDU. Each circuit pair had a separate graphing template developed to facilitate the analysis process. Each template contains graphs that may be edited to narrow in on failure behavior. In the subsequent appendices for each circuit pair, voltages are primarily displayed with the ground filtered out. In the caption for these graphs, the word “Modified” is displayed to differentiate between the original and modified data.

A.8.8 Intermediate-Scale Cable Loading Diagrams

Cable grouping and bundling was widely used for the circuit cables throughout the intermediate scale tests. When looking at the test data in subsequent sections, the orientation (e.g., in direct contact the tray, on top of fuel cables) of the cable bundle within the tray is important to note. The loaded cable tray orientation diagrams represents trays filled with 30 to 40 filler cables used to facilitate hot gas production. The bundled cable tray orientation diagrams illustrate trays that were modified with brackets to contain small bundles of fuel cables as well as the circuits. The specialized cable tray orientation defines the circuit location for two tests, ISTest9 and ISTest10. In both tests, unique cables (i.e., Kerite® and armored cables, respectively) were tested and specific orientations were necessary for the desired test objectives. These tests included thermally monitored cables as well as air temperature data.

In all three tray conditions, the gray background represents filler cables and the white circles represent the circuit cables. For each test, the filler cables surrounding the circuit cables and within the tray were of similar type. In other words, for example, thermoset circuit cables were grouped with the thermoset filler cables. The only exception to this was the cable trays containing only filler cable. In these trays, it was most common to have similar cable types, but a limited amount of dissimilar cables were added if deemed necessary. As the data is presented in subsequent sections, Figure A-76 illustrates the location of the circuit cables within the filler cables. Figure A-77 illustrates the fill cable tray orientations. Figure A-78 and Figure A-79 illustrate the bundled cable tray orientations. Figure A-80 illustrates the specialized fill cable tray orientations.

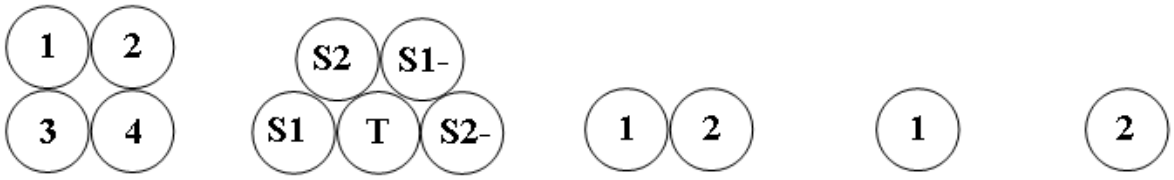

Figure A-76 Circuit cable orientation within the cable trays

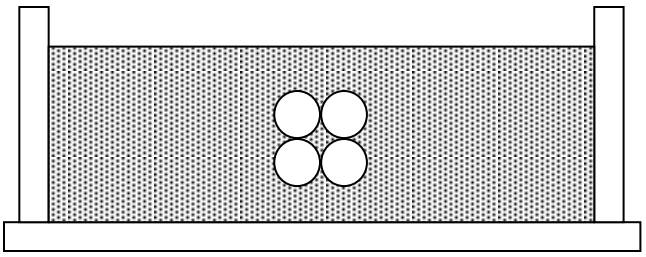

Fill Tray A

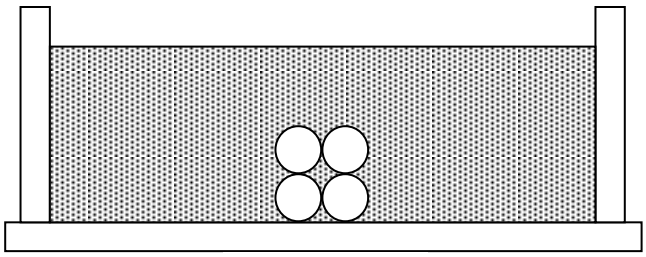

Fill Tray B

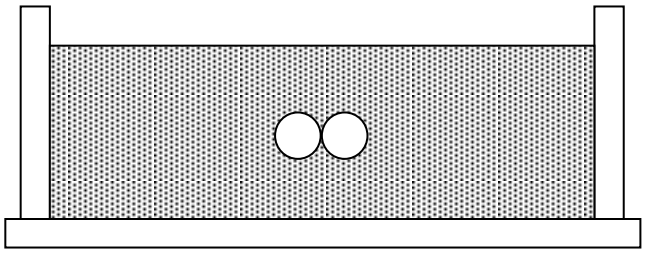

Fill Tray C

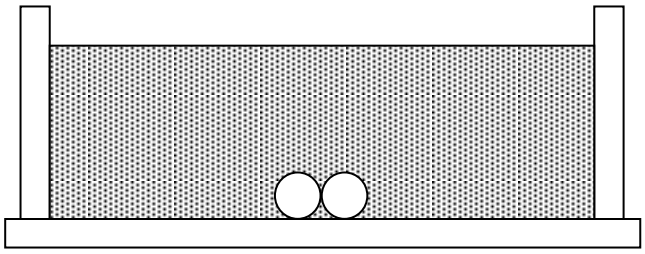

Fill Tray D

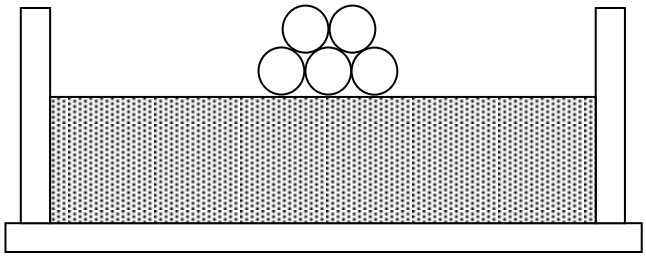

Fill Tray E

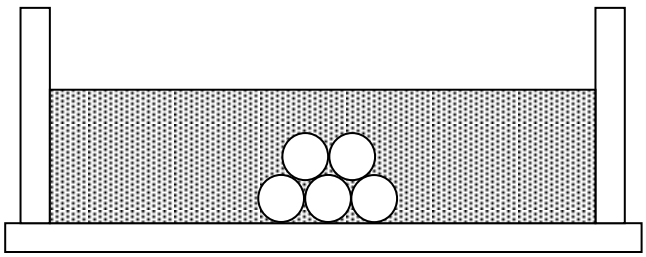

Fill Tray F

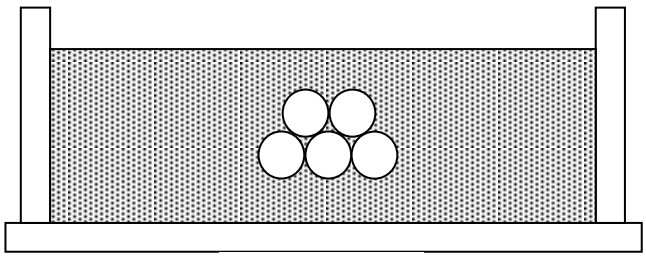

Fill Tray G

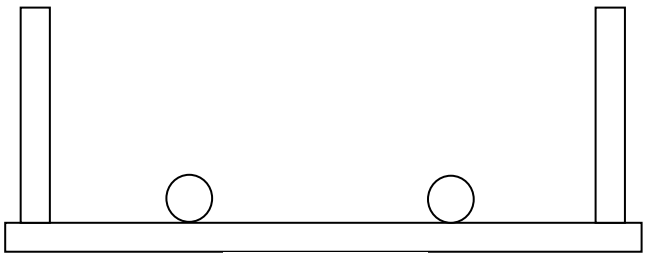

Fill Tray H

Figure A-77 Fill cable tray orientation

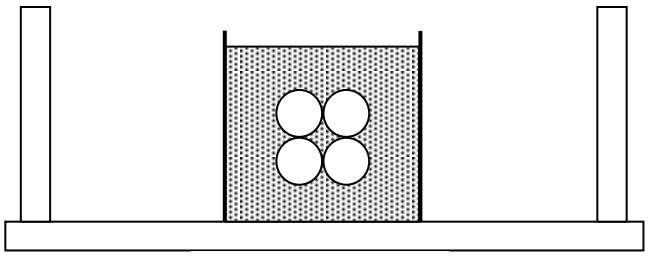

***Bundled* Tray A**

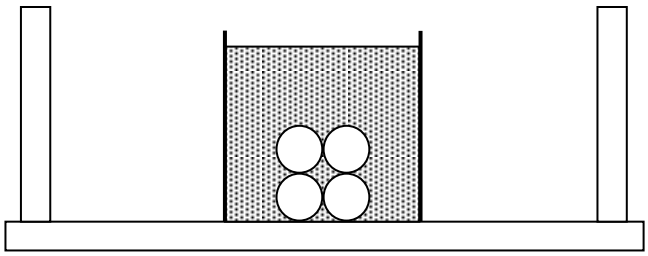

***Bundled* Tray B**

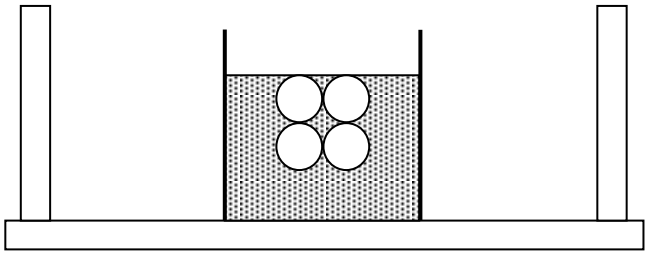

***Bundled* Tray C**

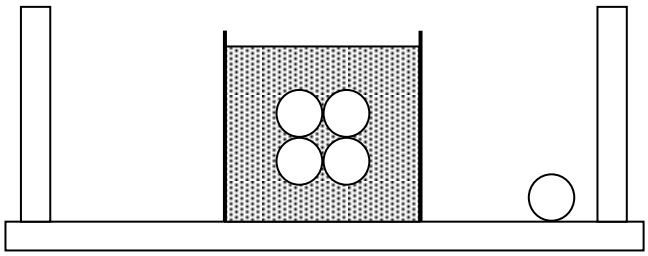

***Bundled* Tray D**

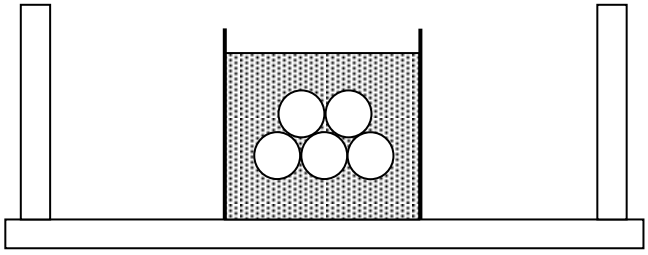

***Bundled* Tray E**

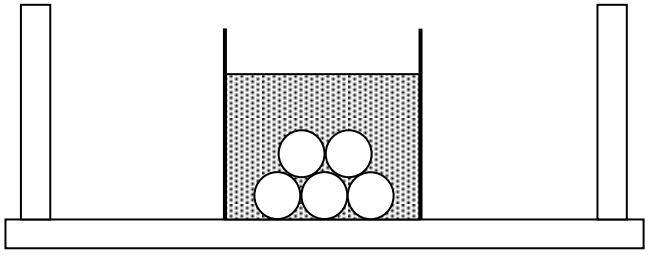

***Bundled* Tray F**

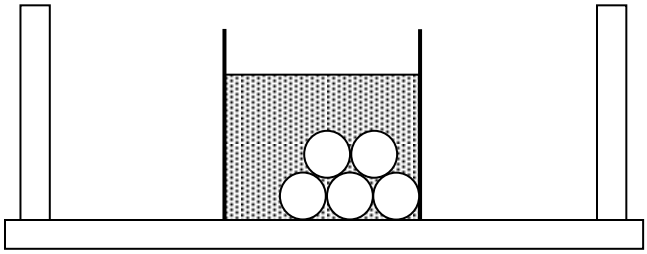

***Bundled* Tray G**

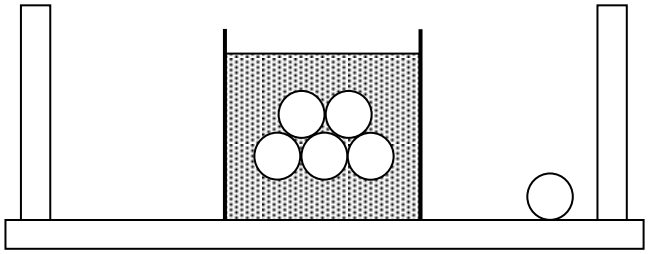

***Bundled* Tray H**

Figure A-78 Bundled cable tray orientation

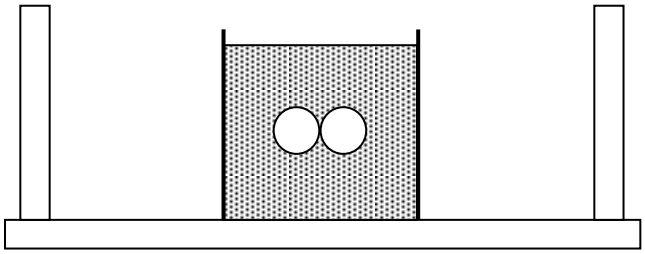

***Bundled* Tray I**

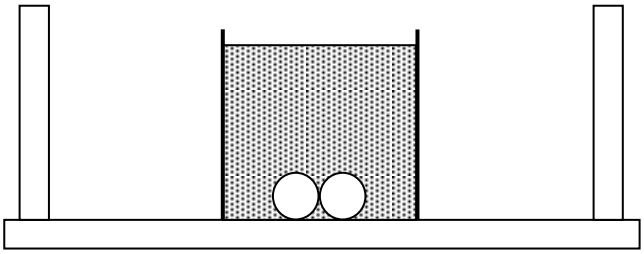

***Bundled* Tray J**

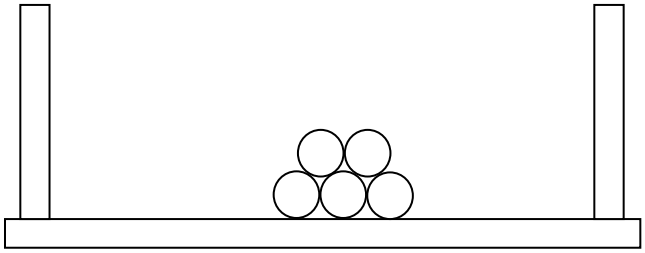

***Bundled* Tray K**

Figure A-79 Bundled cable tray orientation (continued)

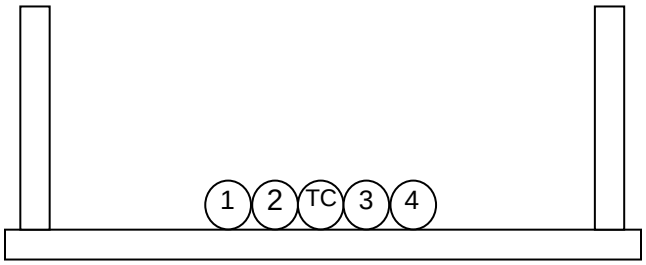

***Specialized* Tray**
A

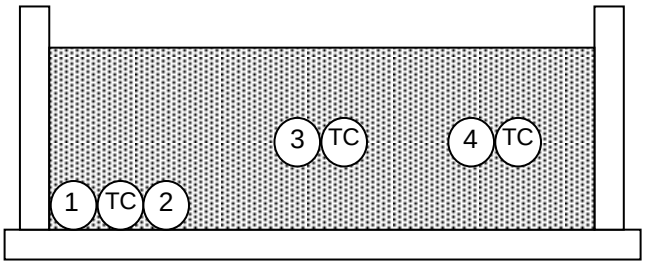

***Specialized* Tray**
B

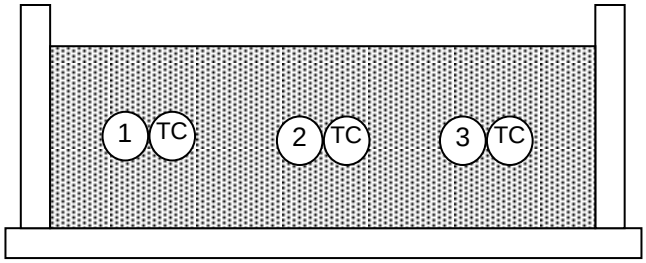

***Specialized* Tray**
C

Figure A-80 Specialized tray fill orientation

A.9 Intermediate-Scale Burner System

Nearly identical to the propylene (propene, C_3H_6)fuel system used in CAROLFIRE, the propylene fuel system was used to feed the gas from externally secured tanks to the sand burner within the bunker facility (Figure A-81). The sand burner was identical to the one used during the CAROLFIRE testing program. Typically, six bottles of propene were connected to 100-psig (6.80 atm) regulators attached to stainless steel flex line. This line connected to Swagelok® fittings and was piped through a ventilation valve, an isolation valve, and pressure gauge before penetrating a through-way into the bunker. The line was connected to an Omega Mass Flow Controller,[8] which regulated the flow of propylene to the sand burner. The digital readout was run from within the bunker to the instrumentation transportainer just outside the bunker.

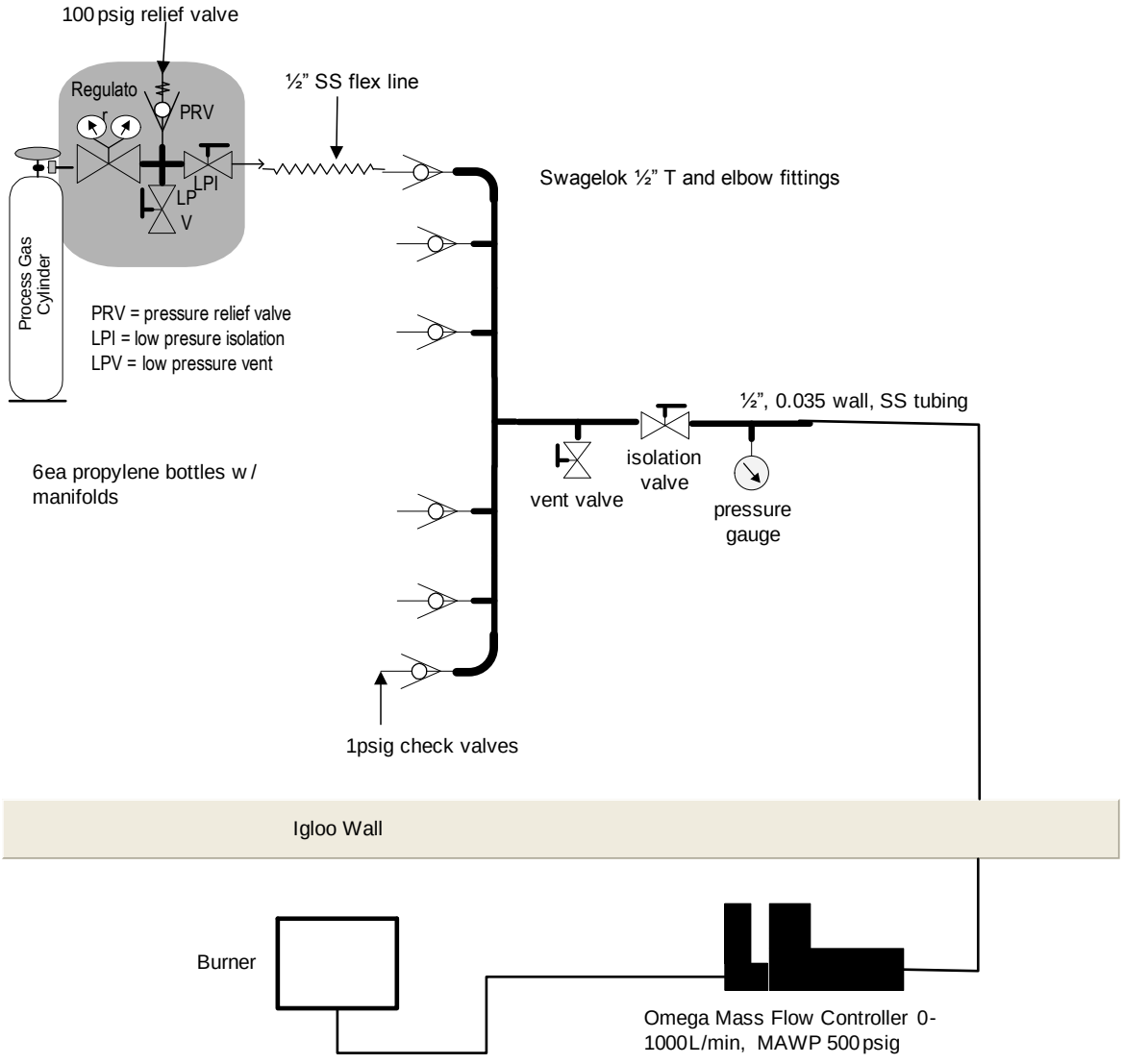

Figure A-81 Illustration of the propene pressure system for the intermediate-scale experiments

[8] Additional information may be ascertained from Omega's product literature found on the following website http://www.omega.com/manuals/index.html?s=all.

The top surface of the burner measured 400 mm (15.75 in.) on a side (outside dimensions). A metal lip around the upper edge of the burner was turned to the inside of the burner on all sides and measures 12 mm (1/2 in.) wide (a piece of standard mild steel angle iron was used to form the top rail of the burner). The sand box burner is illustrated in Figure A-82.

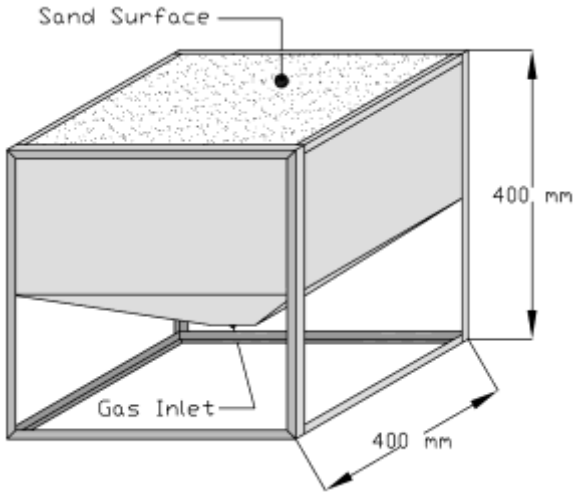

Figure A-82 Illustration of the sand box burner

By itself, the burner stood a total of 400 mm (15.75 in.) high (a nominal cube). The lower half of the burner was an open support framework, while the upper half was an enclosed box section. That is, the upper 200 mm (7.8 in) of each side of the support framework was enclosed with thin steel sheet panels welded and sealed with high-temperature caulk. Below this upper section a four-sided funnel shaped section was welded below the side panels. The lower funnel section acted as a plenum for gas entering the burner. A coarse copper screen was placed at the top of the funnel section and was supported by an X-shaped metal framework at the interface between the funnel section and the upper section side panels. A layer of 6 to 9 mm (1/4 to 3/8 in.) gravel was placed on top of the first screen filling the lower two-thirds of the upper box section. A second (finer) screen was placed on top of the gravel and a layer of course sand filled the upper one-third of the upper box section flush to the top lip of the burner. Gas flowed into the bottom of the sand box, percolated up through the gravel, through the sand, and then burned as a diffusion flame above the sand surface.

For testing, the burner was elevated above the floor of the test enclosure. The top surface of the burner was about 840 mm (33 in.) above the floor of the enclosure. The burner was always placed in the center of the test structure and directly below cable raceway Location A. The flow of gas to the burner was measured and controlled by an electronic flow control valve.[9]

The single largest source of uncertainty associated with the intermediate-scale test conditions was that associated with conversion of the gas burner measure flow rate into an effective HRR. That is, while the gas flow rate was monitored in all tests, the HRR must be calculated. The HRR (MW) can be estimated based on the measured fuel flow rate as follows:

$$HRR = \eta \bullet V_g \bullet \rho \bullet H_c, \qquad \text{(A-1)}$$

[9] The flow controller used was from Omega Controls and is electronic flow controller model FMA5545.

where η is the combustion efficiency, H_c is the heat of complete combustion (45.79 MJ/kg), ρ is the fuel gas density as standard conditions (1.802 kg/m^3), and V_g is the measured fuel gas volume flow rate (m^3/s). All but one of these parameters was either well known or directly measured, the exception being the combustion efficiency. The intent had been to estimate the burner efficiency based on cross-calculation of the HRR based on both the fuel flow rate and oxygen consumption calorimetry based on stack measurements. This proved to be impractical given the extremely long residence times for combustion products in the outer test cell that led to an untenably long delay between gas burner changes and the achievement of steady-state conditions at the stack.

Typical values for this parameter for a sand burner and a fuel such as propene will generally range from 0.8 to 0.9. *Note that throughout this report, whenever a value or plot of the nominal gas burner HRR has been cited, the calculation has assumed a combustion efficiency of 0.85 (85%).* The relatively low combustion efficiency reflects two factors. First, the sand burner creates a diffusion flame that is less efficient than a pre-mixed gas-air flame. Second, propene was chosen as the fuel gas specifically because under diffusion flame burning conditions propene burns with a luminous, sooty flame. However, such burning behavior is also indicative of a less complete, hence less efficient, combustion process than would be obtained with a cleaner-burning fuel gas such as propane. Based on these conditions, 0.85 is considered a reasonable estimate of the overall combustion efficiency of the propene sand burner. Given the range of typically measured sand burner efficiencies, the resulting HRR calculations are estimated to have a nominal uncertainty of ± 5%.

Gas flow to the gas burner was provided through a set-point flow control valve. The flow rate was recorded in standard liters per minute of gas. In practical application, the volume flow rate of the gas as reported by the mass flow meter must be multiplied by a constant "correction factor." The correction factor was specified by the flow controller's manufacturer and corrects for the flow of propene gas as compared to the flow of nitrogen gas against which the valve was calibrated. Hence, Equation A-2 is modified in application as follows:

$$HRR = \eta \bullet 0.4 \bullet V_{g-reported} \bullet \rho \bullet H_c \qquad \text{(A-2)}$$

where 0.4 is the calibration correction factor and $V_{g\text{-reported}}$ is the measured fuel gas volume flow rate as reported by the flow meter.

A.10 Intermediate-Scale Test Burner Settings

The heating protocol for each intermediate scale test is described in Tables A-18 through A-32. It should be noted that the flow rates did not stabilize on one value, but fluctuated by approximately +/–- 3 liters per minute. Additionally, the ambient temperatures (e.g., extreme colds of 0 °F) impacted the performance of the pressure system. These conditions will be noted as appropriate.

Table A-19 Inputs for the heat release rate equation.

Initial Inputs			
Condition	Symbol	Units	Value
Combustion Efficiency	η		0.85
Heat of Combustion	H_c	MJ/kg	45.79
Fuel Gas Density	ρ	kg/m^3	1.802
Correction Factor			0.4

Table A-20 Heat release rate for Intermediate-Scale Test 1.

Intermediate Scale Test 1		
Time (minutes into test)	Burner Flow (L/min)	Heat Release Rate (kW)
0	148.4	173
15	187.2	219
29	214	250
45	239.2	280
60	269.6	315
63	0	0

Table A-21 Heat release rate for Intermediate-Scale Test 2.

Intermediate Scale Test 2		
Time (minutes into test)	Burner Flow (L/min)	Heat Release Rate (kW)
0	146.4	171
15	182	213
25	214	250
33	240	281
41	260	304
46	280	327
49	240	281
52	212	248
56	184	215
60	156	182
64	137.6	161
68	126	147
70	120	140
74	110	129
79	104.4	122
82	99.2	116
87	92	108
97	75.6	88
101	0	0

Intermediate Scale Test 2 was conducted during frigid ambient temperatures. After approximately 46 minutes into the test, the burner flow rate declined steadily until test termination. The cold ambient conditions caused two issues; namely, minor leaking of propene gas from the valves and the freezing of the gas regulators.

Table A-22 Heat release rate for Intermediate-Scale Test 3.

Intermediate Scale Test 3		
Time (minutes into test)	Burner Flow (L/min)	Heat Release Rate (kW)
0	148.4	173
15	180.4	211
28	212.4	248
51	244	285
56	0	0

Table A-23 Heat release rate for Intermediate-Scale Test 4.

Intermediate Scale Test 4		
Time (minutes into test)	Burner Flow (L/min)	Heat Release Rate (kW)
0	124	145
55	244	285
112	0	0

Table A-24 Heat release rate for Intermediate-Scale Test 5.

Intermediate Scale Test 5		
Time (minutes into test)	Burner Flow (L/min)	Heat Release Rate (kW)
0	148	173
15	181.2	212
25	212	248
37	244.8	286
44	0	0

Table A-25 Heat release rate for Intermediate-Scale Test 6.

Intermediate Scale Test 6		
Time (minutes into test)	Burner Flow (L/min)	Heat Release Rate (kW)
0	147.6	173
18	181.6	212
31	212	248
41	0	0

Table A-26 Heat release rate for Intermediate-Scale Test 7.

Intermediate Scale Test 7		
Time (minutes into test)	Burner Flow (L/min)	Heat Release Rate (kW)
0	147.6	173
15	182.8	214
25	210.8	246
36	240.8	281
40	0	0

Table A-27 Heat release rate for Intermediate-Scale Test 8.

Intermediate Scale Test 8		
Time (minutes into test)	Burner Flow (L/min)	Heat Release Rate (kW)
0	149.2	174
24	182.8	214
34	0	0

Table A-28 Heat release rate for Intermediate-Scale Test 9.

Intermediate Scale Test 9		
Time (minutes into test)	Burner Flow (L/min)	Heat Release Rate (kW)
0	148	173
15	180	210
29	213.6	250
39	241.2	282
55	0	0

Table A-29 Heat release rate for Intermediate-Scale Test 10.

Intermediate Scale Test 10		
Time (minutes into test)	Burner Flow (L/min)	Heat Release Rate (kW)
0	148	173
15	182.4	213
25	215.6	252
35	243.2	284
45	260.4	304
57	272	318
66	0	0

Table A-30 Heat release rate for Intermediate-Scale Test 11.

Intermediate Scale Test 11		
Time (minutes into test)	Burner Flow (L/min)	Heat Release Rate (kW)
0	148	173
16	184.4	216
36	211.6	247
46	242.4	283
56	257.2	301
75	0	0

Table A-31 Heat release rate for Intermediate-Scale Test 12.

Intermediate Scale Test 12		
Time (minutes into test)	Burner Flow (L/min)	Heat Release Rate (kW)
0	147.2	172
15	184	215
25	215.6	252
35	246	288
45	262.4	307
65	0	0

Table A-32 Heat release rate for Intermediate-Scale Test Contingency 1.

Intermediate Scale Test Contingency 1		
Time (minutes into test)	Burner Flow (L/min)	Heat Release Rate (kW)
0	143.6	168
17	0	0

Table A-33 Heat release rate for Intermediate-Scale Test Contingency 2.

Intermediate Scale Test Contingency 2		
Time (minutes into test)	Burner Flow (L/min)	Heat Release Rate (kW)
0	119.6	140
17	0	0

A.11 References

Standard 450-1995, “IEEE Recommended Practice for Maintenance, Testing and Replacement of Vented Lead-Acid Batteries for Stationary Applications,” Published by The Institute of Electrical and Electronics Engineers, 3 Park Avenue, New York, NY 10016-5997, June 1995.

Standard 484-2002, “IEEE Recommended Practice for Installation Design and Implementation of Vented Lead-Acid Batteries for Stationary Applications,” Published by The Institute of Electrical and Electronics Engineers, 3 Park Avenue, New York, NY 10016-5997, September 2002.

Standard 485-1997, “IEEE Recommended Practice for Sizing Lead-Acid Batteries for Stationary Applications,” Published by The Institute of Electrical and Electronics Engineering, 3 Park Avenue, New York, NY 10016-5997, May 1997.

NRC FORM 335 (12-2010) NRCMD 3.7

U.S. NUCLEAR REGULATORY COMMISSION

BIBLIOGRAPHIC DATA SHEET

(See instructions on the reverse)

1. REPORT NUMBER (Assigned by NRC, Add Vol., Supp., Rev., and Addendum Numbers, if any.)

NUREG/CR-7100
SAND2012-0323P

2. TITLE AND SUBTITLE

Direct Current Electrical Shorting in Response to Exposure Fire (DESIREE-Fire): Test Results

3. DATE REPORT PUBLISHED

MONTH	YEAR
April	2012

4. FIN OR GRANT NUMBER

USNRC JCN N6579

5. AUTHOR(S)

S.P.Nowlen, J.W.Brown, T.J. Olivier, F.J.Wyant

6. TYPE OF REPORT

Technical

7. PERIOD COVERED *(Inclusive Dates)*

2/26-2010 - 1/30/2012

8. PERFORMING ORGANIZATION - NAME AND ADDRESS *(If NRC, provide Division, Office or Region, U.S. Nuclear Regulatory Commission, and mailing address; if contractor, provide name and mailing address.)*

Sandia National Laboratories
Risk and Reliability Analysis Dept. 6761
P.O. Box 5800
Albuquerque, NM 87185-0748

9. SPONSORING ORGANIZATION - NAME AND ADDRESS *(If NRC, type "Same as above"; if contractor, provide NRC Division, Office or Region, U.S. Nuclear Regulatory Commission, and mailing address.)*

Division of Risk Analysis
Office of Nuclear Regulatory Research
U.S. Nuclear Regulatory Commission
Washington, DC 20555-0001

10. SUPPLEMENTARY NOTES

G. Taylor, NRC Project Manager

11. ABSTRACT *(200 words or less)*

This report presents the results of a series of fire tests performed to assess cable failure modes and effects behavior for direct current (dc)-powered control circuits. The project, known as the Direct Current Electrical Shorting in Response to Exposure Fire (DESIREE-Fire) test project, was sponsored by the U.S. Nuclear Regulatory Commission Office of Nuclear Regulatory Research. The tests were performed by and at Sandia National Laboratories in Albuquerque, NM. The program was conducted with the collaboration of the Electric Power Research Institute (EPRI) and its member utilities. EPRI representatives participated in all phases of program planning, execution, data analysis, and data reporting by providing both peer review and in-kind material support.

The test program involved a series of both small- and intermediate-scale fire tests. Each test exposed one or more electrical control cables commonly used in the existing fleet of U.S. nuclear power plants (NPPs) to fire exposure conditions. Each test cable was connected to one of several circuit simulator units designed to mimic the behavior of typical NPP components. The simulated dc-powered control circuits included motor-operated valves, solenoid-operated valves of various sizes, and a medium voltage circuit breaker unit. Cable electrical performance is monitored throughout each test to determine both the timing and mode of circuit faulting behavior. This report focused on a factual reporting of the test program and test data. Insights regarding dc-powered control circuit cable failure modes and effects are to be addressed separately via a Phenomena Identification and Ranking Table (PIRT) exercises to qualitatively rank fire-induced electrical circuit phenomena and an expert elicitation to provide quantitative numerical estimates to the likelihood of various fire-induced circuit failure configurations. One PIRT panel focused on electrical behavior and the second on implications for probabilistic risk assessment.

12. KEY WORDS/DESCRIPTORS *(List words or phrases that will assist researchers in locating the report.)*

Electric cables, cables, fire, cable failure, fire risk, fire PRA, fire PSA, post-fire safe shutdown, spurious actuaiton, spurious operation, hot short

13. AVAILABILITY STATEMENT

unlimited

14. SECURITY CLASSIFICATION

(This Page)

unclassified

(This Report)

unclassified

15. NUMBER OF PAGES

16. PRICE

Federal Recycling Program

UNITED STATES
NUCLEAR REGULATORY COMMISSION
WASHINGTON, DC 20555-0001

OFFICIAL BUSINESS

NUREG/CR-7100

Direct Current Electrical Shorting in Response to Exposure Fire (DESIREE-Fire): Test Results

April 2012